Nano/micro particle as catalysts for organic reactions and carbon dioxide conversion into cyclic-and poly-carbonates

A Thesis submitted for the degree of

Doctor of Philosophy

By

Venkateswara Rao Velpuri

School of Chemistry

University of Hyderabad

Hyderabad - 500046

India

January 2021

Nano/micro particle as catalysts for organic reactions and carbon dioxide conversion into cyclic- and poly-carbonates

A thesis submitted for the degree of

Doctor of Philosophy

In

CHEMISTRY

By

Venkateswara Rao Velpuri

Reg. No. 15CHPH17

School of Chemistry

University of Hyderabad

Hyderabad - 500046

India

January 2021

Dedicated

to

My Teachers

and

family members

DECLARATION

I hereby declare that the matter embodied in the thesis entitled "**Nano/micro particle as catalysts for organic reactions and carbon dioxide conversion into cyclic- and poly-carbonates**" is the result of investigations carried out by me in the School of Chemistry, University of Hyderabad, India under the supervision of Prof. K. Muralidharan.

In keeping with the general practice of reporting scientific investigations, due acknowledgements have been made wherever the work described is based on the findings of other investigators. Any omission, which might have occurred by oversight or error, is regretted.

K. M 22/1/2021
Signature of Supervisor

K. MURALIDHARAN
Professor
School of Chemistry
University of Hyderabad
Hyderabad - 500 046.

V. V. Rao
Venkateswara Rao Velpuri

Reg. No.: 15CHPH17

CERTIFICATE

This is to certify that the thesis entitled **"Nano/micro particles as catalysts for organic reactions and carbon dioxide conversion into cyclic- and poly- carbonates"** submitted by **Venkateswara Rao Velpuri** with registration number **15CHPH17** in partial fulfillment of the requirements for the award of Doctor of Philosophy (Ph.D.) in the School of Chemistry is a bonafide work carried out by him under my supervision and guidance. This thesis is free from plagiarism and has not been submitted previously in part or full to this or any other University/Institution for any degree or diploma. Further the student has two publications before submission of the thesis for adjudication and has produced evidences for the same in the form of reprints.

Further Parts of this thesis has been:

A. Published as the following article:

1. **Venkateswara rao velpuri** and Krishnamurthi muralidharan, Multicomponant click reaction catalysed by organic surfactant free copper sulfide (sf-CuS) nano micro flowers. *Journal of organometallic chemistry.* **2019**, 884, 59e6560.
2. Sanyasinaidu gottepu, **Venkateswara rao velpuri** and Krishnamurthi muralidharan" Surfactant free metal chalcogenides microparticles consisting of nano size crystallites: room temperature synthesis driven by the supersaturated condition *J. Chem. Sci.* **129** (2017) 1853–1861.

B. Presented in the following conferences:

1. **Oral talk, Venkateswara Rao Velpuri** and Krishnamurthi Muralidharan "*Synthesis of metal Sulphide/Oxide nano/micro particles and their catalytic application for organic transformations*" Oral and poster presentation at 17 annuals in house symposium in Chemfest-2020, School of Chemistry, University of Hyderabad, Hyderabad during 20-21, may 2020
2. **Poster,Venkateswara Rao Velpuri** and Krishnamurthi Muralidharan, "*multicomponent click reaction catalysed by Organic surfactant-free copper sulfide (sf-CuS) nano/micro flowers" poster* presentation at CRSI-National Symposium in Chemistry-24, jointly organized by CSIR-CLRI and IIT-Madras at CSIR-CLRI, Chennai during 08-10th, February 2019.

Further, the student has passed the following courses towards the fulfillment of coursework requirement for Ph.D.:

S. No.	Course Code	Title	Credits	Pass/Fail
1.	CY-801	Research Proposal	3	Pass
2.	CY-802	Chemistry pedagogy	3	Pass
3.	CY-805	Instrumental Methods-A	3	Pass
4.	CY-504	Chemistry of Materials	3	Pass

K. M 22/1/2021

Prof. K. Muralidharan
(Thesis Supervisor)

K. MURALIDHARAN
Professor
School of Chemistry
University of Hyderabad
Hyderabad - 500 046.

Dean
School of Chemistry

Dean
SCHOOL OF CHEMISTRY
University of Hyderabad
Hyderabad-500 046

Contents

CHAPTER – 2

Multicomponent dipolar cycloaddition of phenylacetylene involving aryl halides and epoxides catalyzed by organic surfactant-free CuS nano/micro flowers (sf-CuS)

CHAPTER – 3

NIR absorbing surfactant-free $CuInS_2$ nano/micro particles (sf-CIS) as catalyst for symmetric Glaser–Hay coupling reactions

CHAPTER – 4

High yield room temperature conversion of carbon dioxide into cyclic carbonates catalyzed by mixed metal oxide surfactant-free CuO-ZnO nano/micro-flakes (Cozi-nmf)

CHAPTER – 5

ACKNOWLEDGMENT

All praises to the Almighty of lord Shiva who has bestowed me health and wisdom, which enabled me to complete this study successfully.

In pursuing this study, I owe intellectual as well as personal debts to several people; it would have been impossible to complete this work without their invaluable support and guidance. First and foremost, I would like to express my deepest gratitude to my Supervisor **Prof. K. Muralidharan**, for his advice, patience, encouragement and invaluable guidance throughout the course. His guidance was the beacon light for my research and writing of this thesis. I could not have imagined better supervisor and mentor for my Ph.D. than him. I owe my personal gratitude to my supervisor for giving me time and space to work under his supervision; it was great life experience to owe his thoughts and mentorship. Thank you so much sir.

I would like to thank and owe my personal appreciation to my doctoral committee members **Prof. Tushar Jana** and **Prof. R. Balamurugan** for their constant support, inspiration and ideas throughout my research career. Besides this I pay my homage to present and former Deans of School of Chemistry for their valor and support on various occasions. I am highly thankful to all the faculty members of the school for their timely support and as a source of inspiration and motivation towards carrying my research to new and achievable heights and acting as a torch bearer for students with the aim for pursuing research in their carrier. My acknowledgement would seem to be incomplete if I wouldn't mention and thank **Prof**. **Jai Prakash Gautam** (UOH SEST) for helping Vickers hardness test and non-teaching and technical staff especially Subrahmayam (HRMS operator), Dr. Muvva Durga Prasad (specially known as DP anna), David Mahender (NMR operator), Sunil anna, S. Thurabuddin, Durgesh Singh (NMR operator), Mahesh, B. Anand (N_2 Gas and CO_2 gas), Jagadeesh (SEST UOH student) and Jyoti.

I sincerely thank all the non-teaching staff of School of Chemistry for their help and assistance on various occasions. I specially thank to Mr. Abraham, Mr. Venkatesh anna, Mr. Gupta, Mr. Dilip, Mr. Shetty, Mr. Mallaya Shetty, Mr. Vijay Bhaskar, Mr. Naik, Late Mr. Aleem, Smt. Geeta, Smt. Rani, Smt. Radhika, Mr. David and Mr. Satyanarayana, and Smt.

Vijayalakshmi. I am sincerely thankful to all my colleagues in School of Chemistry for fruitful scientific and social discussions and making my research life productive.

I wish to thank UGC-BSR for fellowship, DST-SERB, UOH-UPE and UGC for providing required instruments, chemicals and facilities.

I feel utmost pride in acknowledging the love and support of my parents (**Koteswara Rao** and **Rukmini**), and my lovely wife (Chetana), without their affections and constant support I was supposed to be nothing. I thank them for always showering me with their prayers which had made me capable to stand against all the challenges that I have faced in my life. Thank you, Dad and Mom, for your unconditional love. The love and consistent support of not only my parents but also my siblings give me courage on each step of my life. I ought to subject my sincere feelings to my family members My grandmother Chittemma, chinnana (bujji babu), Chinnamma (Venkataramana), My babai (Fr. Suneel) My Brothers (Rambabu and Kishore babu), My sisters (Suneetha chelli and Jinni akka), My wife dady and mummy (Nagamalliraju and Laxmi), My wife sisters family (Srihari Rao and Anitha devi, Rajasekhar and Prasanna Jyothi), My school friends Dr. J. Balaraju, Yosepu, and Dass.

I would like to thank my family for an inherent debt in the form of emotional, moral and intellectual support that continue to inspire me attain my dreams.

I am lucky to have friendly colleagues Mallesh anna, Mahender anna, Bala, Allu Suryanarayana, Nagamaiah, Anil, Uma, Prabhakar reddy, Sabari, Sneha pual, Chandrahaas, Rangu prasad, Surender reddy, Satish, Majji, Junaid, Sandeep, Jagjeet, Rambabu, Dr. Sudheer babu, Dr. Suresh anna, Chandu anna, Ashok anna, Sudhir anna, Sunil Anna, Murali Anna Allu Srinu Anna, Nagarjuna Anna, Narayana Anna, Vikranth Anna, Obiah Anna, Nandu Anna, Satish Anna, Naren Anna, Siva Anna, Shoukath, Mohan, Sugata, Ramakrishna, Uday Anna, Harish Anna, Prasad Anna, Srinu Anna, Anif, Sudipta, Ramesh, Surendra, Subho, Rangu, Shruthi, Suresh, Srujana akka, Sneha, Tasnim, Divya mdhuri, Anjana, Radhika. I am thankful for my juniors Ravindar, Vinay, Hemanth, Vamshi, Vinod, Sandeep, Hema, Olivea, Sneha, Sarada, Suman, Aleem, Sumanto, Somanath, Navaneetha, Roja, Padmavathi, Soutrick, Jayakrushna, Mamina, Tausif, Senthil, Arun, Pritam, Ashok, Bhasha, Shailendra, Umashish, Naresh, Laxman, and Venkateshulureddy, Mangababu, Ramunaidu, Santhosh, Rana.

I specially thank my Friend Prema Sai MBA, Bhanu Prakash (ONGC employ), Pondicherry university MSc Batch mates, UOH MSc batch (2015-17), badminton friends for their entertaining cooperation and encouragement.

I would like to pay pay special thanks to my seniors and lab members especially Dr. Srinivas Billakanti, Dr. Sanyasi Naidu, Dr. Manigandan Ramadoss, Dr. Mohan, Dr. Hanumanth Rao, Dr. Praveen kumar Naik, Dr. Ramu Guda, Dr. Manzoor, Dr. Anjana K. O, Anju Joseph, Hemanth Kumar, Ramakrishna and Prachuritha for their support, valuable discussion and encouragement. I am also thankful to my batchmates who joined with me in the school of chemistry 2015 for Ph. D for their timely support and encouragement, especially my special thanks to Senthil Nathan, Ankit Kumar, Anif Pasha, Apurba De, Arun kumar, Harilal, Ramesh, Sadam Hussain, Sandeep, Srinivas, Shankar, Tanmay Kumar, Chandni Singh, Joycy, Mou Mandal, Sameeta Sahoo, Shipra and Tasnim Ahmed. I owe my special privilege to **Narendra anna, Venkata Surya Kumar (my MSc classmate)** and **Chinna Kandula** (UOH physics Ph.d student and Degree friend) who always made himself available to put his valuable efforts for helping me whenever I felt. I also feel positive in thanking to my juniors who showed their love, respect and affection towards me during this tenure.

Finally, I express my sincere regards to all my friends and well-wishers for their moral support, motivation and encouragement.

Venkateswara Rao Velpuri

List of Schemes

List of figures

List of Tables

List of Acronyms

NPs	Nanoparticles
NMs	Nanomaterials
OD	Zero-dimensional
1D	One-dimensional
2D	Two-dimensional
3D	Three-dimensional
CNT	Carbon nanotubes
QDs	Quantum Dots
SAM	Self-assembly monolayers
LB	Langmuir-Blodgett
PMMA	Polymethylmethaacrylate
PVP	Polyvinylpyrrolidine
OLAM	Oleyl amine
DDT	1-dodecanethiol
PANI	Polyaniline
PEDOT	Poly(3,4-ethylenedioxythiophene)
POPD	Poly(O-Phenylenediamine)
LED	Light emitting diodes
DNA	Deoxyribonucleic acid
RNA	Ribonucleic acid
UV	Ultraviolet
RGO	Reduced graphene oxide
THF	Tetrahydrofuran

PEG	Polyethylene glycol
SPE	Solid polymer electrolytes
TBAB	Tetra butylammonium bromide
PHU	Polyhydroxyurethanes
TBD	Triazabicyclodecene (1,5,7-Triazabicyclo [4.4.0] dec-5-ene
CTAB	Cetyltrimethylammonium bromide
HMDS	Hexamethyldisilazane
SF	Surfactant-free
HIV	Human Immunodeficiency Viruse
TLC	Thin Layer Chromatography
sf-CIS-np	Copper Indium Sulfide nanoparticles
DBU	8-diazabicyclo[5.4.0]undec-7-ene
CVD	Chemical vapor deposition
Cozi-nmf	CuO-ZnO nano/micro-flakes
PGE	Phenyl glycidyl ether
HV	Vickers hardness
PC	Polycarbonates
TBAI	Tetra butylammonium iodide
C_3N_4	Carbon nitride
PXRD	Powder X-ray diffraction
SEM	Scanning electron microscopy
FESEM	Field emission scanning electron microscopy
EDS	Energy dispersive spectroscopy
TEM	Transmission electron microscopy

HRTEM	High resolution transmission electron microscopy
SAED	Selected Area electron diffraction
XPS	X-ray photoelectron spectroscopy
TGA	Thermal gravimetric analysis
DSC	Differential scanning calorimeter of polycarbonates
NMR	Nuclear magnetic resonance
FTIR	Fourier-transform infrared spectroscopy
HRMS	High resolution mass spectrometer
FT-IR	Fourier transform infra-red spectroscopy
JCPDS	Joint committee on powder diffraction standards
UV-Vis	Ultraviolet visible spectroscopy

CHAPTER 1

Nano/micro particle catalysis for organic transformation: An introduction

Abstract: Nanomaterials are the most attractive materials as they are prominent in every aspect of science and technology. In the first chapter, we have explained the definition of nanoparticles, their classification, synthetic methods, morphologies, and the application in the various fields from the literature. The procedures for synthesizing metal sulfides and metal oxides, particularly copper sulfides, copper indium sulfide, and copper oxide-zinc oxide composite materials, are described. These metal chalcogenide nano/micro particles are utilized as catalysts in organic transformation. The descriptions of nano/micron sized material-based catalysis for a few organic reactions, specifically, click reactions and Glaser-hay coupling reactions, are included in the chapter. The capturing of CO_2 gas from the atmosphere, then converting it to valuable chemicals is the best method of alleviating environmental pollution. In this chapter, we have described the available chemical methods to produce cyclic- and poly- carbonates.

1.1. Definition of nanomaterials and their classification of based on dimensions

The word nanoparticle stems from the fusion of two words, “nanos” (Greek) and “particulum” (Latin). A nanoparticle has its dimensions ranging from 1 to 100 nanometres. Nanoparticles are invisible to the naked eye, and they present different chemical and physical properties compared to their macroscopic counterparts. They occur in different morphologies like spheres, flowers, rods, wells, wires, flakes, and wafers [1]. The nanoparticles are classified into different types based on size, shape, morphology, and composition.

The nanomaterials are classified based on their growth in the three-dimensional space (Figure 1.1). Zero-dimensional (0D) nanomaterials possess all the nanoscale regime dimensions (all dimensions are lesser than 100 nm). Typically, 0D nanomaterials are a congregation of few atoms or molecules. The one-dimensional nanomaterials (1D) mean that at least one of the dimensions is beyond the nanoscale regime. This type consists of

nanowires, nanorods, and nanotubes [2-3]. The two-dimensional nanomaterials (2D) have two dimensions more than 100 nm. They exhibit shapes similar to a plate-type and consist of nanolayers, nanofilms, and nanocoating [4-6]. Three-dimensional nanomaterials (3D) are materials that do not have restrictions in their measurements to nanometres in any dimension. This group of materials includes bulk powders, diffusions of nanoparticles, nanowires packages, and with multi-nanolayers [7].

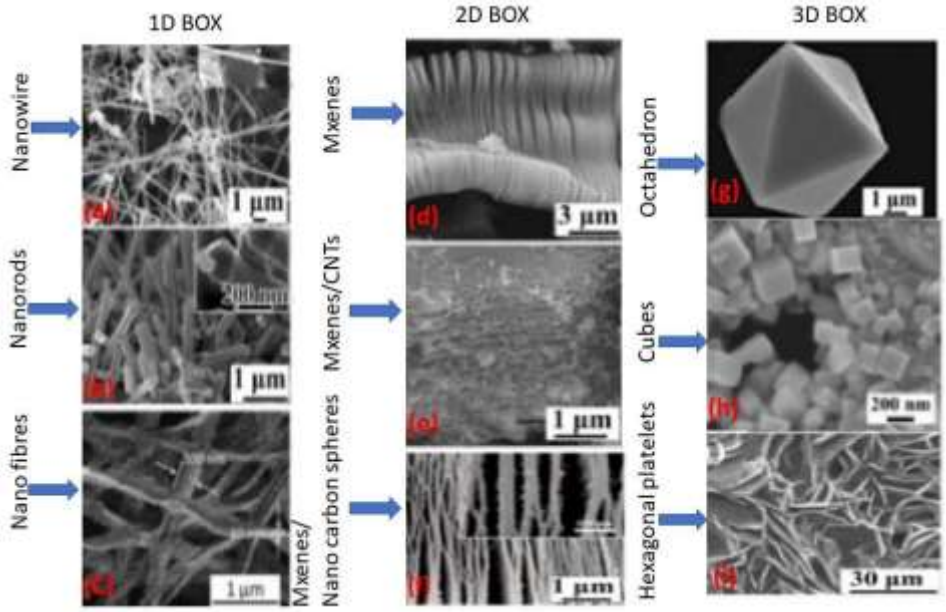

Figure 1.1: Different types of morphologies (8)

1.2. Types of nanomaterials according to their chemical composition

1.2.1. Carbon-based nanostructures

Carbon-based nanomaterials mainly consist of only carbons, and they are grouped into two main classes (Figure 1.2). (a) Fullerenes: an allotrope of carbon, made by the wrapping of single and double-bonded carbon atoms to form closed cages containing 60 carbon atoms. This C60 is the simplest form of carbon-based nanomaterial, which is also known as “buckminsterfullerene.” The C60 molecule derives its spherical structure from the arrangement of carbon atoms at the vertices of a truncated icosahedron. The other forms include C70, C76, C78, and C80, which are used in many medical and biological applications [9]. (b) Carbon nanotubes (CNTs): CNTs applications span across various

fields like electronics, polymers, energetics, biological, and medical because of their diverse but straightforward and efficient synthetic strategies [10].

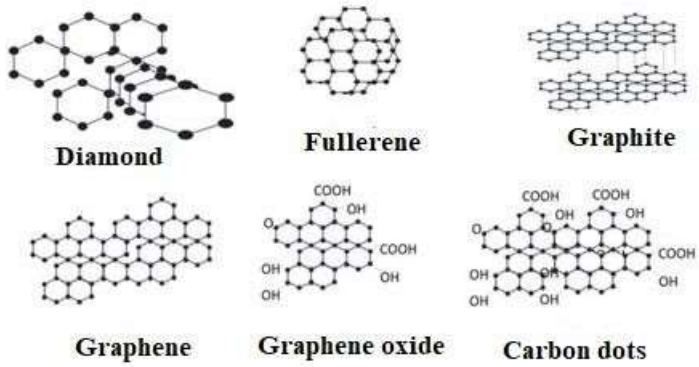

Figure 1.2: Different carbon-based nanomaterials

1.2.2. Inorganic nanoparticles and Quantum dots (QDs)

Inorganic nanoparticles are not composed of carbon. The significant materials in this category are metal and metal oxide-based nanoparticles, and these nanomaterials have a considerable therapeutic impact in clinical science. The mechanisms interaction of noble metal nanoparticles such as Au and Ag with animal and plant cells makes them utilized considerably in health and applications [11]. Various other transition metals like Fe and Zn finds numerous applications in catalysis, transport, optical sensors, solar panels, bioremediation, and detection of biomolecules [12-13]. The transition metal oxides are utilized in cosmetics and sunscreens.

Quantum dots (QDs) are semiconductor materials having nano-sized particles. The commercial properties of QDs arise from quantum size confinement that arises when metal or semiconductor particles are smaller sized than their exciton Bohr radii [14-17]. The fluorescent QDs are used in vivo biomedical imaging [18-20]. The binary metal QDs such as $CdSe_2$, CdS, and CdZn are utilized commonly for biological labeling in animal cells. Various QDs can be developed by combination, such as CdSe-ZnS core-shell nanocrystals that are utilized as bioactive fluorescent probes in imaging, sensing, immunoassays, and in various analysis uses [21].

1.2.3. Organic nanomaterials

Dendrimers, micelles, ferritin and liposomes, are usually called organic nanoparticles (Figure 1.3). Organic nanoparticles are suitable for drug distribution because of their characteristics. The most well-known shapes of organic nanoparticles are nanosphere and nanocapsule. These nanoparticles are naturally degradable and safe. Particles such as micelles and liposomes possess a hollow core called nanocapsules. Also, they are sensitive to thermal and electromagnetic radiation [22]. Many organic polymer-based nanoparticles are reported. The polymeric nature permits their use as controlled and sustained drug release components. It is realized that surface-modified biodegradable polymeric nanoparticles could deliver required drugs beyond the blood-brain barrier for diagnostic and therapeutic uses in neurological disorders [23].

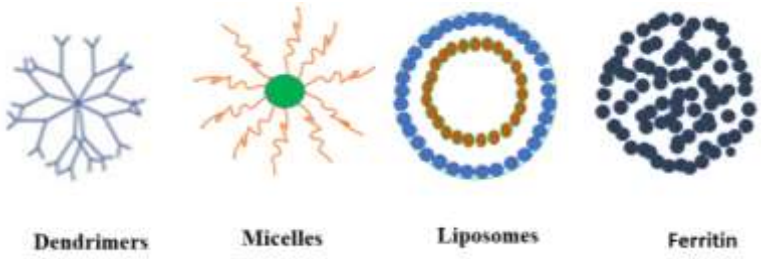

Figure 1.3: Different types of organic nanomaterials

1.2.4. Nanocomposites

The nanocomposites are the combinations of materials of one kind of nanomaterial with another kind (Figure 1.4). The nanomaterials like nanowires or nanofibers can be integrated with bigger size materials. These nanocomposites might be a mixer of metal or carbon-based nanofibers or organic-based nanowires with any metal ceramic, and polymer [24].

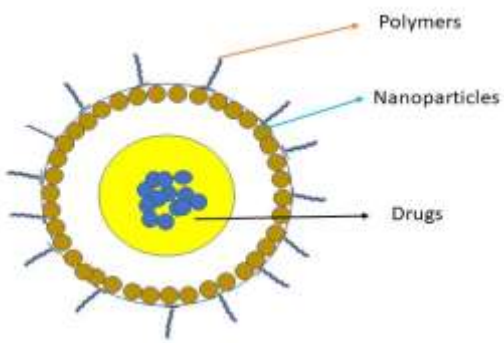

Figure 1.4: Structure of nanocomposites

1.3. Synthetic methods of nano/micro particles

Continues research in nanoscience and technology necessitates the collection of approaches to produce nanoparticles from various materials such as semiconductors, metals, metal oxides, ceramics, and polymers, and many more. Nanomaterials are synthesized by various approaches based on the types (organic, inorganic, QDs, and composites) and nature (size, shape, and orientation). Various techniques have been discovered to produce thermal decomposition, chemical vapor deposition approach, conventional Sol-Gel method, solvothermal approach, hydrothermal synthesis, templating technique, pulsed laser ablation, combustion method, gas phase method, and also microwave synthesis. Generally, these production methods can be organized as Top-down and Bottom-up strategies (Figure 1.5). Both techniques play indispensable roles in the device industry and have their very own benefits and bad marks.

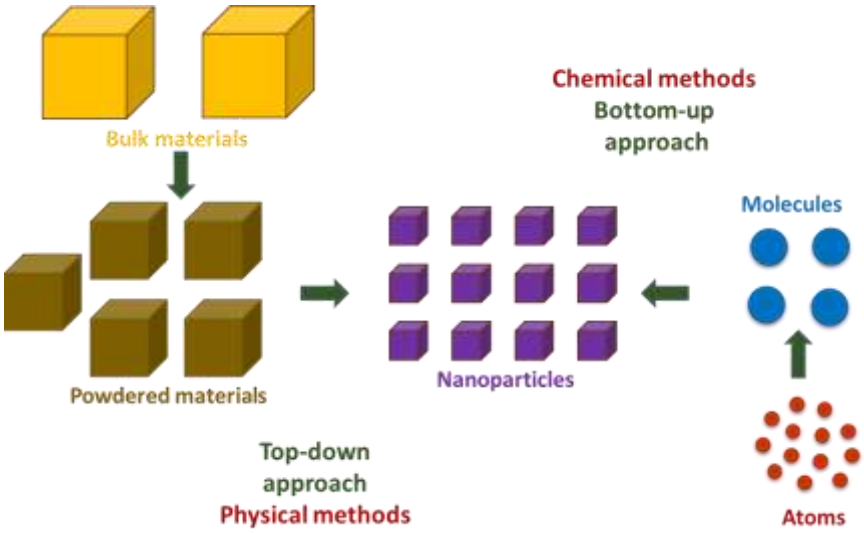

Figure 1.5: Schematic representation of 'bottom-up' and 'top-down' methods for the production of nanoscale materials.

Top to Bottom

The top-down approach involves the solid-state processing of the materials wherein the bigger particles of material are fragmented into smaller sized particles utilizing physical techniques (Figure 1.5). Some of the techniques are applying mechanical stress, high radiation energy, thermal energy or electric energy to trigger material abrasion, and evaporation followed by condensation to produce nanoparticles. Grinding or milling, physical vapor deposition are other examples of Top-down synthesis [25]. These

approaches are beneficial as they were devoid of solvent contamination, also generate uniform monodispersed nanoparticles.

The most significant issue with the top-down technique (physical methods) is the defectiveness of the surface area. For example, the nanoparticles created by the attrition have a reasonably wide dimension distribution and different particle geometry or shape. Furthermore, they might consist of a considerable number of impurities. Such imperfections would definitely sway the physical as well as chemical properties of nanostructures and nanomaterials.

Bottom to Top

The bottom-up production methods of nanomaterials consist of the miniaturization of materials components to the atomic level with different self-assembly processes leading to nanostructure development. In this approach, the nanomaterials are constructed from atom-by-atom or molecule-by-molecule to produce a vast quantity of materials. The bottom-up methods are prominent to produce nanoparticles because of several advantages such as homogenous chemical composition and much better ordering of particle shapes.

The principal methods of the bottom-up approach include

1. Solution-phase strategies (solvothermal synthesis, chemical reduction, sol-gel, sonochemical synthesis, and precipitation).
2. Chemical vapor condensation methods (sputtered plasma processing).
3. Vapor-phase strategies involving deposition (thermo chemical vapor deposition, plasma-enhanced deposition, and plasma arching).
4. Self-assembly methods [electrostatic self-assembly, self-assembly monolayers (SAM) biological templating, and Langmuir-Blodgett (LB) formation].

Many of these methods are still under advancement or are starting to be utilized for nanomaterials' commercial production [26-27].

1.4. Synthesis of metal sulphides nano/micro particles

Chalcogenides of transition metal are valuable semiconducting materials. The properties of these nanomaterials change with the size and shape of the particles and their composition. Production of metal chalcogenides is accomplished employing diverse metal sources like $CuCl_2$, $Cu(OAc)_2$, $CdCl_2$, $InCl_3$, $ZnCl_2$, and $Pb(NO_3)_2$ [28]. The sources of

sulfur are Na_2S, thiourea (CH_4N_2S), elemental sulfur (S), and CS_2 [29]. The surfactant molecules or capping agents used during the production of metal chalcogenide based nanomaterial are oleic acid, amines (alkylamine, hexadecyl amine), thiols (dodecane thiol, 1,6-hexane dithiol), and polymers (PVP, PMMA) [30]. The use of amine-based stabilizing molecules instead of thiol or alcohol is convenient since amines activate the sulfur present in its source material [31]. Within the metal chalcogenide, copper chalcogenides (Cu_2S, CuS, and $Cu_{2-x}Se$) are less harmful material, low-cost, and potentially useful nanomaterial for various applications.

The ternary chalcogenide materials such as $CuInS_2$ and $CuInSe_2$ have good photoconductivity and large absorption coefficients [32]. Further, the bandgap of these materials can be tuned by changing the particle size so that there is a possibility to match the desired region of the solar spectrum [33]. Therefore, there are many interests in synthesizing non-toxic ternary chalcogenide semiconducting nanoparticles ($CuInS_2$ and $CuInSe_2$. These ternary chalcogenide materials are useful in the photocatalytic splitting of water, light emitting diode, nonlinear optical devices, and bio-imaging [34]. Therefore, the preparation of the ternary chalcogenide (I-III-VI group) semiconductor materials has got more interest. Several procedures to synthesize $CuInS_2$ and $CuInSe_2$ have been reported. Some of them include solvothermal, hydrothermal methods, microwave irradiation technique, hot injection technique, and single-source molecular precursor [35]. Some recent significant synthetic methods are mentioned below.

Synthesis of Copper sulfides

Samira Saeednia et al. reported the production of CuS with various sizes and shapes, which was obtained through a typical solvothermal synthesis from the reaction of metal acetate with N-benzylidene ethane and thioamide in ethylene glycol (Scheme 1.1) [36].

$$Cu(CH_3COO)_2\ H_2O + \text{N-benzylidene ethane thioamide} \xrightarrow[\text{40 min, 230 }^{o}C]{\text{Ethylene glycol}} \text{CuS Nanoparticles}$$

Scheme 1.1

Charles W Dunnill et al. reported the synthesis of CuS via direct mixing of elemental of Cu and S powder in hydrazine hydride and water (scheme 1.2). [37].

$$\text{Cu powder} + \text{S powder} \xrightarrow[H_2O,\ 4h,\ 80\ ^{o}C]{\text{Hydrazine hydrate}} \text{CuS Nanoparticles}$$

Scheme 1.2

Production of hexagonal shape CuS has been developed by Mark T. Swihart et al., which was obtained using copper chloride and ammonium sulphide in toluene (scheme 1.3) [38].

$$CuCl_2\ 2H_2O + (NH_4)_2S \xrightarrow[\text{2h, 72 }^{o}\text{C, toluene}]{\text{OLAM}} \text{CuS Nanoparticles}$$

Scheme 1.3

Synthesis of copper indium sulfides

Jonathan E. Halpert et al. reported the synthesis of $CuInS_2$ quantum dots thin film for the perovskite solar cells. The materials were produced by typical single pot synthesis with a high-temperature method using copper(I) iodide, indium(III) acetate, and 1-dodecanethiol (DDT) in 1-octadecene (scheme 1.4) [39].

$$CuI + In(CH_3COO)_3 + C_{12}H_{26}SH \xrightarrow[\text{40 min, 230 }^{o}\text{C}]{\text{olylamine}} CuInS_2 \text{ Nanoparticles}$$

Scheme 1.4

Synthesis (scheme 1.5) of $CuInS_2$ with chalcopyrite structure by hot injection technique using copper(II) chloride, indium(III) chloride, and thiourea was reported by Y. Vahidshad et al. In this reaction, oleyl amine was used as the capping agent [40].

$$CuCl + InCl_3 + CH_4N_2S \xrightarrow[\text{300 }^{o}\text{C, 2 h to 4 h}]{\text{olylamine}} CuInS_2 \text{ Chalcopyrites}$$

Scheme 1.5

Mohammad Yousefi et al. reported the synthesis of $CuInS_2$ produced in very little time using a microwave oven using bis(acetylacetonate)copper (II), indium (III) chloride, and thioacetamide in ethylene glycol (scheme 1.6) [41].

$$Cu(acac)_2 + InCl_3 + C_2H_5NS \xrightarrow[\text{microwave oven (900power,6 min)}]{\text{ethylene glycol}} CuInS_2$$

Scheme 1.6

1.5. Composites of copper oxide and zinc oxide and their synthesis

The semiconducting oxides such as ZnO, TiO_2, CeO_2, ZrO_2, and SnO_2 are appealing materials due to their unique properties. These materials having different nanostructures find applications in various areas including, catalysis [42], photocatalysis [43], solar cells [44], and gas sensors [45]. The metal oxides nanostructures of CuO and ZnO, such as CuO-NiO, CuO-MgO, CuO-TiO_2, NiO-ZnO, ZnO-TiO_2, and CuO-ZnO-ZrO_2, have been studies elaborately because of their exciting surface properties [46-51]. These materials have been used in many fields, including chemical and material sciences owing to their diversified applications. Some of the research areas include catalysis, gas sensors, solar cells, and optoelectronics devices [52]. Some recent interesting synthetic procedures are discussed as follows.

Hyunjoon Song et al. reported the ZnO-CuO Core-Hollow cube nanostructures that was produced by heating zinc acetylacetonate hexahydrate and copper acetylacetonate at 225 °C (scheme 1.7) [53-54].

$$Zn(acac)_2.6H_2O + Cu(acac)_2 \xrightarrow[\text{5 min, 220 }^{o}\text{C, inert condition}]{\text{1,5-PD, PVP}} ZnO\text{-}Cu_2O \xrightarrow[\text{2 h}]{\text{200 }^{o}\text{C}} ZnO\text{-}CuO$$

Scheme 1.7

Bhaskar R. Sathe et al. synthesized hetero structural CuO−ZnO nanocomposites from zinc acetate and copper acetate by chemical synthetic approach by calcination 500 °C (scheme 1.8) [55].

$$Zn(acac)_2 + Cu(acac)_2 \xrightarrow[\text{2) NaOH, stiiring at 80 }^{o}\text{C; 3) Dried, calcinated at 500 }^{o}\text{C}]{\text{1) PVP, stirring}} CuO\text{-}ZnO$$

Scheme 1.8

P. Sathishkumar et al. reported the synthesis of CuO-ZnO by impregnation method using the zinc oxide and aqueous copper sulphate at 550 °C (scheme 1.9) [56].

$$ZnO + CuSO_4.5H_2O \xrightarrow[\text{2) heating at 80 }^{o}C\text{, 24 h}]{\text{1) stirring at 48 h}} CuO\text{-}ZnO$$

3) calcinated at 550 ^{o}C, 5 h

Scheme 1.9

1.6. Applications of nano/micro particles

Nanotechnology is the most motivating advancement used in every aspect of scientific research. Nanomaterials are used in different applications depending on the physical features such as shape, size, and surface characteristics. The nanoparticles have distinct physicochemical, architectural, and morphological features relying on their synthetic methods. These properties are crucial in many applications, such as optical, optoelectronic, atmosphere, electrochemical, and biomedical areas [57]. Some of the exciting applications of nanomaterials are itemized in the table 1.1.

Table 1.1: Applications of nanomaterials in various areas

Application	Materials	Ref
Catalyst	Pt, Pd, Fe	[58]
Photocatalyst	CdS, CuS, BiS_3	[59]
Energetic materials	Al, Bi_2O_3/Al	[60-61]
Water purification	ZnO, γ-Fe_2O_3, CeO_2	[62]
Water splitting	$BiVO_4$, V_2O_5, $SnxV_2O_5$/CdSe/Pt, IrO_2	[63-64]
Electrode materials	Sb_2O_3, TiO_2/MoS_2	[65]
Solar cells	$AgInGaSe_2$, Cu_2ZnSnS_4	[66]
Lasers	Au, CdO, Cu, Ni	[67-69]
LED	AlGaN	[70]
DNA	Pt and Ag nanoparticles	[71]
Fluorescent biological labels	Silicon RNA and pd nanoparticle	[72]
Nano medicine	CdSe Quantum dots	[73]

Catalysts are chemical species that enhance a chemical reaction rate by offering an alternate reaction path to the reaction product, generally by reducing the activation energy. Nanomaterials received considerable interest as reliable catalysts in numerous reactions since they have high surface-to-volume ratio and coordination ability. These properties

offer more active sites per area in contrast with their heterogeneous counter sites. Nanomaterials find substantial use as a catalyst in water purification, decomposition of organic pollutants, and organic transformation reactions. Some of the enticing catalysis by nanomaterials are listed in table 1.2. However, the present description is restricted to two organic reactions; click chemistry and Glaser–Hay homocoupling reaction.

Table 1.2: Applications of nanomaterials as catalyst in organic reactions

Reaction type	Nanoparticle	Ref
β-hydroxy-1,2,3-triazoles	copper(i)@phosphorated SiO_2	[74]
Homo and cross-coupling of terminal alkynes	Cu/C_3N_4 composite	[75]
Homocoupling of arylboronic acids	rgo-ni nanocomposite	[76]
Hydrogenation of Nitroarenes	Ni_3S_4 Nanocatalyst	[77]
Synthesis of cyclic carbonates	porous $ZnSnO_3$ nanocrystals	[78]
C–N bond forming reactions	CuI -zeolite	[79]
Aerobic oxidation of benzyl amine	$MoOx/CeO_2–ZrO_2$	[80]
Oxidation of vanillyl alcohol	Mn-doped CeO_2 mixed oxides	[81]
Alcohol oxidation reactions	Mn_3O_4@POP nano catalyst	[82]

1.7. Nano/micro particles as heterogeneous catalyst for organic reactions

One of the significant advantages of catalysis by nanoparticles is its heterogeneous nature, which allows the regeneration and reuse of catalysts. Few recent pieces of literature on nanomaterials-based catalyzes on the click chemistry, Glaser–Hay homocoupling reaction, and cyclic carbonate synthesis are discussed below.

1.7.1. Click chemistry

Jalal Albadi et al. synthesized 1,4-disubstituted-1H-1,2,3-triazoles from the mixture of benzyl halide or alkyl halide, alkyne, and NaN_3 in the water at reflux condition in the presence of melamine-supported CuO nanocatalyst (scheme 1.10) [83]. Later, they have used $CuO–CeO_2$ nanocomposite as the catalyst to react benzyl bromide and phenylacetylene in the presence of amberlite-supported azide in ethanol as solvent (at the refluxed condition for 65 min) to form corresponding products (scheme 1.11) [84].

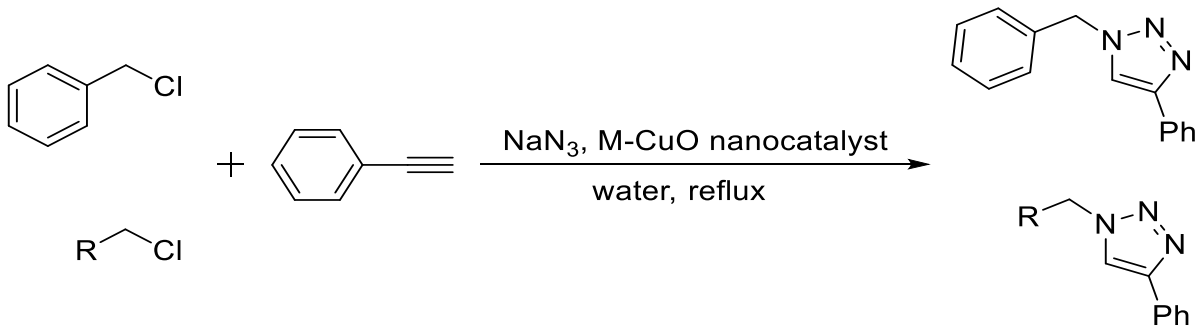

Scheme 1.10

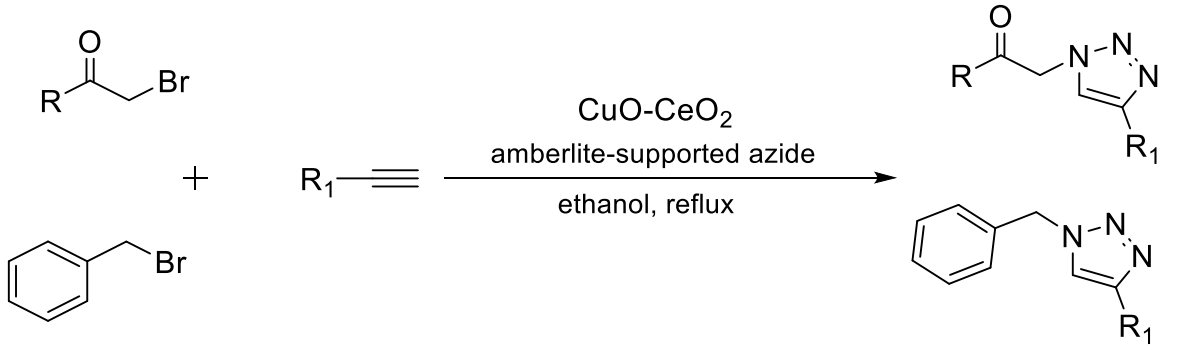

Scheme 1.11

Jun Nie et al. synthesized 1,4-disubstituted-1H-1,2,3-triazoles using CuOx@Nb_2O_5 as the catalyst for benzyl azide reaction with phenylacetylene in THF. This reaction was performed in a quartz test tube irradiated with UV light for 6 h at room temperature under air (scheme 1.12) [85].

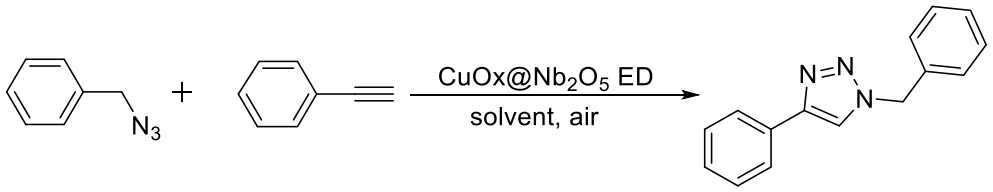

Scheme 1.12

Y. V. D. Nageswar et al. synthesized of 1,4-disubstituted 1,2,3-triazoles by using magnetically separable and reusable $CuFeO_4$ nanoparticles in a one pot reaction in tap water at 70 °C (scheme 1.13) [86].

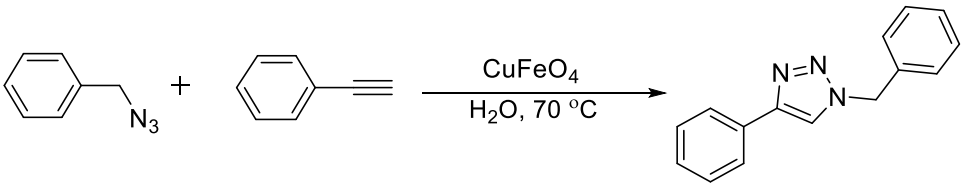

Scheme 1.13

1.7.2. Glaser hay coupling

Yalan Xinget et al. reported the development of green and sustainable synthetic methods for the preparation of 1,4-diphenyl buta-1,3-diyne from phenylacetylene using DBU as the base and copper(II)triflate as catalyst in acetone (Reaction condition: rt, 2–5 h, open air atmosphere) (scheme 1.14) [87].

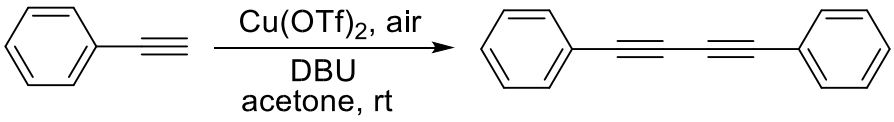

Scheme 1.14

Xiaoquan Yao et al. synthesized Cu/C_3N_4 composite and used it as the catalyst for homo cross coupling of terminal alkynes. For example, diphenylbuta-1,3-diyne synthesis was carried out using phenylacetylene and KOH in the presence of Cu/C_3N_4 as the catalyst at room temperature in isopropyl alcohol for 12 h under an O_2 atmosphere (scheme 1.15) [88].

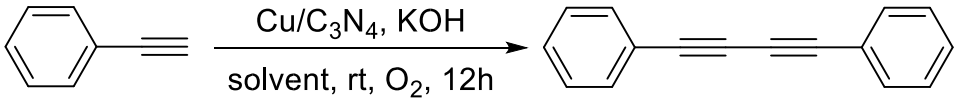

Scheme 1.15

Bianxiang Zhang et al. has established a mild method to synthesize diphenylbuta-1,3-diyne through a room temperature reaction, which used phenyl acetylene as substrate, benzene as an oxidizing agent, Et_3N as the base, and acetonitrile as a solvent in the presence of CuCl (scheme 1.16) [89].

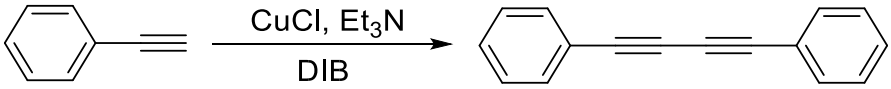

Scheme 1.16

Elham Safaei et al. established a method for the homocoupling of phenylacetylene with a mixture of phenylacetylene while suing L_2^{NIS} Cu (II) as a catalyst in an oxygen atmosphere at room temperature in THF (scheme 1.17) [90].

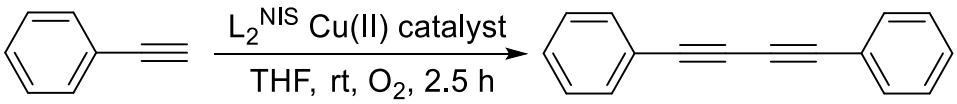

Scheme 1.17

1.8. Capturing and conversion of CO_2 into cyclic and polycarbonates

Owing to the industrial revolution, the atmospheric carbon dioxide (CO_2) level is increasing rapidly, which the primary cause of global is warming. On the other hand, the attractive CO_2 capture reactions represent an alternative and safer way of mitigating the excessive release of it from various industrial sources [91]. The process of capturing waste carbon dioxide (CO_2) released from the heavy industry, and automobile exhaust and the use of renewable carbon resource CO_2 to produce various organic molecules and polymers are the best way to alleviate its excessive release to the environment [92-93] and also advantages as it is an abundant, economic, and non-toxic substance [94]. Therefore, the research on the utility of

CO_2 is attractive for many scientists as it is an inexpensive, non-toxic, non–flammable, abundant carbon feedstock to produce valuable chemicals [95-100].

Cyclic and polycarbonate synthesis from CO_2 and epoxides through a catalytic process is a 100% atom economic reaction established long ago [101]. They are industrially important materials because of their physical properties, and also, they are biodegraded under composting conditions. Cyclic carbonates are fascinating compounds finding a collection of applications such as electrolyte in lithium-ion batteries, [102] polar aprotic solvents [103] intermediates for fine chemicals and building blocks in the manufacture of pharmaceuticals [104]. Polycarbonates are used as solid polymer electrolytes (SPE) [105]. The perpetual challenge is finding a simple route to produce biodegradable and recyclable polycarbonates using CO_2.

1.8.1. Synthesis of cyclic carbonates from CO_2

Highly reactive molecules are used to activate CO_2 using various catalysts. For example, Irina P. Beletskaya et al. used a reusable alumina-supported zinc dichloride as the catalyst for the synthesis of cyclic carbonates from epoxides and CO_2 (4 atm) in a low-pressure reactor but without using any solvent at 60 °C (scheme 1.18) [106].

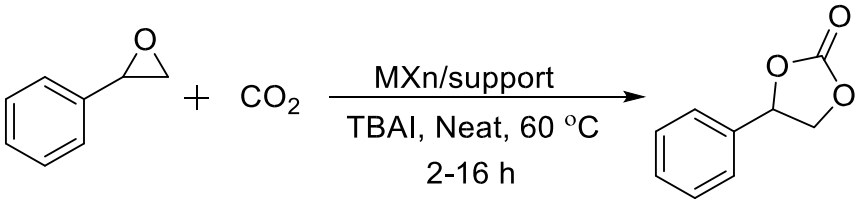

Scheme 1.18

Haibo Chang et al. synthesized 5-membered cyclic carbonates from the epoxide and CO_2 (0.4 MPa) in a mild solvent-free condition at 70 °C in the presence of Succinimide-KI as the efficient binary catalytic system (scheme 1.19) [107].

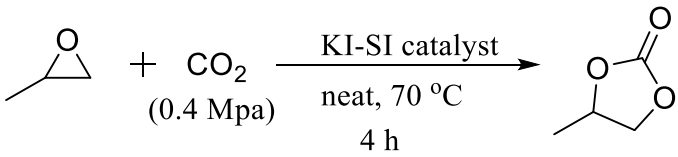

Scheme 1.19

Jie Wu et al. prepared cyclic carbonates by the cycloaddition of CO_2 (1 atm) with epoxides using Al (III)@cage as catalyst at 25 °C for 24 h (scheme 1.20) [108].

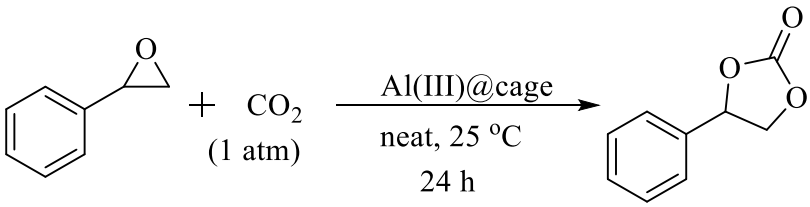

Scheme 1.20

The PIMs was used as the catalyst by Guichun Yang et al. for the reaction of CO_2 with epoxides at 130 °C using 1 MPa pressure of CO_2 for 4 h (scheme 1.21) [109].

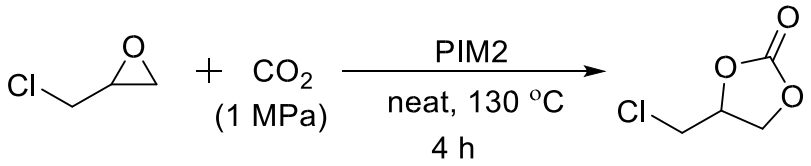

Scheme 1.21

1.8.2. Synthesis of polycarbonates from CO_2

Rukhsana I. Kureshy et al. synthesized cyclic carbonates with a polymer, which is rich with nitrogen content, as an organo-catalyst (CUP) for the reaction of epoxides with CO_2 (6MPa) (at 120 °C, 12 h stirring at 1000 rpm). This material was used for the synthesis of polyurethane via the cycloaddition reactions under similar condition using resorcinol diglycidyl carbonate and diamines (ethane-1,2-diamine and butane1,4-diamine) in DMSO (8 h at 85 °C under air). This reaction yielded the corresponding polyhydroxy urethane (scheme 1.22) [110].

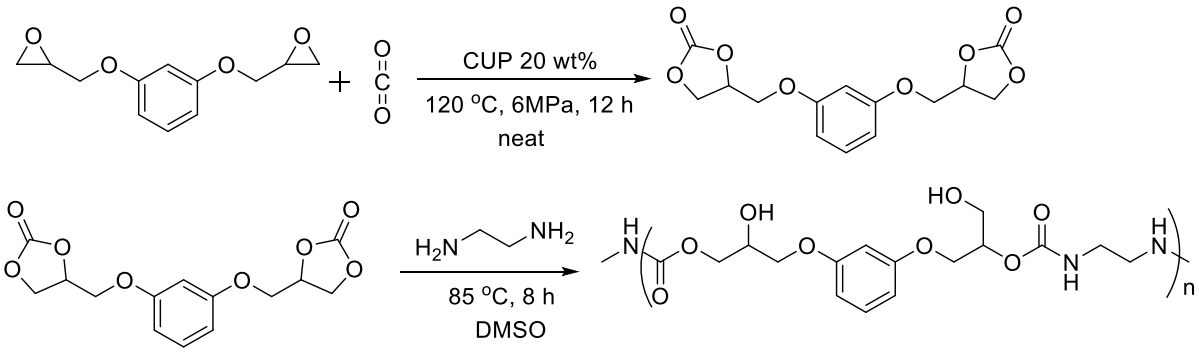

Scheme 1.22

R. Mulhaupt et al. synthesized the cyclic carbonates from CO_2 (30 bar) using tetra butyl ammonium bromide (TBAB) as the catalyst (120−140 °C, 16−26 h). Those cyclic carbonates were converted into polyhydroxyurethanes (PHU) through melt-phase polyaddition in a twin-screw compounder (18−130 min at 100−130 °C under nitrogen atmosphere) (scheme 1.23) [111].

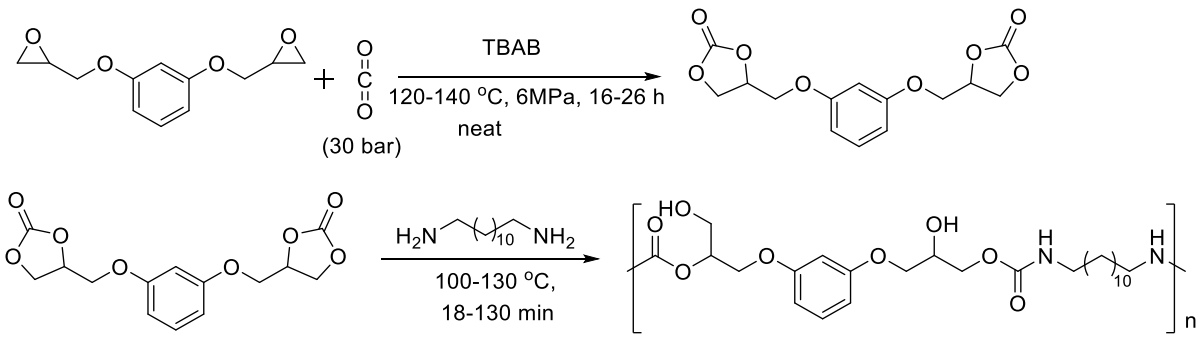

Scheme 1.23

Robert H. Lambeth et al. synthesized poly(hydroxyurethanes) in the presence of organocatalyst and TBD (triazabicyclodecene or 1,5,7-triazabicyclo [4.4.0] dec-5-ene) at room temperature step-growth polymerization between difunctional cyclic carbonates and amines to produce the polymers (scheme 1.24) [112].

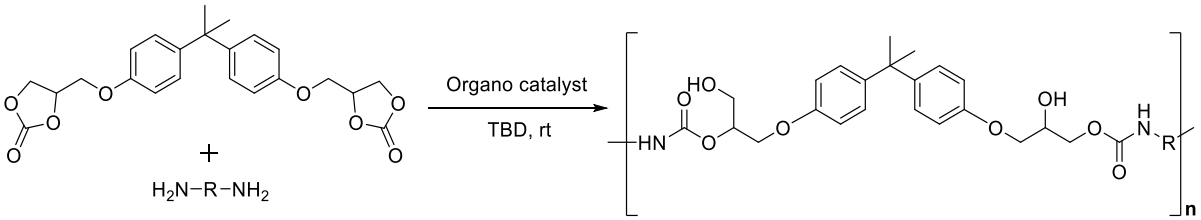

Scheme 1.24

Despite the availability of many efficient catalytic systems [113-118] there are inadequacies in either tedious preparatory procedure of catalyst, separation problem associated with homogeneous catalysis, conversion percentage, or the need to use pure CO_2. Therefore, it is ambitious to capture CO_2 instantly and convert it to polycarbonates without tedious procedures.

1.9. Deficiencies in the chemical synthesis of nano/micro particles and circumventing the problem

Copper sulfides attract researcher because of the variations in their valence states, and stoichiometric compositions. Further, they exhibit differences in nanocrystal morphologies and crystal structures. As discussed in section 1.4, there are many ways to produce binary and ternary metal chalcogenides. However, while synthesizing nanomaterials by the chemical methods (bottom-up approach), we use long-chain organic molecules to surround the particles to stabilize them. These surfactant molecules are known by phrases as stabilizing agents, protecting agents, or passivating agents.

The surfactant molecules have head group(s) possessing the lone pair of electron (N, P, O, and S). Oleyl amine, octylamine, CTAB, pyridine are surfactants having nitrogen-based head group [120]. Alkyl phosphonic acids, TPP, TOP, TOPO, and phosphagens are the capping agents possessing phosphorus-based head group [119]. Long-chain alcohols like octanol, oleoyl alcohol are the surfactant molecules having oxygen-based head groups [120]. Long-chain thiols, cysteine, thiophenes are stabilizing molecules containing sulfur-based head group [121]. These surfactant molecules perform a vital role during the synthesis by way of stabilizing the particle's size. Also, they prevent the nanomaterials from uncontrollable oxidation, controls the particle growth rate. However, these organic molecules create an inorganic-organic interface between them with metal chalcogenides. These intimate interfaces impact the material's properties and their applications.

The organic surfactant molecules affect the nanoparticle's properties of in many ways. Surfactant molecules isolate the adjacent particles and reduce the communication between them. For example, when nanoparticles are used for the catalytic application, the chemical reaction occurs on their surfaces. For the best catalytic activity, adsorption of the substrate on the surface of nanoparticles as well as electron transfer between them should occur. However, the insulating nature of organic molecules hinders the movement of charge carriers, i.e., it affects the electron transfer between inorganic particles and substrate. Thus, the presence of capping restricts or reduces catalytic activity. A straightforward solution to the aforementioned issues is avoiding the use of surfactant molecules while synthesizing nanoparticles.

1.10. Scope and methodology of the thesis

As discussed in sections 1.8 and 1.9, a variety of nanoparticles are tested as the catalyst for the synthesis of organic molecules and polymers. Despite the availability of many efficient catalytic systems for organic C-C and C-N bond formation reactions and carbon dioxide activation, there are inadequacies in either tedious preparatory procedure of catalyst, separation problem associated with homogeneous catalysis, conversion percentage, or the need to use pure CO_2. Despite the variety of reports, the advantage of the surfactant-free surface of nanoparticles is underutilized. Thus, the present work aims to prepare the surfactant-free metals sulfides and mixed metal oxides and use them as the catalyst for organic reactions and carbon dioxide activation. It is also ambitious to capture CO_2 instantly and convert it to polycarbonates without tedious procedures.

The scope of the thesis is described below.

(i) Understanding the effect of organic surfactant molecules while using nano/micro particles as heterogeneous catalysts in organic reactions and carbon dioxide activation.

(ii) Use of surfactant-free metal chalcogenides as a heterogeneous catalyst for click chemistry and Glaser-hay coupling.

(iii) Use of surfactant-free mixed metal oxides as heterogeneous catalyst for the synthesis of 5-membered cyclic carbonates.

(iv) Capturing and conversion of CO_2 into polycarbonates without any cumbersome procedures.

Methodology

Our lab has developed two novel methods of synthesis of metal chalcogenides without using any organic surfactant molecules. In the first method, the materials were prepared at room temperature in a reaction driven by the supersaturated condition, while in the second method; the formation of metal chalcogenides was assisted by hexamethyldisilazane (HMDS – assisted method).

For this present work (Figure 1.7), we have produced the surfactant-free binary and ternary copper sulfides at room temperature under the "supersaturated condition". The binary chalcogenide, surfactant-free CuS nano/micro flowers (**sf-CuS**) was utilized as the catalyst for the click reaction, while surfactant-free $CuInS_2$ nano/micro particles **(sf-CIS-np)** was used as the catalyst for the reaction of Glaser-hay coupling.

The mixed metal oxide surfactant-free CuO-ZnO nano/micro-flakes **(Cozinmf)** composite material was prepared by the simple grinding method, and it was employed for the 5- membered cyclic carbonate synthesis.

We have explored the instantaneous capture of CO_2 through alternative copolymerization with resorcinol diglycidylether and three different amines in one-pot cascade reactions involving polycondensation. These reactions yielded Abrasive materials that are sharp as glass.

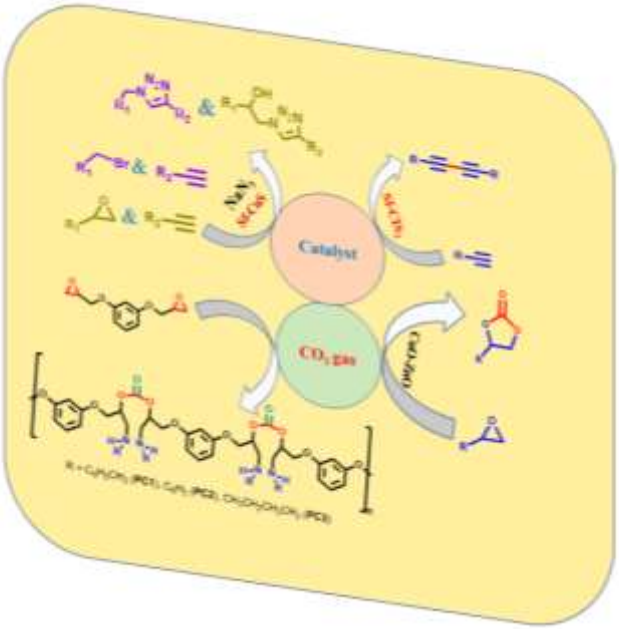

Figure 1.7: Schematic representation of the scope of the present work.

1.11. References:

[1] C. Burda, X. Chen, R. Narayanan, and M. A. El-Sayed, *Chem. Rev.* **2005**, *105*, 1025.

[2] S. J. Hurst, E. K. Payne, L. Qin, and C. A. Mirkin, *Angew. Chem. Int. Ed.* **2006**, *45*, 2672.

[3] A. Gedanken, *Ultrasonics Sonochemistry*. **2004**, *11*, 47.

[4] R. Gui, H. Jin, Y. Sun, X. Jiang and Z. Sun *J. Mater. Chem. A.* **2019**, *7*, 25712.

[5] H. Zhang *Acs nano*. **2015,** *9*, 9451–9469.

[6] C. M. Hangarter, M. Bangar, A. Mulchandani and N. V. Myung, *J. Mater. Chem.* **2010**, *20*, 3131.

[7] I. Ijaz, E. Gilani, A. Nazir and A. Bukhari, *Green chemistry letters and reviews.* **2020**, *13*, 223.

[8] B. X. Dong, F. Qiu, Q. Li, S. L. Shu, H.Y. Yang and Q. C. Jiang, *Nanomaterials.* **2019**, *9*, 1152.

[9] S. H. Friedman, D. L. Decamp, R. P. Sijbesma, G. Srdanov, F. Wudl, and G. L. Kenyon, *J. Am. Chem. Soc.* **1993**, *115*, 6506.

[10] N. C. Mueller and B. Nowack, *Environ. Sci. Technol.* **2008**, *42*, 4447.

[11] S. B. Yaqoob, R. Adnan, R. Muhammad, R. Khan, and Mohammad Rashid, *Frontiers in Chemistry.* **2020**, *8*, 341.

[12] M. auffan, J. rose, T. Orsiere, M. Demeo, A. Thill, O. Zeyons, O.Proux, A. masion, P. Chaurand, O. spalla, A. bott, M. R. Wiesner, and J. Y. Bottero, Nanotoxicology. 2009, 2, 161.

[13] K. Zhou, R. Wang, B. Xu and Y. Li, *Nanotechnology.* **2006,** 17, 3939.

[14] A. P. Alivisatos, *Science.* **1996,** *271*, 933.

[15] L. E. Brus, *Appl. Phys. A.* **1991**, *53*, 465.

[16] W. L. Wilson, P. F. Szajowski, L. E. Brus, *Science*. **1993**, *262*, 1242.

[17] (a) A. Henglein, *Chem. Rev*., **1989,** *89*, 1861. (b) H. Weller, *Angew. Chem. Int. Ed. Engl.* **1993**, *32*, 41.

[18] D. R. Larson, W. R. Zipfel, R. M. Williams, S. W. Clark, M. P. Bruchez, F. W. Wise, W. W. Webb, *Science.* **2003**, *300*, 1434.

[19] M. Bruchez, M. Moronne, P. Gin, S. Weiss and A. P. Alivisatos, *Science*. **2013-2016**, *281*, 5385.

[20] W. C. W. Chan and S. Nie, *Science.* **2016-2018**, *281*, 5385.

[21] A. L. Serrano, R. M. Olivas, J. S. Landaluze and C. Camara, *Anal. Methods.* **2014**, *6*, 38.

[22] D. K. Tiwari, J. Behari and P. Sen, Application of Nanoparticles in Waste Water Treatment. 2008, 3, 417.

[23] C. Roney, P. Kulkarni, V. Arora, P. Antich, F. Bonte, A. Wu, N.N. Mallikarjuana, S. Manohar, H. F Liang, A. R. Kulkarni, H-W Sung, M. Sairam, T. M. Aminabhavi, *Journal of Controlled Release.* **2005**,108, 193 – 214

[24] W. Leea, D. Kima, S. Leea, J. Parka, S. Oha, G. Kima, J. Limb and J. Kima, Nano today. **2018,** *23*, 97.

[25] I. ravani, S. Green, Green Chem. **2011**, *13*, 2638.

[26] Y. Chen, Z. Fan, Z. Zhang, W. Niu, C. Li, N. Yang, B. Chen, and H. Zhang, *Chem. Rev.* **2018**, *118*, 6409.

[27] L. Zhu, M. Gharib, C. Becker, Y. Zeng, A. R. Ziefu, L. Chen, A. M. Alkilany, C. Rehbock, S. Barcikowski, W. J. Parak, and I. Chakraborty J. Chem. Educ. **2020**, *97*, 239.

[28] (a) J. Joo, H. B. Na, T. Yu, J. H Yu, Y. W. Kim, F. Wu, J. Z. Zhang and T. Hyeon,*J.Am. Chem. Soc.* **2003**, *125*, 1110. (b) Du, Y.; Yin, Z.; Zhu, J.; Huang, X.X. J. Wu, Z. Zeng, Q. Yan and H. Zhang, *Nat. Commun*. **2012**, *3*, 1177. (c) X.Peng, *Chem. Eur. J.* **2002**, *8*, 335. (d) Z. A. Peng and X. G. Peng, *J. Am. Chem.Soc.* **2001,** *123*,183. (e) H. Zhang, B. R. Hyun, F. W. Wise and R. D. Robinson, *NanoLett.* **2012,** *12*, 5856.

[29] (a) A. Ghezelbash and B. A. Korgel, *Langmuir*. **2005**, *21*, 9451. (b) M. E. Norako, M. A Franzman, and R. L Brutchey, *Chem. Mater.* **2009**, *21*, 4299. (c) D. Pan, Q. Wang, S. Jiang, X. Ji, L. An, *Adv. Mater.* **2005**, *17*, 176.

[30] (a) K. Mori and Y Nakamura, *J. Org. Chem.*, **1971,** *6*, 3041. (b) S. Mourdikoudis and L. M Liz-Marzán, *Chem. Mater.* **2013**, *25*, 1465. (c) Y. Li, Z. Wang and Y. Ding, *Inorg. Chem.*, **1999,** *38*, 4737.

[31] M. Azad Malik, N. Revaprasadu and P. O.Brien, *Chem. Mater*. **2001**, *13*, 913.

[32] (a) Y.-H. Yang and Y.-T. Chen, *J. Phys. Chem. B.* **2006,** *110*, 17370. (b) H. Zhong, Y. Li, M. Ye, Z. Zhu, Y. Zhou, C. Yang and Y. Li, *Nanotechnology*. **2007**,*18*, 025602. (c) P. M. Allen and M. G. Bawendi, *J. Am. Chem. Soc*. **2008**, *130*, 9240. (d) H. Zhong, S. S. Lo, T. Mirkovic, Y. Li, Y. Ding, Y. Li and G. D. Scholes, *ACS Nano.* **2010**, *9*, 5253. (e) Q. Guo, S. J. Kim, M. Kar, W. N. Shafarman, R. W. Birkmire, E. A. Stach, R. Agrawal and H. W. Hillhouse, *NanoLett*. **2008,** *8*, 2982. (f) M. G. Panthani, V. Akhavan, B. Goodfellow, J. P. Schmidtke, L. Dunn, A. Dodabalapur, P. F. Barbara and B. A. Korgel, *J. Am. Chem. Soc*. **2008**, *130*, 16770. (g) J. Tang, S. Hinds, S. O. Kelley and E. H. Sargent, *Chem. Mater*. **2008,** *20*, 6906.

[33] (a) D. Pan, X. Wang, Z. H. Zhou, W. Chen, C. Xu and Y. Lu, *Chem. Mater*. **2009**, *21*, 2489. (b) Y.-H. A. Wang, X. Zhang, N. Bao, B. Lin, and A. Gupta, *J. Am. Chem.Soc*. **2011,** *133*, 11072. (c) M.-Y Chiang, S.-H. Chang, C.-Y. Chen, F.-W. Yuan and H.-Yu. Tuan, *J. Phys. Chem. C*. **2011**, *115*, 1592.

[34] (a) L. Zheng, Y. Xu, Y. Song, C. Wu, M. Zhang and Y. Xie, *Inorg. Chem.* **2009**, *48*, 4003. (b) W. S. Song and H.Yang, *Chem. Mater.* **2012**, *24*, 1961. (c) H. Zhong, Z. Wang, E. Bovero, Z. Lu, F. C. J. M. van Veggel, and G. D. Scholes, *J. Phys. Chem. C.* **2011**, *115*, 12396. (d) J. Y. Lee, D. H. Nam, M. H. Oh, Y. Kim, H. S. Choi, D. Y. Jeon, C. B. Park and Y. S. Nam, *Nanotechnology*. **2014**, 25, 175702. (e) L. Li, T. J. Daou, I. Texier, T. T. K. Chi, N. Q. Liem and P. Reiss, *Chem. Mater.* **2009**, *21*, 2422. (f) K. Nose, T. Omata and S. Otsuka-Yao-Matsuo,

J. Phys. Chem. C. **2009**, *113*, 3455. (g) H. Zhong, Y. Zhou, M. Ye, Y. He, J. Ye, C. He, C. Yang and Y. Li, *Chem.Mater.* **2008**, *20*, 6434.

[35] (a) J. Xiao, Y. Xie, R. Tang and Y. Qian, *J. Solid State Chem*. **2001**, *161*, 179. (b) Y. Jiang, Y. Wu, X. Mo, W. Yu, Y. Xie and Y. Qian, *Inorg. Chem*, **2000**, *39***,** 2964. (c) Y. Jiang, Y. Wu, S. Yuan, B. Xie, S. Zhang and Y. Qian, *J. Mater. Res*. **2001**, *16*, 2805. (d) A. Pein, M. Baghbanzadeh, T. Rath, W. Haas, E. Maier, H. Amenitsch, F. Hofer, C. O. Kappe and G. Trimmel, *Inorg. Chem*. **2011**, *50*, 193. (e) C.-C. Wu, C.-Y. Shiau, D. W. Ayele, W.-N. Su, M.-Y. Cheng, C.Y. Chiu and B. –J. Hwang, *Chem. Mater*. **2010**, *22*, 4185. (f) S. L. Castro, S. G. Bailey, R. P. Raffaelle, K. K. Banger and A. F. Hepp, *Chem. Mater*. **2003,** *15*, 3142. (g) K. K. Banger, M. H. C. Jin, J. D. Harris, P. E. Fanwick, A. F. Hepp, *Inorg. Chem*. **2003**, *42*, 7713. (h) S. L. Castro, S. G. Bailey, R. P. Raffaelle, K. K. Banger and A. F. Hepp, *J. Phys. Chem. B*, **2004,** *108*, 12429. (i) K. K. Banger, M. H.-C. Jin, J. D. Harris, P. E. Fanwick and A. F. Hepp, *Inorg. Chem*. **2003**, *42*, 7713. (j) B. Koo, R. N. Patel and B. A. Korge, *J. Am. Chem. Soc*. **2009,** *131*, 3134.

[36] S. Shahi, S. Saeednia, P. Iranmanesh, M. H. Ardakani, *Luminescence.* **2020**;1.

[37] R. Mulla, D. R. Jones, and C. W Dunnill *ACS Sustainable Chemistry & Engineering.* **2020,** *8*, 14234-14242.

[38] Y. Liu, M. Liu, and M. T. Swihart *Chem. Mater.* **2017**, *29*, 4783.

[39] Y. Ma, P. Vashishtha, S. B. Shivarudraiah, K. Chen, Y. Liu, J. M. Hodgkiss, and J. E. Halpert, *Sol. RRL*. **2017**, *1*, 1700078.

[40] Y. Vahidshad, R. Ghasemzadeh, A. Irajizad, S. M. Mirkazem *JNS.* **2013**, *3*, 145.

[41] M. Yousefi, M. Sabet, M. S. Niasari, S. Mostafa, H. Mashkani, *J. Clust. Sci.*, **2012,** *23*, 491.

[42] J. B. Joo, M. Dahl, N. Li, F.Zaera and Y. Yin, *Energy Environ. Sci.* **2013**, *6*, 2082.

[43] A. S. Alshammari, L. Chi, X. Chen, A. Bagabas, D. Kramer, A. Alromaeha and Z. Jiang, *RSC Adv.* **2015**, *5*, 27690.

[44] J. Honga, S. Baea, Y. S. Wonb, S. Huha, *J. Colloid and Interface Science*. **2015,** *448*, 467.

[45] D. Hu, B. Han, S. Deng, Z. Feng, Y. Wang, J. Popovic, M. Nuskol, Y. Wangand I. Djerdj, *J. Phys. Chem. C*. **2014**, *118*, 9832.

[46] R. S. Nandhini, G. Mubeen, U. K. Kumar, R. N. Nithya *International Journal of Engineering and Technical Research*. **2019**, *8*, 09.

[47] P. P.Dorneanu, A.Airinei, N. Olaru, M.Homocianu, V. Nica and F. Doroftei. *Materials Chemistry and Physics.* **2014**, *148*, 1029e1035.

[48] S. K. Alla, A. D. Verma, V. Kumar, R. K. Mandal, I. Sinha and N. K. Prasad, M. Janczarek, and E. Kowalska. *Catalysts.* **2017**, *7*, 317.

[49] Md. A. Habib, Md. T. Shahadat, N. M. Bahadur, I. M. Ismail and A. J. Mahmood, *International Nano Letters.* **2013**, *3*,5.

[50] X. Guoa, D. Maoa, S. Wanga, G. Wua and G. Lua, *Catalysis Communications.* **2009**, *10*, 1661

[51] S. Das and V. C. Srivastava, *Nanotechnol Rev*. **2018**, *7*, 267.

[52] K. L. Bae, J. Kim, C. K. Lim, K. M. Nam and H. Song *Nature Communications*. **2017**, 8, 1-8.

[53] J. E. Lee, C. K. Lim, H. J. Park, H. Song, S.Y. Choi, and D. S. Lee *ACS Appl. Mater. Interfaces.* **2020,** *12*, 35688.

[54] S. M. Mali, S. S. Narwade, Y. H. Navale, S. B. Tayade, R. V. Digraskar, V. B. Patil, A. S. Kumbhar, and B. R. Sathe, *ACS Omega.* **2019**, *4*, 20129.

[55] P. Sathishkumar, R. Sweena, J. J. Wub, S. Anandan *Journal of Chemical Engineering*. **2011,** *171*, 136.

[56] C. Dhand, N. Dwivedi, X. J. Loh, A. N. J. Ying, N. K. Verma, R. W. Beuerman, R.

L. narayanan and S. Ramakrishna, *RSC Adv.* **2015,** *5*, 105003.

[57] R. Abazari, F. Heshmatpour, and S. Balalaie, *ACS Catal.* **2013**, *3*, 139.

[58] B. G. Kumar, B. Srinivas and K. Muralidharan, *Materials research bulletin.* **2017**, *89*, 108.

[59] K. Jayaraman, K. V. Anand, S. R. Chakravarthy, and R. Sarath, *American Institute of Aeronautics and Astronautics*. **2007**, *45*, 1-9.

[60] V. Kumar Patel, R. Kant, A. choudhary, M. Painuly, S. Bhattacharya, *Defence Technology*. **2019**, *15*, 98e105.

[61] C. Santhosh, V. Velmurugan, G. Jacob, S. K. Jeong, A. N. Grace and A. Bhatnagar *Chemical Engineering Journal.* **2016**, *306*, 1116.

[62] S. A. Razek, M. R Popeil, L. Wangoh, J. Rana, N. Suwandaratne, J. L. Andrews, D. F Watson, S. Banerjee and L. F. J Piper, *Electron. Struct.* **2020**, *2*, 023001.

[63] R. Zhang, P. E. Pearce, Y. Duan, N. Dubouis, T. Marchandier, and A. Grimaud, *Chem. Mater.* **2019,** *31*, 8248.

[64] A. Mishra, A. Mehta, S. Basu, S. J. Malode, N. P. Shetti, S. S. Shukla, M. N. Nadagouda, T. M. Aminabhavi, *Materials Science for Energy Technologies*. **2018,** 1, 182.

[65] X. Zhang, Q. Sun, M. Zheng, Z. Duan and Y. Wang, *Nanomaterials*. **2020**, *10*, 547.

[66] A. M. Mostafa, S. A. Yousef, W. H. Eisa, M. A. Ewaida, E. A. Al-Ashkar, *Applied Physics A.* **2017**, *123*, 774.

[67] E. Paulis, U. Pacher, M. J. J. Weimerskirch, T. O. Nagy, W. Kautek, *Applied Physics A.* **2017**, *123*, 790.

[68] L. Gavrila, Florescu, F. Dumitrache, M. Balas, C. T. Fleaca, M. Scarisoreanu, I. P. Morjan, E. Dutu, A. Ilie, A. M. Banici, C. Locovei and G. Prodan, *Applied Physics A.* **2017**, 123, 802.

[69] X. Yi, H. Sun, Z. Li, J. Sun, T. Liu, X. Wang, X. Zhang, Z. Guo, *Optics and Laser Technology*. **2018,** *106*, 469.

[70] A. Samanta, and I. L. Medintz, *Nanoscale*. **2016**, *8*, 9037.

[71] M. Bruchez Jr, M. Moronne, P. Gin, S. Weiss and A. P. Alivisatos, *Science.* **1998,** 281**,** 2013.

[72] M. Kiani, N. Rabiee, M. Bagherzadeh, A. M. Ghadiri, Y. Fatahi, R. Dinarvand, and J. Thomas, *Nanotechnology, Biology, and Medicine*. **2020**, *30*, 102297.

[73] H. Naeimi and V. Nejadshafiee *New J. Chem.* **2014**, *38*, 5429.

[74] H. Xu, K. Wu, J. Tian, L. Zhu and X. Yao *Green Chem.* **2018**, *20*, 793.

[75] K. Murugan, D. Nainamalai, P. Kanagaraj, S. G. Nagappan, S. P. swamy *Appl Organomet Chem.* **2020**, *34*, e5778.

[76] B. Srinivas, B. Ganesh Kumar, and K. Muralidharan**,** *ChemistrySelect*. 2017, *2*, 4753.

[77] S.Roy, B. Banerjee, A. Bhaumik and Sk. M. Islam, *RSC Adv.* **2016**, *6*, 31153.

[78] A. R. swamy, A. N. Prasad, and B. M. Reddy, *Current Organic Chemistry.* **2016,** *20*, 1.

[79] A. R. swamy, P. Sudarsanam, B. G. Rao, B. M. Reddy, *Res Chem Intermed.* **2016,** *42*, 4937.

[80] S. Ramana, B. G. Rao, P. V. swamy, A. R. swamy, B. M. Reddy, *Journal of Molecular Catalysis A: Chemical.* **2016**, *415*, 113.

[81] K. Dhanalaxmi, S. Ramana, S. K. Kundu, B. M. Reddy, A. Bhaumik and J. Mondal, *RSC Adv.* **2016**, *6*, 36728.

[82] M. Rajabi, J. Albadi, A. Momeni, *Research on Chemical Intermediates.* **2020**, 46,3879.

[83] J. Albadia, J. A. Shiranb and A. Mansournezhad., *j. chem. sci.* 2014, 126, 147.

[84] B. Wang, J. Durantini, J. Nie, A. E. Lanterna, and J. C. Scaiano, *J. Am. Chem. Soc.* **2016,** *138*, 13127.

[85] B. S. P. Anil Kumar, K. Harsha Vardhan Reddy, B. Madhav, K. Ramesh, Y. V. D. Nageswar, *Tetrahedron Letters.* **2012**, *53*, 4595.

[86] M. K. Holganz, L. Trigour, S. Elfarr, Y. Seo, J. Oiler, Y. Xing, *Tetrahedron Letters*. **2019**, *60*, 1179.

[87] H. Xu, K. Wu, J. Tian, L. Zhu, and X. Yaoa, *J. Name*, **2013**, *00*, 1.

[88] M. Y. Kang, Y. Guo, H. Shi, M. S. Ye, and B. Zhang, *Chemistry Select.* **2018,** *3*, 7054 .

[89] M. Nasibipour, E. Safaei, G. Wrzeszcz and A. Wojtczak, *New J. Chem.* **2020,** *44*, 4426.

[90] M. North, R. Pasquale and C. Young, *Green Chem.* **2010**, *12*, 1514.

[91] R. A. Meyers, *Conversion of CO_2 into Polymers, Encyclopedia of Sustainability Science and Technology*, **2018**, Springer Science+Business Media, LLC, Springer Nature.

[92] B. Metz, O. Davidson, H. C. de Coninck, M. Loos, and L. Meyer (eds.), *IPCC Special Report on Carbon Dioxide Capture and Storage. Prepared by Working Group III of the Intergovernmental Panel on Climate Change (IPCC)*, **2005**, 442 pp, Cambridge University Press, Cambridge, United Kingdom and New York, NY, USA.

[93] T. Sakakura, J. Choi and H. Yasuda, *Chem. Rev*. **2007**, *107*, 2365.

[94] R. Dalpozzo, N. Della Ca, B. Gabriele and R. Mancuso, *Catalysts.* **2019**, *9*, 511.

[95] A.H. Liu, Y.L. Dang, H. Zhou, J.J. Zhang, X.-B. Lu, *ChemCatChem*. **2018**, *10*, 2686.

[96] S. Wu, Y. Zhang, B. Wang, E. H. M. Elageed, L. Ji, H. Wu, G. Gao, *Eur. J. Org. Chem*. **2017**, *3*, 753.

[97] R. Dalpozzo, N. Della Ca, B. Gabriele and R. Mancuso, *Catalysts.* **2019**, *9*, 511.

[98] D. Y. C. Leung, G. Caramanna, M. M. Maroto-Valer, *Renewable and Sustainable Energy Reviews*. **2014**, *39*, 426.

[99] M. Mikkelsen, M. Jorgensen and F. C. Krebs, *Energy Environ. Sci*. **2010**, *3*, 43.

[100] M. North, R. Pasquale and Carl Young, *Green Chem*. **2010**, *12*, 1514.

[101] J. N. Appaturi, F. Adam, *Applied Catalysis B: Environmental.* **2013**, *136*, 150.

[102] K. Xu *Chem. Rev.* **2004**, *104*, 4303.

[103] B. Schaffner *Chem. Rev*. **2010**, *110*, 4554.

[104] J. P. Parrish, R. N. Salvatorea and K. Woon Junga, *Tetrahedron*. **2000**, *56*, 8207.

[105] David R. Moore, M. Cheng, E. B. Lobkovsky, G. W. Coates, *J. Am. Chem. Soc*. **2003**, *125*, 11911.

[106] G. N. Bondarenko, E.G. Dvurechenskaya, O. G. Ganinaa, F. Alonsob, I. P. Beletskaya *Applied Catalysis B: Environmental.* **2019**, *254*, 380.

[107] Q. Li, H. Chang, R. Li, H. Wang, J. Liu, S. Liu, C. Qiao, T. Lin, *Molecular Catalysis.* **2019**, *469*, 111.

[108] Y. Wang, J. Nie, C. Lu, F. Wang, C. Ma, Z. Chen, G. Yang. *Microporous and Mesoporous Materials.* **2020,** *292*, 109751.

[109] C. K. Ng, R. W. Toh, T. T. Lin, H. K. Luo, T. S. A. Hor and J. Wu, *Chem. Sci.* **2019**, *10*, 1549.

[110] S. Verma, G. Kumar, A. Ansari, R. I. Kureshy and N. H. Khan, *Sustainable Energy Fuels.* **2017**, *1*, 1620.

[111] V. Schimp, J. B. Max, B. Stolz, B. Heck, and R. Mülhaupt, *Macromolecules*. **2019**, *52*, 320.

[112] R. H. Lambeth, T. J. Henderson, *polymer.* **2013**, *5*, 5568.

[113] J. Zhang, J. Yang, T. Dong, M. Zhang, J. Chai, S. Dong. T. Wu, X. Zhou and G. Cui, Small, **2018**, *14*, 1800821.

[114] S. Verma, G. Kumar, A. Ansari, R. I. kureshy and N. H. Khanab, *Sustainable Energy Fuels*, **2017,** *1*, 1620.

[115] J. Sun and D. Kuckling, *Polym. Chem.* **2016**, *7*, 1642.

[116] S. Bian, C. Pagan, A. A. Andrianova, Artemyeva, and G. Du, *ACS Omega.* **2016**, *1*, 1049.

[117] S. Ghosh, A. Ghosh, S. Biswas, M. Sengupta, D. Roy, and Sk. M. Islam, *Chemistry Select*. **2019**, *4*, 3961.

[118] R. H. Lambeth, T. J. Henderson, *Polymer*. **2012**, *54*, 5568.

[119] (a) C. Graf, S. Dembski, A. Hofmann and E. Ruhl, *Langmuir*. **2006**, *22*, 5604. (b) P. Bao, C. Zhong, D. M. Vu, J. P. Temirov, R. B. Dyer and J. S. Mar-tinez, *J. Phys. Chem. C.* **2007**, *111*, 12194. (c) A. Kairdolf, M. C. Mancini, A. M. Smith, S. M. Nie, *Anal. Chem***. 2008**, *80*, 3029.

[120] (a) G. chmid and A. Lehnert, *Angew. Chem. Int. Ed. Engl*. **1989**, *28*, 780. (b) W. W. Weare, S.M. Reed, M.G. Warner, J.E. Hut-chinson, *J. Am. Chem. Soc*. 2000, **122**, 12890. (c) L. R. Becerra, C. B. Murray, R. G. Griffin and M. G. Bawendi, *J. Chem. Phys*. **1994**, *100*, 3297. (d) M. Green, *J. Mater. Chem.* **2010**, *20*, 5797.

[121] (a) A. Chastellain, A. Petri and H. Hofmann, *J. Colloid Interface Sci*. 2004, **278**, 353. (b) C. P. Shah, M. Kumar and P N Bajaj, *Nanotechnology*, 2007, **18**, 385607-385613.

CHAPTER 2

Multicomponent dipolar cycloaddition of phenylacetylene involving aryl halides and epoxides catalyzed by organic surfactant-free copper sulfide nano/micro flowers (sf-CuS)

Abstract

The azide-alkyne cycloaddition (Huisgen reaction) is one of the most powerful and widely used copper-mediated reactions. In many such reactions, use of metal or metal oxide nanoparticles as the catalyst is more appealing because of the increased catalytic activity attributed to the large surface to volume ratio. However, the nano/micro particles are synthesized often in the presence of long chain organic molecules as capping or stabilizing agents. These organic molecules cover the active centers and restrict or reduce their catalytic activity. Therefore, we have synthesized the copper sulfide (sf-CuS) nano/micro particles without having organic surfactant molecules as the capping agent. These particles with a flower-like architecture (micro flowers, **mf**) were obtained readily under the supersaturated condition at room temperature. In these particles, the surface was freely available for adsorption and desorption reactions. When utilized as a catalyst in multicomponent cycloaddition reactions, the sf-CuS **mf** exhibited excellent catalytic activity compared with some other nanoparticles with surfactants. This sf-CuS **mf** catalyzed the one-pot synthesis of 1,2,3-triazole and β-hydroxy-1,2,3-triazole effectively from a variety of benzyl bromide derivatives epoxides respectively. Both these reactions proceeded in the presence of azide and phenylacetylene in the water at room temperature. The catalyst was reusable, and there was no catalyst leaching observed during reactions. Synthesis of β-hydroxy triazoles and 1,2,3-triazoles under exceptionally mild conditions with high yields proved the sf-CuS **mf** as the catalyst as a robust and recyclable catalyst.

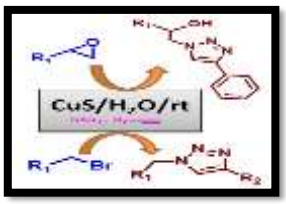

2.1. Introduction

Synthesis of nano/micro particles is fascinating in organic chemistry since they are used as heterogeneous catalysts in organic reactions. The capping agents or surfactants that are used commonly in the synthesis of metal chalcogenides nanoparticles are; amines (hexadecyl amine, alkyl amine), oleic acid, polymers (PVP, PMMA), thiols (1-Dodecanethiol, 1, 6hexanedithiol) [1-3]. However, the collective properties of nanomaterials are not utilized fully [4-9] because of the presence of organic surfactant molecules around the nano/micro particles that are synthesized *via* conventional chemical synthetic methods. When the metal nano/micro particles are used as a catalyst, the chemical reaction occurs on the surface of the particles. The presence of capping molecules would hide the active centers and restrict or reduce the catalytic activity so that capping agents or surfactant molecules around the particles may contribute negatively to the target applications [10].

In recent years metal is decorated on nanomaterials and these materials are used as heterogeneous catalysts in organic reactions such as heck reaction (Pd/CuO) [11], Suzuki cross-coupling reaction (Pd−CuO@Hol S-1) [12], Sonagashira coupling reaction (Cu/CuO) [13], Heisenberg 1, 3-dipolar reaction (CuNPs/MagSilica) [14], copper(I)-catalyzed synthesis of azoles by Sharpless [15], copper(I)-catalyzed azide-alkyne [3 + 2] cycloaddition by Sharpless and Finn [16] and so on. The substituted triazoles are exciting materials in organic synthesis, coordination chemistry, and N-heterocyclic chemistry [17-21].

Substituted triazoles play an essential role in opening calcium channels in cells, particularly [22] at 1 and 4 positions of triazole. They also show biological activities as anti-cancer, antiHIV therapy, anti-bacterial [23-27] and anti-allergy molecules [28-30]. Agricultural and industrial applications of such compounds include herbicides, fungicides, agrochemicals [31], optical brighteners [32], fluorescence chemosensory [33] corrosion retarding agents, dyes, and solar cells [34-37]. Further, the heterocyclic compounds that are rich in nitrogen atoms can be used as high energy materials [38].

The formation of 1,2,3-triazole derivatives is known to proceed through heisenbug 1,3dipolar cycloaddition of organic azides and alkynes using CuAAC as a catalyst [38-41]. In recent years, multi-component click synthesis of 1,2,3-triazoles from both *in-situ* azidolysis of benzyl halide in the presence of alkynes and β-hydroxy-1,2,3-triazoles *via*

in-situ azidolysis of epoxides in the presence of alkynes have been developed [42-44]. Some heterogeneous catalysts used in the dipolar cycloaddition are polyurea encapsulated copper(I) chloride [45], CuNP/C [46], $CuFe_2O_4$ [47], Cu/Cu_2O [48], [$AQ_2Cu(II)$-$APSiO_2$] [49], copper(I)@phosphorated SiO_2 [50], SiO_2-CuI [51], Clay–Cu(II)/$NH_2NH_2 \cdot H_2O$ [52], GO@PTA-Cu [53] and copper(I) in ionic liquids [54]. Albeit several catalytic systems have been used for dipolar cycloaddition, in pursuit of catalyst working under mild condition and developing simple method of production of nano catalyst, we have synthesized surfactant-free copper sulfide (sf-CuS) particles having micro flower (**mf**) like architecture formed by the self-assembly of nanoparticles.

Herein, we report the synthesis of surfactant-free copper sulfide micro flowers (**sf-CuS mf)** in an efficient and straightforward synthetic process, and its practical use in the synthesis of both benzyl halide linked 1,2,3- triazoles and *β*-hydroxy- 1,2,3-triazoles *via* dipolar cycloaddition of azide and alkyne in the presence of benzyl halide and epoxide. The synthesis described here was performed in water, and so it was safer, greener, and used inexpensive, recyclable surfactant free heterogeneous catalyst. The above synthetic procedure satisfied the most of green chemistry principles such as (a) one-pot multicomponent synthesis (atom economy) (b) reactions in a water medium (green solvent) (c) using of readily separable and recyclable heterogeneous catalyst (d) involving simple workup procedure.

2.2. Results and Discussion

In recent times, the azide-alkyne cycloaddition (Huisgen reaction) has emerged as one of the most powerful and widely utilized copper-mediated reactions. However, many reactions catalyzed by metal or metal oxide nanoparticles are more appealing because of the increased catalytic activity attributed to the large surface to volume ratio. In general, the nano/micro particles used as the catalyst are produced in the presence of long chain organic molecules as capping or stabilizing agents. These capping agents on the nano/micro particles cover the active centers and restrict or reduce their catalytic activity. To outwit this problem, we have developed a method of synthesis of metal chalcogenides without capping agent so that the catalyst surface is freely available for adsorption and desorption reactions [10].

In the present work, we have prepared surfactant-free copper sulfide (**sf-CuS)** under the supersaturated condition in a simple chemical reaction wherein sulfur was dissolved while $LiBH_4$ and $Cu(CH_3COO)_2 \cdot H_2O$ were suspended in dry tetrahydrofuran (THF). The reaction was conducted for one hour at room temperature and in an inert atmosphere to avoid any oxidation. The partial solubility of the metal source and fast reactivity in the presence of $LiBH_4$ provided a thermodynamically favorable condition [55] which induced the nucleation of particles. Since the reaction was at room temperature, the digestion process was avoided [56-60] which supplemented the formation of black powder of CuS having nano/micro flower like architecture. These micron-sized flower-like particles (**mf**) were formed by the self-assembly of nanoflakes [61]. These metal chalcogenide **mf** were formed under the supersaturated condition, and no surfactant molecules were used during synthesis. The particles were stable, and no agglomeration was observed. The material was characterized by PXRD, SEM, and spectroscopic techniques (Figure 2.1) [10]. Since no organic surfactant molecules were surrounding the particles, the catalyst surface was freely available for reactions and that significantly favored high activity in the reactions of click chemistry and epoxy ring opening.

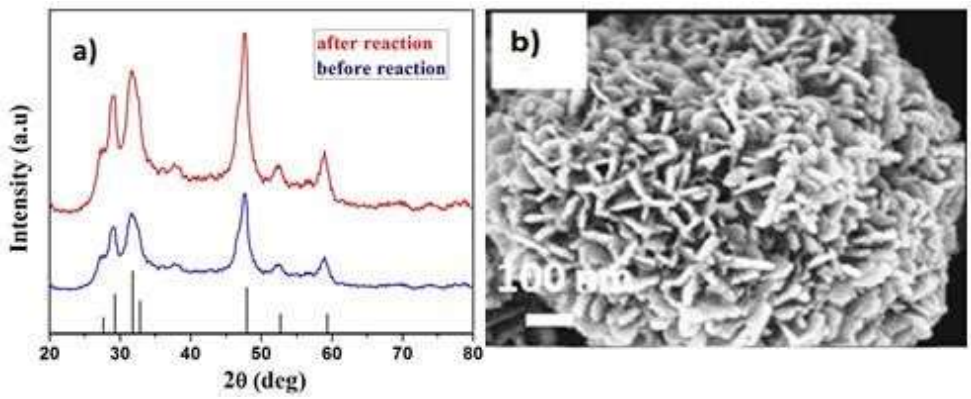

Figure 2.1: (a) X-ray diffraction of sf-CuS mf, (b) SEM images of sf-CuS mf

2.2.1. Catalytic activity

The catalytic activity of **sf-CuS mf** having the unhindered surface in the multicomponent synthesis of 1, 2, 3-triazoles in the dipolar cycloaddition reactions was investigated. The experiments began with optimizing the reaction conditions for the multicomponent synthesis of 1, 2, 3-triazoles from benzyl halide, sodium azide and phenylacetylene (Scheme 2.1).

Later the reaction was extended to the synthesis of β-hydroxy 1, 2, 3-triazoles from epoxy derivatives, sodium azide and phenylacetylene (Scheme 2.2). This reaction proceeded *via in-situ* ring opening of epoxides followed by the reaction with phenylacetylene. In both reactions, water was used as the solvent at room temperature. The results were very encouraging since the reactions completed in 5-12 h, and yielded of the desired products quantitatively.

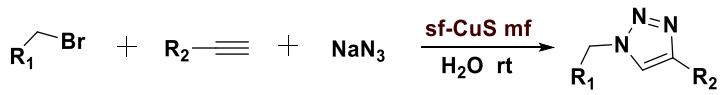

Scheme 2.1: Three component synthesis of 1,2,3-triazoles from organic halides catalyzed by sf-CuS mf

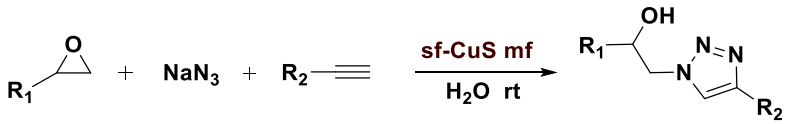

Scheme 2.2: Three component synthesis of β-hydroxy-1,2,3-triazoles from epoxides catalyzed by sf-CuS mf in water

In order to optimize the reaction conditions, the reactions were performed by varying the quantity of catalyst and using different solvents. Progress the reaction was monitored by means of TLC. At the end of the reaction, the catalyst was separated by filtration and worked up using ethyl acetate and water. There was no difference in yield and reaction time when catalyst loading was reduced to 15 mg, 10 mg, and 5 mg. However, when 2 mg of the catalyst was used, it required a longer time for the completion of the reaction (above 12 h). Consequently, it was decided to use 5 mg of the catalyst for further studies. Similarly, few more reactions were performed in various solvents to choose the medium of the reaction (Table 2.1). In DMF 45%, DMSO 20% yield was obtained. Among all solvents tried, water was the best solvent to produce the products in good yields. Other than these solvents no product spot was observed in TLC. Therefore, water was chosen as the reaction medium for all reactions.

Table 2.1: Solvent optimization of for the synthesis of scheme 1 in the model reaction

Entry	Solvent	Time (h)	Yield (%)
1	CH_3OH	24	no
2	n-butanol	24	no
3	CH_3CN	24	no
4	$CHCl_2$	24	no
5	$CHCl_3$	24	no
6	DMSO	24	20
7	DMF	24	45
8	H_2O	6	92

Different benzyl bromides substituted with halides and methyl were reacted with sodium azide and terminal alkynes to form 1,2,3- triazoles using **sf-CuS mf** as catalyst under optimized condition (Table 2.2). Similarly, a series of different aryl epoxy, cyclic epoxy and alkyl-substituted epoxy derivatives, sodium azide, and terminal alkynes to form *β*-hydroxy 1,2,3- triazole using **sf-CuS mf** as catalyst and water as solvent at room temperature (Table 2.3). The crude products from all reactions were purified by column chromatography and then characterized by ^{1}H and ^{13}C NMR spectral data. Almost all these reactions (except table 2.2, entries 4 and 5) yielded the corresponding product in more 90 % yield in water as the solvent

Table 2.2 : Synthesis of 1, 2, 3 triazole derivatives by CuS

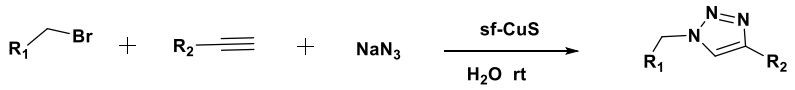

Entry	benzyl bromide (R1)	alkyne (R2)	time	product	yield%
1	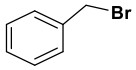	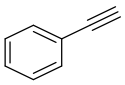	6h	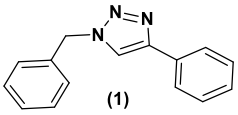 (1)	96%
2	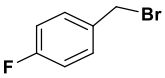	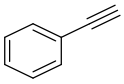	5h	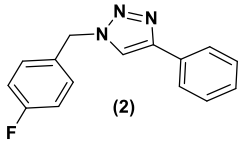 (2)	95%
3	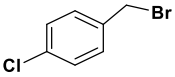	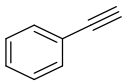	7h	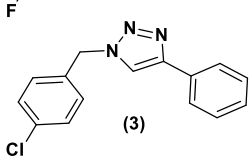 (3)	92%
4	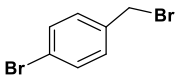	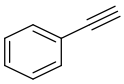	9h	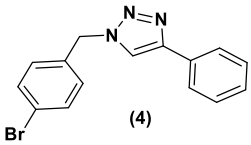 (4)	90%
5	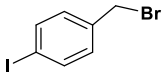	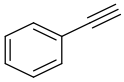	12h	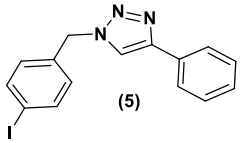 (5)	87%
6	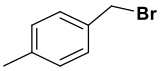	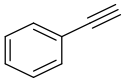	8h	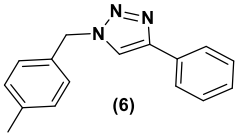 (6)	92%
7	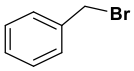	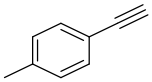	6h	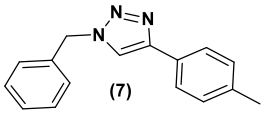 (7)	95%
8	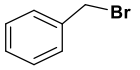	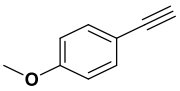	6h	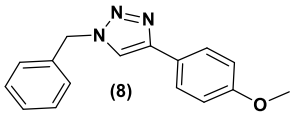 (8)	96%
9	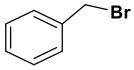	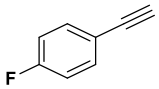	5h	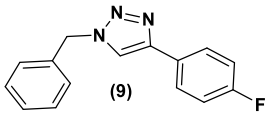 (9)	97%

Table 2.3: Synthesis of β-hydroxy 1,2,3-triazole derivatives by CuS

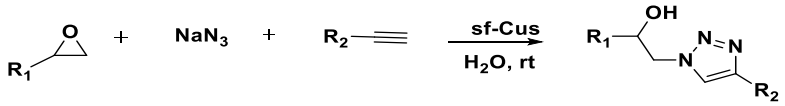

Entry	epoxide (R1)	alkyne (R2)	time	product	Yield%
1	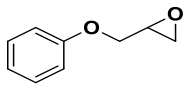	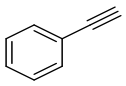	6h	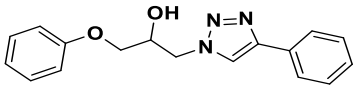 (10)	92%
2	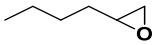	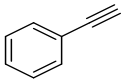	8h	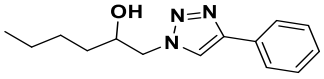 (11)	89%
3		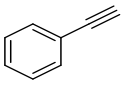	8h	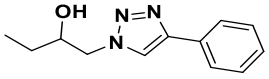 (12)	86%
4		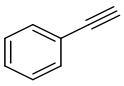	10h	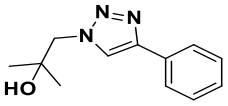 (13)	82%
5	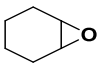	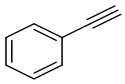	12h	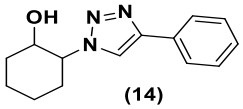 (14)	79%
6	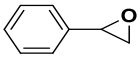	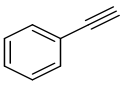	5h	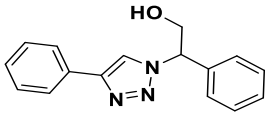 (15)	91%
7	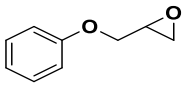	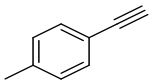	7h	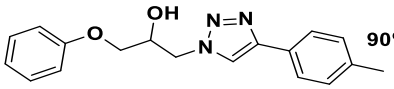 (16)	90%
8	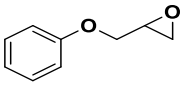	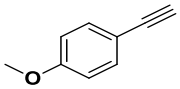	7h	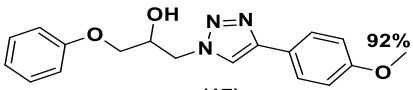 (17)	92%
9	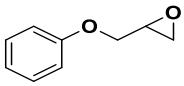	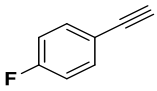	6h	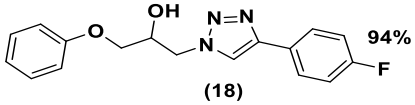 (18)	94%

Though many catalysts are known, the **sf-CuS mf** used here was obtained in a simple reaction condition, and the products were obtained in excellent yield. The performance of the various catalysts in the model reaction (styrene oxide, sodium azide, and phenylacetylene) was compared (Table 2.4) to understand the effect of **sf-CuS** micro flowers as the catalyst. Most of those catalysts were used at above 60°C except for Cu/Cu_2O while our **sf-CuS mf** was working at the room temperature (This work). Further, most of the literature on scheme 1 type model reaction was only within benzyl azide and phenylacetylene (two reactants) whereas we are presenting the catalyst which can work in multicomponent reactions.

Table 2.4: Comparison table of numerous catalysts with various Synthesis of 1, 4 disubstituted β hydroxy 1, 2, 3 triazoles (for the compound **15)**

Catalyst	**Substrate**	**Time (h)**	**Temperature (**°C)	**Yield (%)**	**Ref**
CPSi	Styrene Oxide	1	60	94	50
Cu/Cu_2O	Styrene Oxide	2	RT	75	48
$AQ_2Cu(II)$-$APSiO_2$	Styrene Oxide	4	60	82	49
$CuFe_2O_4$	Styrene Oxide	6	60	87	47
Cu Nano particles	Styrene Oxide	8	100	83	46
Cu(I) in Ionic liquids	Styrene Oxide	10	80	95	54
Sf-CuS mf	**Styrene Oxide**	**5**	**RT**	**91**	**This work**

2.2.2. Leaching study and recyclability of sf-CuS mf as catalyst

Leaching study was performed to confirm the heterogeneous catalysis for the reaction shown in scheme 1. For this purpose, a reaction was stopped after the formation of around 20% product, and the catalyst was separated from the reaction mixture. The reaction was continued without the catalyst for 8 h, but no considerable product formation was observed. This observation explained that the reaction was working under heterogeneous catalysis. The lifetime of the catalyst and its reusability play an essential

role in the practical applications of such heterogeneous systems. In order to take advantage of heterogeneous nature of our catalyst, a set of experiments were performed in which both 1,2,3-triazole from *in-situ* azidolysis of benzyl halide in the presence of alkynes (scheme 2.1) and epoxy ring opening followed by cycloaddition of azide (scheme 2.2) and phenylacetylene using the recycled **sf-CuS mf**. After the completion of the first reaction, the product was extracted using ethyl acetate, and the catalyst was recovered by simple decantation and dried at 50 °C. A new reaction was performed with new reactants under the same conditions using the recovered **sf-CuS mf**. We have also performed a recycling experiment in Scheme1 using 5 mmol of reagents. After completion of the reaction, the catalyst was recovered and reused for the next cycle thus confirming that **sf-CuS mf** could be reused for five times with little change in its activity (Figure 2.2).

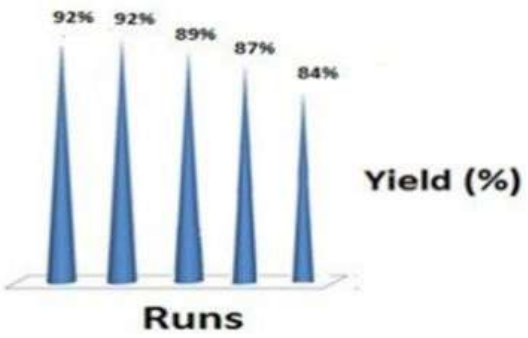

Figure 2.2: Recycling results of the sf-CuS mf catalyst in the synthesis of triazoles

2.3. Conclusions

Surfactant-free copper sulfide (**sf-CuS)** catalyst has been utilized successfully for one-pot synthesis of triazoles by cycloaddition of both benzyl halide derivatives- alkyne and epoxide derivatives – alkyne in the presence of sodium azide. The desired products were obtained at ambient temperature while the reactions were performed in water. Most of the reactions proceeded faster with the exception of aliphatic epoxide in the case of epoxide derivatives. While in benzyl halide derivatives, less electronegative substituted benzyl halide derivative (Bromo and Iodo) were slower compared with other (flouro and

chloro). The catalyst can be recycled and reused for five times without losing its activity.

2.4. Experimental procedure

2.4.1. Materials

The chemicals $Cu(OAC)_2$, S, and all the phenyl bromide derivatives, phenyl acetylene derivatives, Lithium borohydride were purchased from Sigma-Aldrich Chemical Co and used as such. Anhydrous Na_2SO_4 and NaN_3 were purchased from Merck, India. Solvents used for all reactions were dried and distilled through the standard procedure and then used for workup and column chromatography. The yields of the compounds reported here are isolated yields. All reported yields are isolated yields.

2.4.2. Instrumentation

Bruker (500 and 400 MHz) NMR spectrometers were used to acquire ^{1}H NMR and ^{13}C NMR spectra at room temperature using $CDCl_3$ as solvent. Chemical shifts (ppm, δ) are reported downfield of TMS. Thin-layer chromatography (TLC) was done using aluminium plates coated with silica gel 60-120 mess (purchased from MERCK) and was visualized under 254 nm UV light. Column chromatography was performed using column packed silica gel (120–240 mesh).

2.4.3. Synthesis of catalyst (sf-CuS-mf)

Sulphur (40 mg, 1.3 mmol) was dissolved in 15 mL of dry tetrahydrofuran (THF) in a 50 mL two neck RB flask, to that $LiBH_4$ (59 mg, 2.5 mmol) and $Cu(CH_3COO)_2{\cdot}H_2O$ (250 mg, 1.2 mmol) were added. The reaction mixture was stirred at room temperature under nitrogen atmosphere for 1 h. Initially, the color of the solution was dark brown, and after the completion of reaction it turned to dark green along with the evolution of gaseous side product(s). After one-hour, volatile side products and solvent were removed by applying high vacuum. The obtained crude product was washed with methanol (40 mL) followed by THF (40 mL) to remove side products (copper acetate, lithium salt) and unreacted S, and then centrifuged. The residue was dried under vacuum for 6 h to get catalyst as a black powder of **sf-CuS** micro flowers. The catalyst was characterized by PXRD and SEM techniques.

2.4.4. Synthesis of 1, 2, 3-triazole from benzyl bromide derivatives, sodium azide and alkyne

NaN_3 (65 mg, 1.0 mmol), the benzyl bromide (1 mmol), and the alkyne (1 mmol) were added to a suspension of sf-**CuS** (5 mg) in water. The reaction mixture was stirred at room temperature and monitored by TLC until all the starting materials were converted to products. The solid was obtained by filtration and washed by DCM (3 ×10 mL). The ex-traction of aqueous phase with DCM was also performed without loss of product, and collected organic phase were dried with anhydrous Na_2SO_4, and concentrated in vacuum. The product was purified through a silica gel column chromatography as corresponding *β*-hydroxy 1, 2, 3triazoles. All the products were confirmed by usual spectral methods (^{1}H-NMR, ^{13}C NMR).

1-benzyl-4-phenyl-1H-1, 2, 3-triazole:

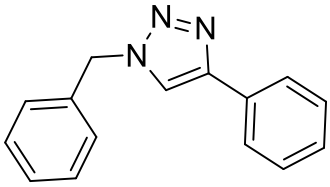

Melting point : 128-129 ^oC (White solid).

^{1}H NMR (500 MHz, $CDCl_3$) : δ = 7.83-7.81 (m, 2H), 7.68 (s, 1H), 7.43 – 7.38 (m, 5H) 7.35 –7.32 (m, 3H), 5.59 (s, 2H).

^{13}C NMR (126 MHz, $CDCl_3$) : δ =148.2, 134.6, 130.5, 129.1, 128.8, 128.1, 128.0, 125.7, 119.4 and 54.2.

HRMS calculated for $C_{15}H_{13}N_3$: $[M+H]^+$: 236.1182, found: 236.1184.

1-(4-flourobenzyl)-4-phenyl-1H-1,2,3-triazole:

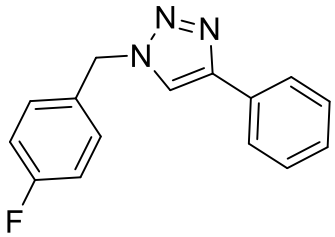

Melting point : 123-125 ^{o}C (white solid).

^{1}H NMR (500 MHz, $CDCl_3$) : δ = 7.80-7.78 (m, 2H), 7.65 (s, 1H), 7.42 – 7.38 (m, 2H), 7.33 – 7.05 (m, 5H), 5.55 (s, 2H).

^{13}C NMR (126 MHz, $CDCl_3$) : δ =164.1, 161.6, 148.3, 129.9,129.1, 128.8, 128.2, 125.7, 119.3, 116.2, 116.0, 115.9, 115.6, 53.4 and 52.0.

HRMS calculated $C_{15}H_{12}FN_3$: $[M+H]^+$: 254.1081, found: 254.1082.

1-(4-Chloro benzyl)-4-phenyl-1H-1,2,3-triazole:

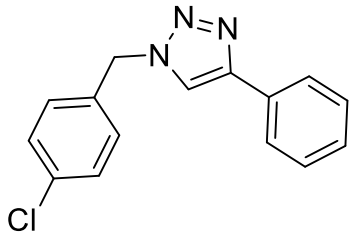

Melting point :141-143 ^{o}C (white solid).

^{1}H NMR (500 MHz, $CDCl_3$) : δ = 7.83-7.80 (m, 2H), 7.68 (s, 1H), 7.44 – 7.34 (m, 7H), 5.55 (s, 2H).

^{13}C NMR (126 MHz, $CDCl_3$) : δ =148.4, 134.8, 133.1, 130.3, 129.3, 129.1, 128.8, 128.3, 125.7, 119.4 and 53.5.

HRMS calculated for $C_{15}H_{12}ClN_3$: $[M+H]^+$: 270.0714, found: 270.0716.

1-(4-bromobenzyl)-4-phenyl-1H-1,2,3-triazole:

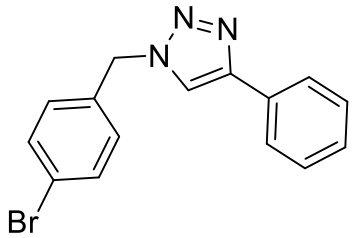

Melting point :150-152 ^{o}C (white solid).

^{1}H NMR (500 MHz, $CDCl_3$) : δ = 7.78-7.80 (m, 2H), 7.66 (s, 1H), 7.51 (d, 8Hz, 2H),7.40 (t, 7Hz, 2H), 7.33 (t, 7Hz, 1H) 7.17 (d, 8Hz, 2H), 5.55 (s, 2H).

^{13}C NMR (126 MHz, $CDCl_3$) : δ =148.4, 133.7, 132.3, 130.3, 129.6, 129.5, 128.8, 128.3, 125.7, 125.6, 122.9, 119.4, and 53.5.

HRMS calculated for $C_{15}H_{12}BrN_3$: $[M+H]^+$: 315.0220, found: 315.0221.

1-(4-Iodobenzyl)-4-phenyl-1H-1,2,3-triazole:

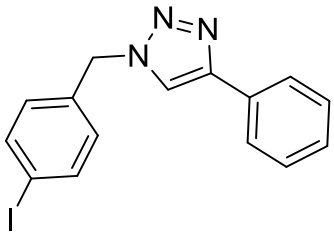

Melting point: :153-155 ^{o}C (white solid).

^{1}H NMR (500 MHz, $CDCl_3$) : δ = 7.81 (d, 7Hz, 2H), 7.73 (d, 8Hz, 2H),7.68 (s, 1H), 7.42 (t, 7Hz, 2H), 7.34 (t, 7Hz, 1H) 7.06 (d, 8Hz, 2H), 5.55 (s, 2H).

^{13}C NMR (126 MHz, $CDCl_3$) : δ =148.4, 138.3, 134.3, 132.3, 130.3, 129.8, 129.6, 128.8, 128.2, 120.7, 119,4, 94.5, 53.6 and 53.5.

HRMS calculated for $C_{15}H_{13}I\ N_3$: $[M+H]^+$: 362.0162, found: 362.0164.

1-(4-methylbenzyl)-4-phenyl-1H-1,2,3-triazole:

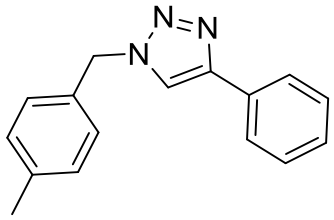

Melting point : 112-114 ^{o}C (white solid).

^{1}H NMR (500 MHz, $CDCl_3$) : δ = 7.82-7.79 (m, 2H), 7.65 (s, 1H), 7.43-7.39 (m, 2H), 7.35-7.30 (m, 1H), 7.25-7.20 (m, 4H), 5.55 (s, 2H), 2.38 (s, 3H).

^{13}C NMR (126 MHz, $CDCl_3$) : δ =148.1, 138.7, 131.6, 130.6,129.8, 128.7, 128.15, 128.12, 125.7, 119.3, 54.0 and 21.1.

HRMS calculated for $C_{15}H_{13}N_3$: $[M+H]^+$: 250.1382, found: 250.1384.

1-benzyl-4-p-tolyl-1H-1,2,3-triazole:

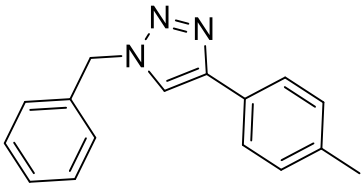

Melting point : 142-143 ^{o}C (Pale yellow solid)

^{1}H NMR (500 MHz, DMSO-d6) : δ = 8.59 (s, 1H), 7.73 (d, 8Hz, 2H), 7.42-7.34(m, 5H), 7.25 (d, 8Hz, 2H), 5.63 (s, 2H), 2.32 (s, 3H).

^{13}C NMR (126 MHz, DMSO-d6) : δ =147.1, 137.6, 136.5, 129.9, 129.2, 128.6, 128.3, 125.5, 121.6, 53.4 and 21.3.

HRMS calculated for $C_{15}H_{13}N_3$: $[M+H]^+$: 250.1382, found: 250.1384.

1-benzyl-4-(4-methoxyphenyl)-1H-1,2,3-triazole:

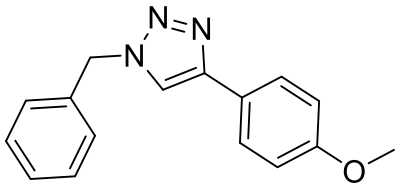

Melting point : 140-142 ºC (White solid).

^{1}H NMR (500 MHz, DMSO-d6) : δ = 7.75-7.73 (d, 8Hz, 2H), 7.59 (s, 1H), 7.41-7.38 (m, 3H), 7.33-7.31 (m, 2H), 6.96-6.94 (m, 2H), 5.58 (s, 2H), 3.84 (s, 3H).

^{13}C NMR (126 MHz, DMSO-d6) : δ =159.6,148.12, 134.7, 129.1, 128.7, 128.0, 127.0, 123.2, 118.6, 114.2, 55.3, 54.2 and 30.9.

HRMS calculated for $C_{16}H_{15}N_3O$: $[M+H]^+$: 266.1211, found: 266.1214.

1-benzyl-4-(4-fluorophenyl)-1H-1,2,3-triazole:

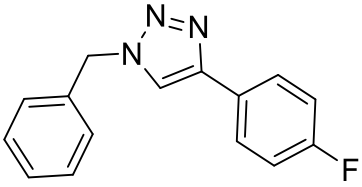

Melting point : 112-113 ºC (White solid).

^{1}H NMR (500 MHz, DMSO-d6) : δ = 7.80-7.77 (m, 2H), 7.63 (s, 1H), 7.42-7.39 (m, 3H), 7.34-7.32 (m, 2H), 7.13-7.09 (m, 2H), 5.59 (s, 2H).

^{13}C NMR (126 MHz, DMSO-d6) : δ =161.4, 134.5, 129.2, 128.8, 128.1, 127.49, 127.41, 126.7, 119.2, 115.9,115.7 and 54.5.

HRMS calculated for $C_{15}H_{12}FN_3$: $[M+H]^+$: 254.1021, found: 254.1024.

2.4.5. Syntesis of *β*-hydroxy 1, 2, 3-triazole from benzyl bromide derivatives, sodium azide and alkyne:

NaN_3 (65 mg, 1.0 mmol), the epoxide (1 mmol), and the alkyne (1 mmol) were added to a suspension of **sf-CuS** (5 mg). The reaction mixture was stirred at room temperature and monitored by TLC until all the starting materials were converted to products. The solid was obtained by filtration and washed by DCM (3 ×10 mL). The extraction of aqueous phase with DCM was also performed without loss of product, and collected organic phase were dried with anhydrous Na_2SO_4, and concentrated in vacuum. The product was isolated through a silica gel column chromatography as corresponding *β*-hydroxytriazoles. All the products were confirmed by usual spectral methods (^{1}H-NMR, ^{13}C NMR).

3-Phenoxy-2-(4-phenyl-1H-1,2,3- triazol-1-yl)propan-1-ol:

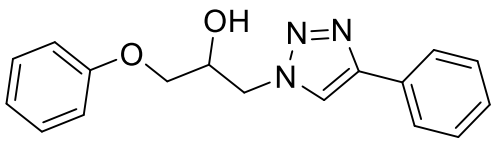

Melting point	:126-128 ^oC (pale yellow solid)
^{1}H NMR (500 MHz, $CDCl_3$)	: δ = 7.89 (s, 1H), 7.78-7.75 (m, 2H), 7.43- 7.39 (m, 2H), 7.34-7.35 (m, 1H), 7.32-7.30 (m,1H) 7.03-6.99 (m, 1H), 6.95-6.92 (m, 2H), 4.75 (dd, J=3 Hz, J = 11 Hz, 1H), 4.61-4.54 (m, 2H), 4.09-4.00 (m, 2H), 3.57 (s, 1H).
^{13}C NMR (126 MHz, $CDCl_3$)	: *δ* = 158.0, 147.7, 130.2, 129.6, 129.5, 128.8, 128.2, 125.6, 121.6, 121.3, 114.5, 68.9, 68.7 and 53.03
HRMS calculated for $C_{17}H_{17}N_3O_2$	: $[M+H]^+$: 296.1398, found: 296.1398.

2-(4-Phenyl-1H-1,2,3-triazol-1-yl)hexan-1-ol:

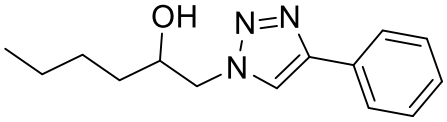

Melting point : 92-93 ^{o}C (white solid)

1H NMR (500 MHz, CDCl3) : δ = 7.83 (s, 1H), 7.76-7.74 (m, 2H), 7.40-7.37 (m, 2H), 7.32-7.29 (m, 1H), 4.49 (dd, J = 3 Hz, J = 11 Hz, 1H), 4.27-4.22 (m, 2H), 4.13-4.11 (m, 1H), 2.89 (S, 1H) 1.55-1.49 (m, 3H), 1.42-1.33 (m, 3H), 0.92 (t, J=7 Hz, 3H).

^{13}C NMR (126 MHz, CDCl3) : δ = 147.4, 130.4, 128.8, 128.1, 126.0, 125.6, 121.0, 56.1, 34.1, 27.5, 22.5 and 13.9.

HRMS calculated for $C_{14}H_{19}N_3O$: $[M+H]^+$: 246.1571, found: 246.1573.

2-(4-phenyl-1H-1,2,3-triazol-1-yl)butan-1-ol:

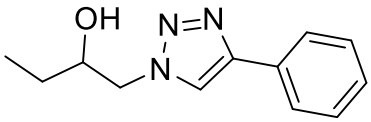

Melting point :110-112 ^{o}C (White solid)

^{1}H NMR (500 MHz, $CDCl_3$) : δ = 7.82 (s, 1H), 7.71 (d, J=7 Hz, 2H),7.37 (t, J=8Hz, 2H), 7.31-7.28 (m, 1H), 4.49 (dd, J = 3 Hz, J = 14Hz 1H), 4.26-4.22 (m, 1H), 4.09-4.04 (m, 1H), 1.60-1.59 (m, 3H), 1.05 (t, J=7 Hz, 3H).

^{13}C NMR (126 MHz, CDCl3) : δ =147.3, 130.3, 128.8, 128.1, 125.5, 121.1, 55.9, 27.4, and 9.8.

HRMS calculated for $C_{12}H_{15}N_3O$: $[M+H]^+$: 218.1252, found: 218.1254.

2-methyl-2-(4-phenyl-1H-1,2,3-triazol-1-yl)propan-1-ol:

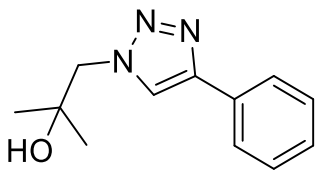

Melting point : 125-126 ^{o}C (white solid)

^{1}H NMR (500 MHz, $CDCl_3$) : δ = 7.91 (s, 1H), 7.83 (d, J=8Hz, 2H), 7.44-7.40 (m, 2H), 7.36-7.31 (m, 1H), 4.37 (s, 2H), 1.27 (s, 6H).

^{13}C NMR (126 MHz, CDCl3) : δ = 147.5, 130.5, 128.8, 128.1, 129.3, 125.5, 121.2, 70.5, 60.4, and 27.1.

HRMS calculated for $C_{12}H_{15}N_3O$: $[M+H]^+$: 218.1246, found: 218.1247

2-(4-phenyl-1H-1,2,3-triazol-1-yl)cyclohexanol:

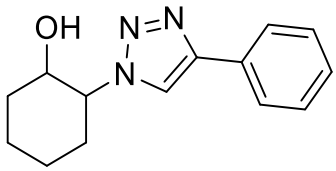

Melting point : 168-170 ^{o}C (white solid)

^{1}H NMR (500 MHz, $CDCl_3$) : δ = 7.80 (s, 1H), 7.78-7.76 (m, 2H), 7.41 (t, 2H), 7.35-7.32 (m, 1H), 4.24-4.18 (m,1H),4.13-4.07 (m,1H), 3.22 (S, 1H) 2.27-2.24 (m, 2H), 2.01-1.89 (m, 1H), 1.61-1.49 (m, 4H).

^{13}C NMR (126 MHz, CDCl3) : δ = 147.3, 128.8, 128.0, 125.6, 119.4, 72.6, 66.9, 33.6, 31.6, 24.7, and 24.0.

HRMS calculated for $C_{14}H_{17}N_3O$: $[M+H]^+$: 244.1493, found: 244.1496.

2-phenyl-2-(4-phenyl-1H-1,2,3-triazol- 1-yl)ethanol:

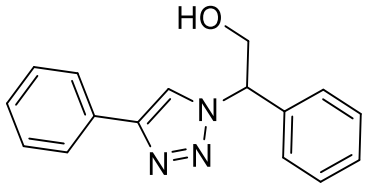

Melting point :122-124 ^{o}C (white solid)

^{1}H NMR (500 MHz, $CDCl_3$) : δ = 7.76 (s, 1H), 7.74 (d, 2H), 7.39- 7.35 (m, 5H), 7.29-7.27 (m, 2H), 5.72-5.69 (m, 1H) 4.63-4.59 (m, 1H), 4.25-4.21 (m, 1H), 3.88 (s, 1H).

^{13}C NMR (126 MHz, $CDCl_3$) : δ = 207.1, 147.6, 136.1, 130.2, 129.1, 128.9, 128.8, 128.2, 127.1, 125.6, 120.5, 67.2, 64.9, and 30.8.

HRMS calculated for $C_{16}H_{15}N_3O$: $[M+H]^+$: 266.1238, found: 266.1239.

3-phenoxy-2-(4-toulyl-1H-1,2,3-triazol-1-yl)propan-1-ol:

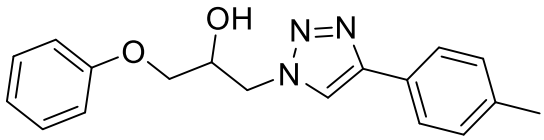

Melting point : 126-128 ^{o}C (colorless solid)

^{1}H NMR (500 MHz, $CDCl_3$) : δ = 7.85 (s, 1H), 7.65-7.63 (m, 2H), 7.33- 7.30 (m, 2H), 7.21 (d, J=7Hz, 2H), 7.02-6.99 (m,1H) 6.94-6.92 (m, 2H), 4.74-4.72 (m,1H), 4.58-4.52 (m, 2H), 4.16-4.01 (m, 3H).

^{13}C NMR (126 MHz, $CDCl_3$) : δ = 158.1, 147.7, 138.0, 129.6, 129.5, 127.4, 125.6, 121.5, 121.0, 114.6, 68.9, 68.8, 53.0,29.7 and 21.2.

HRMS calculated for $C_{18}H_{19}N_3O_2$: $[M+H]^+$: 310.1524, found: 310.1525

1-(4-(4-methoxyphenyl)-1H-1,2,3- triazol-1-yl)-2-phenoxyethan-1-ol: (pale yellow oily)

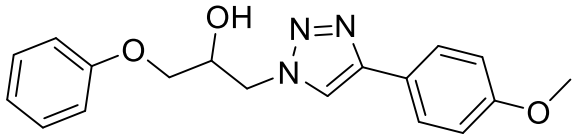

^{1}H NMR (500 MHz, $CDCl_3$) : δ = 7.81 (s, 1H), 7.70-7.69 (d, 2H), 7.33- 7.29 (m, 2H), 6.95-6.92 (m, 5H), 4.75-4.72 (m,1H), 4.59-4.53 (m, 2H), 4.07-3.99 (m, 2H) 3.85 (S, 3H) 3.60 (S, 1H).

^{13}C NMR (126 MHz, $CDCl_3$) : δ = 159.1,158.0, 147.6, 129.6, 129.5, 127.0, 123.0, 21.6, 121.2, 120.4, 114.6, 114.5, 114.2, 69.0, 68.7, 55.3 and 52.9.

HRMS calculated for $C_{18}H_{19}N_3O_3$: $[M+H]^+$: 326.1412, found: 326.1413

1-(4-(4-fluorophenyl)-1H-1,2,3- triazol-1-yl)-2-phenoxyethan-1-ol: (colorless liquid)

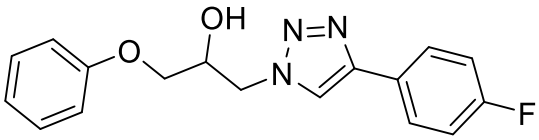

^{1}H NMR (500 MHz, $CDCl_3$) : δ = 7.86 (s, 1H), 7.73-7.72 (d, 2H), 7.34- 7.29 (m, 3H), 7.03-6.92 (m, 4H), 4.76-4.73 (m,1H), 4.60-4.56 (m, 2H), 4.09-4.00 (m, 2H),3.75 (S, 1H).

^{13}C NMR (126 MHz, $CDCl_3$) : δ = 159.6,158.0, 147.6, 129.6, 129.5, 127.0, 123.0, 121.6, 121.2, 120.4, 114.54, 114.55, 114.2, 69.0, 68.7, 55.3 and 52.9.,

HRMS calculated for $C_{17}H_{16}FN_3O_2$: $[M+H]^+$: 314.1215, found: 314.1217.

2.5. Reference

[1] Q. Lu, F. Gao and D. Zhao, *Nano Lett.* **2002**, *2*, 725.

[2] E. C. Greyson, J. E. Barton and T. W. Odom, *Small*. **2006**, *2*, 368.

[3] A. Rabkin, N. Belman, J. Israelachvili and Y. Golan, *Langmuir*. **2012**, *28*, 15119.

[4] P. Roy, K. Mondal and S. K Srivastava, *Cryst. Growth Des.* **2008**, *8*, 1530.

[5] P. Roy and S.K. Srivastava, *Mater.Lett.* **2007,** *61*, 1693.

[6] S. Hsu, K. On and A. R. Tao, *J. Am. Chem. Soc.* **2011**, *133*, 19072.

[7] W. Bryks, M. Wette, N. Velez, S. Hsu and A. R. Tao, *J. Am. Chem. Soc.* **2014**, *136*, 6175.

[8] S. Hsu, W. Bryks and A. R. Tao, *Chem. Mater.* **2012**, *24*, 3765.

[9] S. Hsu, C. Ngo and A. R. Tao, *Nano Lett.* **2014**, *14*, 2372

[10] S. Gottepu, V. R. Velpuri and K. Muralidharan, *J. Chem. Sci.* **2017,** *129*, 1853.

[11] M. Nasrollahzadeh, S. M. Sajadi, A. Rostami-Vartooni, M. Bagherzadeh, *J. Colloid Interface Sci.* **2015,** *448*, 106.

[12] C. Dai, X. Li, A. Zhang, C. Liu, Song, X. Guo, *RSC Adv.* **2015**, *5*, 40297.

[13] J. H. Kou, A. Saha, C. Bennett-Stamper, R. S. Varma, *Chem. Commun.* **2012**, *48*, 5862.

[14] F. Nador, M. A. Volpe, F. Alonso, A. Feldhoff, A. Kirschning, G. Radivoy, Appl. Catal., A. **2013,** *455*, 39.

[15] F. Himo, T. Lovell, R. Hilgraf, V. V. Rostovtsev, L. Noodleman, K. B. Sharpless, Fokin, *J. Am. Chem.* Soc. **2005**, *127*, 210.

[16] Qian Wang, Timothy R. Chan, Robert Hilgraf, Valery V. Fokin, K. B. Sharpless and M. G. Finn, *J. Am. Chem. Soc.* **2003**, *125*, 3192.

[17] A. S. Felten, N. Petry, B. Henry, N. Pellegrini-Moïse and K. Selmeczi, *New J. Chem.* **2016**, *40*, 1507.

[18] M. Bakthadoss, N. Sivakumar, A. Devaraj and P. V. Kumar, *RSC Adv.* **2015**, *5*, 93447.

[19] M. Rajeswari, S. Kumari and J. M. Khurana, *RSC Adv.* **2016**, *6*, 9297.

[20] S. Q. Bai, L. Jiang, A. L. Tan, S. C. Yeo, D. J. Young and T. S. A. Hor, *Inorg. Chem. Front.* **2015**, *2*, 1011.

[21] S. Q. Bai, L. Jiang, D. J. Young and T. S. A. Hor, *Aust. J. Chem.* **2016,** *69*, 372.

[22] V. Calderone, I. Giorgi, O. Livi, E. Martinotti, E. Mantuano, A. Martelli, A. Nardi, *Eur. J. Med. Chem.* **2005**, *40*, 521.

[23] C. Menendez, A. Chollet, F. Rodriguez, C. Inard, M. R. Pasca, C. Lherbet, M. Baltas, *Eur. J. Med. Chem.* **2012,** *52*, 275.

[24] F.C. da Silva, M. C. B. de Souza, I. I. Frugulhetti, H. C. Castro, L. O. Silmara, T. M. L. de Souza, D. Q. Rodrigues, A. M. Souza, P. A. Abreu, F. Passamani, *Eur. J. Med.Chem*. **2009**, *44*, 373.

[25] T. W. Kim, Y. Yong, S. Y. Shin, H. Jung, K. H. Park, Y. H. Lee, Y. Lim, K.Y. Jung, *Bioorg. Chem.* **2015**, *59*, 1.

[26] J. N. Sangshetti, R. R. Nagawade, D. B. Shinde, *Bioorg. Med. Chem. Lett.* **2009**, *19*, 3564.

[27] M. F. Mady, G. E. Awad, K. B. Jorgensen, *Eur. J. Med. Chem.* **2014**, *84*, 433.

[28] D. R. Buckle, D. J. Outred, C. J. M. Rockell, H. Smith and B. A. Spicer, *J. Med.Chem.* **1986**, *29*, 2267.

[29] D. R. Buckle, D. J. Outred, C. J. M. Rockell, H. Smith and B. A. Spicer, *J. Med.Chem.* **1983**, *26*, 251.

[30] C. J. Buckle and D. R. Rockell, *J. Chem. Soc.* **1982,** *1*, 627.

[31] M. Z. Griffiths and P. L. A. Popelier, *J. Chem. Inf. Model*. **2013**, *53*, 1714.

[32] N. Gouault, J. F. Cupif, A. Sauleau and M. David, *Tetrahedron Lett.* **2000**, *41*, 7293.

[33] (a) E. Hao, T. Meng, M. Zhang, W. Pang, Y. Zhou and L. Jiao, *J. Phys. Chem. A.* **2011**, *115*, 8234. (b) S. A. Ingale and F. Seela, *J. Org. Chem.* **2012**, *77*, 9352. (c) C. Y.Wang, J. F. Zou, Z. J. Zheng, W. S. Huang, L. Li and L.-W. Xu, *RSC Adv*. **2014**, *4*, 54256.

[34] H.Wamhoff, A. R. Katritzky and C. W. Rees, Comprehensive *Heterocyclic Chemistry*, **1984**, *5*, 669.

[35] M. Gouault, N. Cupif, J. F. Sauleau and A. David, *Tetrahedron Lett.* **2000**, *41*, 7293.

[36] A. C. Lees, B. Evrard, T. E. Keyes, J. G. Vos, C. J. Kleverlaan, M.Alebbi and C. A. Bignozzi, *Eur. J. Org. Chem*. **1999,** 2309.

[37] D. srinivas, VD. Ghule, SP. Tewari, K. Muralidharan, *Chem. Eur. J.* **2012**, *18*,15031.

[38] A. Domling and I. Ugi, *Angew. Chem., Int. Ed.* **2000**, *39*, 3169.

[39] R. Huisgen, *Pure Appl. Chem.* **1989**, *61*, 613.

[40] R. Huisgen, G. Szeimies and L. Moebius, *Chem. Ber.* **1965**, ***98***, 4014.

[41] C. S. Radatz, L.do. A. Soares, E. F. Vieira, D. Alves, D. Russowsky and P. H. Schneider, *New J. Chem.* **2014**, *38*, 1410.

[42] G. Kumaraswamy, K. Ankamma and A. Pitchaiah, *J. Org. Chem*. **2007**, *72*, 9822.

[43] K. R. Reddy, C. U. Maheswari, M. L. Kantam and P. C. Division, *Synth. Commun*. **2008**, *38*, 2158.

[44] J. S. Yadav, B. V. S. Reddy, G. M. Reddy and D. N. Chary, *Tetrahedron Lett*. **2007,** *48*, 8773.

[45] Y. Chen, W-Q. Zhang, B-X. Yu, Y-M. Zhao, Z-W. Gao, Y-J. Jian, L-W. Xu, *Green Chem.* **2016**, *18*, 6357.

[46] F. Alonso, Y. Moglie, G. Radivoy, and M. Yus, *J. Org. Chem.* **2011**, *76*, 8394.

[47] B. S. P. Anil Kumar, K. H. V. Reddy, G. Satish, R. U. Kumar and Y. V. D.Nageswar, *Tetrahedron Letters.* **2012**, *53*, 4595.

[48] H. E. Shahri, H. Eshghi, J. Lari, S. A. Rounagh, *Appl Organometal Chem*. **2017**, e3947.

[49] H. Sharghi, A. Khoshnood, M. M. Doroodmand , R. Khalifeh, *J Iran Chem. Soc.* **2012**, *9*, 231.

[50] H. Naeimi, V. Nejadshafiee, *New J. Chem.* **2014**, *38*, 5429.

[51] T. Shamim and S. Paul, *Catal Lett.* **2010,** *136*, 260–265

[52]H.N.M Elnagdy, K. Gogoi, A.A. Ali and D.Sarma, *Appl Organometal Chem.*, **2018**, *32*, e3931

[53] H. Naeimi and Z. Ansarian, *Inorganica Chimica Acta*. **2017,** *466*, 417–42

[54] N. Singh, *C. R. Chimie*. **2015**, *18*, 1257.

[55] B. Li, Y. Xie and Y. Xue, *J. Phys. Chem C.* **2007**, *111*, 12181.

[56] V. P. P. Weimarn, *Chem. Rev.* 1925, *2*, 217.

[57] A. E. Nielsen, *Acta. Chem. Scand.* **1960**, *14*, 1654.

[58] R. A Johnson and J. D. O'ourke, *J. Am. Chem. Soc*. **1954,** *76*, 2124.

[59] R. A. Day. Jr. and A. L. Underwood, 6th *ed.*, *Quantitative analysis*, Pearson Education India; Sixth edition, (**2015)**.

[60] D. A Skoog, D. M West, F. J Holler and S. R Crouch, *Fundamental analytical chemistry*. Cengage Learning **(2004).**

[61] B. G Kumar and K. Muralidharan, *Eur. J. Inorg. Chem.* **2013,** *32*, 2102.

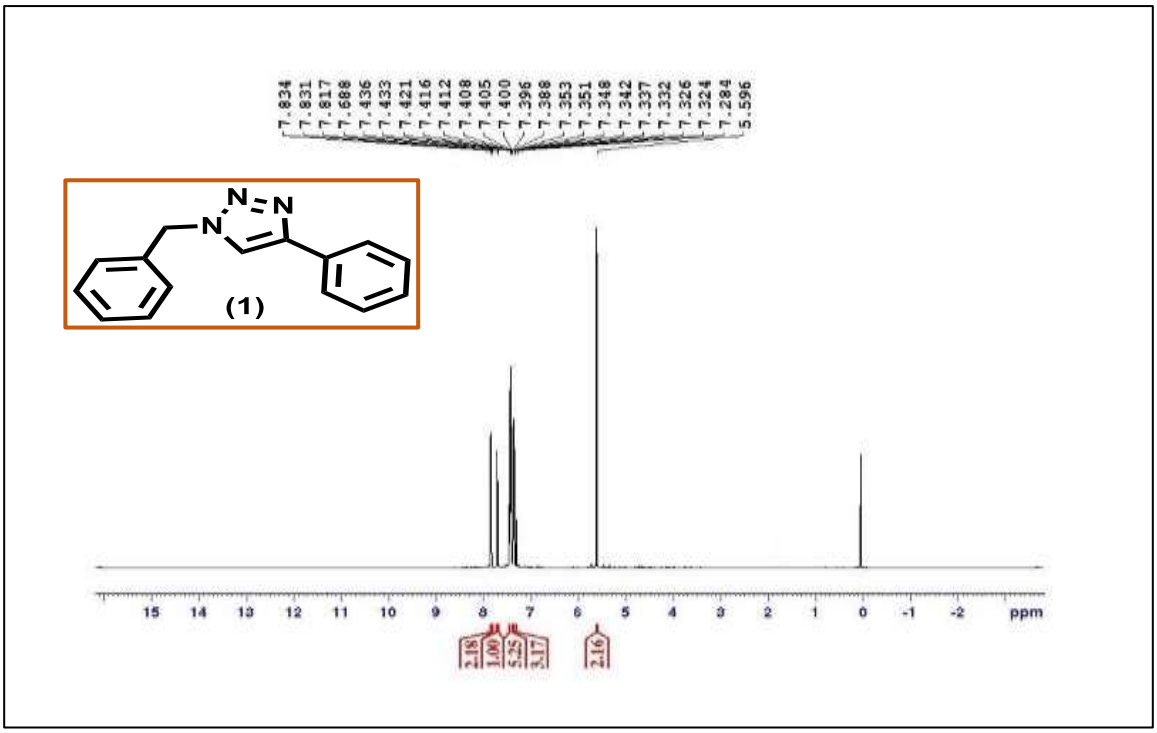

Figure 2.3: ^{1}HNMR spectrum of the compound 1

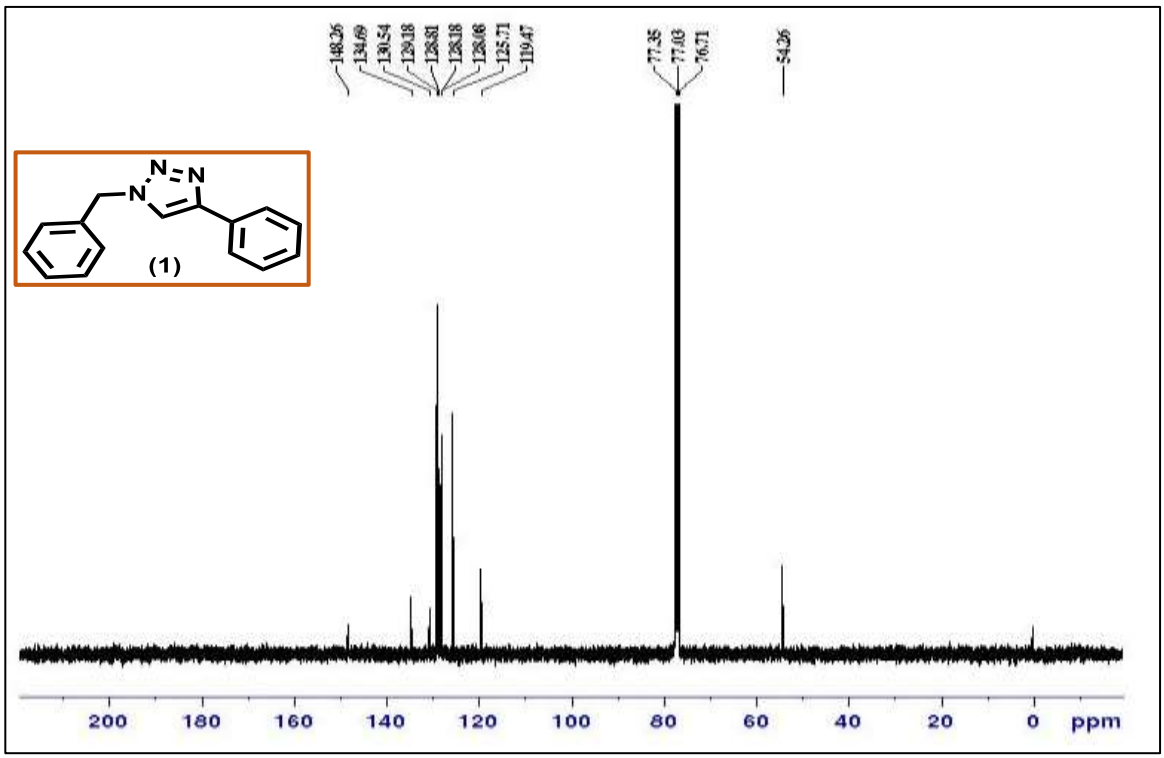

Figure 2.4: ^{13}C NMR spectrum of the compound 1

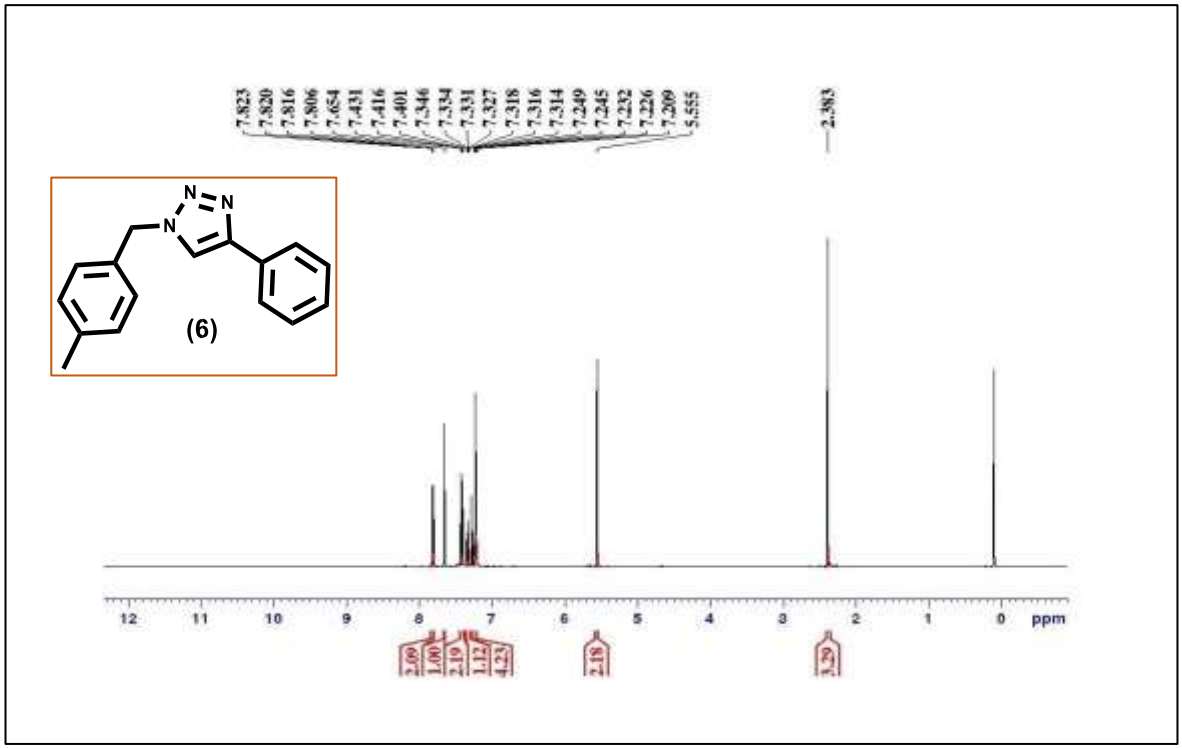

Figure 2.5: ^{1}H NMR spectrum of the compound 6

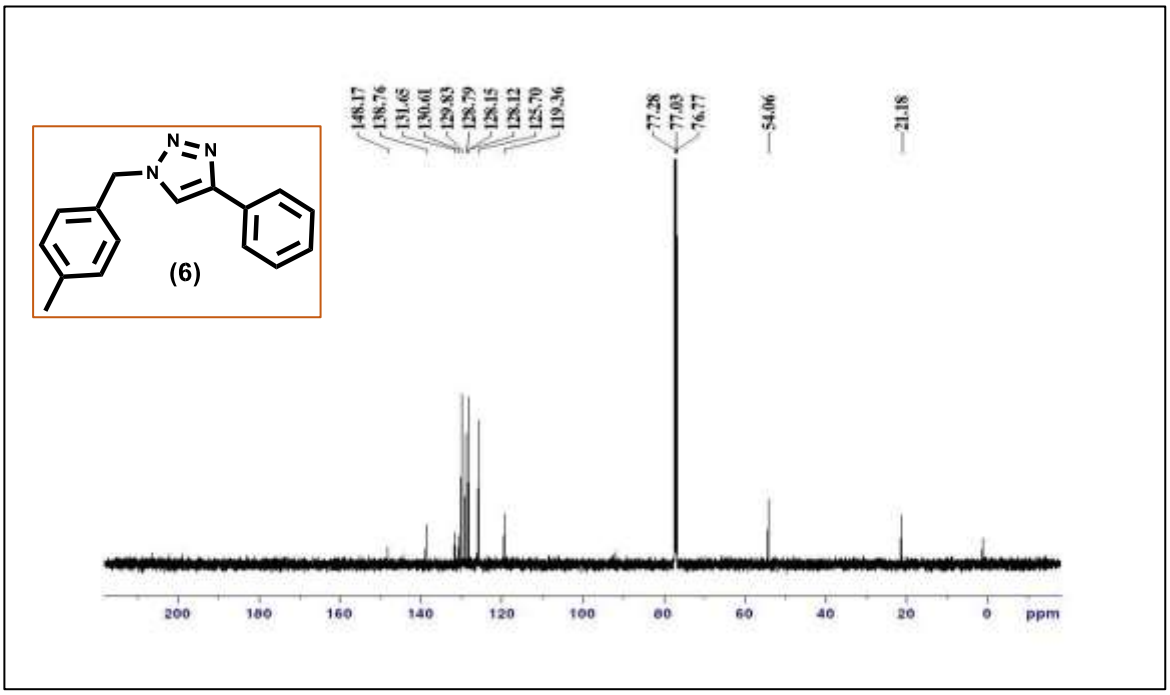

Figure 2.6: ^{13}C NMR spectrum of the compound 6

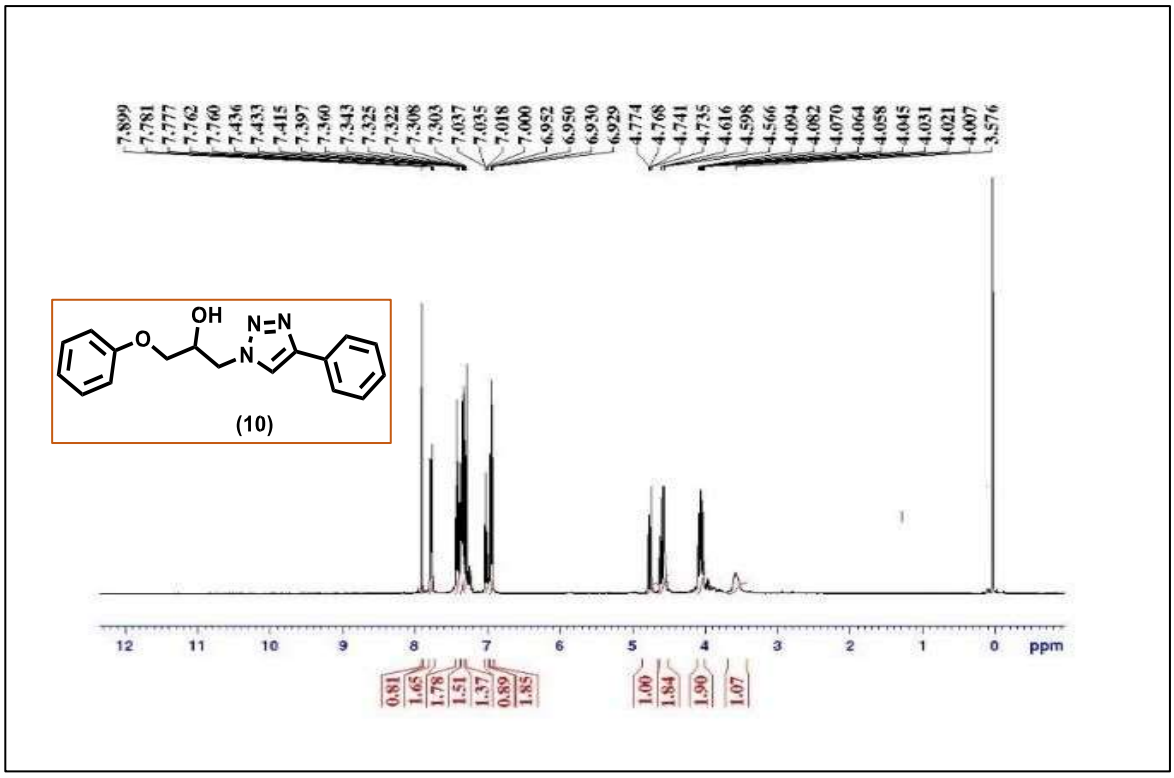

Figure 2.7: ^{1}H NMR spectrum of the compound10

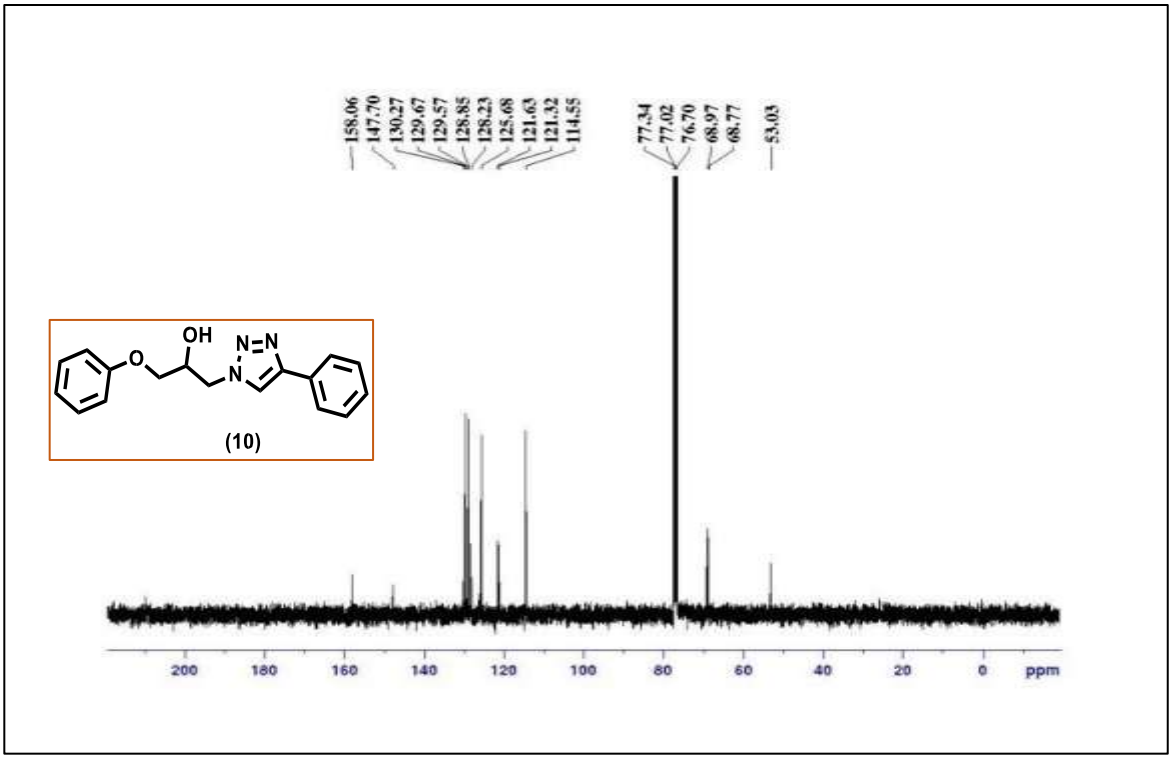

Figure 2.8: ^{13}C NMR spectrum of the compound10

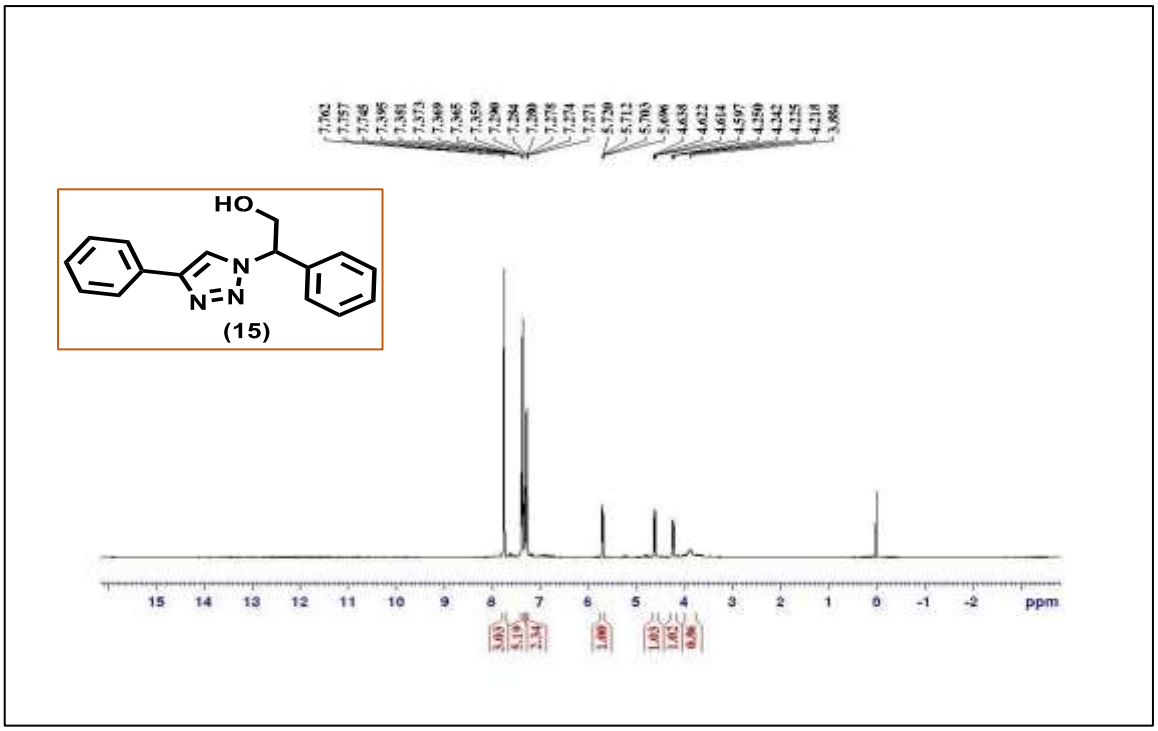

Figure 2.9: ^{1}H NMR spectrum of the compound15

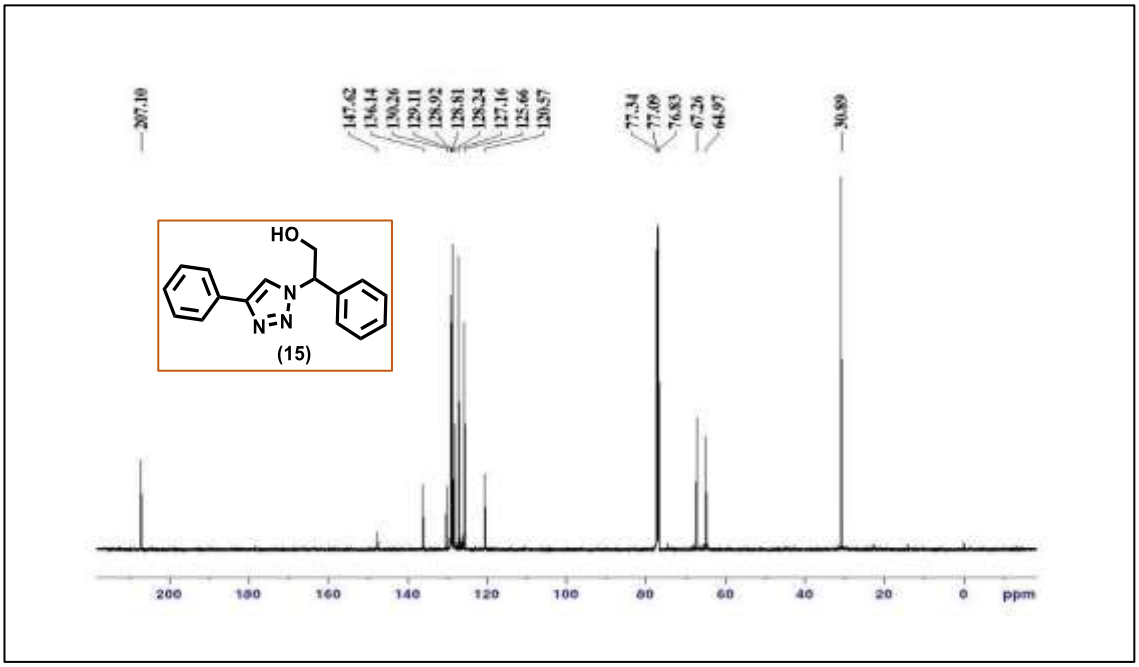

Figure 2.10: ^{13}C NMR spectrum of the compound15

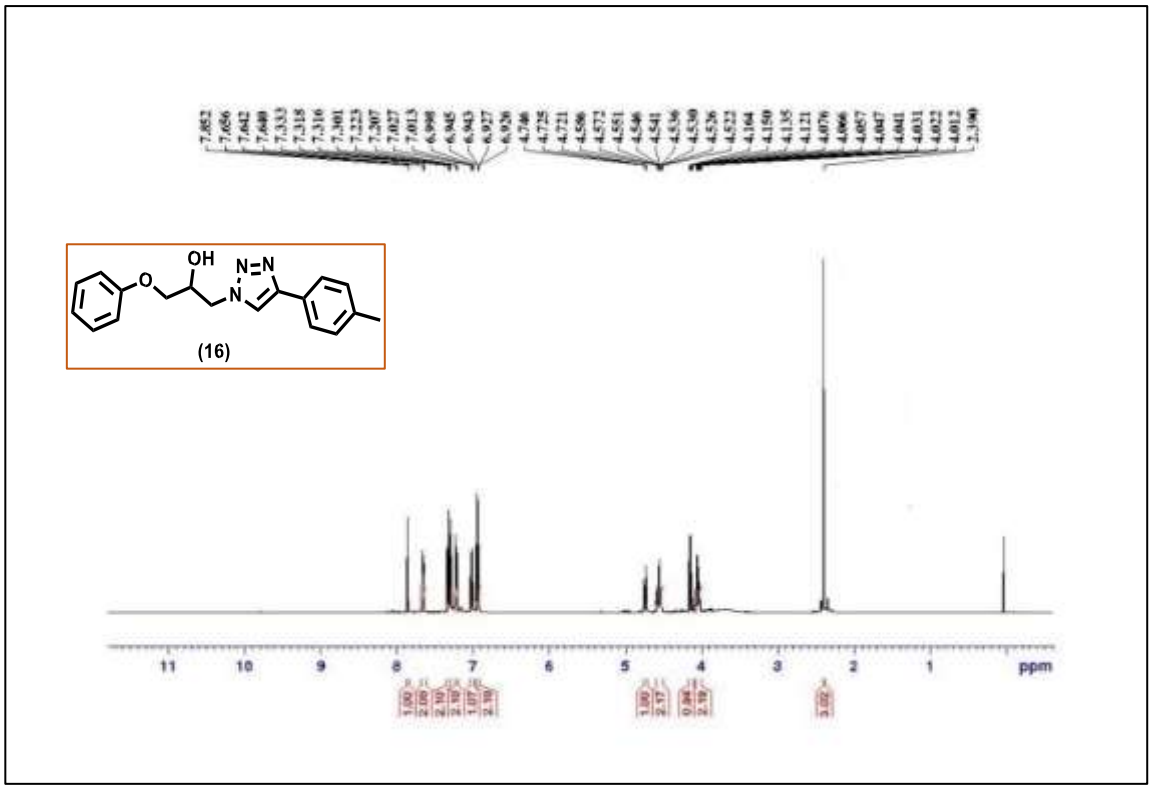

Figure 2.11: ^{1}H NMR spectrum of the compound16

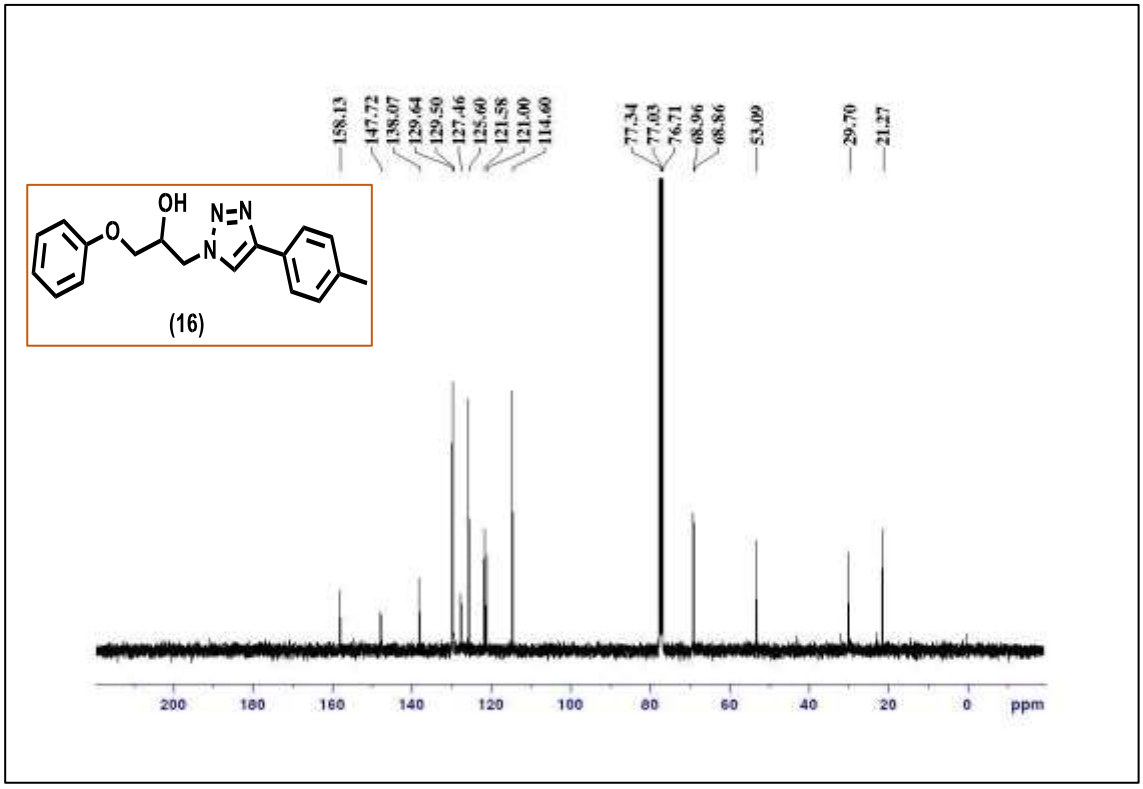

Figure 2.12: ^{13}C NMR spectrum of the compound 16

CHAPTER 3

NIR absorbing surfactant-free $CuInS_2$ nano/micro particles (sf-CIS-np) as catalyst for symmetric Glaser–Hay coupling reactions

Abstract

Catalysis by $CuInS_2$ nanoparticles in the coupling reaction of substituted phenylacetylenes is presented in this chapter. The $CuInS_2$ nano/micro particles (**sf-CIS-np**) were prepared in a simple reaction without using any surfactant molecules. They were used as the catalyst in the dimerization of 1, 3-diyne derivatives while using of 8-diazabicyclo[5.4.0]undec-7-ene (DBU) as the base. These Glassar-Hay coupling reactions were conducted at room temperature in acetonitrile (Time: 4-7 h, depending on the substrate) using 10 mg of **sf-CIS-np**. The maximum yield obtained in these reactions was 97%, while the catalyst was reused for five cycles with little difference in its efficiency.

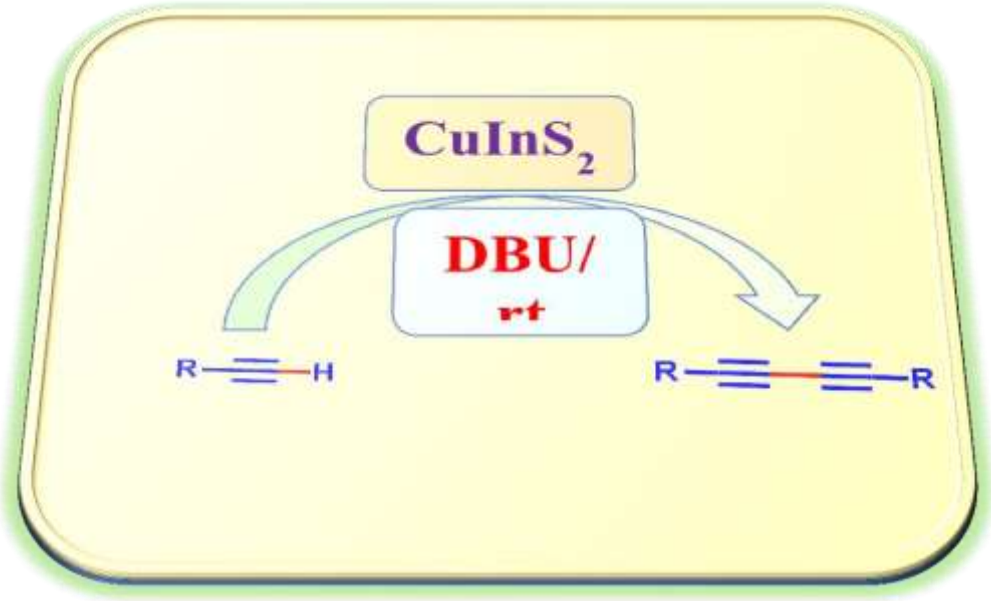

3.1. Introduction

The non-toxic ternary chalcogenide semiconducting nanoparticles such as $CuInS_2$, $CuInSe_2$, and $CuIn_xGa_{1-x}Se_2$ are attractive materials for various uses. Among the I-III-VI group-based materials, $CuInS_2$ possess good photoconductivity, large absorption coefficients, and bandgap value matching with the visible solar spectrum [1-7]. The bandgap of this material can be adjusted by altering the particle size, which provides the probability to match a particular part of the solar spectrum [8-10]. The tenability gives the material a choice to be very useful in solar cells, photocatalytic splitting of water [11], light-emitting diodes [12-13], bio-imaging [14-15], and nonlinear optical devices [16-17]. Because of these applications, the synthesis of ternary chalcogenide semiconductor materials has received more interest. Some of the methods available to synthesize $CuInS_2$ are elemental hydrothermal [18], solvothermal method [19-20], microwave irradiation technique [21-22], single-source molecular precursor [23-25], and hot injection techniques [26-27].

Producing 1,3-diynes via coupling of terminal alkynes to is appealing to the synthetic community. 1,3-Diynes present in numerous natural products, and they are useful as bioactive and pharmaceutical compounds with antifungal, antibacterial, anti-HIV, antiinflammatory, or anticancer activities [28-32]. These compounds also serve as basic building blocks for synthesizing many advanced materials including conjugated polymers, molecular wires, and liquid crystals, [33-34]. These applications made it attractive in recent decades. The Glaser–Hay reaction is one of the conventional synthetic methods available for the construction of conjugated 1,3-diynes is [35]. This reaction was reported first by Carl Andreas Glaser in 1869, where the copper salts were used as the catalysts. Much progress has been made in the past decade to improve this methodology, where copper received the most attention [36].

At present, two methods are used extensively to synthesize 1,3-diyne derivatives. The first method make use of alkenyl halides possessing leaving groups that undergo elimination under basic conditions with a copper catalyst to yield the desired 1, 3-diyne [37]. The other method is the transition metal-catalyzed homocoupling reaction of terminal alkynes in the presence of a base or ligand [38]. For example, recently, Elhamifar

and co-workers reported the synthesis of 1, 3-diyne in ionic liquid using novel nanoporous organo silica-supported Pd and CuI as a catalytic combination [39]. Significant endeavors have been made to design and synthesize more efficient and feasible catalysts to improve the catalytic activity compared to this Pd/Cu bi-metallic framework for oxidative coupling of terminal alkynes. Transition metals such as Pd [40], Cu [41], Ni [42], Co [43], and Ti [44] were tested in many places. Some other catalysts employed for alkyne coupling include RGO-Ni [45], L_2^{NIS} Cu^{II} [46], CuI [47], GO@Cu(II) [48], and SiO_2/SSQ/Au [49]. However, there are still challenges in catalysis, such as the use of expensive and toxic catalysts, the constraint of using complex ligands, and harsh reaction conditions.

The ternary transition metal sulfides such as $ZnIn_2S_4$, $CdIn_2S_4$, and $CdLa_2S_4$ can directly function as photocatalysts for visible-light-induced organic transformations without any ancillary modifications [50]. Thus, these materials occupy a prominent place in the heterogeneous catalysis for many organic transformations such as C-C, C-N, and C-S coupling reactions, oxidation, and reduction reactions [51]. However, it can be noted that despite many catalytic applications of ternary metal sulfides as a photocatalyst for organic transformation, their catalytic activity for C-C coupling reactions specifically for 1,3-diyne synthesis is unexplored. Our research group at the University of Hyderabad has been concentrating on developing green and sustainable heterogeneous catalysts for organic transformation.

The synthetic method plays a significant role in determining the material's properties by controlling size and shape. The control can be attained in the wet chemical synthetic method by changing reaction temperature, solvent, surfactant, nature of precursors, and other reaction conditions. However, whatever the method may be, the easy availability of the material's surface for catalysis without any hindrance is indispensable. Earlier, in our group, surfactantfree synthesis of binary and ternary metal chalcogenides was developed [52-53]. Chapter 2 described the multicomponent dipolar cycloaddition catalyzed by surfactant-free CuS nano/micro flowers (**sf-CuS mf**). We have explored the catalytic activity of surfactant-free $CuInS_2$ nanoparticles (**sf-CIS-np**) for useful transformations of alkynes in our continuing endeavor.

This chapter reports the catalytic activity of ternary metal chalcogenide nano/micro particles (**sf-CIS-np**) produced by chemical synthetic approach without using any surfactants or templates. The synthesis of **sf-CIS-np** was reported earlier from our lab

(2015 Sanyasinaidu gottapu, Synthesis and characterization of metal (Al) and metal chalcogenides nanoparticles). In this present work, it is used as a catalyst in the dimerization of 1, 3-diyne derivatives in the presence of DBU as the base. The synthesis explained here was carried out in acetonitrile, and the heterogeneous catalyst was recyclable readily.

3.2. Results and discussion

3.2.1. Production of $CuInS_2$ (sf-CIS-np) nanoparticles and its characterization

Many synthetic methods such as hot injunction method, thermal decomposition of single precursor, hydrothermal or solvothermal, template-assisted growth, soft template way, microwave irradiation, sonochemical techniques, CVD, and electrochemical methods are developed to prepare semiconducting binary metal chalcogenide nanoparticles [54]. However, only a few methods are available for the synthesis of ternary metal chalcogenide nanocrystals. This is because in ternary systems, three elements are involved in the reaction, and it is necessary to consider the reactivity of all elements. If the reactivity is not controlled, elements will form two different binary compounds or nucleus growth into heterodimers. A simple solution-phase surfactant-free synthesis of $CuInS_2$ nanoparticles (**sf-CIS**) was developed in our lab. In this reaction, the limited solubility of the metal sources and fast reactivity them with $LiBH_4$ driven the formation of nano/micro particles under a thermodynamically favorable condition that encouraged the nucleation of particles. We have prepared **sf-CIS-np** at ambient temperature in less time (3h) without using any template or surfactant molecules in the present work. To synthesize $CuInS_2$ nanoparticles, $Cu(OAc)_2$, $InCl_3$, and S are used in 1:1:2 ratio respectively while $LiBH_4$ was used as a reducing agent (Scheme 3.1). The final product was characterized by PXRD patterns, EDX, FESEM, and UV–Vis-NIR spectrum.

$$Cu(OAc)_2 + InCl_3 + LiBH_4 + S \xrightarrow[\text{reflux, 3h}]{\text{toluene}} CuInS_2$$

Scheme 3.1: Synthesis of copper indium sulfide nanoparticles

PXRD pattern (Figure 3.1) of **sf-CIS-np** showed the obtained product had a tetragonal crystal structure (a=b=5.523 Å, c=11.12 Å) with body-centered lattice (JCPDS # 89-6095). In PXRD spectrum, the obtained broad diffraction peaks around (2θ) =27.8, 32.3, 54.7, 75.2 (°) were matching with the (1 1 2), (2 0 0), (1 1 6) and (3 2 5) planes of the tetragonal crystal structure. No other characteristic peaks were corresponding to

$Cu(OAc)_2$, Cu_2O, CuO, CuS, and In_2S_3, or any other phase of $CuInS_2$. These observations established the phase purity of **sf-CIS-np**. The energy EDAX spectrum (Figure 3.2) of **sf-CIS-np** was consistent and substantiated the presence of elements Cu, In, and S in the material and there were no other elements present.

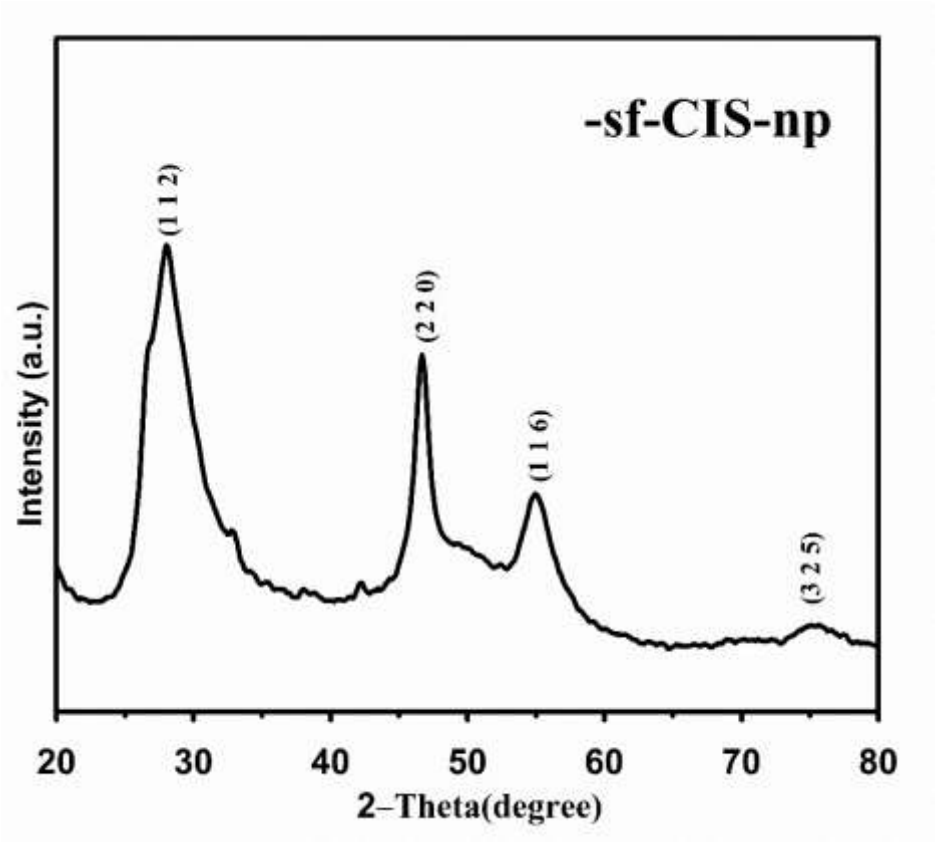

Figure 3.1: Powder X-ray diffraction (PXRD) of **sf-CIS-np**

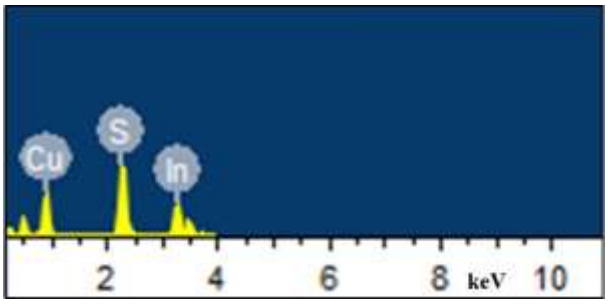

Figure 3.2: Energy dispersive X-ray analysis (EDAX) spectrum of **sf-CIS-np**

The FESEM images were acquired to perceive the shape and size of the **sf-CIS-np**. The FESEM image of **sf-CIS-np** (Figure 3.3) depicted spherical aggregates of particles of sizes ranging from 30-50 nm. The UV-Visible -NIR spectrum of **sf-CIS-np** (Figure 3.4) showed the absorption maximum at 468 nm.

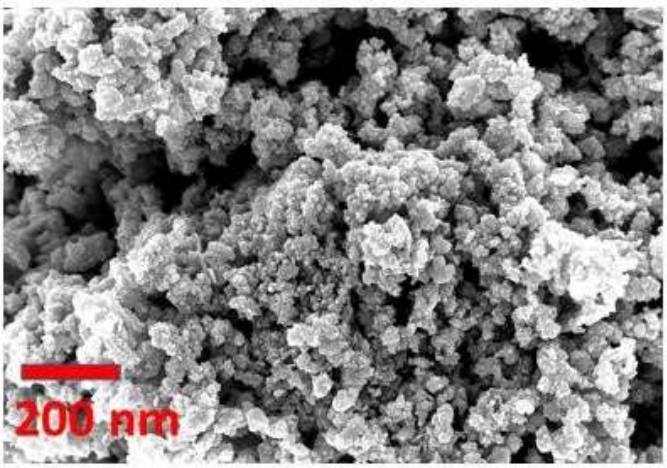

Figure 3.3: FE-SEM images of **sf-CIS-np**

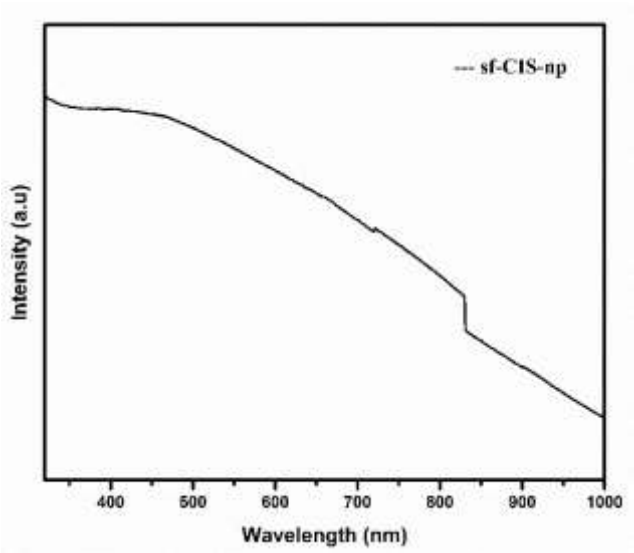

Figure 3.4: UV–Vis–NIR spectrum of **sf-CIS-np**

3.2.2. Catalytic application

Numerous reactions are catalyzed by metal salts, bimetallic systems as well as metal composite nanoparticles. The catalysis by nanoparticles is much more enticing due to the boosted catalytic activity associated with the huge surface area to volume ratio. However, in the synthesis of nanoparticles, long-chain organic molecules are used as stabilizing molecules. These molecules surrounding the nano/micro particles hide the active centers and limit or minimize their catalytic activity. We have produced **sf-CIS-np** by solution-phase method at moderate temperature without using any surfactants or templates to outsmart this issue. In this material, the catalyst surface was freely available for adsorption

and desorption reactions because no organic surfactant molecules were surrounding the particles,

As discussed earlier, (section 3.1) dimerization of acetylene derivatives via Glaser-Hay coupling has arisen as one of the most effective and extensively used Cu-catalyzed reactions to produce 1,3-diynes. The free, unhindered surface on **sf-CIS-np** is expected to influence activity significantly when used as the catalyst in the reactions of 1,3-diynes synthesis. Therefore, we tested the catalytic activity of **sf-CIS-np** in the Glaser-Hay coupling reaction using various substituted phenylacetylene. In all cases, the reaction progress was watched by TLC. Further, the reaction product was purified by eluting via column chromatography and the products were characterized using NMR spectral data (^{1}H and ^{13}C).

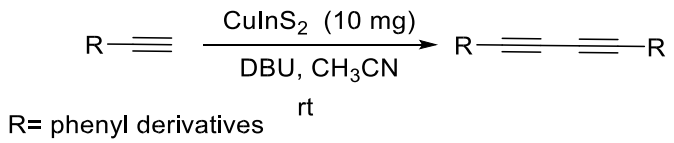

Scheme 3.2: Synthesis of homocoupling of phenyl acetylene derivatives

First, the reaction conditions were optimized to synthesize 1,3-diynes from phenylacetylene using different bases and solvents through homo-coupling reaction (Scheme 3.2). Few reactions were carried out in different solvents to pick the medium of the reaction. No product was obtained in water and dimethylformamide, whereas the yields (in brackets) in other solvents are as follows; Methanol (34%), dichloromethane (39%), n-butanol (20%), chloroform (56%). It was found that the reaction progressed perfectly in acetonitrile and (Table 3.1, entry 5) while the yields were low when the reaction was performed in other solvents (Table 3.1, entries 1–4). When acetonitrile was utilized as a solvent, the reactions were completed in 4-7 h at room temperature and quantitatively yielded the preferred products. While we screened various bases for the phenylacetylene coupling reaction, the base DBU provided the best result compared with other bases like NaOH, KOH and triethyl amine.

Table 3.1: Optimization of reaction condition for coupling reaction

Entry	Solvent	Time (h)	Yield (%)
1	Methanol	24	34
2	Dichloro methane	24	39
3	n-butanol	24	20
4	Chloroform	24	56
5	Acetonitrile	4	96
6	Water	24	no
7	DMF	24	no

Few reactions were done by altering the catalyst quantities in various solvents to find a sufficient quantity of catalyst required for the reaction. The progression of all these reaction was checked by TLC. The catalyst **sf-CIS-np** was isolated at the end of the reaction by filtering. Furthermore, the product was worked-up with ethyl acetate and water. There was no change in yield when the catalyst's amount in the reaction was 20, 15, 10, and 5 mg. While 5 mg of **sf-CIS-np** was utilized, the reaction prolonged much for the completion (above 12 h). Therefore, it was chosen to utilize 10 mg of **sf-CIS-np** for further investigations. After optimizing conditions (rt, 4-7 hours), the reaction was generalized with 10 mg of **sf-CIS-np** as the catalyst; DBU as the base; acetonitrile as the solvent. With this condition, various substituted benzyl acetylenes were reacted to form 1,3-diynes (Table 3.2). Mostly, all these reactions (except Table 3.2, entries 3, 7, and 8) produced the respective products in greater than 95% yields at room temperature.

Numerous catalysts for the coupling reactions were described in the literature. The efficiency of the different catalysts in the coupling reaction (phenylacetylene as substrate) was compared (Table 3.3) to recognize the impact of surfactant-free catalyst. Most of those catalysts were used at a temperature above 80 °C except for CuI and L_2^{NIS} Cu^{II}, while our **sfCIS-np** was working at room temperature and required less amount of catalyst (10mg) except GO@Cu(II)**.** Further, **sf-CIS-np** studied here was prepared in easy reaction conditions while the products were obtained in good yield.

Table 3.2: Synthesis of homocoupling of phenyl acetylene derivatives

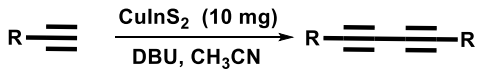

Entry	Substrate	Time	product	Yield%
1	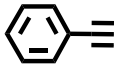	4	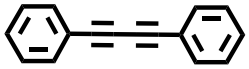	96%
2	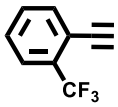	6	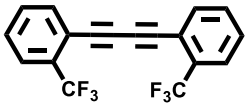	99%
3		5	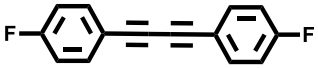	80%
4	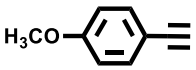	4	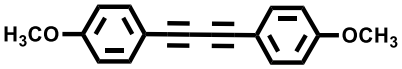	97%
5	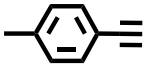	4	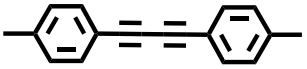	95%
6		6	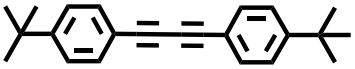	96%
7	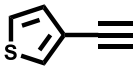	7	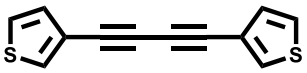	79%
8	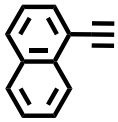	5	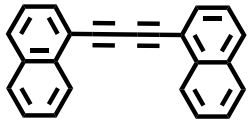	75%
9	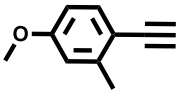	6	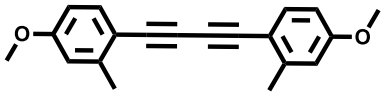	95%
10	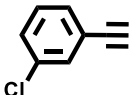	5	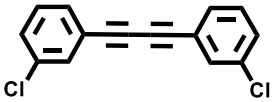	97%

Table 3.3: Comparison results from numerous catalysts used for the Glaser-Hay coupling

Catalyst	Substate	Catalyst load (mg)	Time (h)	Temperature (°C)	Yield (%)	Ref
RGO-Ni	Phenylacetylene	50	3	85	99	[61]
L_2^{NIS} Cu(II)	Phenyl acetylene	63	2.5	RT	100	[62]
CuI	Phenyl acetylene	28	12	RT	98	[63]
GO@Cu(II)	Phenyl acetylene	10	2	80	99	[64]
SiO_2/SSQ/Au	Phenyl acetylene	18	18	80	99	[65]
sf-CIS-np	**Phenyl acetylene**	**10**	**4 h**	**RT**	**96**	**This work**

3.2.3. Leaching study and recyclability of sf-CIS-np as catalyst

A leaching study was executed on the heterogeneous catalysis in the Glaser-Hay coupling reaction (scheme 3.2). Thus, the reaction was stopped after around 20% product formation, and **sf-CIS-np** was isolated from the reaction mixture. It was then allowed to progress without **sf-CIS-np** for further 8 h, yet no significant increase in the amount of product was observed. This observation revealed the functioning of heterogeneous catalysis in these reactions.

The reusability of the catalyst plays an important role in deciding the real use of such heterogeneous systems. Therefore, experiments were done in which alkynes (5mmol of reagents) were reacted utilizing the recovered **sf-CIS-np**. After the initial reaction, the product was removed using ethyl acetate, and **sf-CIS-np** was recovered by decanting the reaction mixture, and then it was dried at 60 °C. A fresh reaction was carried out with new reactants under similar conditions applying the recovered **sf-CIS-np**. After completing the reaction, the catalyst was recycled by following the cycle in the same manner. This study confirmed that **sf-CIS-np** may be reused for five times with little modification in its activity (Figure 3.5).

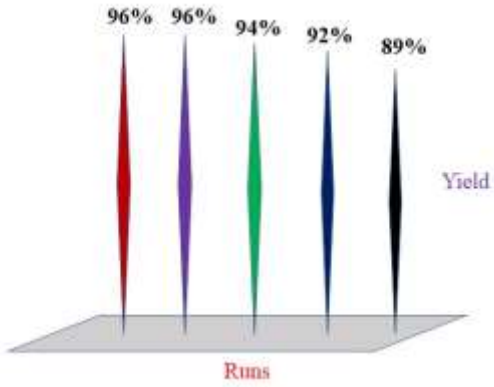

Figure 3.5: Bar diagram showing the results of recycling of **sf-CIS-np** as catalyst in the Glaser-Hay coupling

3.3. Conclusion

The copper-indium-sulfide ($CuInS_2$) nanoparticles (**sf-CIS-np**) were prepared without using any surfactant molecules. These nanoparticles were used as the heterogeneous catalyst for homo-coupling reactions involving phenylacetylene derivatives. The reaction optimization studies established that 10 mg of **sf-CIS-np** is sufficient to complete the reactions within 4-7 h at room temperature, depending on the substrate. These reactions gave the best result when the base DBU and solvent acetonitrile were used. The maximum yield obtained in these reactions was 97%. The catalyst was reused for five cycles with little difference in its efficiency.

3.4. Experimental section

3.4.1. Materials

The chemicals, $CuCl_2$, $InCl_3$, S, and all the phenyl acetylenes were purchased from SigmaAldrich Chemical Co and used without any purification process. Anhydrous Na_2SO_4 were purchased from Merck, India. Solvents were dried and distilled through the standard procedure and then used for workup and column chromatography. TLC was done using aluminium plates coated with silica gel 60-120 mess, which was purchased from MERCK. The yields of the compounds reported here are isolated yields. Schlenk line technique was applied to maintain the standard air-free conditions.

3.4.2. Instrumentations

The following instruments were used to characterize the **sf-CIS-np** samples. (i) Bruker D8 Xray diffractometer [λ (Cu-Kα) = 1.54A°, scan rate of 1°/min], (ii) Ultra 55 Carl Zeiss Field Emission Scanning Electron Microscopy (Operating voltage = 10 kV), (iii) JASCO UVVisible-NIR Spectrophotometer MODEL V-770, (iv) Buchi B-540 apparatus for melting points, and (v) Bruker (500 or 400 MHz) NMR spectrometer.

For microscopic analyses, and the **sf-CIS-np** samples dispersed in methanol were dropped on the glass plate and then mounted on a stub using conductive carbon tape. ^{1}H NMR and ^{13}C NMR spectra of organic compounds in $CDCl_3$ were acquired in at ambient temperature.

3.4.3. Synthesis of surfactant-free $CuInS_2$ nanoparticles (sf-CIS-np)

In the systematic procedure, the sulfur powder (0.058g, 1.8 mmol) was dissolved in of dry toluene (10 ml) in a two neck round bottom flask (50 ml). Then, $InCl_3$ (200 mg, 0.9 mmol), Cu $(OCOCH_3)_2$ (164 mg, 0.9 mmol), and $LiBH_4$ (98 mg, 4.49 mmol) were added. The reaction mixture inside the flask was refluxed until the reaction mixture turned black (approximately for 3 h) with stream nitrogen. Then, the stirring was stopped and the volatile compounds were evacuated by applying high-vacuum. To remove unreacted lithium salts, starting materials, and other side products, the resultant product was washed using methanol and toluene by sonication followed by centrifugation methods. It was dried 6 h under vacuum to get black $CuInS_2$ nanoparticles (**sf-CIS**). The obtained product was characterized by using different techniques such as PXRD, FESEM, EDX, and UV–Vis absorption spectroscopy.

3.4.4. Typical procedure for homocoupling reactions

A mixture of phenylacetylene (0.052 g, 0.50 mmol), 8-diazabicyclo 5.4.0 undec-7-ene (DBU) (0.074 g, 0.50 mmol) and **sf-CIS-np** (10 mg) in acetonitrile (1.0 mL) was stirred under air (at rt, 4 h). The reaction progress was monitored by TLC, and finally the suspended material was filtered to get back the catalyst. Afterward, the filtrate was diluted with saturated aqueous NH_4Cl, and the water layer was extracted repeatedly by

$CH_3COOC_2H_5$. All organic extracts were mixed together, washed with brine, and dried over Na_2SO_4. It was concentrated under reduced pressure to get the crude substance, which was purified by eluting through a column packed with silica gel using n-hexane to obtain the corresponding diyne as a white solid.

Spectral data of homocoupling of phenyl acetylene derivatives

1,4-diphenyl buta-1,3-diyne:

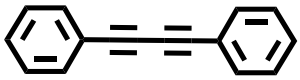

(1)

Melting point	: 85-86 °C (white solid).
^{1}H NMR (400 MHz, $CDCl_3$)	: δ= 7.55-7.57 (m, 4 H), 7.35-7.40 (m, 6 H).
^{13}C NMR (101MHz, $CDCl_3$)	: δ= 132.5, 129.2, 128.4, 121.7, 81.5, 73.9.
HRMS	: $[M + H]^+$ = m/z 203.

1,4-Bis(2-(trifluoromethyl)phenyl)buta-1,3-diyne:

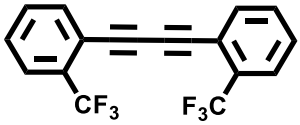

(2)

Melting point	: 67−69 °C (white solid).
^{1}H NMR (400 MHz, $CDCl_3$)	: δ = 7.70-7.75 (m, 4H), 7.49−7.57 (m, 4H);
^{13}C NMR (101 MHz, $CDCl_3$)	: δ = 135.1, 131.4, 129.0, 126.0, 124.3, 122.2, 119.8, 78.7, and 78.5.
HRMS	: $[M+H]^+$ = m/z 339.

1,4-bis(p-fluorophenyl) buta-1,3-diyne:

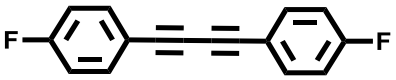

(3)

Melting point	: 192-193 °C (white solid).
^{1}H NMR (400 MHz, $CDCl_3$)	: δ= 7.52-7.56 (m, 4H), 7.04-7.09 (m, 4H).
^{13}C NMR (101 MHz, $CDCl_3$)	: δ= 164.1, 162.4, 134.5, 117.8, 116.0, 115.8, 80.6, 73.7.
HRMS	: $[M+H]^+$ = m/z 239.

1,4-bis(p-methoxyphenyl) buta-1,3-diyne:

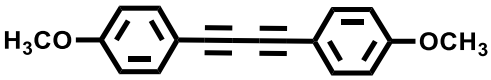

(4)

Melting point	: 134−135 °C (white solid).
^{1}H NMR (500 MHz, $CDCl_3$)	: δ= 7.46-7.50 (m, 4H), 6.86-6.89 (m, 4H), 3.85 (s, 6H).
^{13}C NMR (126 MHz, $CDCl_3$)	: δ= 160.2, 134.0, 114.0, 114.11, 80.9, 73.2, 55.4.
HRMS	: $[M + H]^+$ = m/z 263.

1,4-Bis(4-ethylphenyl)buta-1,3-diyne:

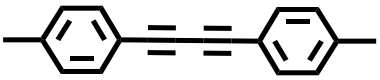

(5)

Melting point : 181−183 °C (white solid).

^{1}H NMR (400 MHz, $CDCl_3$) : δ= 7.44 (d, J = 8 Hz, 4 H), 7.16 (d, J =8 Hz, 4 H), 2.39 (s, 6 H);

^{13}C NMR (101 MHz, $CDCl_3$) : δ= 139.4,139.2, 132.3,132.1, 129.5, 118.4, 81.4, 72.9, 21.7.

HRMS : $[M + H]^+$ = m/z 231.

1,4-Bis(4-(tert-butyl)phenyl)buta-1,3-diyne: (colour less liquid)

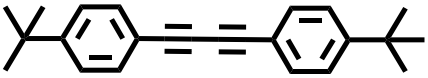

(6)

^{1}H NMR (500 MHz, $CDCl_3$) : δ= 7.48-7.50 (m, 4H), 7.37-7.39 (m, 4H), 1.34 (s, 18H);

^{13}C NMR (126 MHz, $CDCl_3$) : δ= 152.5, 132.0, 125.2, 118.9, 81.4, 73.4, 34.5, and 31.1 ppm;

HRMS : $[M + H]^+$ = m/z 315.

1,4-dithienyl buta-1,3-diyne:

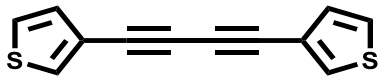

(7)

Melting point : 111-112 °C (white solid).

^{1}H NMR (400 MHz, $CDCl_3$) : δ= 7.61-7.62 (m, 2H), 7.30-7.32 (m, 2H), 7.19-7.29 (m, 2H).

^{13}C NMR (101 MHz, $CDCl_3$) : δ= 131.2, 130.1, 125.6, 120.9, 76.5, 73.5.

HRMS : $[M + H]^+$ = m/z 215.

1,4-dinaphthyl buta-1,3-diyne:

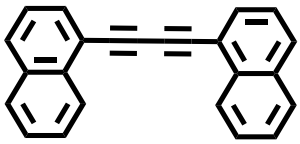

(8)

Melting point : 171-172 °C (yellow solid).

^{1}H NMR (500 MHz, $CDCl_3$) : δ= 8.46 (d, J = 8.3 Hz, 2H), 7.91 (d, J = 8.3 Hz, 2H), 7.87 (d, J = 8.3 Hz, 2H), 7.84 (dd, J = 7.2, 1.3 Hz, 2H), 7.64-7.68 (m, 2H), 7.56-7.61 (m, 2H), 7.47-7.51 (m, 2H).

^{13}C NMR (126 MHz, $CDCl_3$) : δ= 144.1, 133.9, 133.1, 132.0, 129.7, 128.4, 127.2, 126.7, 126.2, 125.2, 119.5, 80.9, 76.6.

HRMS : $[M + H]^+$ = m/z 303.

1,4-Bis(4-methoxy-2-methylphenyl)buta-1,3-diyne:

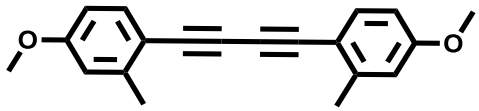

(9)

Melting point : 66−68 °C (white solid).

^{1}H NMR (500 MHz, $CDCl_3$) : δ= 7.45 (d, J = 9.0 Hz, 2H), 6.77 (d, J = 2.5 Hz, 2H) 6.70−6.73 (m, 2H), 3.83 (s, 6H), 2.49 (s, 6H);

^{13}C NMR (126 MHz, $CDCl_3$) : δ= 160.2, 143.5, 134.3, 115.2, 114.1, 111.4, 80.8, 76.4, 55.1, and 20.7;

HRMS : $[M + H]^+$ = m/z 291.

(10) 1,4-bis(3-chlorophenyl)buta-1,3-diene:

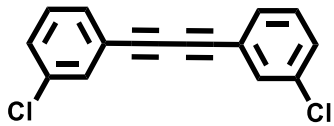

(10)

Melting point : 174−176 °C (white solid).

^{1}H NMR (500 MHz, CDCl3) : δ= 7.47 (t, J = 8 Hz, 1H), 7.44 (t, J = 8 Hz, 1H), 7.38 (t, J = 8 Hz, 1H), 7.36 (t, J = 8 Hz, 1H), 7.33-7.34 (m,1 H), 7.31-7.32 (m,1 H), 7.21-7.24 (m, 2H);

^{13}C NMR (126 MHz, CDCl3) : δ= 134.3, 132.2,130.6, 130.2, 129.7, 123.2, 80.5, 74.6.

HRMS : $[M + H]^+$ = m/z 271.

3.5. References

[1] Y. H. Yang and Y.-T. Chen, *J. Phys. Chem. B.* **2006**, *110*, 17370.

[2] H. Zhong, Y. Li, M. Ye, Z. Zhu, Y. Zhou, C. Yang and Y. Li, *Nanotechnology*. **2007**, *18*, 025602.

[3] P. M. Allen and M. G. Bawendi, *J. Am. Chem. Soc.* **2008**, *130*, 9240-9241.

[4] H. Zhong, S. S. Lo, T. Mirkovic, Y. Li, Y. Ding, Y. Li and G. D. Scholes, *ACS Nano*. **2010,** *9*, 5253.

[5] Q. Guo, S. J. Kim, M. Kar, W. N. Shafarman, R. W. Birkmire, E. A. Stach, R. Agrawal and H. W. Hillhouse, *Nano Lett.* **2008**, *8*, 2982.

[6] M. G. Panthani, V. Akhavan, B. Goodfellow, J. P. Schmidtke, L. Dunn, A. Dodabalapur, P. F. Barbara and B. A. Korgel, *J. Am. Chem. Soc*. **2008**, *130*, 16770.

[7] J. Tang, S. Hinds, S. O. Kelley and E. H. Sargent, *Chem. Mater.* **2008,** *20*, 6906.

[8] D. Pan, X. Wang, Z. H. Zhou, W. Chen, C. Xu and Y. Lu, *Chem. Mater***. 2009**, *21*, 2489.

[9] Y. H. A. Wang, X. Zhang, N. Bao, B. Lin, and A. Gupta, *J. Am. Chem. Soc.* **2011**, *133*, 11072.

[10] M. Y Chiang, S.-H. Chang, C.-Y. Chen, F.-W. Yuan and H.-Yu. Tuan, *J. Phys. Chem. C.* **2011**, *115*, 1592.

[11] L. Zheng, Y. Xu, Y. Song, C. Wu, M. Zhang, and Y. Xie, *Inorg. Chem.* **2009**, *48*, 4003.

[12] W. S. Song and H.Yang, *Chem. Mater.* **2012**, *24*, 1961.

[13] H. Zhong, Z. Wang, E. Bovero, Z. Lu, F. C. J. M. van Veggel, and G. D. Scholes, *J. Phys. Chem. C.* **2011**, *115*, 12396.

[14] J. Y. Lee, D. H. Nam, M. H. Oh, Y. Kim, H. S. Choi, D. Y. Jeon, C. B. Park and Y.S. Nam, *Nanotechnology*. **2014**, *25*, 175702.

[15] L. Li, T. J. Daou, I. Texier, T. T. K. Chi, N. Q. Liem and P. Reiss, *Chem. Mater.* **2009,** *21*, 2422.

[16] K. Nose, T. Omata and S. Otsuka-Yao-Matsuo, *J. Phys. Chem. C*. **2009**, *113*, 3455.

[17] H. Zhong, Y. Zhou, M. Ye, Y. He, J. Ye, C. He, C. Yang and Y. Li, *Chem. Mater*. **2008**, *20*, 6434.

[18] J. Xiao, Y. Xie, R. Tang and Y. Qian, *J. Solid State Chem.* **2001,** *161*, 179.

[19] Y. Jiang, Y. Wu, X. Mo, W. Yu, Y. Xie and Y. Qian, *Inorg. Chem*. **2000,** *39*, 2964.

[20] Y. Jiang, Y. Wu, S. Yuan, B. Xie, S. Zhang and Y. Qian, *J. Mater. Res.* **2001**, *16*, 2805.

[21] A. Pein, M. Baghbanzadeh, T. Rath, W. Haas, E. Maier, H. Amenitsch, F. Hofer, C. O. Kappe and G. Trimmel, *Inorg. Chem.* **2011**, *50*, 193.

[22] C. C. Wu, C. Y. Shiau, D. W. Ayele, W. N. Su, M. Y. Cheng, C. Y. Chiu and B. J. Hwang, *Chem. Mater*. **2010**, *22*, 4185.

[23] S. L. Castro, S. G. Bailey, R. P. Raffaelle, K. K. Banger and A. F. Hepp, *Chem. Mater.* **2003,** *15*, 3142.

[24] K. K. Banger, M. H. C. Jin, J. D. Harris, P. E. Fanwick, A. F. Hepp, *Inorg. Chem*. **2003,** *42*, 7713.

[25] S. L. Castro, S. G. Bailey, R. P. Raffaelle, K. K. Banger and A. F. Hepp, *J. Phys.Chem. B.* **2004**, *108*, 12429.

[26] K. K. Banger, M. H.-C. Jin, J. D. Harris, P. E. Fanwick and A. F. Hepp, *Inorg. Chem.* **2003**, *42*, 7713.

[27] B. Koo, R. N. Patel and B. A. Korge, *J. Am. Chem. Soc.* **2009**, *131*, 3134.

[28] M. L. Lerch, M. K. Harper and D. J. Faulkner, *J. Nat. Prod.* **2003**, *66*, 667.

[29] M. Ladika, T. E. Fisk, W. W. Wu, and S. D. Jons, *J. Am. Chem. Soc.* **1994**, *116*, 12093.

[30] S. F. Mayer, A. Steinreiber, R. V. A. Orru, and K. Faber, *J. Org. Chem*. **2002**, *67*, 9115.

[31] G. Zeni, R. B. Panatieri, E. Lissner, P. H. Menezes, A. L. Braga, and H. A. Stefani, *Org. Lett.* **2001**, *3*, 819.

[32] A. Stiitz, *Angew. Chem. Int. Ed. Engl.* **1987**, *26*, 320.

[33] J. Liu, J. W. Y. Lam, and B. Z. Tang, *Chem. Rev.* **2009**. *109*, 5799.

[34] T. Kitamura, C. H. Lee, Y. Taniguchi, and Y. Fujiwara, *J. Am. Chem. Soc.* **1997**, *119*, 619.

[35] H. Xu, K. Wu, J. Tian, L. Zhu and X. Yao, *Green Chem*. **2018**, *20*, 793.

[36] A. Kusuda, X. H. Xu, X. Wang, E. Tokunaga and N. Shibata, *Green Chem.* **2011**, *13*, 843.

[37] L. Mahendar, B. V. Ramulu and G. Satyanarayana, *Synthetic communications*. **2017**, *47*, 1151.

[38] M. Nasibipour, E. Safaei, G. Wrzeszcz and A. Wojtczak, *New J. Chem.* **2020**, *44*, 4426.

[39] Dawood Elhamifar, Afrooz Eram, Ramin Moshkelgosha, *Microporous and Mesoporous Materials.* **2017**, *252*, 173.

[40] Serena Perrone, Fabio Bona and Luigino Troisi, *Tetrahedron.* **2011**, *67*, 7386.

[41] K. Kamata, S. Yamaguchi, M. Kotani, K. Yamaguchi, and N. Mizuno, *Angew. Chem. Int. Ed.* **2008**, *47*, 2407.

[42] T. P. Cheng, B. S. Liao, Y. H. Liu, S. M. Peng and S. T. Liu, *Dalton Trans.* **2012**, *41*, 3468.

[43] G. Hilt, C. Hengst and M. Arndt, *Synthesis.* **2009**, *3*, 395.

[44] P. Bharathi and M. Periasamy, *Organometallics.* **2000**, *19*, 5511.

[45] K. Murugan, D. Nainamalai, P. Kanagaraj, S. G. Nagappan and S. Palaniswamy, *Appl Organomet Chem*. **2020**, *34*, e5778.

[46] M. Nasibipour, E. Safaei, G. Wrzeszcz and A. Wojtczak, *New J.Chem.* **2020**, *44*, 4426.

[47] G. Cheng, H. Zhang and X. Cui, *RSC Adv.* **2014**, *4*, 1849.

[48] L. Chaabane, E. Beyou, D. Luneau, and M. H. V. Baoua, *Journal of Catalysis.* **2020**, *388*, 91–103

[49] C. A. Didoa, Felipe L. Coelhoa , Maurício B. Clossa , Monique Deona , F. Horowitz, F. Bernardi, P. H. Schneider, E. V. Benvenutti, *Applied Catalysis A, General.* **2020**, *594*, 117444.

[50] H. Hao, and X. Lang, *ChemCatChem*. **2019**, *11*, 1378.

[51] K. Soni, M. Chauhan and S. Deka, *Front. Mater*. **2019**, *6*, 273.

[52] M. A. Pandit, B. Srinivas, K. Muralidharan, *J. Environ. Chem. Eng*. **2020**, *8*, 103542.

[53] B. Srinivas, M. A. Pandit, K. Muralidharan, *ACS Omega.* **2019**, *4*, 14970.

[54] (a) G. Mao, W. Dong, D. G. Kurth and H. Mohwald, *Nano Lett.* **2004**, *4*, 249. (b) L. Gao, E. Wang, S. Lian, Z. Kang, Y. Lan and D. Wu, *Solid State Commun.* **2004**, *130*, 309. (c) S. Wang and S. Yang, *Chem. Phys. Lett.*, **2000**, *322*, 567. (d) Q. Lu, F. Gao and D. Zhao, *Nano Lett.* **2002**, *2*, 725.

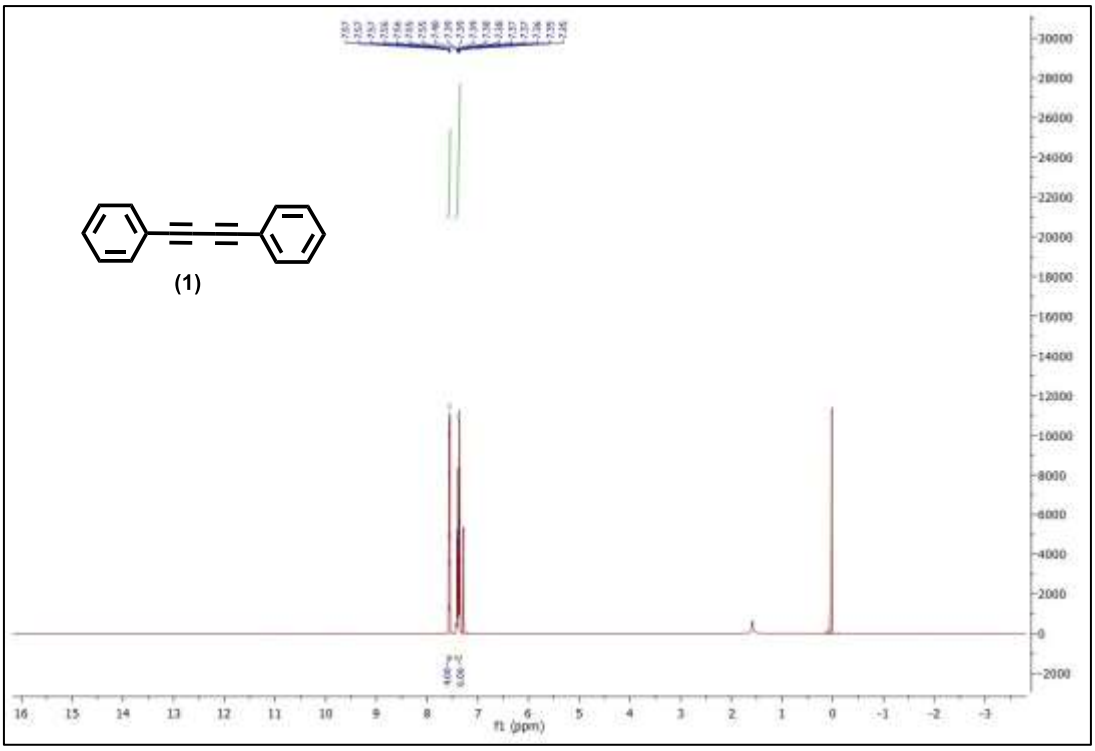

Figure 3.6: ^{1}H NMR spectrum of the compound 1

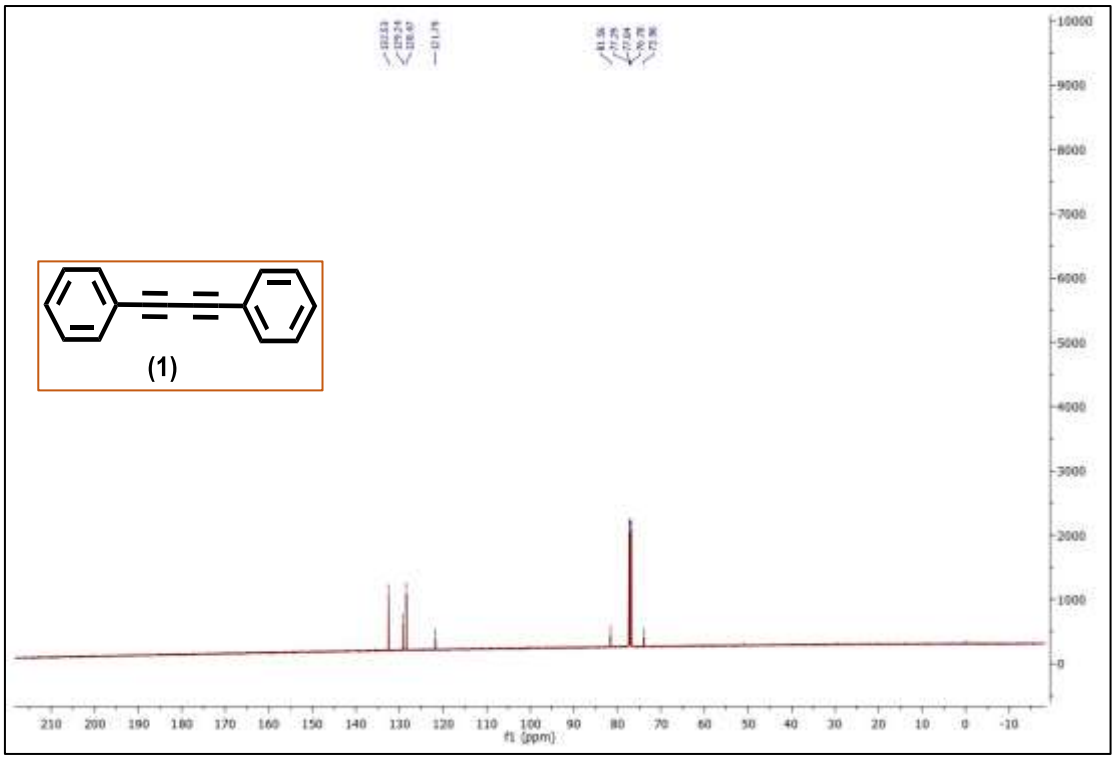

Figure 3.7: ^{13}C NMR spectra of the compound1

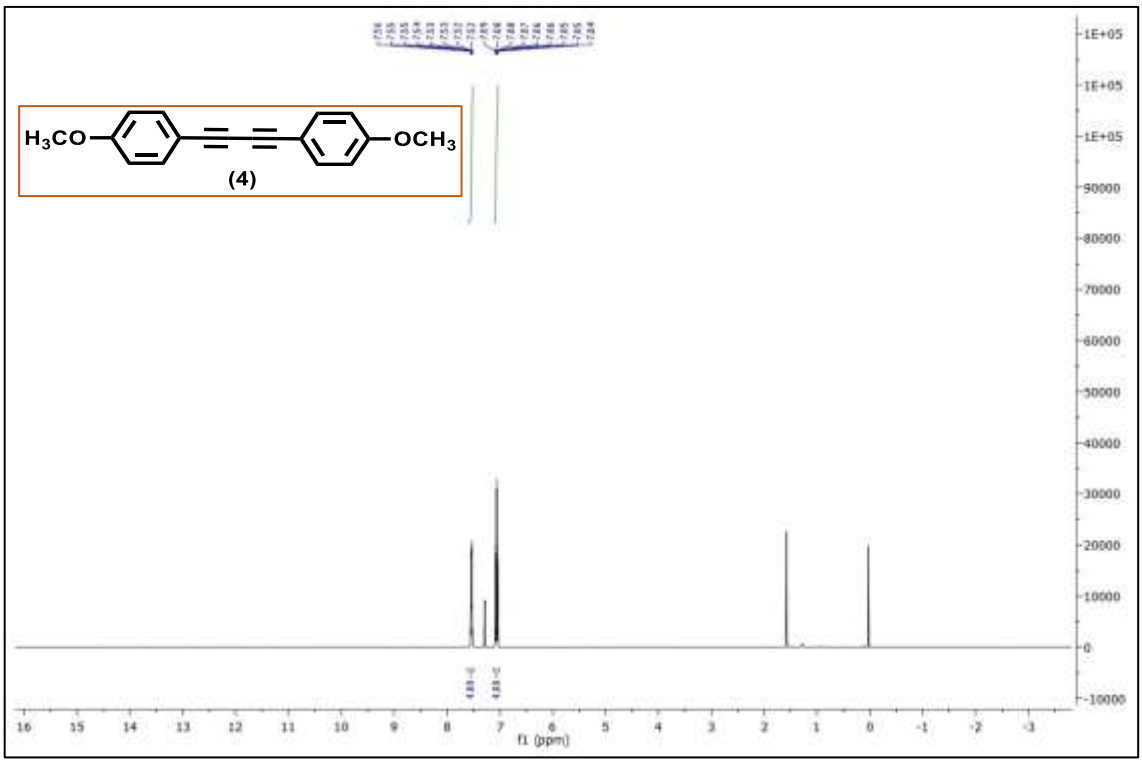

Figure 3.8: ^{1}H NMR spectrum of the compound4

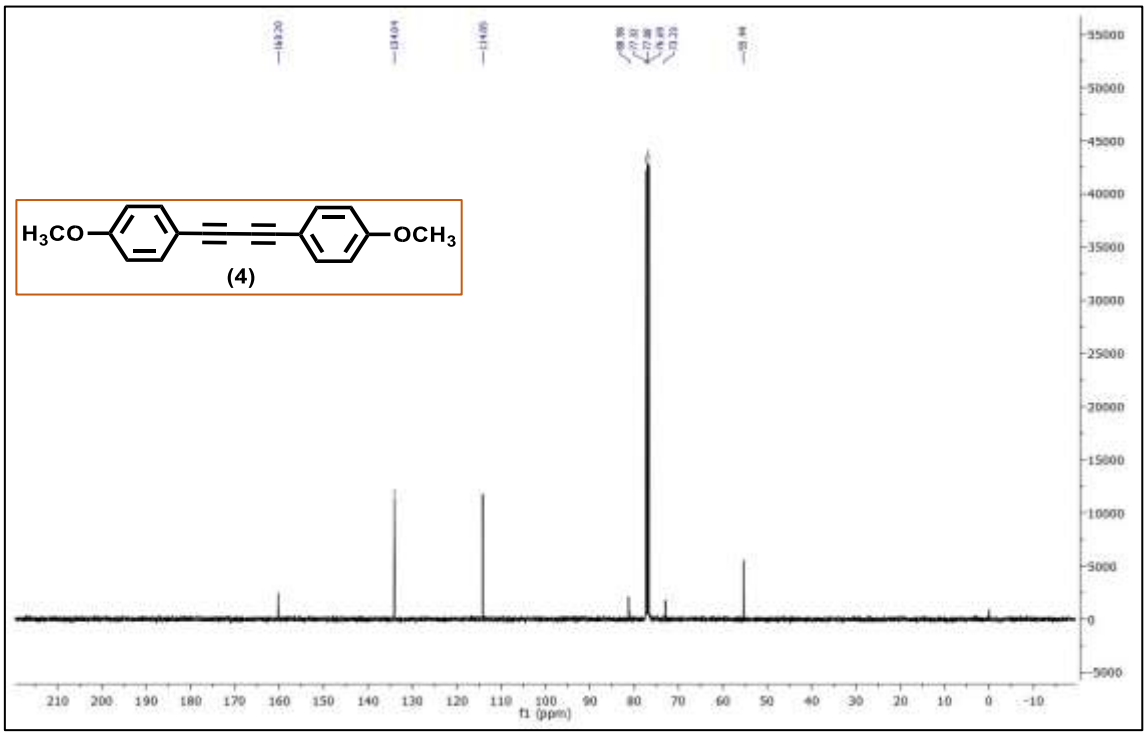

Figure 3.9: ^{13}C NMR spectra of the compound 4

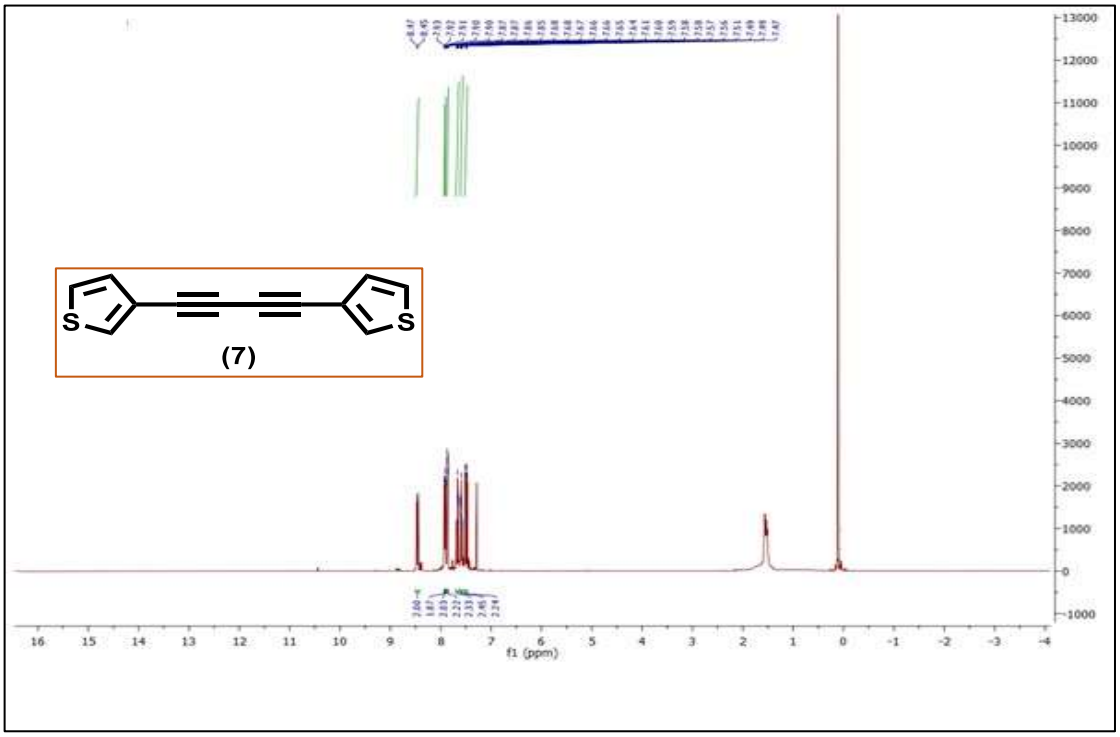

Figure 3.10: ^{1}H NMR spectrum of the compound7

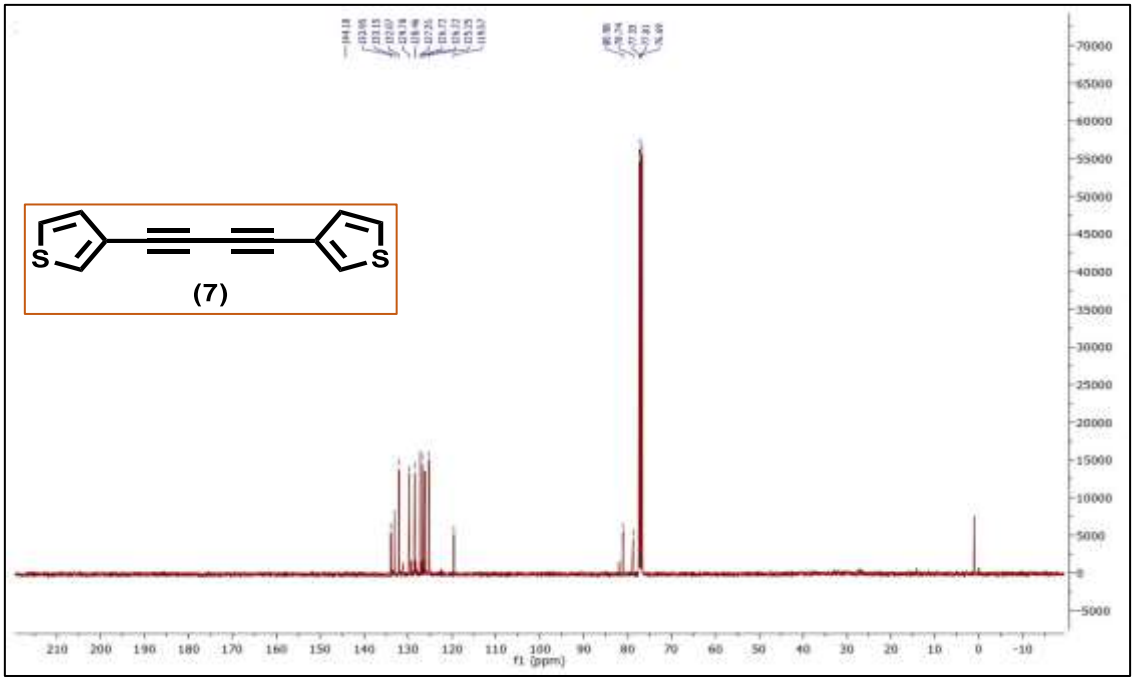

Figure 3.11: ^{13}C NMR spectra of the compound 7

CHAPTER 4

High yield room temperature conversion of carbon dioxide into cyclic carbonates catalyzed by mixed metal oxide (CuO-ZnO) nano/micro-flakes (Cozi-nmf)

Abstract: Capturing and converting carbon dioxide (CO_2) into useful organic molecules and polymers is the best way of alleviating excessive release of it from industrial sources to the environment. Cyclic carbonate synthesis by cycloaddition from CO_2 and epoxides through a catalytic process is a 100% atom economic reaction established five decades ago. Despite the availability of many efficient catalytic systems, there are shortcomings in either tedious preparatory procedure of catalyst, separation problem associated with homogeneous catalysis, or the requirement of pure CO_2. In this work, we report the catalytic system based on copper and zinc mixed metal oxides (CuO-ZnO) nano/micro-flakes (**Cozi-nmf**) for cycloaddition reaction of CO_2 with various epoxides at room temperature. These reactions were performed under solvent-free conditions. The novel recyclable heterogeneous catalyst was prepared via a simple procedure successfully at room temperature by grinding process. The synthesis of both catalyst and cyclic carbonates described here is greener and used inexpensive source materials to produce them. The yields of the synthesized cyclic carbonates were more than 95%, except for many reactions. The high efficiency of **Cozi-nmf** as a catalyst is explained based on the availability of the bare catalyst surface, which promoted the hindrance free movement of electrons and adsorption of substrate effectively.

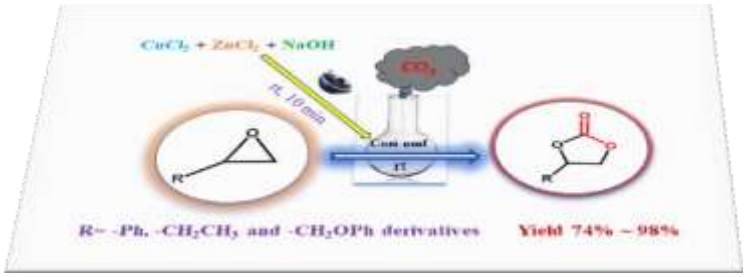

4.1. Introduction

Owing to the industrial revolution, the atmospheric carbon dioxide (CO_2) level is increasing rapidly, which is the primary cause of global-warming. On the other hand, the attractive CO_2 capture reactions represent an alternative and safer way of mitigating the excessive release of it from various industrial sources [1]. Using CO_2 it is possible to prepare many organic compounds by carboxylation reaction and specific transformation reactions into carboxylic acids, organic carbonates, urea, and methanol [2]. The use of renewable carbon resource CO_2 to produce various organic molecules and polymers has advantages as it is an abundant, economic, and nontoxic substance [3]. Therefore, the efficient methods that convert carbon dioxide into valuable chemicals have drawn much attention [4].

Cyclic carbonates are fascinating compounds finding range of applications such as electrolyte in lithium-ion batteries [5], polar aprotic solvents [6] intermediates for fine chemicals and building blocks in the manufacture of pharmaceuticals [7]. The cyclic carbonates with different functional groups are used as the precursor materials for polymeric materials like polycarbonates, polyurethanes, and polyesters [8]. Further, it is possible to tune the properties such as hydrophilicity, bio adhesion, and biodegradation by integrating various functional groups into the polymer chain [9]. The production of cyclic carbonates from CO_2 through cycloaddition reactions with epoxides is a 100% atom economic process established five decades ago [10]. However, because of the low reactivity and thermal stability of CO_2, the transformation of it into several useful products always involves a principal step of activating CO_2 molecules [11].

There are many reports on the development of catalytic systems to activate CO_2. Until now, the catalysts for the reaction of epoxides with CO_2 are confined to materials such as ionic liquids [12], organic metal complexes [13], organocatalysts, and quaternary ammonium [14]. Some of the known catalytic systems for epoxide–CO_2 coupling includes Al (III)@cages [15], $Ti(HPO_4)_2 \cdot H_2O$ [16], $ZnCl_2/Al_2O_3$ [17], succinimide-KI [18], PCN222(Co) [19], PIM2 [20] and some complexes [21] of Zn, Co, Mo, Pd, Cr, Cu, Mg, Al, and Sn. Much of the catalytic systems reported to the cyclic carbonate synthesis are homogeneous catalysts. Further, many of these reactions need high pressures of pure

CO_2 to induce the reaction with epoxides at temperatures. At this juncture, it is worth mentioning that pure CO_2 is obtained by purifying flue gases containing large amounts of CO_2 released from power plants and industrial furnaces. These purification processes are typically time-consuming and involve additional cost and energy. Despite the good catalytic behavior manifested by the catalysts mentioned above, their intrinsic homogeneous nature precludes re-utilization and limits their practical application on an industrial scale, especially those involving tedious preparation procedures [22]. Therefore, it is essential to develop highly stable and efficient heterogeneous catalysts for converting industrial CO_2 at atmospheric pressure and the mild temperature [22].

The chemical reactions occur on the catalyst's surface. To use metal oxides in the form of nano/micro particles as a catalyst in any reaction, their active centers at the surface should be free from any hindrance and exposed to the interaction with the substrate. Moreover, a critical scan in the literature revealed that most reactions through different physical and chemical pathways required high temperatures to produce copper oxide-zinc oxide (CuO-ZnO) nanocomposite [23]. Therefore, we have designed a simple procedure and synthesized the CuO-ZnO nano/micro-flakes (**Cozi-nmf**) successfully with the exposed surface and explored their catalytic activity for CO_2 capture reactions. We have synthesized CuO and ZnO in a 1:1 ratio to attain a high specific surface area. We have established the novel recyclable heterogeneous catalysis of **Cozi-nmf** having exposed surfaces for reaction of CO_2 with various epoxides at room temperature without use of any solvent. The synthesis described here is greener and used inexpensive source materials to produce catalyst and cyclic carbonates.

4.2. Results and discussion

4.2.1. Room temperature preparation of catalyst (Cozi-nmf) and its characterization

The procedure involved in the synthesis of materials determines their usability on a large scale. In the present work, **Cozi-nmf** was produced at room temperature by the solvent-free grinding method easily within 10 minutes. The required product was purified by water. The X-ray diffraction pattern gave preliminary information on the formation of **Cozi-nmf**. The typical powder XRD pattern (Figure 4.1) obtained from the sample of **Cozi-nmf** exhibited diffraction peaks at 2θ values of 31.6, 34.3, 36.0, 47.3, 56.5, 62.7, 66.1, 67.7 and 68.8 (°) respectively. The representative (hkl) planes of the corresponding

diffraction peaks (100), (002), (101), (102), (110), (103), (200), (112) and (201) were identified to the ZnO wurtzite phase (JCPDF No:036-1451). However, diffraction peaks at 2θ values of 31.6, 34.3, 36.0, 38.5, 47.3, 48.4, 53.5, 56.5, 57.9 and 61.3 (°) were identified to the lattice planes of [(110), (002), ($\bar{1}$11), (111), ($\bar{1}$12), ($\bar{2}$02), (020), (021), (202) and (113)], which were matching with CuO monoclinic phase (JCPDS No: 80-0076). Further, the existence of three diffraction peaks at 2θ values of Cu at 31.3°, 34.3° and 36.1° being overlapped completely with ZnO diffraction peaks with the variation of 0.85-1.14°, which established the formation of ZnO-CuO composite material.

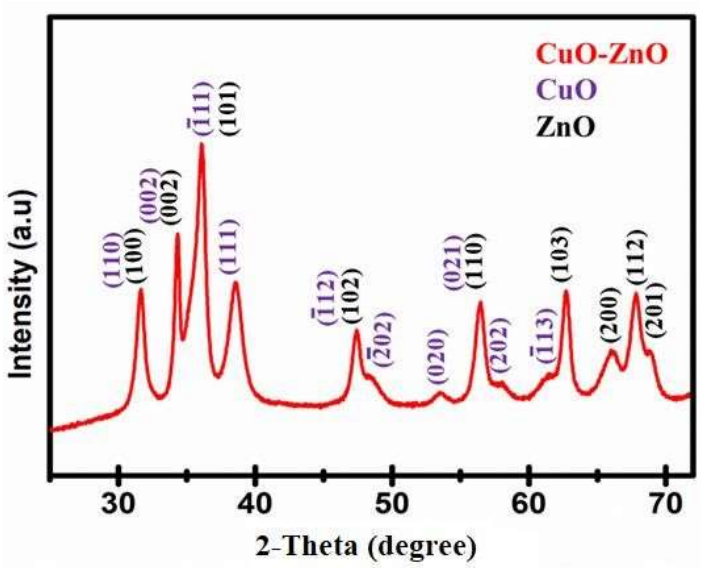

Figure 4.1: PXRD pattern of **Cozi-nmf**

The morphological features and elemental compositions of **Cozi-nmf** were visualized through electronic microscopes. The FESEM images (Figures 4.2a and b) exposed the formation of flake-like particles of CuO-ZnO composite materials (**Cozi-nmf)** with thickness in nanometer's order while overall size in microns. The elemental mapping images by EDS (Figure 4.2c) demonstrated the presence of oxygen, zinc and copper elements throughout architecture while the atomic ratio was matching with CuO-ZnO (Cu: Zn: O=1:1:2) (Figures 4.2d, e, and f). The TEM, HRTEM and SAED analysis of **Cozi-nmf** are shown in figure 4.3. The crystallinity of material was evident clearly from the HRTEM image (Figure 4.3c.) The selected area electron diffraction (SAED) indicated (Figure 4.3d) corresponds to the plane (110) at d spacing value at 2.7Å of CuO

, and the plane (101) at d spacing value at 2.4Å ZnO indicated the formation of CuO-ZnO composite material and the bright spots revealed the high crystalline nature.

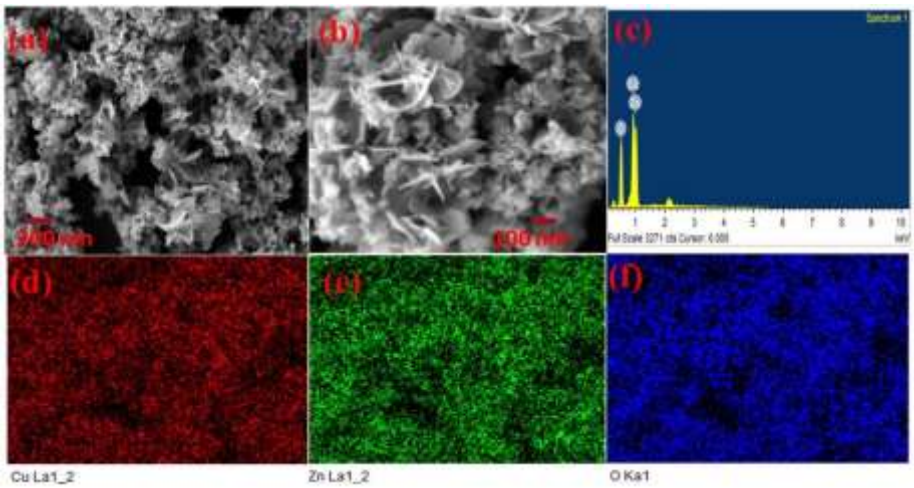

Figure 4.2: FE-SEM image of **Cozi-nmf**, 200 nm a) 100 nm b), EDS spectrum c), Cu, Zn, O elemental mapping (d, e, f)

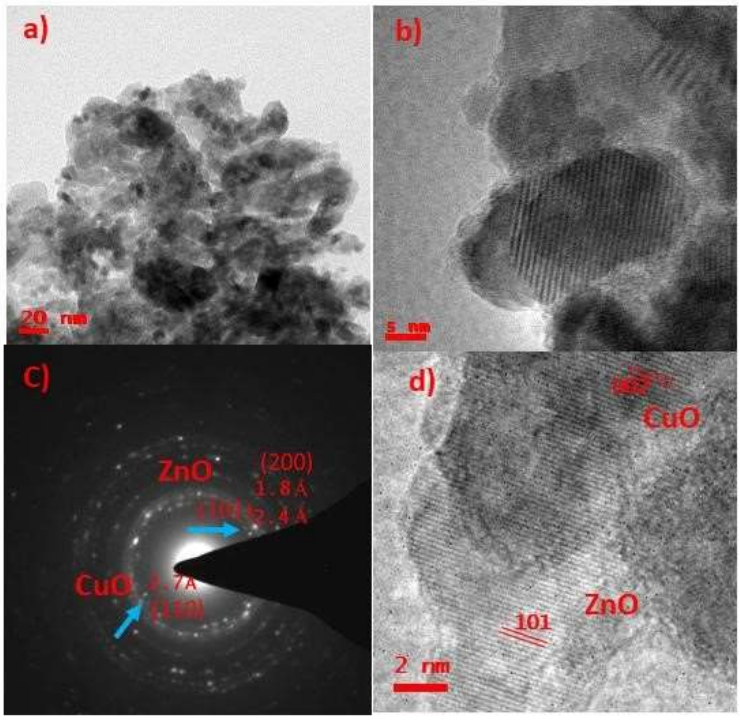

Figure 4.3: TEM image of **Cozi-nmf** at 20 nm magnification (a), high resolution Image of **Cozi-nmf** (b,d) and SAED pattern (c)

X-ray photoelectron spectroscopy (XPS) analyses (Figure 4.4) of **Cozi-nmf** disclosed the oxidation state of elements in the composite. First, the XPS survey spectra of the sample confirmed the presence of Cu, Zn, and O atoms in **Cozi-nmf**. There are no other elements observed except Si and C from the glass plate (Figure 4d). The Zn2p spectra showed two symmetric peaks, the peak around 1024.0 eV corresponds to the Zn2p3/2, and the one around 1047.1 eV is assigned to Zn 2p1/2, indicating the oxidation state of Zn (II) ion in the sample (Figure 4a). In the Cu2p spectrum, the peaks around 934.5 eV and 955.5 eV in all the samples confirmed the presence of Cu 2p3/2 and Cu 2p1/2, indicating the oxidation state of Cu (II) (Figure 4b). The O 1s peaks observed around 533.3 eV was assigned to oxygen (Figure 4.4c).

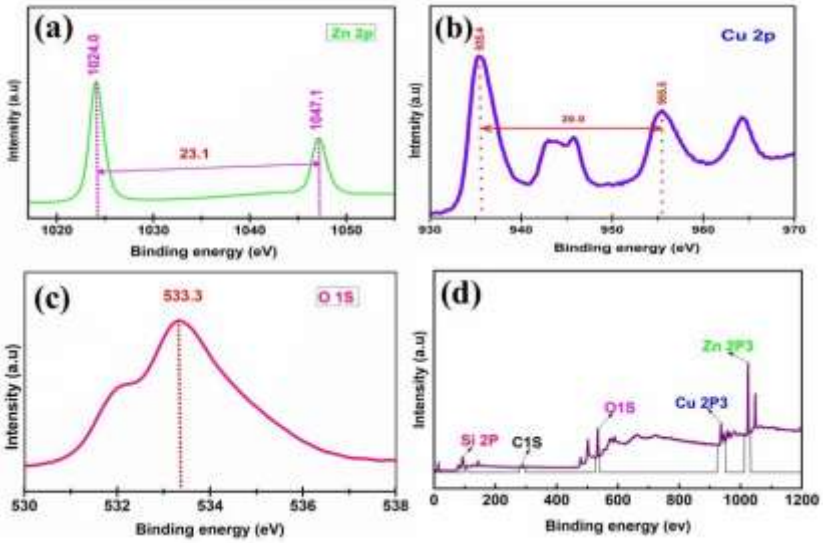

Figure 4.4: XPS spectrum of **Cozi-nmf** (a) Zn 2p, (b) Cu 2p, (c) O 1s and (d) Survey spectrum

4.2.2. Stability and surface area

The thermal stability of **Cozi-nmf** was investigated by thermal gravimetric analysis (TGA). The composite **Cozi-nmf** underwent a sharp weight loss of about 6.3% upto 250 ^{o}C, corresponding to the surface adsorbed residues (Figure 4.6). After an initial weight loss, the composite was losing weight of about 4 % slowly stable upto 800 °C. The availability of surface freely for the interaction with the substrate is essential for effective catalysis. Therefore, the specific surface area of **Cozi-nmf** was measured based on single gas adsorption at a constant temperature, while nitrogen gas was used as an adsorbate.

The N_2 adsorption-desorption isotherm of **Cozi-nmf** (Figure 4.5) was determined in the pressure range "P/P0 of 0–1.0", and the surface area was calculated as 45.8 m^2 g^{-1}. Envisioning here is that this entire surface area will be available for catalysis without any hindrance for the catalytic activity to produce cyclic carbonates.

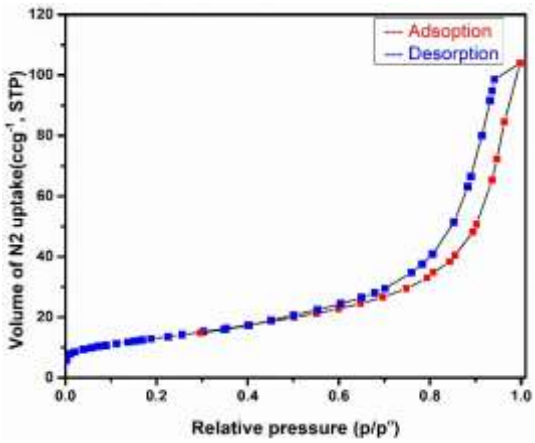

Figure 4.5: N_2 adsorption and desorption isotherm of **Cozi-nmf**

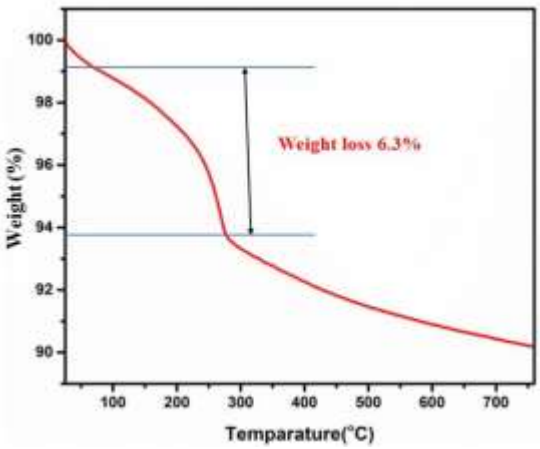

Figure 4.6: Thermogravimetric analysis of **Cozi-nmf**

4.2.3. Catalytic activity

The metal oxides in the form of nano/micro particles are preferred as catalysts compared to their bulk counterparts because of increased surface area. However, many chemical synthesis procedures of nanoparticles use various long-chain surfactant molecules to stabilize the size of the particles. These organic surfactant molecules not only hide the surface but also hinder the electron movement. Therefore, it is imperative to produce a catalyst whose surface should be free from any hindrance and exposed for substrate

interaction. Thus, **Cozi-nmf** is an attractive material for catalysis. We chose the coupling of phenyl glycidyl ether (**PGE**) with CO_2 using **Cozi-nmf** as a catalyst to give phenyl glycidyl carbonate (**PGC**) as the model reaction (Scheme 4.1). First, we have scanned the reaction conditions (time and temperature) and keeping CO_2 pressure at 1 atm to optimize the cyclic carbonates yield. Among the various reactions tried with solvents like toluene, CH_3CN, CH_3OH, $CHCl_3$, DMSO, DMF, and H_2O, the reaction without solvent showed superior activity compared to other solvents (Table 4.1).

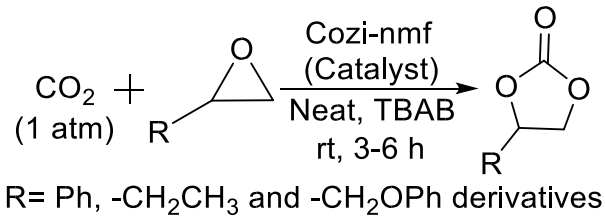

Scheme 4.1: Reaction of terminal epoxides and CO_2 at 1 bar pressure

Table 4.1: Solvent optimization using the model reaction the presence of **Cozi-nmf**

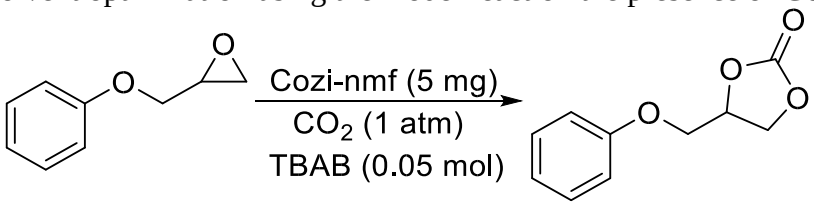

Entry	Solvent	Time (h)	Yield (%)
1	CH_3OH	24	15
2	toluene	24	20
3	CH_3CN	24	23
4	H_2O	24	no
5	$CHCl_3$	24	26
6	DMSO	24	no
7	DMF	24	no
8	No solvent	6	97

To test the advantage of having mixed metal oxide composite as the catalyst, we have performed controlled reactions of PGE with CO_2 under the optimized condition in the presence of ZnO and CuO nanoparticles, also the catalyst **Cozi-nmf** (Table 4.2). The reaction did not yield any product when conducted without **Cozi-nmf**. The observed yield of PGC in the presence of ZnO and CuO was 15% and 35%, while a much higher 97% yield was obtained using **Cozi-nmf** as the catalyst. The high surface area of **Cozi-nmf** that available freely without any capping agent was the reason for better catalytic activity in this CO_2 fixation reaction.

Table 4.2: Synthesis of phenyl glycidyl carbonates with different catalysts

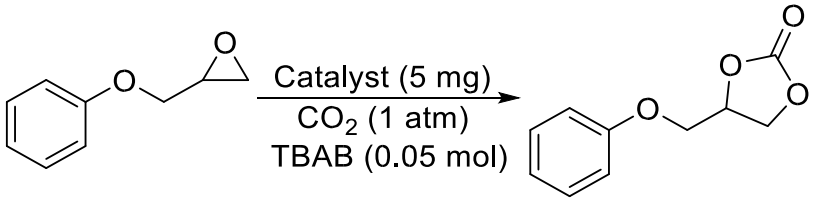

Entry	Epoxide	Catalyst	Yield (%)
1	2	CuO	35
2	2	ZnO	15
3	2	Cozi-nmf	97

The reaction without solvent at room temperature for 3 h using scanty of **Cozi-nmf** (5 mg, 0.06 mmol) and CO_2 at 1 atm pressure (Table 4.3, entry 8) gave the best result in terms of time and yield (98%). In contrast, with less than 5 mg of **Cozi-nmf**, the reaction became sluggish with a low product yield. Using the optimized reaction conditions, we have tested the performance of **Cozi-nmf** for the reaction of CO_2 with substituted epoxides. Phenyl glycidyl ether substituted with electron-donating [-CH_3 -OCH_3, -$C(CH_3)_3$] and electron-withdrawing groups (-Cl, -Br, -Ph) were used as the substrate in the reactions. As shown in Table 4.3 (entries 1–11), most substrates were converted efficiently to cyclic carbonates respectively with excellent selectivity and high conversion. It was observed that terminal epoxides with both electron-withdrawing and electron-donating groups were converted into the respective cyclic carbonates with quantitative yields (93–98%) within 3-6 h. Other than phenyl glycidyl ether, we have attempted the

reaction with two more substrates, styrene oxide (Table 4.3, entry1) and 1, 2 epoxy butane (Table 4.3, entry 11). It is noteworthy that the aliphatic substrate, 1, 2 epoxy butane yielded the corresponding cyclic carbonate with lower conversion (Table 4.3, entry 11, 74%).

We have compared the catalytic activity of **Cozi-nmf** with that of known heterogeneous catalysts used for the production of cyclic carbonates (Table 4.4). The comparative study showed that other reported reactions involved use of protic compounds, additives, and solvents for epoxide activation. Moreover, those catalytic systems required either high pressure [24], high temperature to activate CO_2, whereas our designed **Cozi-nmf** having high Lewis acidic nature of surface might facilitate CO_2 insertion at rt with 1 atm pressure. The simplicity of synthesis makes **Cozi-nmf** stand in a better position.

Table 4.3: Cyclic carbonate synthesized by using **Cozi-nmf** as catalyst

(1) 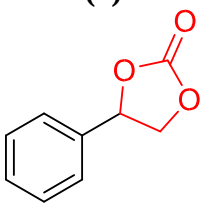 **Yield: 93%** **Time: 4 h**	**(2)** 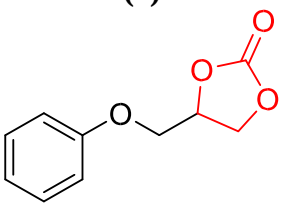 **Yield: 97%** **Time: 3 h**	**(3)** 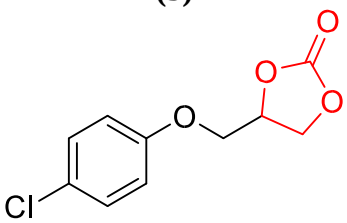 **Yield: 95%** **Time: 4 h**
(4) 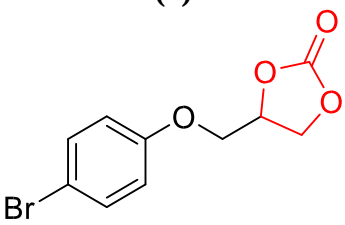 **Yield: 94%** **Time: 5 h**	**(5)** 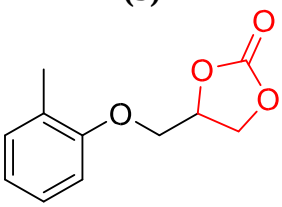 **Yield: 97%** **Time: 3 h**	**(6)** 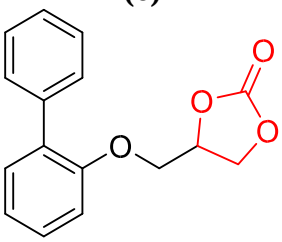 **Yield: 93%** **Time: 6 h**
(7) 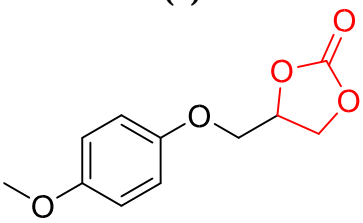 **Yield: 96%** **Time: 4 h**	**(8)** 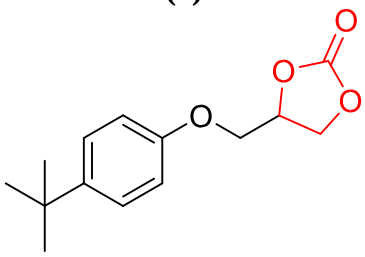 **Yield: 98%** **Time: 3 h**	**(9)** 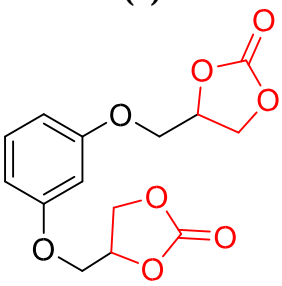 **Yield: 90%** **Time: 6 h**
(10) 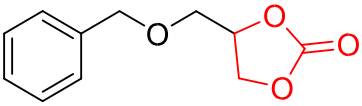 **Yield: 93%** **Time: 6 h**	**(11)** 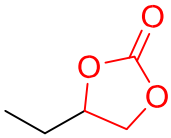 **Yield: 74%** **Time: 6 h**	--

Reaction conditions: epoxide (1 mmol), **Cozi-nmf** (5 mg), rt, 1 atm of CO_2. Yields of isolated pure product.

Table 4.4: Comparative study on the catalytic activity of **Cozi-nmf** with numerous catalysts using PGE as substrate

Catalyst	CO_2 (bar)	Time (h)	Temperature (°C)	Yield (%)	Ref
Al(III)@cages	1	48	RT	54	15
$Ti(HPO_4)_2 \cdot H_2O$	1	6	RT	87	16
$ZnCl_2/Al_2O_3$	1	4	100	100	17
Succinimide-KI	0.4	6	70	94	18
PCN-222(Co)	1	18	50	90	19
PIM2	1	8	130	96	20
Cozi-nmf	**1**	**3**	**RT**	**97**	**This work**

4.2.4. Recyclability of Cozi-nmf as catalyst

A heterogeneous catalyst needs to be examined for its recoverability, ease of separation, and reusability. The reusability of **Cozi-nmf** was examined using the illustrative reaction between CO_2 and PGE to yield cyclic carbonate. The reaction mixture was centrifuged after the reaction time to separate the solid **Cozi-nmf**. Then, it was washed scrupulously with distilled H_2O followed by CH_3OH and dried for 5 h in an oven at 100 ^oC before reuse. As seen in figure 4.7 the catalyst can be efficiently recycled and reused five times. The results indicated that after 5-time reuse of catalyst, the product's yield decreased from 97% to 90%.

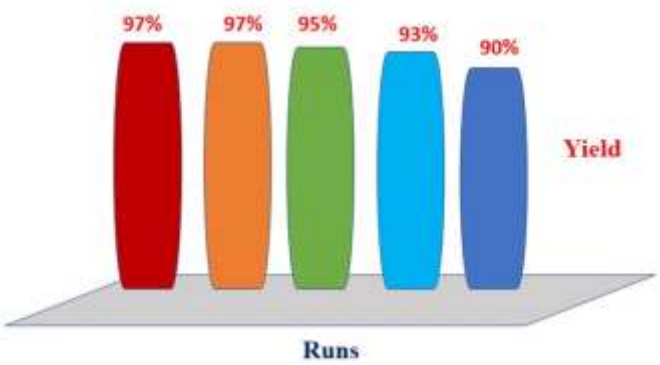

Figure 4.7: Bar diagram showing results of recycling of **Cozi-nmf** in the synthesis of cyclic carbonates.

4.3. Conclusion

We have synthesized **Cozi-nmf** with a high surface area of around 45.8 $m^2 g^{-1}$ by grinding method within 10 min. It was used as the catalyst to activate CO_2 for cycloaddition reaction with various epoxides to produce cyclic carbonates. The syntheses described here were performed in solvent-free conditions and used inexpensive and recyclable surfactant-free heterogeneous catalysts. The yields of the synthesized products were more than 95% except for styrene and aliphatic carbonates. The high efficiency of **Cozi-nmf** as a catalyst is because of the availability of the bare catalyst surface, which promoted the hindrance free movement of electrons and adsorption of substrate effectively. The simplicity in the synthesis of catalyst and cyclic carbonates promises large-scale industrial use of the method.

4.4. Experimental Section

4.4.1. Materials

$ZnCl_2$, $CuCl_2$ and epoxides were purchased from Sigma-Aldrich, while anhydrous NaOH was purchased from Merck, India. Solvents used for the reactions were dried and distilled using standard procedure and then used for work up and column chromatography. TLC was done using commercially available (MERCK) aluminium plates coated with silica gel (60-120 mess).

4.4.2. Instrumentation

Instruments used to characterize **Cozi-nmf** are similar to the description in section 3.4.2. TEM images of **Cozi-nmf** were acquired by using an "FEI Technai G2 20 STEM instrument" at an acceleration voltage of 200 kV. XPS spectra were recorded in a Thermo Scientific K Alpha spectrometer equipped with a micro-focused monochromatic X-ray source (Al Kα, spot size ~ 400 μm) operating at 70 W.

The **Cozi-nmf** sample was suspended in isopropanol and then dispersed on ITO plates to record FESEM micrographs. The **Cozi-nmf** sample for TEM analyses were dispersed in isopropanol, and 1-2 drops of dispersion were dripped onto a carbon-coated copper grid

(200 mesh). An optimum concentration of **Cozi-nmf** was drop-casted onto a quartz substrate for the XPS analysis.

^{1}H NMR and ^{13}C NMR spectra of cyclic carbonates in $CDCl_3$ were acquired at room temperature using Bruker (500 or 400 MHz) NMR spectrometer. The chemical shifts (δ) are reported in ppm scale downfield from the internal standard TMS (δ = 0.0). High-resolution mass spectra (HRMS) were recorded using ESI-TOF techniques.

TGA was recorded on a PerkinElmer – STA 6000. Surface area analysis was determined from the BET analysis, which was recorded by the Quanta chrome instrument. Melting points of cyclic carbonates were measured on a Buchi B-540 apparatus.

4.4.3. Synthesis of nanocomposite copper oxide -zinc oxide (CuO-ZnO) nano/micro-flakes (Cozi-nmf)

The grinding process for synthesizing **Cozi-nmf** is described as follows: $CuCl_2$ (2 mmol) and $ZnCl_2$ (2 mmol) were mixed uniformly by grinding in an agate mortar until the mixture turned black (approximately for 5 min). After that solid NaOH (8 mmol) was added into the mortar, and continued the grinding for another 10 min. The resultant black mass was gathered and washed several times using water followed by absolute methanol through the centrifugation process. Then the residue was dried at 60 °C to get light black powder of **Cozi-nmf**. The whole grinding process was operated in air atmosphere at room temperature.

4.4.4. Synthesis of cyclic carbonate from CO_2 and epoxide

In a typical reaction (Scheme 4.1), epoxide (1mmol), t-butyl ammonium bromide (0.05mol), and catalyst, **Cozi-nmf** (5mg) were placed in a 50mL round bottom flask filled with CO_2 gas from a CO_2 cylinder. After mixing them, CO_2 gas flow was continued purging through the needle dipped in the reaction mixture. The reactions were continued at rt for 3–6 h, and CO_2 was provided by a gas cylinder (1atm) connected to the flask. After completing the reaction, it was worked up with water and ethyl acetate and dried using anhydrous Na_2SO_4. Then, ethyl acetate was evaporated under a vacuum and the residue was purified by eluting through a column packed with silica gel using ethyl acetate and hexane to get the purified cyclic carbonates. Compounds were characterized based on their spectroscopic data (^{1}H, ^{13}C NMR, and HRMS), which were compared to those reported in the literature.

Spectral data of cyclic carbonates

4-phenyl-1,3-dioxolan-2-one:

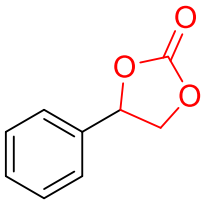

Melting point : 57 °C (White solid).

^{1}H NMR (500 MHz, $CDCl_3$) : δ=4.32 (1H, t, J=8 Hz), 4.80 (1H, t, J=8 Hz), 5.68 (1H, t, J=8 Hz), 7.30-7.37 (2H, m), 7.40-7.44 (2H, m)

^{13}C NMR (126 MHz, $CDCl_3$) : 71.11, 77.93, 125.79, 129.16, 129.64, 135.78, 154.79

HRMS calculated for $C_9H_8O_3$: $[M+Na]^+$: 187.1571, found: 187.1572.

4-(Phenoxymethyl)-1,3-dioxolan-2-one:

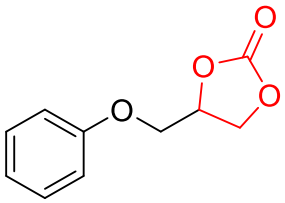

Melting point : 96-97 °C (White solid)..

^{1}H NMR (400 MHz, $CDCl_3$) : δ=4.16-4.18 (1H, dd, J=10 Hz, J= 7 Hz), 4.24-4.27 (1H, dd, J=10 Hz, 6 Hz), 4.54-4.57 (1H, q), 4.64 (1H, t, J=8 Hz), 5.02-5.07 (1H, m), 6.92-6.94 (m, 2H), 7.02-7.05 (1H, m), 7.31-7.34 (2H, m)

^{13}C NMR (101 MHz, $CDCl_3$) : δ=66.25, 66.93, 74.04, 114.65, 122.04, 129.70, 154.56, 157.76.

HRMS calculated for $C_{10}H_{10}O_4$: $[M+Na]^+$: 217.0471, found: 217.0471.

4-((4-Chlorophenoxy)methyl)-1,3-dioxolan-2-one:

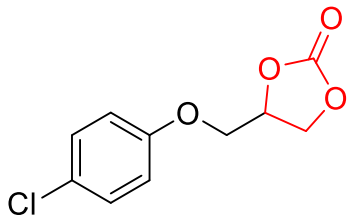

Melting point : 101-102 °C (White solid).

^{1}H NMR (500 MHz, $CDCl_3$) : δ=4.11-4.15 (1H, dd, J=10 Hz, 7 Hz), 4.22-4.26 (1H, dd, J=10 Hz, 7 Hz), 4.52-4.56 (1H, q), 4.64 (1H, t, J=8 Hz), 5.02-5.07 (1H, m), 6.84-6.88 (2H, m), 7.25-7.29 (2H, m) and

^{13}C NMR (126 MHz, $CDCl_3$) : 66.10, 67.27, 73.96, 115.94, 127.03, 129.40, 129.62 154.55, 156.36.

HRMS calculated for $C_{10}H_9ClO_4$: $[M+ H]^+$: 228.0212, found: 228.0212.

4-((4-Bromo phenoxy)methyl)-1,3-dioxolan-2-one:

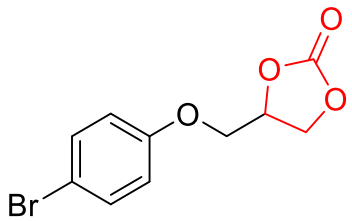

Melting point :103-104 °C (White solid).

^{1}H NMR (500 MHz, $CDCl_3$) : δ= 4.12-4.14 (1H, dd, J=10 Hz, 7 Hz), 4.22-4.25(1H, dd, J= 10Hz, 6 Hz), 4.52-4.55 (1H, q), 4.64 (1H, t, J=8Hz), 5.03-5.07 (1H, m), 6.80-6.83 (2H, m), 7.38-7.43(2H, m) and

^{13}C NMR (126 MHz, $CDCl_3$) : 66.11, 67.22, 74.00, 114.32, 116.45, 132.34,132.55, 154.59, 156.89.

HRMS calculated for $C_{10}H_9BrO_4$: $[M]^+$: 271.9565, found: 271.9562,

$C_{10}H_9BrO_4$: $[M+2]^+$: 273.9540, found: 273.9540

4-((o-Tolyloxy)methyl)-1,3-dioxolan-2-one:

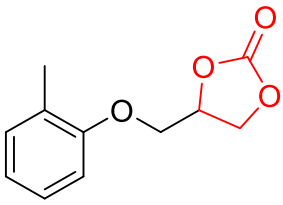

Melting point : 96 °C (White solid).

^{1}H NMR (500 MHz, $CDCl_3$) : δ= 2.24 (3H, s), 4.14–4.17 (1H, dd, J=13 Hz, 7 Hz), 4.27-4.30 (1H, dd, J=14 Hz, 7 Hz), 4.59-4.62 (1H, q), 4.66 (1H, t, J= 8 Hz), 5.06-5.10(1H, m), 6.78-6.81 (1H, t, J=5 Hz), 6.93-6.96 (1H, m), 7.17-7.20 (2H, m)

^{13}C NMR (126 MHz, $CDCl_3$) : 16.00, 66.27, 66.99, 74.22, 110.79, 121.67, 126.90, 131.10, 154.83, 155.74.

HRMS calculated for $C_{11}H_{12}O_4$: $[M+ NH_4]^+$: 226.0957, found: 226.0957

4-(([1,1'-biphenyl]-2-yloxy)methyl)-1,3-dioxolan-2-one: Isolated yield: 93%, white solid,

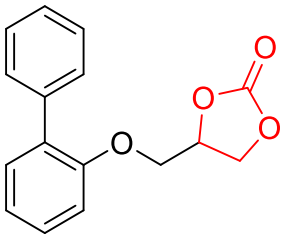

Melting point :105-107 °C (White solid).

^{1}H NMR (500 MHz, $CDCl_3$) : δ= 3.60-3.70 (2H, m), 3.96-4.02 (2H, m), 4.06-4.08 (1H, m), 7.01(1H, d, J=8Hz), 7.09 (1H, t, J=7Hz) 7.32-7.36 (3H, m) 7.43 (2H, t, J= 7Hz) 7.50 (2H, d J= 7Hz)

^{13}C NMR (126 MHz, $CDCl_3$) : δ=63.63, 70.17, 70.49, 113.23, 121.81, 127.14, 128.15, 128.77, 129.38, 130.90, 131.49, 138.36, 155.28.

HRMS calculated for $C_{16}H_{14}O_4$: $[M+Na]^+$: 293.0797, found: 293.0798.

4-((4-methoxyphenoxy)methyl) -1,3-dioxolan-2-one:

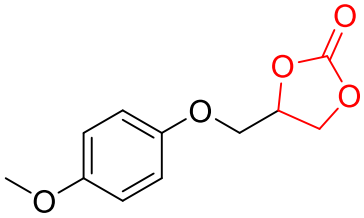

Melting point : 99-100 °C (white solid).

^{1}H NMR (400 MHz, $CDCl_3$) : δ= 3.13 (3H, s), 4.24 (2H, d, J=4Hz), 4.62-4.64 m), 5.00-5.06 (1H, m), 6.89-6.97 (3H, m), 7.01-7.06 (1H, m).

^{13}C NMR (101 MHz, $CDCl_3$) : 55.90, 66.42, 69.39, 74.45, 112.57,116.77, 121.04, 123.49, 147.46, 150.43, 154.77.

HRMS calculated for $C_{11}H_{12}O_5$: $[M+H]^+$: 225.0637, found: 225.0636.

4-((4-(tert-Butyl)phenoxy)methyl)-1,3-dioxolan-2-one:

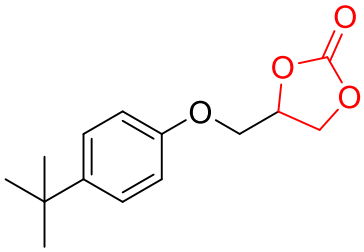

Melting point : 98-100 °C (white solid).

^{1}H NMR (500 MHz, $CDCl_3$) : δ=1.31 (9H, s), 4.14-4.17 (1H, dd, J=10 Hz, 7 Hz), 4.22-4.25 (1H, dd, J=11 Hz, 6 Hz) 4.52 (1H, q), 4.62 (1H, t, J =8 Hz), 5.01-5.06 (1H, m), 6.85-6.88 (2H, m),7.32-7.34 (2H, m)

^{13}C NMR (126 MHz, $CDCl_3$) : 31.45, 34.15, 66.30, 67.06, 74.10, 114.17, 126.47, 144.88, 154.60, 155.55.

HRMS calculated for $C_{14}H_{18}O_4$: $[M+ NH_4]^+$: 268.1420, found: 268.1420.

4,4'-((1,3-phenylenebis(oxy))bis(methylene))bis(1,3-dioxolan-2-one): (Colorless gel)

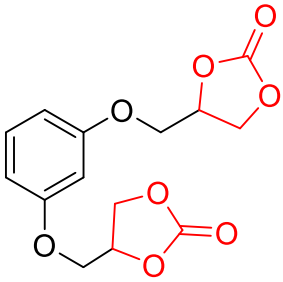

^{1}H NMR (400 MHz, $CDCl_3$) : δ=4.11-4.14 (2H, dd, J=Hz), 4.23-4.25 (2H, dd, J =Hz, Hz), 4.51-4.54 (2H, q), 4.63 (2H, t, J=Hz), 5.03-5.07 (2H, m), 6.49 (1H, d, J=Hz), 6.55-6.57 (2H, d, J= Hz), 7.19-7.23 (1H, t, J= Hz) and

^{13}C NMR (101 MHz, $CDCl_3$) : 66.14, 67.10, 67.15, 74.05, 101.97, 102.06, 107.95, 130.41, 154.81, 154.82, 159.06.

HRMS calculated for $C_{14}H_{14}O_8$: [M+ Na] $^{+}$: 333.0958, found: 333.0958.

4-((Benzyloxy)methyl)-1,3-dioxolan-2-one: (Colorless liquid)

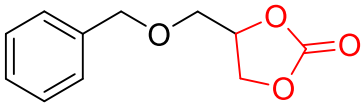

^{1}H NMR (400 MHz, $CDCl_3$) : δ=3.62-3.65 (1H, dd, J=11 Hz, 7Hz), 3.71-3.74 (1H, dd, J=11Hz, 7 Hz), 4.39-4.42 (1H, q), 4.50 (1H, t, J=8 Hz), 4.57-4.65 (2H, m), 4.82-4.85 (1H, m), 7.31-7.33(3H, m) 7.36–7.39 (2H, m)

^{13}C NMR (101 MHz, $CDCl_3$) : 66.32, 68.84, 73.73, 75.00, 127.78, 128.11, 128.60, 137.06, 154.93.

HRMS calculated for $C_{11}H_{12}O_4$: [M+ NH_4] $^{+}$: 226.0954, found: 226.0953.

4-ethyl-1,3-dioxolan-2-one: (Colorless liquid)

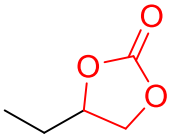

^{1}H NMR (500 MHz, $CDCl_3$) : δ= 0.98-1.031 (3H, m), 1.71-1.85 (2H, m), 4.05-4.09 (1H, q), 4.50-4.53 (1H, t, J=8 Hz), 4.62-4.68 (2H, m).

^{13}C NMR (126 MHz, $CDCl_3$) : 19.72, 68.97, 77.96, 155.06.

HRMS calculated for $C_5H_8O_3$ [M+ NH_4] $^{+}$: 134.1539, found: 134.1530.

4.5. References:

[1] M. North, R. Pasquale and Carl Young, *Green Chem.* **2010**, *12*, 1514.

[2] M. Mikkelsen, M. Jorgensen and F. C. Krebs, *Energy Environ. Sci*. **2010,** *3*, 43.

[3] T.Sakakura, J. Choi and H. Yasuda, *Chem. Rev*.**2007**, *107*, 2365.

[4] R. Dalpozzo, N. Della Ca, B. Gabriele and R. Mancuso, *Catalysts.* **2019**, *9*, 511.

[5] K. Xu, *Chem. Rev.* **2004**, *104*, 4303.

[6] B. Schaffner, *Chem. Rev*. **2010**, *110*, 4554.

[7] J. P. Parrish, R. N. Salvatorea and K. Woon Junga, *Tetrahedron*. **2000**, *56*, 8207.

[8] S. Verma, G. Kumar, A. Ansari, R. I. kureshy and N. H. Khanab, *Sustainable Energy Fuels*. **2017**, *1*, 1620.

[9] S. Wu, Y. Zhang, B. Wang, E. H. M. Elageed, L. Ji, H. Wu, and G. Gao, *Eur. J. Org. Chem*. **2017**, 753.

[10] J. N.Appaturi, F. Adam, *Applied Catalysis B: Environmental*. **2013**, *136*, 150.

[11] C. Maeda, Y. Miyazaki and T. Ema, *Catal. Sci. Technol*. **2014,***4*, 1482.

[12] Lina Hana, Haiqing Lib, S. Choia, M. Parka, S. Leea, Y. Kima, D. Parka, *Applied Catalysis A: General.* **2012,** *429*, 67.

[13] H. Vignesh Babu and K.Muralidharan, *RSC Adv.* **2014**, *4*, 6094.

[14] J. Langanke, L. Greiner and W. Leitner, *Green Chem.***2013**, *15*, 1173.

[15] C. K. Ng, R. W. Toh, T. T. Lin, H. Luo, T. S. Andy Hor and J. Wu, *Chem. Sci*. **2019**, *10*, 1549.

[16] A. H. Chowdhury, I. H. Chowdhury and Sk. M. Islam, *Ind. Eng. Chem. Res.* **2019**, *58*, 11779.

[17] G. N. Bondarenkoa, E. G. D Vurechenskay, O. G. Ganin, F. Alonso, I. P. Beletskay, *Applied Catalysis B: Environmental*. **2019**, *254*, 380.

[18] Q. Li, H. Chang, R. Li, H. Wang, J. Liu, S. Liu, C. Qiao and T. Lin, *Molecular Catalysis*. **2019,** *469*, 111.

[19] S. Carrasco, A. S. Marco and B. M. Matute, *Organometallics.* **2019**, *38*, 3429.

[20] Y. Wang, J. Nie, C. Lu, F. Wang, C. Ma, Z. Chen and G. Yang, *Microporous and Mesoporous Materials.* **2020,** *292,* 109751.

[21] (*a*) Y.-M. Shen, W.-L. Duan and M. Shi, *J.Org.Chem.* **2003**, *68*, 1559. (*b*) A. Decortes, M. M. Belmonte, J. Benet-Buchholz and A. W. Kleij, *Chem. Commun.* **2010**, *46*, 123. (*c*) R. M. Haak, A. Decortes, E. C. Escudero-Adan, M. M. Belmonte, E. Martin, J. Benet-Buchholz and A. W. Kleij, *Inorg. Chem.* **2011**, *50*, 7934. (*d*) A. Decortes, A. M. Castilla and A. W. Kleij, *Angew. Chem. Int. Ed.* **2010**, *49*, 9822. (*e*) Z. Wang, Z. Bu, T. Cao, T. Ren, L. Yang and W. Li, *Polyhedron*, **2012,** *32*, 86. (*f*) R. L. Paddock and S. T. Nguyen, *Chem. Commun.* **2004,** *23,* 1622. (*g*) A. Berkessel and M. Brandenburg, *Org. Lett.* **2006, 8**, 4401. (*h*) G. P. Wu, S-H. Wei, X-B. Lu, W-M. Ren and D. J. Darensbourg, *Macromolecules.* **2010,** *43,* 9202. (*i*) R. L. Paddock and S. T. Nguyen, *J. Am. Chem. Soc.* **2001**, *123*, 11498. (*j*) D. J. Darensbourg, J. C. Yarbrough, C. Ortiz and C. C. Fang, *J. Am. Chem. Soc.* **2003**, *125*, 7586, (*k*) X-B. Lu, R. He and C-X. Bai, *J. Mol. Catal. A: Chem.* **2002**, *186*, 1. (*l*) X-B. Lu, Y-J. Zhang, K. Jin, L-M. Luo and H. Wang, *J. Catal.* **2004**, *227*,537, (*m*) M. Alvaro, C. Baleizao, E. Carbonell, M. E. Ghoul, H. Garcia and B. Gigante, *Tetrahedron.* **2005**, *61*, 12131.

[22] J. N. Appaturi, F. Adam, *Applied Catalysis B: Environmental.* **2013**, *136*, 150.

[23] S. Harish, J. Archana, M. Sabarinathan, M. Navaneethan, K.D. Nisha, S. Ponnusamy, C. Muthamizhchelvan, H. Ikeda, D.K. Aswal, Y. Hayakawa, *Applied Surface Science*. **2017**, *418*, 103.

[24] T. Werner and N. Tenhumberg, *Journal of CO_2 Utilization*. **2014**, *7*, 39.

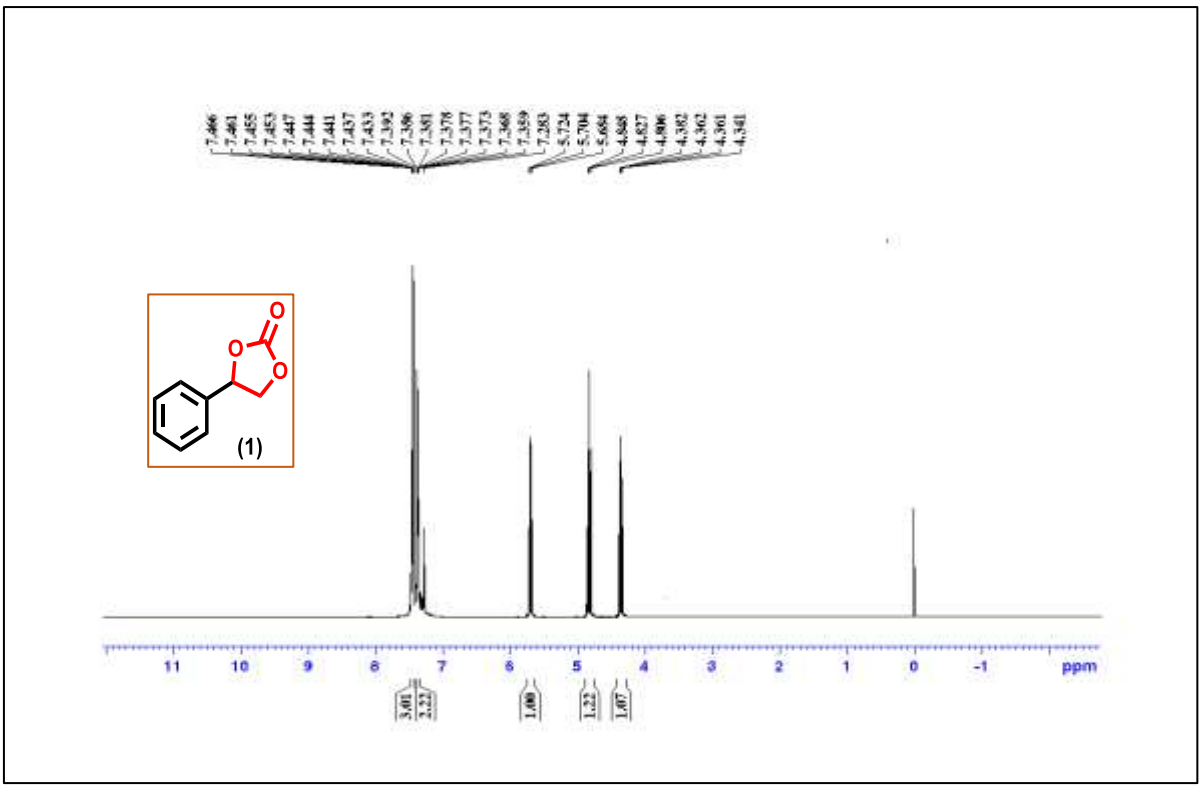

Figure 4.8: ^{1}H NMR spectrum of the compound1

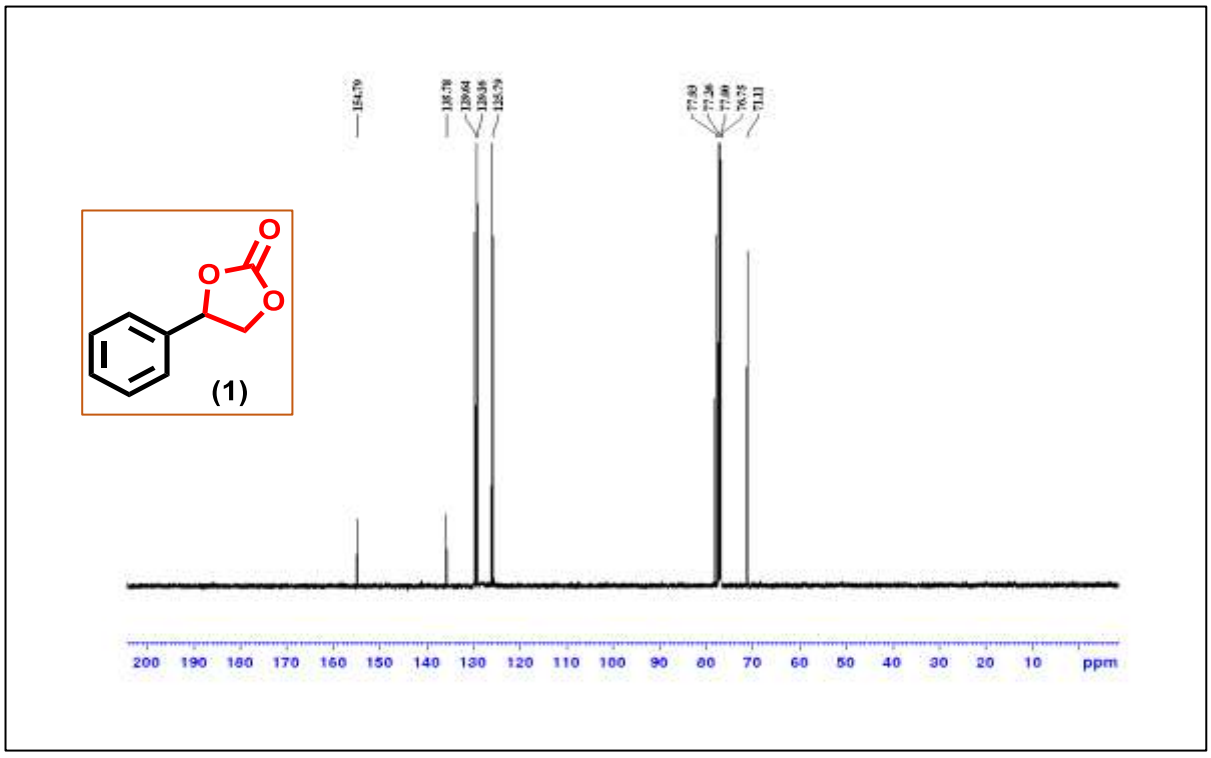

Figure 4.9: ^{13}C NMR spectra of the compound 1

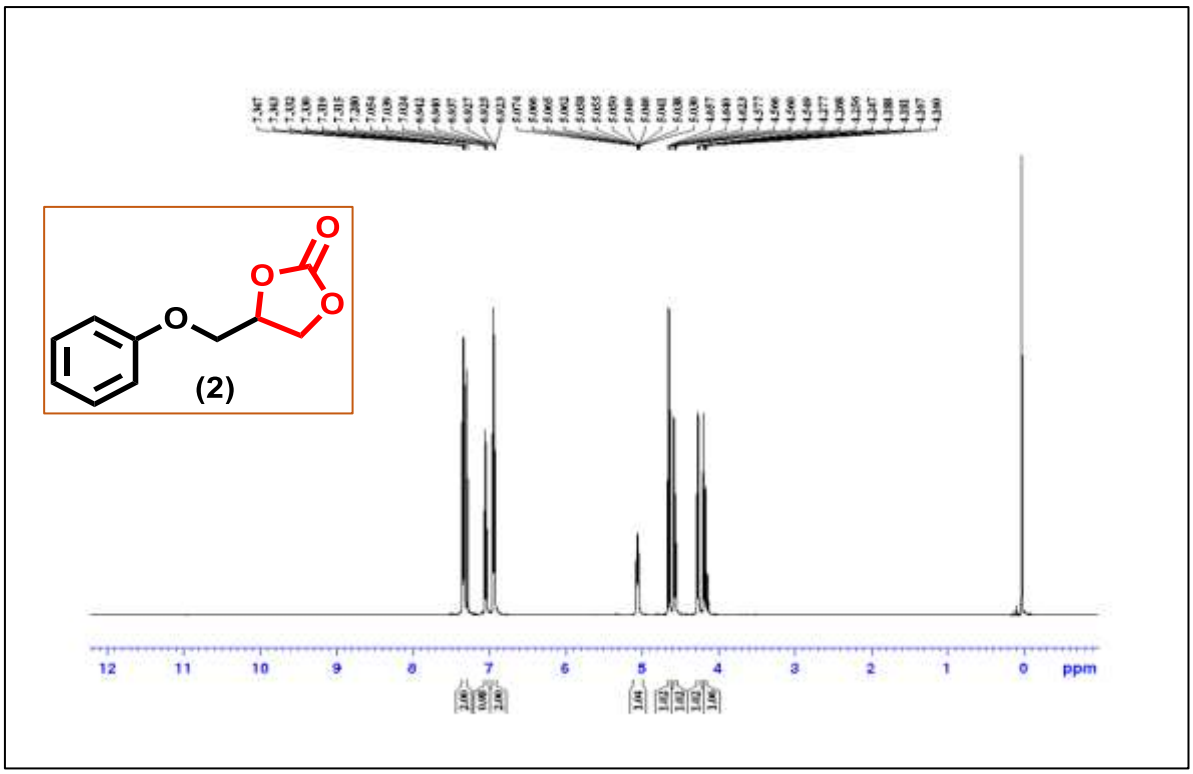

Figure 4.10: ^{1}H NMR spectrum of the compound 2

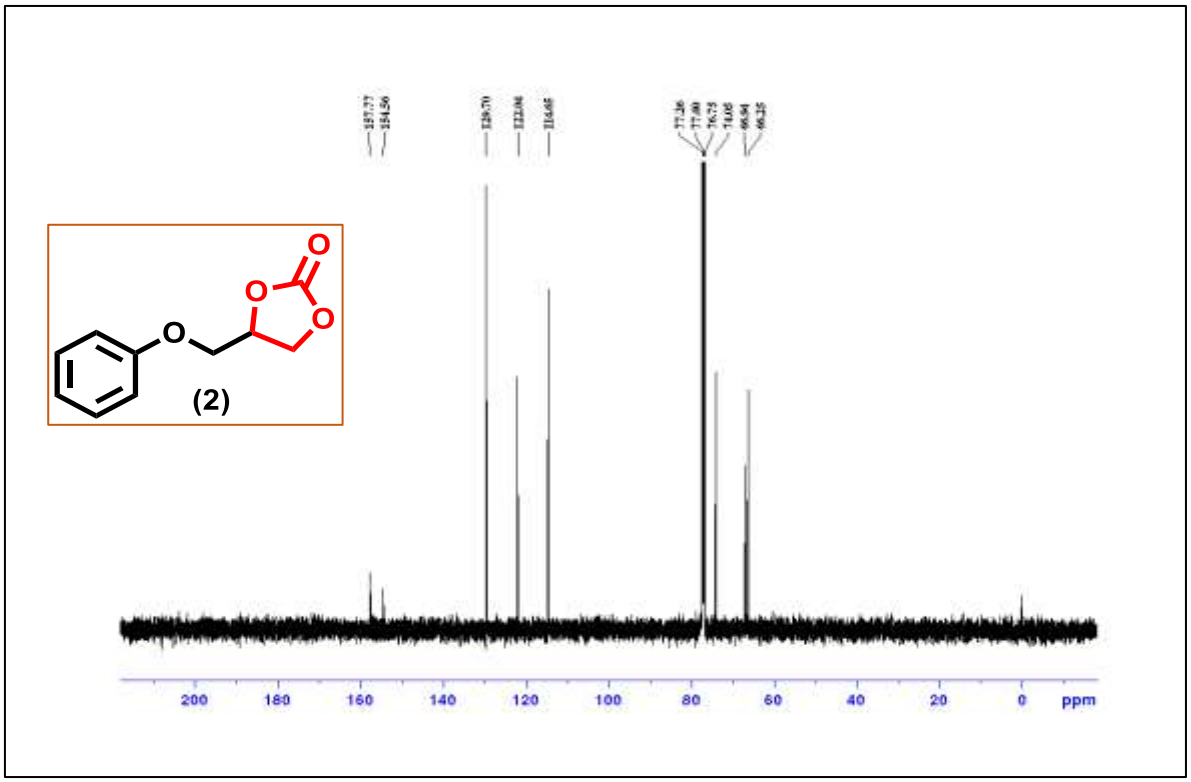

Figure 4.11: ^{13}C NMR spectra of the compound 2

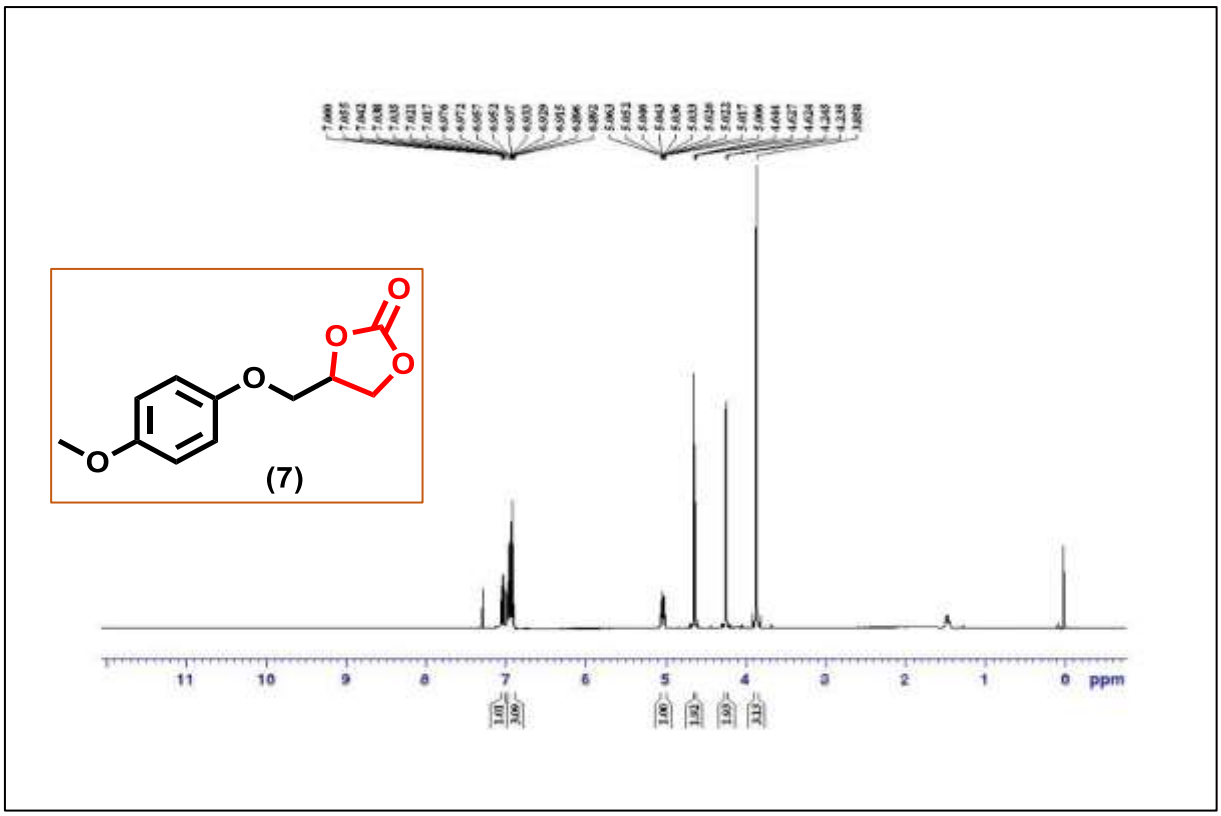

Figure 4.12: ^{1}H NMR spectra of the compound 7

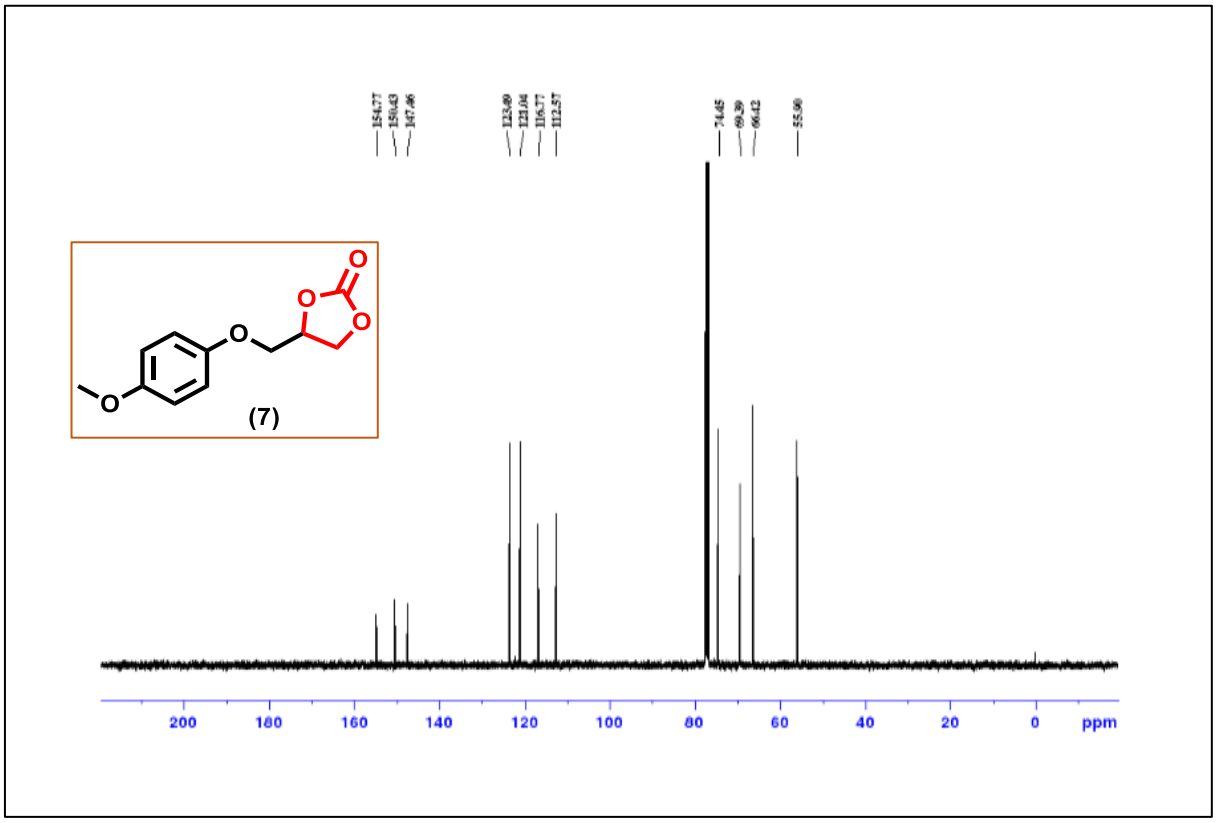

Figure 4.13: ^{13}C NMR spectra of the compound 7

CHAPTER 5

Instantaneous capture of carbon dioxide by resorcinol diglycidylether in cascade reactions comprising bulk co-polymerization

Abstract:

Capture and conversion of carbon dioxide (CO_2) to organic materials is an enticing reaction to mitigate its excessive release into the atmosphere. Herein, we report instantaneous capture of CO_2 through bulk copolymerization in three-component cascade reactions. The atom economic reactions of CO_2 with resorcinol diglycidylether (or 1,3-di(glycidoxy)benzene) and three different amines in the presence of a non-nucleophilic base 1,8-diazabicyclo[5.4.0]undec-7-ene (DBU) yielded three polycarbonates. The activation of CO_2 and reaction with co-monomer completed within 10-15 min at 100 °C but without any catalyst and solvent. The ring-strain induced reactivity of oxiranes and the proton-removing ability of the sterically hindered non-nucleophilic base have driven the copolymerization reactions. All these polycarbonates were hard and glassy with hardness upto 24.26 HV

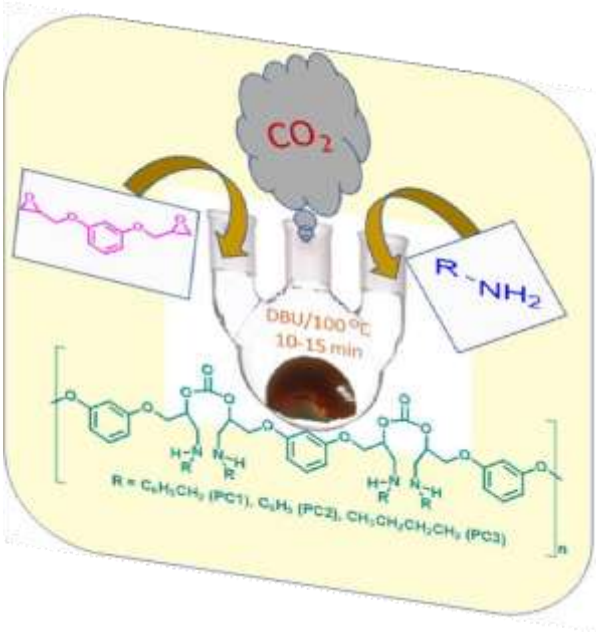

5.1. Introduction

The process of capturing waste carbon dioxide (CO_2) released from the heavy industry and automobile exhaust, and converting it to organic compounds or polymeric materials are the best way to alleviate its excessive release to the environment [1]. Therefore, the research on the utility of CO_2 is attractive for many scientists as it is an inexpensive, non-toxic, non– flammable, abundant carbon feedstock to produce valuable chemicals [2-3. Cyclic and polycarbonate synthesis from CO_2 and epoxides through a catalytic process is a 100% atom economic reaction established long ago. However, CO_2 is a thermodynamically stable highly oxidized molecule that deters its usefulness as a starting material for preparing various useful organic materials. In this present work, we report instantaneous capture of CO_2 through bulk copolymerization with resorcinol diglycidylether and three different amines in one-pot cascade reactions involving bulk co-polymerization. These reactions yielded material with remarkable hard and sharp characteristics. As a rare observation, these polymers possessed hardness upto 24.26 HV as determined by Vickers micro hardness tester using the diamond pyramid shape intender.

Cyclic and polycarbonates are industrially important materials because of their physical properties, and also, they are biodegraded under composting conditions. Further, while cyclic carbonates are utilised as the solvent for electrolytes in Li-ion rechargeable batteries, polycarbonates are used as solid polymer electrolytes (SPE) [4]. The perpetual challenge is finding a simple route to produce biodegradable and recyclable polycarbonates using CO_2. Highly reactive molecules are used to activate CO_2 in the presence of various catalysts. Despite the availability of many efficient catalytic systems [5], there are inadequacies in either tedious preparatory procedure of catalyst, separation problem associated with homogeneous catalysis, conversion percentage, or the need to use pure CO_2. Therefore, it is ambitious to capture CO_2 instantly and convert it to polycarbonates without tedious procedures.

Some of the best-practiced methods of preparing polycarbonates are direct polycondensation with CO_2, ring-opening polymerization of cyclic carbonates, caprolactones, and ring-opening followed by copolymerization of epoxides [6]. There are many reports on developing catalytic systems to activate CO_2 to polycarbonates via

alternating copolymerization of CO_2/epoxides. Earlier, we reported ring-expansion and ring-opening polymerization of epoxides using Cu(II), Zn(II), and Cd(II), complexes of 2,5-bis{N-(2,6diisopropylphenyl)iminomethyl} pyrrole, wherein Zn(II) complexes provided the best result [7].

A recent report by Williams and co-workers [8] showed the advantages of using an indium phosphasalen ring-opening polymerization catalyst to overcome similar Al-salen catalyst system's low activity. In such recent efforts, notably, the ring expansion of diglycidylethers occurred upon reaction with CO_2 in the presence of either organopolymer catalyst [9] (60 bar CO_2 at 120 °C, 12 h) or tetrabutylammonium bromide [10] (30 bar CO_2 at 85 °C, 16-26 h). Those bis(cyclic carbonates) were converted to polycarbonates by condensation polymerization at temperatures 85 – 130 °C in the presence of diamines. Ringopening polymerization of resorcinol diglycidylether yielded a cross-linked polyether via cationic photo polymerization on exposure UV light [11]. All these studies revealed the complexity involved in the ring-opening polymerization of diglycidylethers to capture CO_2 either in the form of catalyst or undesired product formation. Further, it is imperative to look towards a collection of carbon mitigation strategies, rather than a single method. In this chapter, we report straight forward synthesis of polycarbonates from CO_2 using resorcinol diglycidylether driven by a sterically hindered non-nucleophilic base.

5.2. Results and discussion

5.2.1. Co-polymerization of CO_2 with resorcinol diglycidylether

The epoxides being three-membered strained heterocycle is much more reactive than simple ethers and thus susceptible to a variety of nucleophilic and electrophilic attack. To design a fast and reliable method to capture CO_2, we intended to utilize the ring-strain induced reactivity of diglycidylethers and high basicity of the sterically hindered non-nucleophilic base 1,8-Diazabicyclo[5.4.0]undec-7-ene (DBU). Thus, in our present reactions (Scheme 1), resorcinol diglycidylether [IUPAC name: 1,3-bis(oxiran-2-ylmethoxy)benzene] yielded polycarbonates (**PC1**, **PC2** and **PC3**) directly in cascade reactions involving three different amines and CO_2 in the presence of DBU. In a model reaction to optimize reaction conditions, resorcinol diglycidylether (10 mmol) and benzylamine (1.09 mmol) were reacted with CO_2 gas without solvent at 100 °C wherein

DBU (1.09 mmol) was added. The reaction was performed in a 50 mL RB flask connected to the Schlenk line through which continuous flow of CO_2 gas was maintained. Within 10 min, the reaction mixture was turned form a liquid state to abrasive solid material stopping the reaction automatically. Under the optimized reaction condition, the reaction of resorcinol diglycidylether with three different amines in the presence of CO_2 yielded polycarbonates, *i.e.*, from benzylamine (**PC1**), aniline (**PC2**), and butylamine (**PC3**) (Scheme 5.1).

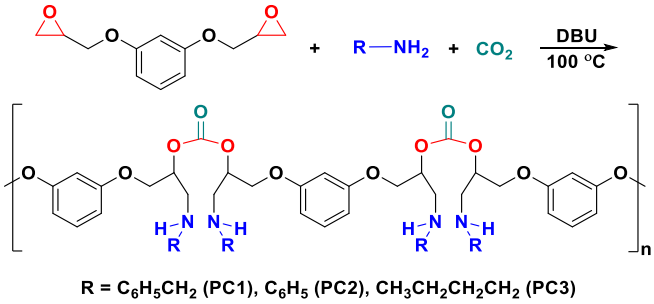

Scheme 5.1: General synthesis of polymers from epoxy CO_2 and amine derivative

The condensation polymerization with CO_2 occurred only in virtue of the chemical functionality formed by an amine reaction with epoxide rings of resorcinol diglycidylether. All steps in these cascade reactions happened within 10-15 min at 100 °C but without any catalyst and solvent. The proton-removing ability of a base without any other side reactions helped direct alternative copolymerization involving three components in cascade reactions. It is worth mentioning that, in a similar reaction condition, in the presence of TBAI, simple oxirane was reported to yield oxazolidinone [12].

The plausible mechanism of polymer formation is shown in Scheme 5.2. In this reaction, DBU's role was to remove a proton from the amine, which in turn reacted with the two epoxy groups to open the ring at the primary carbon position and formed the two anions. From two molecules of epoxy, the oxy anions reacted with CO_2 gas to form the desired polymer. To understand the role of CO_2, we have performed a reaction with resorcinol diglycidylether, amine, and DBU without using CO_2 gas, but no polymerization product was formed from this reaction.

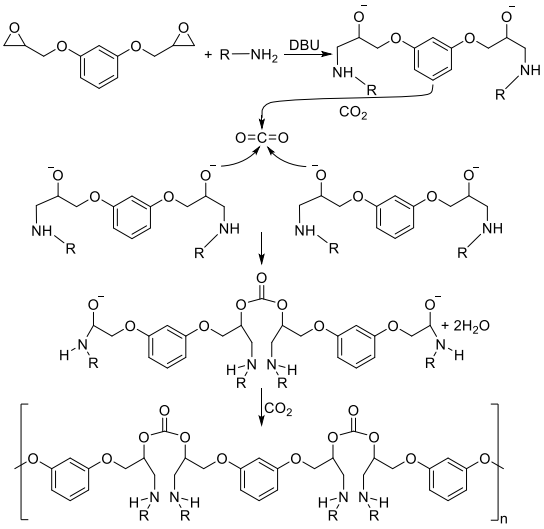

Scheme 5.2: Plausible mechanism for the formation of polycarbonate from resorcinol diglycidylether, amines and CO_2 gas

5.2.2. Structural and thermal characterization of polycarbonates

The challenge was to characterize the polycarbonates produced. All three polymers were not soluble in any solvents from polar to non-polar solvents like DMSO, DMF, acetonitrile, THF, chloroform, DCM, isopropanol, methanol, acetone, toluene, ether, ethyl acetate, water, n-hexane, n-heptane, and cyclohexane. Therefore, the polymers were removed from the reaction vessel by breaking it. They were all strong abrasive solids and sharp like glass, Actual photos polymers, **PC1, PC2,** and **PC3** are shown in Figure 5.1. The polymers were crushed with a hammer and ground to obtain powders, which were washed repeatedly with solvents to remove unreacted starting materials and soluble impurities. The structures of three polymers were confirmed by solid-state ^{13}C NMR and IR spectral data and further characterized by thermal analyses.

Table 5.1: Spectral data and thermal properties of polycarbonates

Polymer	^{13}C NMR-MAS (ppm)	IR (cm^{-1})	T_d (°C)	T_g (°C)	Hardness (HV)
PC1	160.67 (-**C**=O and -O**Ar** carbon), 130.42, 111.30, 105.49 (Aromatic carbons), 70.89 (Aliphatic carbons)	1746	318	77	24.99±0.87
PC2	160.56 (-**C**=O and -O**Ar** carbon), 130.62, 111.10, 105.47 (Aromatic carbons), 70.71 (Aliphatic carbons)	1739	343	109	6.23±0.41
PC3	160.82 (-**C**=O and -O**Ar** carbon), 131.60, 111.01,104.16 (Aromatic carbons), 69.82 (**C**H_2 OPh, -**C**HOCO and -**C**H_2CH-NH), 30.57 (-**C**$H_2$$CH_2$-NH), 21.13(**C**$H_2$-$CH_2$), 14.60 (**C**$H_3$ -CH_2)	1792	315	125	19.65±0.43

^{13}C NMR = Solid state NMR-MAS spectral data; IR = carbonyl stretching frequency in IR spectra; T_d = Decomposition temperature; T_g = Glass transition temperature; HV = Vickers Pyramid Number

Carbon signals of the **PC1**, **PC2**, and **PC3** appeared at expected chemical shifts in the ^{13}C NMR-MAS spectra. In the ^{13}C NMR-MAS spectrum of **PC1** (Figure 5.1), the signal of the aliphatic carbons (C1, C2, C3, and C4 in Figure 5.1) appeared as a single broad peak at δ 70.89 ppm. The signal of the aromatic carbon atoms (C5, C6, C7, C8, C9, C10 and C15 in Figure 5.1) appeared at δ = 130.42 ppm, while other aromatic carbon atoms (C12, C14, and C16 in Figure 5.1) appeared like broad doublet peak at δ 105.49 and 111.30 ppm. The carbons attached with oxygen atoms in the aromatic ring (C11 and C13 in Figure 5.1) and carbonyl carbon C17 were appearing merged at δ 160.67 ppm. The FTIR spectrum of **PC1** presented strong absorption bands at 1746 cm^{-1} pertaining to the carbonyl C=O stretching vibration. Aromatic ring stretching frequency appeared at 1590, 1489, and 1450 cm^{-1}, aromatic ortho-substituted group stretching frequency appeared at 760 and 685 cm^{-1}. For the -CH group, two stretching frequencies appeared at 2926 and 2875 cm^{-1}, -C-O- group stretching frequency appeared at 1180, 1148, 1080, and 1038 cm^{-1} Hydrogen bonding -NH group stretching frequency appeared at 3406 cm^{-1} (Figure 5.2).

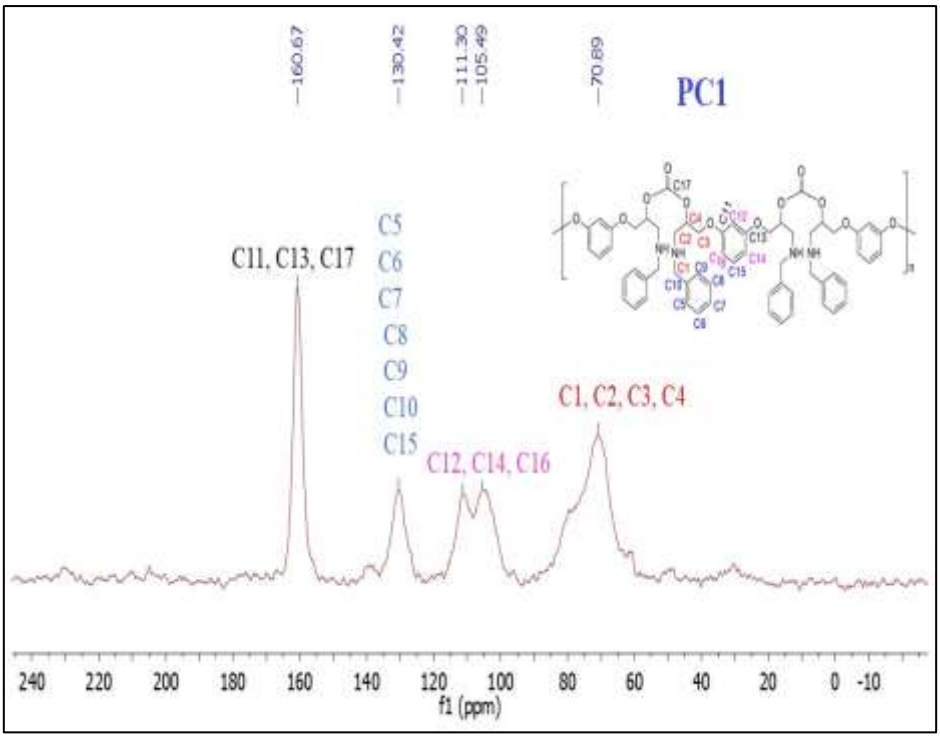

Figure 5.1: ^{13}C NMR-MAS spectrum of **PC1** and its structure of with carbon mapping

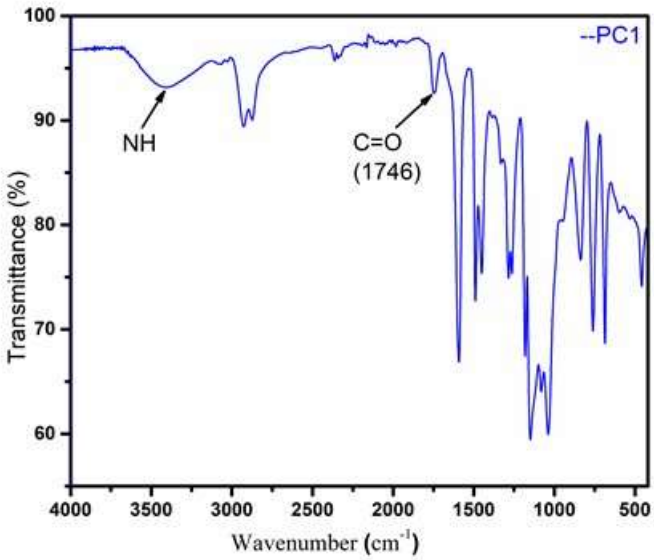

Figure 5.2: FTIR spectrum of **PC1**

The thermal properties of polycarbonates produced *i.e.*, **PC1**, **PC2** and **PC3** were examined with DSC (Figure 5.3) and TGA (Figure 5.4). The Tg values of the polymers seem to vary considerably from 77 to 125 °C (Table 5.1, Column 5) depending on the amine comonomer. The Tg value of the aliphatic substituted polymer (**PC3**) is higher than that of the aromatic aniline substitution (**PC2**), while the benzylamine substitution (**PC1**) gave the lowest Tg value. This observation may be due to the restricted the movement of the polymer chains caused by the aromatic rings, and the flexibility imparted by the presence of aliphatic segments in the polymer backbone. The TGA thermograms (Figure 5.4) demonstrated typical sharp one-stage characteristics with fast weight loss arising at decomposition temperatures for **PC1** and **PC3**, while butylamine incorporated polymer showed initial weight loss sacred at 110 °C. In particular, the thermograms of **PC3** showed very good thermal stability (Table 5.1, Column 4).

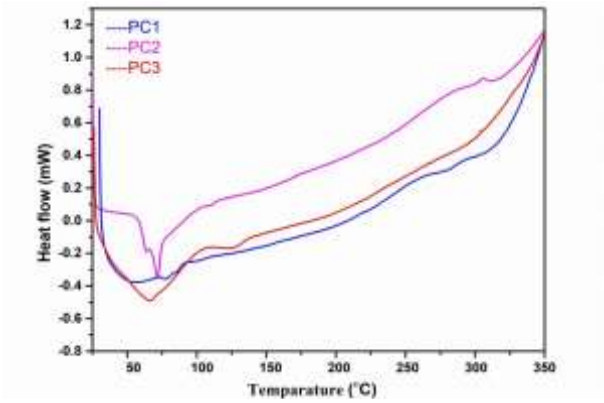

Figure 5.3: Differential scanning calorimeter of polycarbonates, PC1, PC2 and PC3

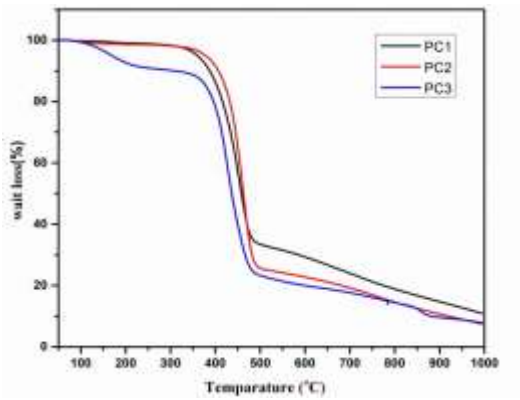

Figure 5.4: Thermal gravimetric analysis of polycarbonates, PC1, PC2 and PC3

5.2.3. Hardness of polycarbonates

Many different plastics are often used in friction and wear applications, such as in bearings, bushings, gears, and chain guides. Plastic hardness is a measure of resistance to penetration of plastic by a harder body [13]. Hence, it is a crucial engineering parameter for constructing devices, industrial parts, or consumer products. The microhardness of polymers is also influenced by various microstructures of polymers and composites [14]. For example, the microhardness of poly(methylmethacrylate) was improved by reinforcing with polypropylene to make the mechanical property suitable for prosthetic dentistry [15]. Synthesized poly carbonates of actual photos (first row), samples (second row), and morphology of Vickers indent (third row) of polymers, **PC1, PC2,** and **PC3** were shown in figure 5.5.

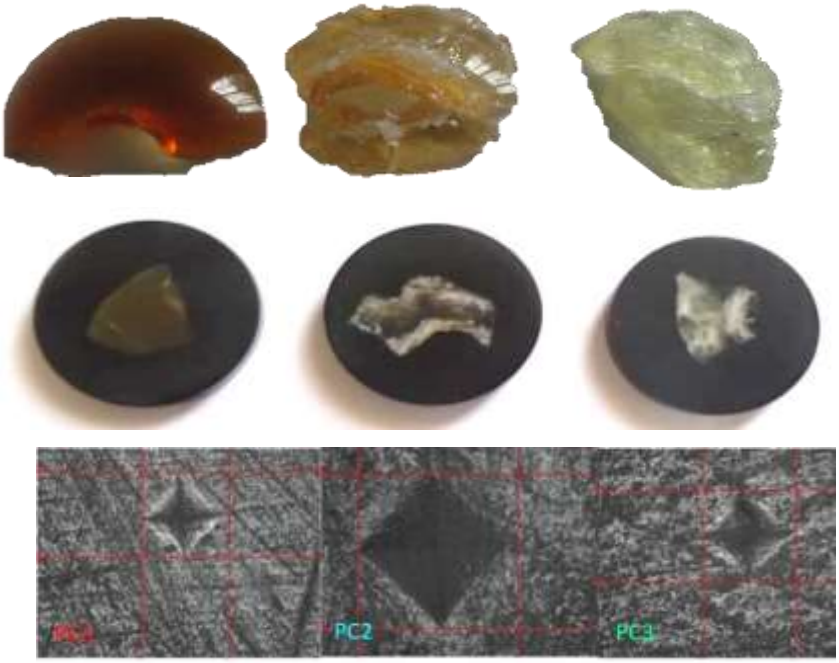

Figure 5.5: Actual photos (first row), samples (second row), and morphology of Vickers indent (third row) of polymers, **PC1, PC2,** and **PC3** in the order from left to right

The basic principle of measuring hardness is to test the material's ability to resist plastic deformation when a force is applied from a standard source. The different hardness scales have been popular in different industries and different disciplines of science and technology. The Vickers hardness test is the most widely used testing methodology [16] for evaluating the mechanical performance of materials since the results in this method

are independent of the indenter load [17]. Since the obtained polymers were hard and glassy, we have determined their hardness by Vickers microhardness tester (Table 5.1, column 6). The polymer with aromatic group attached directly (**PC2**) showed lowest value of hardness Vickers hardness scale, whereas benzyl group attached polymer (**PC1**) showed the highest value of 24.99±0.87 HV. The polymer with the pure aliphatic chain possed the hardness value of 19.65±0.43 HV. We have confirmed the hardness value after 6 trails of each sample (Table 5.2).

Table 5.2: Vickers hardness of samples of **PC1**, **PC2** and **PC3**

Trail	PC-1	PC-2	PC-3
I	24.31±0.35	6.30±0.17	20.01±0.2
II	25.60±0.43	6.10±0.2	19.01±0.14
III	25.35±0.3	6.19±0.15	20.20±0.18
IV	25.48±0.37	6.27±0.25	19.14±0.22
V	24.11±0.32	6.33±0.2	19.81±0.13
VI	25.12±0.45	6.21±0.18	19.75±0.17
Average	**24.99±0.87**	**6.23±0.41**	**19.65±0.43**

5.3. Conclusion

In summary, instantaneous capture of carbon dioxide through bulk copolymerization in three component cascade reactions was established. Three different polycarbonates were obtained by changing the amines used in the reactions. These reactions were driven by the proton removing ability of a non-nucleophilic base and the release of ring-strain imparted by the three-member oxiranes heterocycles. All these polycarbonates were insoluble in any solvent but they were very hard. Considering the fast with which the reaction occurred and the hardness of the materials, the method reported here has potential for large-scale industrial application.

5.4. Experimental section

5.4.1. Materials

Resorcinol diglycidyl ether, benzyl amine, aniline, butyl amine and 1,8-Diazabicyclo [5.4.0] undec-7-ene, (DBU) were purchased from Sigma-Aldrich.

5.4.2. Instrumentation

Solid state ^{13}C NMR spectra were acquired using **ECX400** - Jeol 400 MHz High Resolution Multinuclear FT-NMR Spectrometer. IR spectra were recorded on a neat FTIR spectrophotometer. The Tg of polycarbonates were measured by Differential Scanning Calorimeter (DSC) operated with a heating rate of 10 °C/min. TG analyses were carried out on a PerkinElmer – STA 6000 was performed on a PerkinElmer – STA 6000 coupled with a PerkinElmer–Clarus SQ8S mass spectrometer.

Hardness test

The hardness of polycarbonates was determined using Vickers hardness testing method using square based diamond pyramid as indenter (Figure 5.6). This kind hardness refers to the resistance to permanent deformation when the material is subjected to a continual load. The Vickers hardness measurements of polycarbonates (**PC1**, **PC2** and **PC3**) were performed using a Tinius Olsen Micro – Vickers Hardness – FH006 Series tester. In this method, the force is applied with the help of an indenter on the sample material. The hardness of samples with a 500 g (HV0.5) load was measured at an indentation time of 20 s using Diamond pyramid shape Intender. This intender can be used for all materials irrespective of hardness. The hardness values were measured immediately after indentation. In all cases, six measurements were taken and averaged.

Figure 5.6. Image of measuring of hardness

5.4.3. General procedure of production of polycarbonate from the reaction of epoxide, amine and CO_2

In a typical reaction, DBU (1.09 mmol), epoxide (10 mmol) and amine derivatives (1.09 mmol) were introduced into a Schlenk flask (10 mL). The reaction was continued at 100°C for 10 min with flow of CO_2. When the reaction mixture turned to strong solid material, the flow of gas was stopped and allowed to reach room temperature. Product was not soluble in any solvent and so the reaction flask was broken to get polymers. To know the structure of the product, the material was crushed with hammer and grinded to get powder. It was washed by organic solvents to remove any unreacted starting materials and DBU. To confirm the structure of product, solid state ^{13}C NMR-MAS and IR spectra were recorded.

Spectral data and characterization of PC2

In the solid state ^{13}C NMR-MAS spectrum of PC2 (Figure 5.7), the signal of the aliphatic carbons (C1, C2 and C3 in Figure 5.7) appeared at one broad peak at 70.71 ppm. The signal of the aromatic carbon atoms of the ring (C4, C5, C6, C7, C8, C9, and C14 in Figure 5.7) appeared at δ 130.62 ppm, while other set of aromatic carbon atoms (C11, C13 and C15 in Figure 5.7) appeared like broad doublet peak at δ 105.47 and 111.10 ppm. The carbons attached with oxygen (C10, C12) and the carbonyl carbon C16 were appearing merged at δ = 160.56 ppm.

The FTIR spectra of PC2 (Figure 5.8) showed strong absorption bands at 1739 cm^{-1} due to the carbonyl C=O stretching vibration. Hydrogen bonding -NH group stretching frequency appeared at 3350 cm^{-1}. For -CH group, two stretching frequency appeared at 2931, 2878 and, 2833 cm^{-1}. Aromatic group stretching frequency appeared at 1592, 1490, and 1450 cm^{-1}. The aromatic ortho substituted group stretching frequency appeared at 756 and 685 cm^{-1}. The -C-O- group stretching frequency appeared at 1127, 1181, 1153, 1081 and 1022 cm^{-1}.

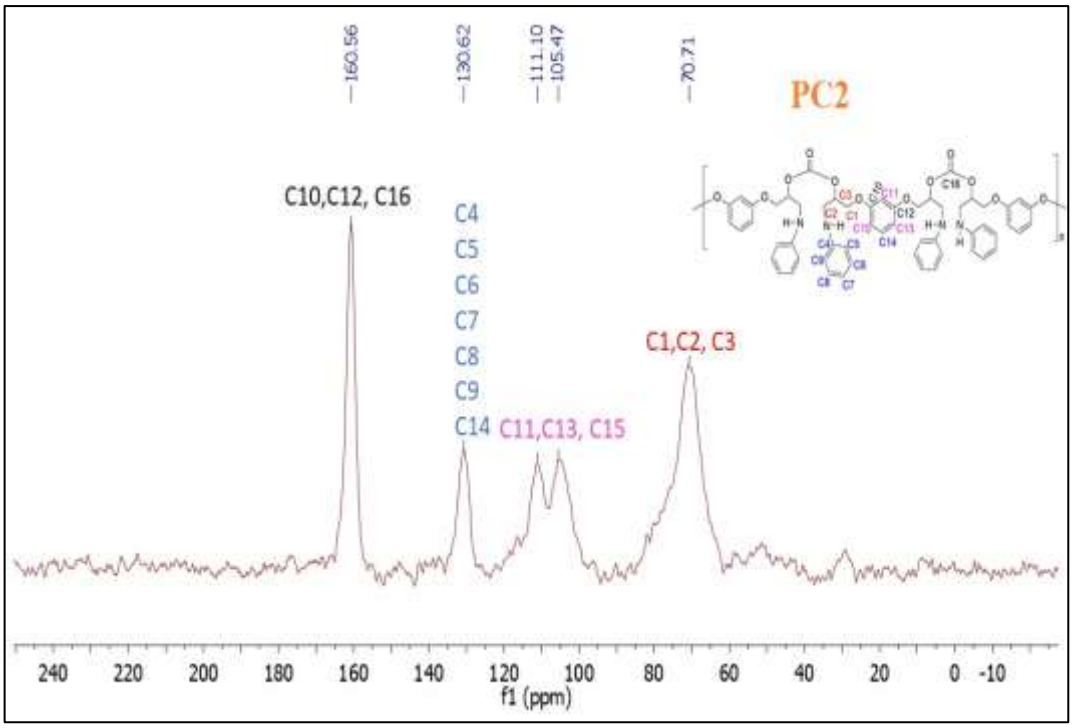

Figure 5.7: ^{13}C NMR-MAS spectrum of **PC2** and its structure of with carbon mapping

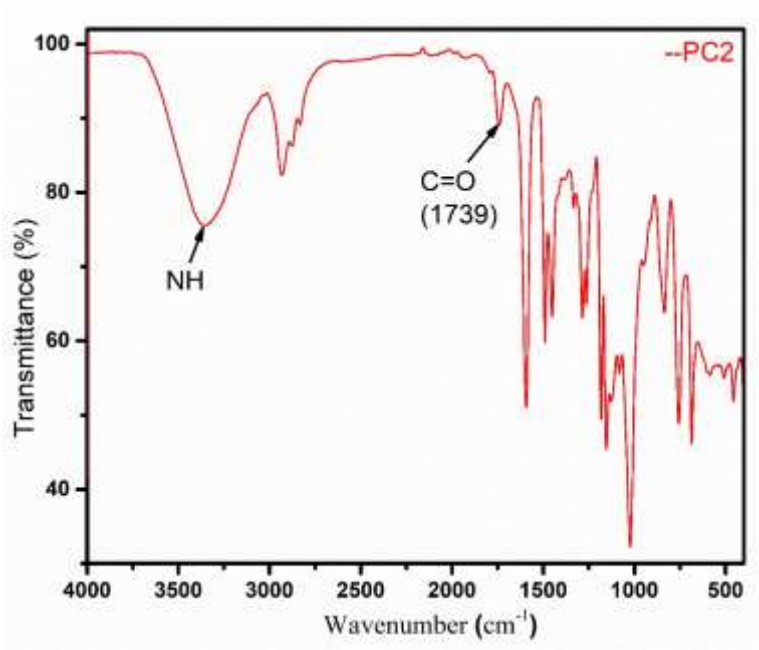

Figure 5.8: FTIR spectrum of **PC2**

Spectral data and characterization of PC3

In the solid state ^{13}C NMR-MAS spectrum of PC3 (Figure 5.9), the signal of the aliphatic carbons, C7 (Figure 5.9) appeared at δ 14.60 ppm, while C5 and C6 (Figure 5.9) appeared as a broad peak at 21.13 ppm. The signal of C4 appeared at δ 30.57 ppm, while other aliphatic carbons (C1, C2, C3, and C4 in Figure 5.9) appeared as one broad at 69.82 ppm. The signal of the aromatic ring carbon C10 appeared at δ 130.60 ppm and remaining ring carbons C9, C11 and C13 appeared like broad doublet peak at δ 104.16 and 111.05 ppm. The carbon attached to oxygen (C8, C12 and C14 in Figure 5.9) and carbonyl carbons were appearing merged at δ 160.82 ppm.

The FTIR spectra of PC3 showed (Figure 5.10) strong absorption bands at 1792 cm^{-1} due to the carbonyl C=O stretching vibration. Hydrogen bonding -NH group stretching frequency appeared at 3373 cm^{-1}. Aromatic group stretching frequency appeared at 1592, 1490 and 1451 cm^{-1}, The aromatic ortho substituted group stretching frequency appeared at 746 and 684 cm^{1}. For -CH group, two stretching frequency appeared at 3008, 2930 and 2875 cm^{-1}. The -C-O- group stretching frequency appeared at 1180, 1154 and 1045 cm^{-1}. The polymers **PC1, PC2** and **PC3** were confirmed from spectral data solid state ^{13}C NMR (table 5.1, column 2) and carbonyl functional group of the FTIR spectral data (table 5.1, column 3)

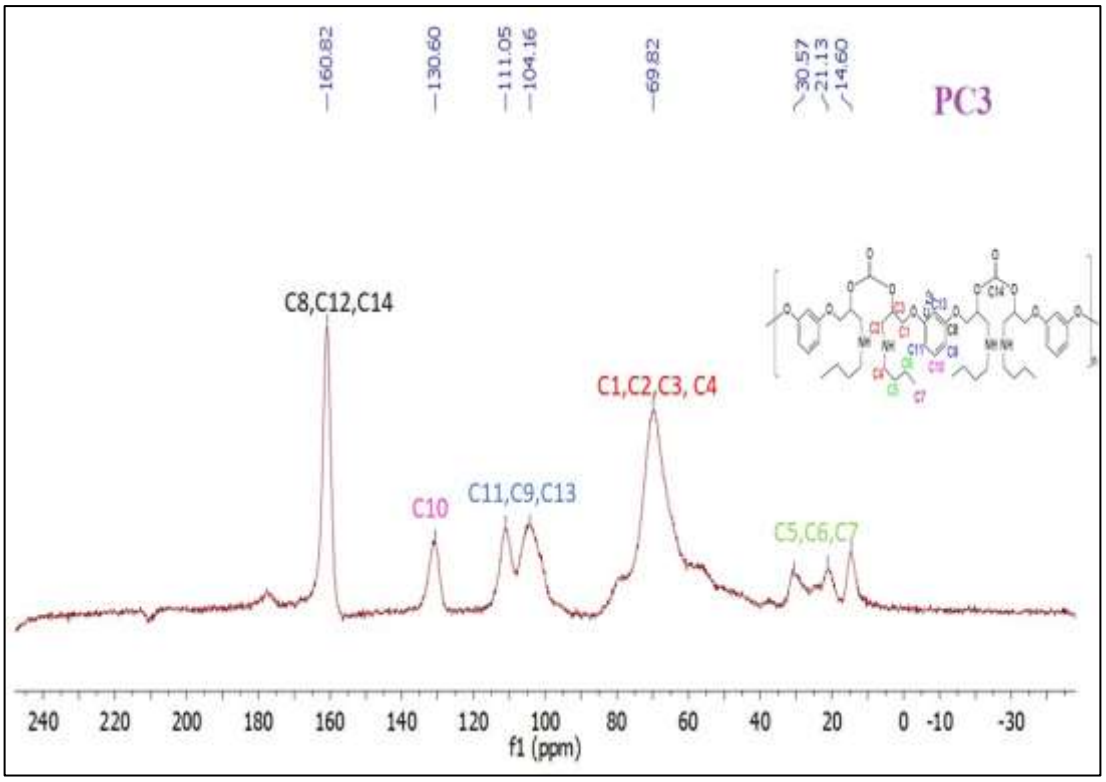

Figure 5.9: ^{13}C NMR-MAS spectrum of **PC3** and its structure of with carbon mapping

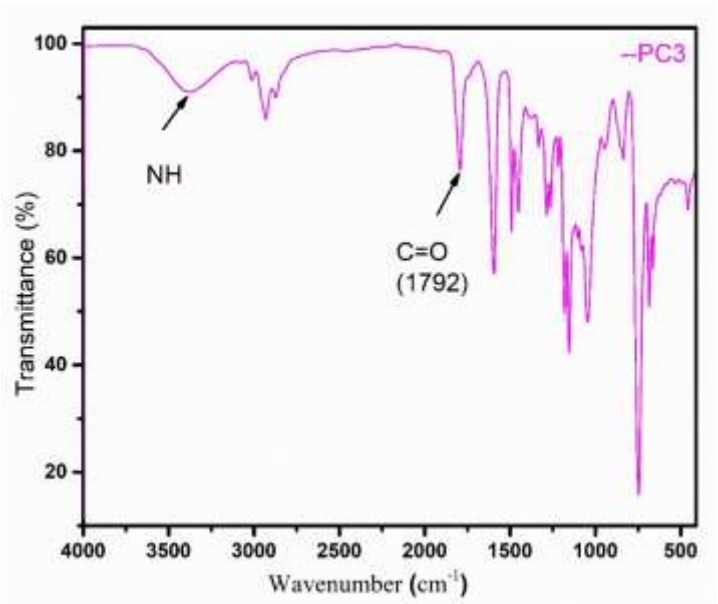

Figure 5.10: FTIR spectrum of **PC3**

5.5. References:

[1] (a) R. A. Meyers (ed.), Conversion of CO_2 into Polymers, Encyclopedia of Sustainability Science and Technology, **2018**, Springer Science+Business Media, LLC, Springer Nature; (b) B. Metz, O. Davidson, H. C. de Coninck, M. Loos, and L. Meyer (eds.), IPCC Special Report on Carbon Dioxide Capture and Storage. Prepared by Working Group III of the Intergovernmental Panel on Climate Change (IPCC), **2005**, 442 pp, Cambridge University Press, Cambridge, United Kingdom and New York, NY, USA.

[2] (a) S. Wu, Y. Zhang, B. Wang, E. H. M. Elageed, L. Ji, H. Wu, G. Gao, *Eur. J. Org. Chem*. **2017**, 3, 753. (b) R. Dalpozzo, N. Della Ca, B. Gabriele and R. Mancuso, *Catalysts.* **2019**, *9*, 511. (c) D. Y. C. Leung, G. Caramanna, M. M. Maroto-Valer, *Renewable and Sustainable Energy Reviews*. **2014**, *39*, 426.

[3] (a) M. Mikkelsen, M. Jorgensen and F. C. Krebs, *Energy Environ. Sci*. **2010**, *3*, 43. (b) M.North, R. Pasquale and Carl Young, *Green Chem*. **2010**, *12*, 1514.

[4] J. Zhang, J. Yang, T. Dong, M. Zhang, J. Chai, S. Dong. T. Wu, X. Zhou, G. Cui, *Small.* **2018**, *14*, 1800821.

[5] (a) S. Verma, G. Kumar, A. Ansari, R. I. Kureshy and N. H. Khanab, *Sustainable Energ Fuels.* **2017**, *1*, 1620. (b) J. Sun and D. Kuckling, *Polym. Chem*. **2016**, *7*, 1642. (c) S. Bian, C. Pagan, A. A. Andrianova, Artemyeva, and G. Du, *ACS Omega*. **2016**, 1, 1049. (d) S. Ghosh, A. Ghosh, S. Biswas, M. Sengupta, D. Roy, and Sk. M. Islam, *ChemistrySelect*. **2019**, *4*, 3961. (e) R. H. Lambeth, T. J. Henderson, *Polymer*. **2012**, *54*, 5568. (f) David R. Moore, Ming Cheng, Emil B. Lobkovsky, Geoffrey W. Coates, *J. Am. Chem. Soc*. **2003**, *125*, 11911. (g) A. H. Liu, Y.L. Dang, H. Zhou, J. J. Zhang, X-B. Lu, *ChemCatChem.* **2018**, *10*, 2686.

[6] (a) B. Grignard, S. Gennen, C. Jérôme, A. W. Kleij and C. Detrembleur, *Chem. Soc. Rev*. **2019**, *48*, 4466. (b) R. Muthuraj, T. Mekonnen, *Polymer*, **2018**, *145*, 348. (c) D. J. Darensbourg, *Chem. Rev*. **2007**, *107*, 2388.

[7] (a) H. V. Babu and K. Muralidharan, *RSC Adv.* **2014**, *4*, 6094. (b) H. V. Babu and K. Muralidharan, *Polymer.* **2014**, *55(1),* 83. (c) H. V. Babu and K. Muralidharan, *Dalton Trans.* **2013**, *42*, 1238.

[8] A. Thevenon, A. Cyriac, D. Myers, A. J. P. White, C. B. Durr, and C. K. Williams, *J. Am. Chem. Soc*. **2018**, *140*, 6893.

[9] V. Schimpf, J. B. Max, B. Stolz, B. Heck, and R. Mülhaupt, *Macromolecules*. **2019**, *52*, 320.

[10] S. Verma, G. Kumar, A. Ansari, R. I. Kureshy and N. H. Khan, *Sustainable Energy Fuels*. **2017**, *1*, 1620.

[11] Q-B. Nguyen, N-H. Nguyen, A. R. de Anda, V-H. Nguyen, D-L. Versace, V. Langlois, S. Naili, E. Renard, *J Appl. Polym. Sci*. **2020**, *137*, e49051.

[12] M. Lv, P. Wang, D. Yuan and Y. Yao, *ChemCatChem*, **2017**, *9*, 4451.

[13] B. J. Briscoe, S.K. Sinha, (**1999**) *Hardness and Normal Indentation of Polymers*. In: G.M. Swallowe (eds) *Mechanical Properties and Testing of Polymers. Polymer Science and Technology Series*, Vol 3. Springer, Dordrecht.

[14] (a) V. A. Soloukhin, J. C. M. Brokken-Zijp, O. L. J. van Asselen, and G. de With, *Macromolecules.* **2003**, *36*, 7585. (b) R. J. Crawford, *Polymer Testing.* **1982**, *3*, 37.

[15] M. Mathew, K. Shenoy, K S Ravishankar, *Int. J. Scientific Study*. **2014**, *2*, 71.

[16] (a) W. Weiler, *NASF Surface technology white papers.* **2019**, *83*, 13. (b) R. L. Smith and G. E. Sandland, *Proceedings of the Institution of Mechanical Engineers*. **1922**,*1*, 623.

[17] (a) I. M. Low, C. Shi, *J. Mater. Sci. Lett*. **1998**, *17*, 1181. (b) I. Narisawa, Ishikawa and T. Nonak, *Kobunshi Ronbunshu*. **1988**, *45*, 777.

SUMMARY AND CONCLUSION

The nano/micro particles are synthesized often in the presence of long chain organic molecules as capping or stabilizing agents. These organic molecules cover the active centres and restrict or reduce their catalytic activity. Considering the above fact, we have been successful in synthesizing various metal sulphides and oxides without involvement of surfactant molecules. In these materials, the surface was freely available for adsorption and desorption reactions. Since there is no hindrance for the movement of electrons, it was anticipated to influence their catalytic efficiency. Thus, the present work emphasized the single step synthesis of different nano/micro materials of metal sulphides/oxides without surfactant molecules and their role as catalysts towards organic reactions.

Capturing and converting carbon dioxide (CO_2) into useful organic molecules and polymers is the best way of alleviating excessive release of it from industrial sources to the environment. The present work also emphasized the conversion of CO_2 to cyclic and polycarbonate with and without using catalyst in simple reactions.

We have successfully synthesized sf-CuS, sf-$CuInS_2$ and composite CuO-ZnO nano/ micro particles under supersaturated conditions. The significant characteristics of nano/ micro materials without surfactant molecules are their insoluble nature in many organic solvents. However, the solubility issue has become advantageous since they could be used in heterogeneous catalysis. In many such reactions, use of these metal sulphides or metal oxide nanoparticles as the catalyst was more appealing because of the increased catalytic activity attributed to the large surface to volume ratio with unhindered electron movement.

In the First study, we have synthesized the copper sulfide (sf-CuS) nano/micro particles without having organic surfactant molecules as the capping agent. These particles with a flower-like architecture (micro flowers, **mf**) were obtained readily under the supersaturated condition at room temperature. The catalyst has been utilized successfully for one-pot synthesis of triazoles by cycloaddition of both benzyl halide derivatives- alkyne and epoxide derivatives – alkyne in the presence of sodium azide and exhibited excellent catalytic activity compared with some other nanoparticles with surfactants. Both these reactions proceeded in the presence of azide and phenylacetylene in the water at room temperature. The desired products were obtained at ambient

temperature while the reactions were performed in water. The catalyst can be recycled and reused for five times without losing its activity and there was no catalyst leaching observed during reactions.

The copper-indium-sulfide ($CuInS_2$) nanoparticles (**sf-CIS-np**) were prepared in a simple without using any surfactant molecules. These nanoparticles were used as the heterogeneous catalyst for Glassar-Hay homo-coupling reactions involving phenylacetylene derivatives. They were used as the catalyst in the dimerization of 1, 3-diyne derivatives while using of 8-diazabicyclo[5.4.0]undec-7-ene (DBU) as the base, in acetonitrile using 10 mg of **sf-CIS-np** at room temperature within 4-7 h, depending on the substrate. The reaction optimization studies established that 10 mg of **sf-CIS-np** is sufficient to complete the reactions within 4-7 h at room temperature, depending on the substrate. The catalyst was reused for five cycles with little difference in its efficiency. The catalyst can be recycled and reused for five times without losing its activity and there was no catalyst leaching observed during reactions.

In this thesis, we have reported the catalytic system based on copper and zinc mixed metal oxides (CuO-ZnO) nano/micro-flakes (**Cozi-nmf**) for cycloaddition of CO_2 with various epoxides at room temperature under solvent-free conditions. The novel recyclable heterogeneous catalyst was prepared via a simple procedure successfully at room temperature and the catalyst (**Cozi-nmf)** with a high surface area of around 45.8 m^2 g^{-1} by grinding method within 10 min. It was used as the catalyst for cycloaddition of CO_2 with various epoxides to produce cyclic carbonates. The syntheses described here were performed in solvent-free conditions and used inexpensive and recyclable surfactant-free heterogeneous catalysts. The high efficiency of **Cozi-nmf** as a catalyst was because of the availability of the bare catalyst surface, which promoted the hindrance free movement of electrons and adsorption of substrate effectively. The simplicity in the synthesis of catalyst and cyclic carbonates promises large-scale industrial use of the method.

We have established instantaneous capture of carbon dioxide through bulk copolymerization in three-component cascade reactions. The atom economic reactions of resorcinol diglycidylether with three different amines and CO_2 in the presence of 1,8-Diazabicyclo[5.4.0]undec-7-ene (DBU) yielded three polycarbonate. The activation of CO_2 and reaction with comonomer completed within 10-15 min at 100°C but without any

catalyst and solvent. The ring-strain induced reactivity of three-member epoxide heterocycles and the proton-removing ability of the sterically hindered non-nucleophilic base have driven the copolymerization reactions. All these polycarbonates were insoluble in any solvent but they were very hard. Considering the fast with which the reaction occurred and the hardness of the materials, the method reported here has potential for large-scale industrial application. All these polycarbonates were hard and glassy with hardness upto 24.26 HV.

List of publications

List of Publications

1. **Venkateswara rao Velpuri** and Krishnamurthi muralidharan, Multicomponant click reaction catalysed by organic surfactant free copper sulfide (sf-CuS) nano micro flowers. *Journal of organometallic chemistry.* **2019**, 884, 59e6560.

2. Sanyasinaidu gottepu, **Venkateswara rao Velpuri** and Krishnamurthi muralidharan* Surfactant free metal chalcogenides microparticles consisting of nano size crystallites: room temperature synthesis driven by the supersaturated condition *J. Chem. Sci.* **2017,** 129 1853–1861.

Publications: to be Submitted/Under Revision:

3. **Venkateswara rao Velpuri** and Krishnamurthi muralidharan, High yield room temperature conversion of carbon dioxide into cyclic carbonates catalysed by mixed metal oxide (CuO-ZnO) nano/micro flakes (Cozi-nmf) (Applied organometallic chemistry).

4. **Venkateswara rao Velpuri** and Krishnamurthi muralidharan, Instantaneous capture of carbon dioxide by 1, 3-bis(oxirane) in cascade reactions comprising polycondensation to yield hard glassy materials.

Posters and Oral presentations

1) Sanyasinaidu Gottapu, **Venkateswara Rao Velpuri** and Krishnamurthi Muralidharan "Room Temperature Synthesis of Surfactant free Metal Chalcogenides Microparticles Consisting of Nano size Crystallites" poster presentation at 15 annuals in house symposium in Chemfest-2018 at University of Hyderabad, Hyderabad during 9-10, March 2018
2) **Venkateswara Rao Velpuri** and Krishnamurthi Muralidharan "*Synthesis of metal Sulphide/Oxide nano/micro particles and their catalytic application for organic transformations*" Oral and poster presentation at 17 annuals in house symposium in Chemfest-2020, School of Chemistry, University of Hyderabad, Hyderabad during 20-21, may 2020
3) **Venkateswara Rao Velpuri** and Krishnamurthi Muralidharan, "*multicomponent click reaction catalyzed by Organic surfactant-free copper sulfide (sf-CuS) nano/micro flowers" poster* presentation at CRSI-National Symposium in Chemistry-24, jointly organized by CSIR-CLRI and IIT-Madras at CSIR-CLRI, Chennai during 08-10th, February 2019.
4) **Venkateswara Rao Velpuri** and Chinappan Shivasankaran "Understanding the electronic structure and bonding analysis of metal azide complexes'' poster presentation at national conferences on frontier areas in chemistry (NCFAC-2011), Dept. of chemistry, Pondicherry university, Puducherry during 22, December 2011

J. Chem. Sci. Vol. 129, No. 12, December 2017, pp. 1853–1861.
https://doi.org/10.1007/s12039-017-1381-4

REGULAR ARTICLE

Surfactant free metal chalcogenides microparticles consisting of nano size crystallites: room temperature synthesis driven by the supersaturated condition

SANYASINAIDU GOTTAPU, VENKATESWARA RAO VELPURI and KRISHNAMURTHI MURALIDHARAN*
School of Chemistry, University of Hyderabad, Prof. C. R. Road, Gachibowli, Hyderabad, Telangana 500 046, India
E-mail: murali@uohyd.ac.in

MS received 26 July 2017; revised 15 September 2017; accepted 25 September 2017; published online 11 November 2017

Abstract. A versatile methodology for the production of organic surfactant-free metal chalcogenide microparticles consisting of nano crystallites at room temperature in a short time is described. The reaction of various metal sources with $LiBH_4$ in the presence of either S or Se yielded their corresponding CuS, Cu_2S, CdS and $Cu_{2-z}Se$ microparticles. These micron size particles are aggregates of nano crystallites. The reactivity of $LiBH_4$ and supersaturated condition helped in the formation nanocrystals. The first observation of metal source dependent morphology of particles produced under identical reaction condition is also discussed. The morphology of CuS particles obtained in these reactions was varying with the change of metal source used in the reaction. Interestingly, the reactions producing metal chalcogenide microparticles also yielded borane (BH_3) as a side product.

Keywords. Metal chalcogenides; copper sulphide; copper selenide; micro flowers.

1. Introduction

The synthesis of metal chalcogenide (S, Se, Te) nano/micro size particles is fascinating since they possess properties that depend on the composition of material, size and shape of the particles.[1] The unique optical properties of these metal chalcogenides made them useful for multiple potential applications in biological,[2,3] light emitting and photovoltaic devices.[4–8] Among the metal sulphides, copper sulphide (CuS) is a less hazardous material, and relatively cheap. It is an important p-type semiconductor and exhibits many unusual electronic, optical, and other physical and chemical properties. It has great potential in a versatile range of applications such as optical filters, superionic materials, solar radiation absorbers, catalysts, nanometer-scale switches, high-capacity cathode material in lithium secondary batteries, superconductors, chemical sensors and thermoelectric cooling material.[7–11] Therefore, copper sulphide is a valuable material for the construction of devices for various applications.

Copper sulphide has attracted significant interests because of the variations in stoichiometric compositions, valence states, nanocrystal morphologies and differences in the crystal structures.[12] The variation in stoichiometric compositions of copper sulphide resulted in five polymorphic forms, *viz.* chalcocite (Cu_2S), djurleite ($C_{1.95}S$), digenite ($Cu_{1.8}S$), anilite ($Cu_{1.7}S$) and covellite (CuS).[12] Copper sulphide was synthesized using the following methods; *viz.*, thrombolysis, template assisted growth, microwave irradiation, hydrothermal or solvothermal, sonochemical techniques, CVD, soft template way and electrochemical method.[13–19] However, those methods are expensive and complicated because of the presence of surfactants and templates that introduce impurities to the products. Further, a selective synthesis of one of the polymorphs is a challenge.

*For correspondence

Electronic supplementary material: The online version of this article (https://doi.org/10.1007/s12039-017-1381-4) contains supplementary material, which is available to authorized users.

The collective properties of nanomaterials are not utilized fully[12] because of the presence of organic surfactant molecules around the nano/micro particles that synthesized via regular chemical synthetic methods. Further, the capping agents or surfactants molecules around the particles may contribute negatively to the targeted applications. A few important points needing attention are,[20] (i) Capping agents isolate the neighbouring particle and decrease the communication between them. (ii) Shielding nature of capping agents hinders the charge carriers and thus affects the electronic devices made out of them. (iii) When the metal nano/micro particles are used as a catalyst, the chemical reaction occurs on the surface of the particles. The presence of capping would hide the active centres and restricts or reduce the catalytic activity. (iv) The surfactant molecules around nano/micro particles used for biological applications can be toxic for the human. All these observations suggest that it is crucial to design a method to produce applied nanomaterials without organic molecules surrounding.

Understanding the mechanism of formation of nanoparticles would help to develop a novel synthetic method. When the particles are formed in a reaction, the size of the particles is determined by the relative rates of two competitive processes, i.e., nucleation and the growth of nuclei to form large particles. The particle size of a freshly formed material is determined by the mechanism that predominates. In a reaction, if nucleation dominates, a material containing a large number of small particles are obtained, and if the growth predominates, a small number of large particles of the material are obtained. Altogether, it is desirable to design a reaction condition suitable for the formation of the product by altering the reaction temperature and solubility of reactants. Hence, we have developed a simple room temperature synthetic method to produce surfactant or template-free metal sulphides and selenides. Herewith, we have described the syntheses of CuS, $Cu_{2-z}Se$, Cu_2S and CdS micron size particles and evolution of BH_3 from the same reactions.

2. Experimental

2.1 *Materials and synthetic procedure*

The chemicals used in the syntheses, copper acetate [$Cu(CH_3COO)_2 \cdot H_2O$] (98.0% purity), copper nitrate [$Cu(NO_3)_2 \cdot 3H_2O$] (99.9% purity), copper chloride ($CuCl_2 \cdot 2H_2O$) (99% purity), cadmium chloride ($CdCl_2$) (tech grade) and lithium borohydride ($LiBH_4$) (95% purity) were purchased from Sigma-Aldrich India and used as received. All the solvents were purified using standard procedures.

2.2 *Instruments and sample preparation*

Powder X-ray diffraction (PXRD) was carried out by using Bruker D8 X-ray diffractometer [λ (Cu-Kα) = 1.54 Å] at scan rate of 1∘/min. The UV-Visible-NIR spectra of samples dispersed in methanol were recorded using Shimadzu UV-3600/Vis spectrophotometer. The Fourier transform infrared (FT-IR) spectra (KBr pellet) were recorded using Jasco 5300 spectrophotometer. Field Emission Scanning Electron Microscopy (FESEM) images were obtained in Ultra 55 Carl Zeiss instrument; for this purpose the samples were dispersed in methanol and kept on glass plate. Transmission electron microscopy (TEM) images were obtained using FEI Technai G^2 20 STEM instrument operated at an acceleration voltage of 200 kV. The TEM samples were prepared by dispersing the compound in methanol followed by sonication for 3 min. Then, sonicated solution was dispersed immediately (otherwise it will settle down) on carbon coated nickel grids (200 mesh). $^{31}P\{^1H\}$, ^1H, ^{11}B NMR spectra were acquired in a Bruker Avance 400 MHz using 85% HPO_4, $SiMe_4$ and BF_3-ether, respectively as the standard references.

2.3 *Synthesis of CuS micro flowers*

In a typical reaction, sulphur (40 mg, 1.3 mmol) was dissolved in 15 mL of dry tetrahydrofuran (THF) in a 50 mL two neck RB flask, to that $LiBH_4$ (59 mg, 2.5 mmol) and $Cu(CH_3COO)_2 \cdot H_2O$ (250 mg, 1.2 mmol) were added. The reaction mixture was stirred at room temperature under nitrogen atmosphere for 1 h. Initially, the colour of the solution was dark brown, and after the completion of reaction it turned to dark green along with the evolution of gas(es). After one hour, volatile side products and solvent were removed by applying high vacuum. The obtained crude product was washed with methanol (40 mL) followed by THF (40 mL) to remove side products (copper acetate, lithium salt) and unreacted S, and then centrifuged. The residue was dried under vacuum for 6 h to get a black powder of CuS micro flowers, which was characterized by PXRD and other techniques. Following the same procedure, the synthesis of CuS was carried out using two different precursors; $CuCl_2 \cdot 2H_2O$ [250 mg, 1.5 mmol, sulphur (47 mg, 1.5 mmol), $LiBH_4$ (47 mg, 2.9 mmol),] and $Cu(NO_3)_2 \cdot 3H_2O$. [250 mg, 1.0 mmol, sulphur (33 mg, 1.0 mmol), $LiBH_4$ (45 mg, 2.1 mmol)].

2.4 *Synthesis of Cu_2S nano/micro particles*

In a typical reaction, sulphur (20 mg, 0.6 mmol) was dissolved in 15 mL of dry THF in a 50 mL two neck RB flask, to that $LiBH_4$ (59 mg, 2.5 mmol) and copper acetate (250 mg, 1.2 mmol) were added. The reaction mixture was stirred for 1 h at room temperature under the nitrogen atmosphere after that volatile side products and solvent were removed under vacuum. Obtained crude product was washed with methanol

(40 mL) and THF to remove side products and unreacted precursor and then centrifuged. The product was dried under vacuum for 6 h to obtain a brown powder of Cu_2S nano/micro particles.

2.5 *Synthesis of CdS micro particles*

In typical a reaction, sulphur (44 mg, 1.4 mmol) was dissolved in 15 mL of dry THF in a 50 mL two neck RB flask and then added $LiBH_4$ (60 mg, 2.8 mmol) and cadmium chloride (250 mg, 1.4 mmol). The reaction mixture was stirred for 1 h at room temperature under the nitrogen atmosphere after that volatile side products and solvent were removed under vacuum. Obtained crude product was washed with methanol (40 mL) and THF to remove side products and unreacted precursor and then centrifuged. The product was dried under vacuum 6 h to obtain a yellow powder of CdS micro particles.

2.6 *Synthesis of $Cu_{2-z}Se$ micro particles*

In a typical reaction, selenium powder (49 mg, 0.6 mmol) was added in 5 mL of dry THF in a 50 mL two neck RB flask, to that $LiBH_4$ (59 mg, 2.5 mmol) and copper acetate (250 mg, 1.2 mmol) were added. The reaction mixture was stirred for 1 h at room temperature under the nitrogen atmosphere after that volatile side products and solvent were removed under vacuum. Obtained crude product was washed with methanol (40 mL) and THF to remove side products and unreacted precursor and then centrifuged. The product was dried under vacuum 6 h to obtain a black powder of $Cu_{2-z}Se$ micro particles.

2.7 *Confirmation of BH_3 by trapping as phosphine-borane complex*

To confirm the formation of BH_3 in all above reactions, four separate reactions were conducted where PPh_3 (721 mg, 2.7 mmol) was added to the mixture of $LiBH_4$ and one of the metal sources [$Cu(CH_3COO)_2 \cdot H_2O$, $Cu(NO_3)_2 \cdot 3H_2O$, $CuCl_2 \cdot 2H_2O$, $CdCl_2$], but in the absence of S and Se. The reaction mixture was stirred at room temperature for 1 h under nitrogen atmosphere. The reaction mixture was filtered, and the solvent of the filtrate evaporated to obtain a crude product, which was dissolved in methanol and recrystallized to get pure PPh_3:BH_3 adduct. It was characterized by multinuclear NMR spectral data and single crystal X-ray diffraction studies. $^{31}P\{^1H\}$ NMR (δ ppm in $CDCl_3$): broad merged lines at 20.86 and 20.36. ^{11}B NMR (δ ppm in $CDCl_3$): -37.94 (m). ^1H NMR (δ ppm in $CDCl_3$): 7.63–7.44 (three set of multiplets, 15H, Ph), 1.3–0.92 (poorly resolved multiplet, 3H, BH_3) (Figures S1–S3 in Supplementary Information). The structure of PPh_3:BH_3 was confirmed by single crystal X-ray crystallography (Figure S4 in Supplementary Information). When the same reactions were conducted in the presence of sulphur a large amount of phosphine sulphide was also obtained due to due to sulphur bonding with phosphorous[37] as confirmed from $^{31}P\{^1H\}$ NMR spectrum (a peak at δ 43.34 ppm) (Figure S2 in SI).

2.8 *Procedure for conversion of acids to alcohols*

Acids to alcohols conversions *via* hydroboration were conducted similarly to metal sulphide/selenide syntheses by adding calculated quantity (2.7 mmol) of each acid separately. The amount of acid to be added was decided by assuming evolution of one mole BH_3 for each mole of $LiBH_4$ used in the reactions. The reactants were added in THF sequentially as sulphur or selenium, $LiBH_4$, metal sources and then organic acid. These reaction mixtures were stirred at room temperature for 3 h under nitrogen atmosphere.

The products were filtered and extracted with ether. The ether extract was washed with 3N NaOH (30 mL) three times followed by brine solution and then dried over anhydrous Na_2SO_4. Evaporation of organic layer yielded alcohols. Structures of acids and corresponding alcohols are depicted in the Table S17 (in Supplementary Information). As determined by the ^1H NMR spectra of crude reaction mixtures, presumably, the majority of acid molecules were converted alcohol while remaining decomposed (Yield: 30–40%). The formation of alcohols in these reactions was confirmed from the appearance of benzylic -CH_2-peak around 4.6 ppm in ^1H NMR spectra (Figure S18 in Supplementary Information).

3. Results and Discussion

3.1 *Formation of copper chalcogenides*

With the aim of producing organic surfactant free nano/micro particles, various metal sources were reacted with $LiBH_4$ at room temperature in the presence of sulphur or selenium. These reactions yielded respective metal sulphide (CuS, Cu_2S and CdS) or selenide [$Cu_{2-z}Se$ (z = 0–0.28)] microparticles within 1 h (Table 1). All three copper sources, copper acetate [$Cu(CH_3COO)_2 \cdot H_2O$], copper nitrate [$Cu(NO_3)_2 \cdot 3H_2O$], copper chloride ($CuCl_2 \cdot 2H_2O$), in the presence of sulphur (metal sources : S = 1:1), on reactions with $LiBH_4$ (two equivalents with respect to metal sources) yielded hexagonal covellite phase of CuS. While the reaction of $LiBH_4$ (two equivalents with respect to metal sources) with copper acetate [$Cu(CH_3COO)_2 \cdot H_2O$] in the presence of lesser amount of sulphur [$Cu(CH_3COO)_2 \cdot H_2O$:S = 2:1] yielded hexagonal-Cu_2S. The same reaction in the presence of one equivalent of selenium [$Cu(CH_3COO)_2 \cdot H_2O$:Se = 1:1] yielded $Cu_{2-z}Se$ (z = 0 − 0.28). A similar reaction of $CdCl_2$ with $LiBH_4$ (two equivalents) in the presence of sulphur ($CdCl_2$:S = 1:1) yielded phase pure CdS. These metal sulphides and selenide nano/micro particles were characterized by powder X-ray diffraction patterns and HRTEM.

Table 1. Production of metal chalcogenides.

xM-Salt + yE + nLiBH$_4$ → M$_x$E$_y$ + nBH$_3$ ↑ + nLi-Salt
M = Metal; E = S, Se. Reaction condition: THF, rt, 1 h.

M Salt	E	Reaction stoichiometry	Product
$Cu(CH_3COO)_2 \cdot H_2O$	S	x = 1, y = 1, n = 2	CuS
$Cu(NO_3)_2 \cdot 3H_2O$	S	x = 1, y = 1, n = 2	CuS
$CuCl_2 \cdot 2H_2O$	S	x = 1, y = 1, n = 2	CuS
$Cu(CH_3COO)_2 \cdot H_2O$	S	x = 1, y = 0.5, n = 2	Cu_2S
$CdCl_2$	S	x = 1, y = 1, n = 2	CdS
$Cu(CH_3COO)_2 \cdot H_2O$	Se	x = 1, y = 0.5, n = 2	$Cu_{2-z}Se$ (Z = 0-0.28)

The selective production of any one of the polymorphic forms of copper sulphide is essential to use them for any device making. Interestingly, the standardized reaction scheme shown in Table 1 was useful to produce selectively CuS, $Cu_{2-z}Se$ ($z = 0-0.28$), Cu_2S and CdS nano/micro particles at room temperature. Besides, hydrated water in metal sources did not seem to affect the preferred products. Since the method developed here was reproducible, inexpensive and consume very less time they have the potential to be used for the production of various metal sulphides.

3.2 *BH_3 evaluation and in-situ organic reactions*

In organic, inorganic and materials chemistry, several reactions are known where $LiAlH_4$, $LiBH_4$, $NaBH_4$, and KBH_4 are used as hydride sources and reducing agents.[21] However, only a few reports explained the fate of Al and B presented in these reducing agents after the reactions.[22] In the earlier reports,[13c,23] we have established the evolution BH_3 in the reaction of $LiBH_4$ with $ZnCl_2$ or $PbNO_3$. Similarly, in the present study, all reactions involving $LiBH_4$ and various metal sources yielded the BH_3 gas along with metal chalcogenides. The formation of BH_3 was confirmed by trapping it with PPh_3 as BH_3:PPh_3 adduct and subsequent characterization by spectral data and single crystal X-ray diffraction studies (Figures S1–S4 in Supplementary Information).

The mixture of $NaBH_4/I_2$ is known to produce BH_3 and the utility of this reaction has been well established.[24] The borohydrides (BH_4^-) are used as hydride source in the variety of organic reactions.[22b,25] Methods of enhancement of reactivity and selectivity of borohydride for applications in organic synthesis have been studied thoroughly.[26] To confirm further, when a few organic acids (aromatic and aliphatic acids) were added to the reaction of $LiBH_4$ and metal sources [$Cu(CH_3COO)_2 \cdot H_2O$, $Cu(NO_3)_2 \cdot 3H_2O$, $CuCl_2 \cdot 2H_2O$, $CdCl_2$], the hydroboration reaction occurred quickly utilizing the *in situ* generated BH_3. Subsequent hydrolysis yielded the corresponding alcohols (yield: 30–40%). This functional group transformation is possible *via* hydroboration. Altogether, the formation of BH_3 in these reactions appears to be common in the reactions of metal borohydrides with metal halides and metal salts. Formation of gaseous side product eased the removal of boron from the reaction.

$$LiBH_4 + \text{M-Salt} \rightarrow \text{Li-Salt} + M^{n+} + BH_3\uparrow + H^+ \ (M = \text{Cu or Cd})$$
$$H^- + E \rightarrow E^{2-} + H^+ \ (E = \text{S or Se})$$
$$M^{n+} + E^{2-} \rightarrow M_xE \ (x = 1 \text{ or } 2)$$

Scheme 1. Plausible reaction pathway for the formation of metal chalcogenides and BH_3.

The formation of metal chalcogenides and BH_3 in these reactions can be explained as follows. A few reports explained the formation NaHE (E = S, Se, Te) in the reaction of $NaBH_4$ in the presence of water.[22e] The NaHE subsequently reacted with metal chlorides yielding metal chalcogenides. However, as mentioned earlier, the evolution BH_3 in the reaction of $LiBH_4$ with $ZnCl_2$ or $PbNO_3$ and $NaBH_4$ with $CoCl_2$ and I_2 are also documented.[13c,23,25] Further, we performed control reactions wherein $LiBH_4$ was reacted with anhydrous metal sources ($Cu(CH_3COO)_2$, $Cu(NO_3)_2$, and $CuCl_2$) in the absence of chalcogens. All these reaction also liberated BH_3. The reactions of $LiBH_4$ with hydrated metal sources accelerated the reactions. Therefore, the sequence of reactions might be as shown in Scheme 1. First, $LiBH_4$ reacted with metal sources forming lithium salts (LiCl, $LiNO_3$, and LiOAc), and then hydride ions from (BH_4^- reacted with the metal sources to liberate BH_3 and H^-.

3.3 *Characterization of metal chalcogenides*

The PXRD (Figure 1) patterns of CuS (JCPDS #06-0464, a = 3.792Å and c = 16.344 Å) showed the formation hexagonal covellite phase in all three reactions. Absence of other characteristic peaks corresponding

to copper acetate, copper oxide, sulphur and Cu_2S, or any other phase of CuS confirmed the phase purity of the products. Interestingly, PXRD pattern of the product from 2:1 [$Cu(CH_3COO)_2 \cdot H_2O$: S = 2:1] reaction showed a selective formation of hexagonal-Cu_2S (JCPDS #89-2670), (Figure S5 in Supporting Information).The selective formation of either CuS or Cu_2S in the above reaction confirmed the stoichiometry control in the reaction. PXRD patterns of $Cu_{2-z}Se$ (z = 0–0.28) (JCPDS #06-0680) (Figure S6 in Supporting Information) and CdS (JCPDS #89-0440) (Figure S7 in SI) showed the formation of pure fcc phases of both microparticles. Peaks in the diffraction pattern were broadened in all cases due to the nano size of the particles. The Vis-NIR spectrum of CuS and Cu_2S dispersed in methanol showed the absorption edge at 683 nm and 568 nm respectively (Figures S8–S9 in SI). Both microparticles had absorption band spanning into NIR region. The materials with NIR absorption are reported to be useful in photoacoustic contrast agent for deep tissue imaging and Photothermal ablation therapy for cancer cells.[27]

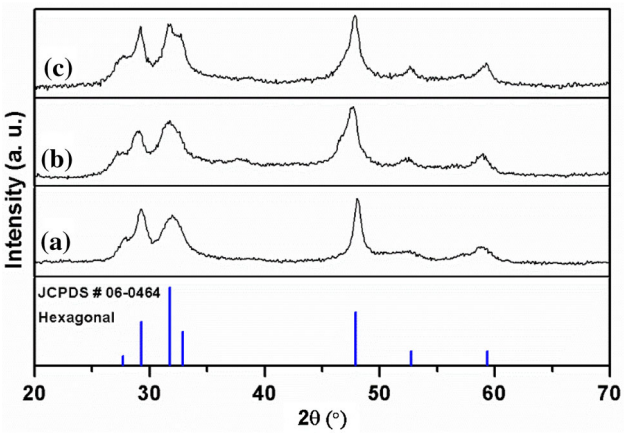

Figure 1. Powder X-ray diffraction (PXRD) patterns of CuS obtained (a) $CuCl_2$, (b) $Cu(OAc)_2$, (c) $Cu(NO_3)_2$ as metal sources.

In last few years, there has been focus on the synthesis of CuS particles existing in different shapes such as nanoflakes, nanotubes, microspheres, flower-like structures, nanowires, nanorods, urchin-like structures, and nanoribbons.[28–33] In these reactions, the morphology of products obtained under identical conditions was varying with the change of metal sources (Table 2). Typical FESEM image (Figures 2a, b) revealed the formation of "rose-flower" like architecture when copper acetate was used in the reaction. These microflowers were constituted through self-assembly of numerous nanoflakes. The width of the flakes ranged within 5–10 nm and length of flakes were within 40–200 nm. When copper chloride was the metal source, aggregated CuS particles having "cauliflower" like architecture were formed (size: 50–200 nm, (Figures 2c, d). When copper nitrate was used, randomly shaped aggregates of CuS particles with a size range of 20–40 nm (Figures 2e, f) were obtained. All these microflowers consisted of nano crystallites. The average sizes of nano crystallites calculated using Scherrer formula is around 30 nm [31.7 nm (when metal source was $CuCl_2$); 30.1 nm (when metal source was $Cu(OAC)_2$; 30.1 nm (when metal source was $Cu(NO_3)_2$] (Table S2 in Supporting Information).

Images of Cu_2S particles showed aggregation of "peanut-shaped" particles (Figures 2g, h). Similarly, many $Cu_{2-z}Se$ particles were seen plate-like in FESEM as while some of were having hexagons (Figure S10 in SI). CdS particles were an aggregation of spherical particles with size range 20–30 nm (Figure S11 in SI).

Table 2. Reaction condition and particles sizes of various Products[a].

Metal source	Concentration of metal sources in (Molarity)[b]	Product	Particles shapes and sizes
$Cu(CH_3COO)_2 \cdot H_2O$	0.083	CuS	nano flakes which self-assembled to form rose flowers architecture 5–10 nm (flake width) 40–200 nm (flake length)
$Cu(NO_3)_2 \cdot 3H_2O$	0.098	CuS	Nanoparticles 20–40 nm
$CuCl_2 \cdot 2H_2O$	0.069	CuS	Cauliflower shape 100–200 nm
$Cu(CH_3COO)_2 \cdot H_2O$	0.083	Cu_2S	Peanut shaped 50–100 nm (length) 20–30 nm (width)
$Cu(CH_3COO)_2 \cdot H_2O$	0.083	$Cu_{2-z}Se$	
$CdCl_2$	0.083	CdS	Spherical nanoparticles 20–30 nm

[a]reaction time 1 hour, [b]solvent THF.

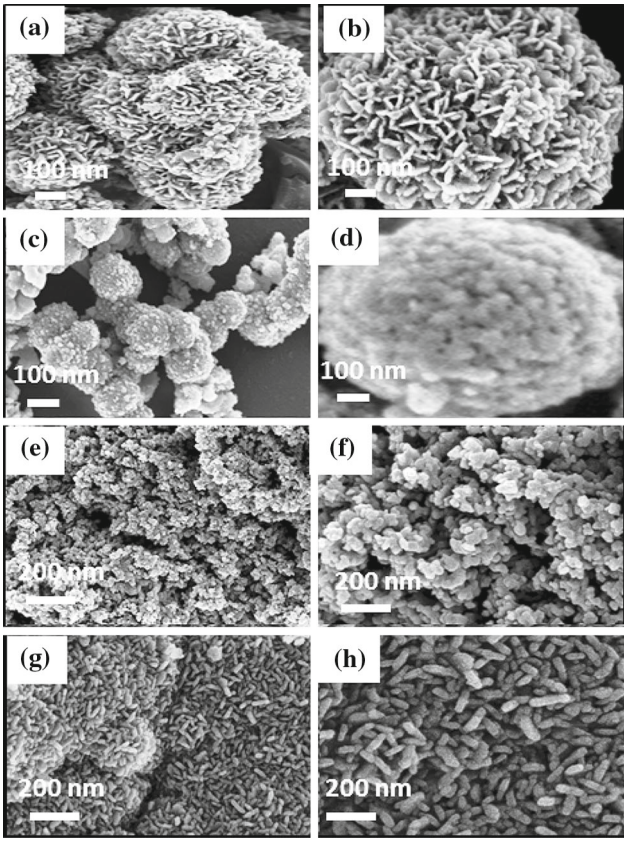

Figure 2. FESEM images of CuS: (a, b) rose-flower like architecture obtained when copper acetate was metal source, (c, d) cauliflower like aggregation obtained from copper chloride, (e, f) Randomly shaped nanoparticles were obtained from copper nitrate. (g, h) peanut shaped Cu_2S nanoparticles.

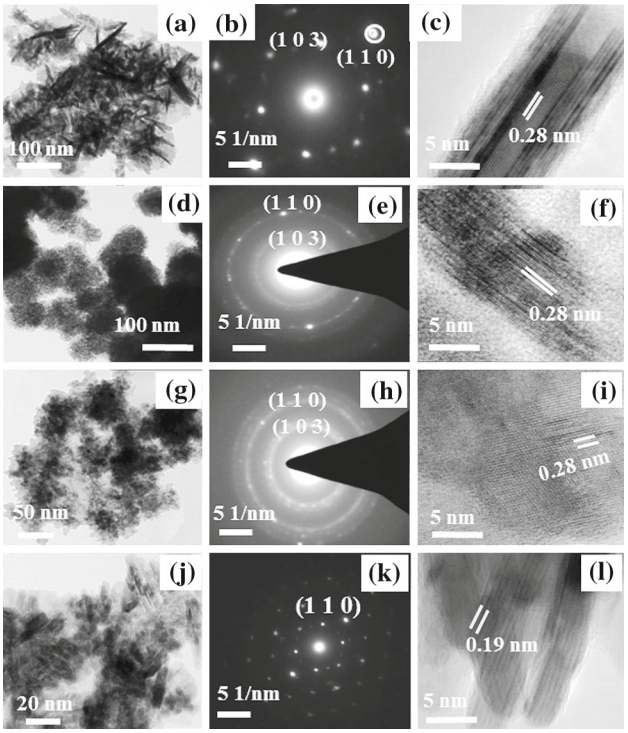

Figure 3. TEM image of CuS, rose flowers architecture (a), SAED (b), HRTEM (c) obtained from copper acetate. Cauliflower-like nano structure (d), SAED (e), HRTEM (f) obtained from copper chloride. Randomly shaped nanoparticles (g), SAED (h), HRTEM (i) obtained from copper nitrate and TEM image of Cu_2S peanut shaped nanoparticles (j), SAED (k), HRTEM (l).

Figure 3 depicts TEM and HRTEM images along with SAED patterns. Morphologies and sizes seen in TEM images (Figure 3a) of CuS obtained using three different copper sources were consistent with that observed in FESEM. SAED patterns of CuS nano/micro particles obtained in reactions where copper acetate was metal source clearly showed (1 0 3) and (1 1 0) planes revealing the crystalline nature of CuS nanoflakes. HRTEM images (Figure 3c) clearly showed a lattice spacing of 0.28 nm, which was consistent with the distance between the (1 0 3) lattice planes observed in pure hexagonal covellite phase of CuS (JCPDS #06-0464). Similarly, the SAED patterns and HRTEM of CuS obtained from two other reactions also showed lattice planes (1 0 3) and (1 1 0) matching with PXRD patterns of CuS hexagonal covellite phase. TEM analysis of Cu_2S showed a peanut like nanostructure of length 50–100 nm and width 20–30 nm (Figures 3j, k, l). SAED and HRTEM images clearly showed a lattice spacing of 0.19 nm, which was consistent with the distance between the (1 1 0) lattice planes.

3.4 *Formation of surfactant free nanoparticle and their purity*

It is necessary to avoid heterogeneous impurities to achieve full utilization[19] of properties of the hierarchical superstructure. Since surfactants molecules or capping agents do not contribute to the application requirements, they are considered as impurities of nano/micro particles. Hence, the purity of metal chalcogenides was collectively assessed by elemental analysis, PXRD pattern and FT-IR spectra. Elemental analyses of the particles reported here (CuS Cu_2S, CdS and $Cu_{2-z}Se$) using Energy Dispersive X-ray Spectroscopy (EDAX) (Figures S12–15 in Supporting Information) proved the presence of the respective elements (Cu, Cd, S, and Se) in the materials. The results were consistent for various samples of every material and confirmed the absence of carbonaceous impurities.

Further, PXRD spectra did not show any amorphous regions corresponding to any organic materials. Clear PXRD patterns matching the targeted materials and the absence of any other compounds (within the detectable limit of PXRD) or other phases confirmed the purity

of materials reported here. Further confirmation about the absence of organic moieties was obtained from FT-IR spectra. The FT-IR spectra (Figure S16 in Supporting Information) of CuS, Cu_2S, CdS and $Cu_{2-z}Se$ obtained from the reactions described here showed no signal for any organic impurity confirming the absence of any organic molecules around the particles. Thus, our reactions yielded the nanomaterials without organic molecules surrounding it.

Agglomeration is a common phenomenon of metal nanoparticles which induces the growth of nuclei leading to the formation of bigger particles. Capping agents are required to ensure colloid stability during synthesis of nanoparticles. Interestingly, it was observed that the metal sulphide nano/micro particles, obtained in the present as well as in the past studies, did not agglomerate.[13] Xie and co-workers[34] suggested the formation of thermodynamically stable structure under right growing conditions, which can yield nanoparticles. Thus the formation nanoparticles can be explained by invoking the necessity of ripening phenomenon for the particle growth. The digestion is a much-needed process practiced in gravimetric analyses to obtain large crystals of metal sulphides, sulphates and salts where there are no metallic bonds. The Ostwald ripening process[35] helps the growth of particles during digestion. This observation gives a clue that if the condition is not favouring the growth, the particles will remain in nano-regime. Therefore, in any reaction to produce nanoparticles, it is necessary to create a condition favouring the nucleation instead the growth of particles.

Von Weimarn's theory[36] of relative supersaturation and subsequent studies explained nucleation vs. particles growth as factors deciding the sizes of particles formed in a reaction. According to the theory, increased solubility of products and elevated temperature would yield particles of bigger sizes. Consequently, the saturated conditions, room temperature reactions, and fast reactions should not support the growth of the nucleus but should produce smaller particles. The reaction conditions and particle sizes of various products obtained are listed in Table 2. The data in the table showcases the influence of reaction condition on the size of particles. Since both the starting materials and products described in the present reactions were only sparingly soluble in THF, the room temperature reactions favoured thermodynamically stable sizes for the particles. However, since there was no other factor supporting the growth of nuclei, these metal sulphide particles remained in nano size after synthesis. Those nano crystallites self-assembled and formed rigid microflower.[13b] Thus, the method described here is useful to produce nano/micro particles without surfactants or any other templates. Nevertheless, the method needs optimization to produce uniform particle size.

4. Conclusions

A versatile method for the syntheses of organic free CuS, Cu_2S, CdS and $Cu_{2-z}Se$ nano/microparticles at room temperature within one hour is described. All these materials were characterized thoroughly using PXRD patterns and electron microscopic images. The supersaturated condition and the strong reactivity of $LiBH_4$ drove the formation of metal chalcogenide nano/micro particles. After the synthesis, the particles remained in nano sizes as long as the compounds were stable. The method was reproducible and can be extended for the production of many metal sulphides.

The reduction reactions producing metal chalcogenide microparticles also yielded borane (BH_3), which was characterized by trapping it with PPh_3. Evolution of BH_3 in the reactions of $LiBH_4$ with various metal sources established the formation of it as a regular phenomenon. The morphology of CuS particles obtained in these reactions was varying with a change of metal source used in the reaction. To the best of our knowledge, this is the first observation of metal source dependent morphology of nano/microparticles obtained under identical reaction condition.

Supplementary Information (SI)

NMR spectra of Ph_3P, PXRD spectra of Cu_2S, $Cu_{2-z}Se$, CdS, UV-Vis-NIR spectra of CuS and Cu_2S, EDAX spectra of CuS, Cu_2S, $Cu_{2-z}Se$, CdS, FESEM images of $Cu_{2-z}Se$, CdS, FTIR spectrum of CuS, ^1H NMR spectrum of reaction mixture and table containing reactions of acid to alcohol conversion using *in situ* generated BH_3 are available as Supplementary Information at www.ias.ac.in/chemsci.

Acknowledgements

The authors thank the Centre for Nanotechnology at the University of Hyderabad for the TEM facility. SNG acknowledges UGC -India for doctoral fellowship. The work is supported by DST-SERB of India under project No: SB/S1/IC-47/2013.

References

1. (a) Wang X L and Swihart M T 2015 Controlling the Size, Shape, Phase, Band Gap, and Localized Surface Plasmon Resonance of $Cu_{2-x}S$ and Cu_xIn_yS Nanocrystals *Chem. Mater.* **27** 1786; (b) Foglia S, Suber L and Righini M

2001 Size tailoring of CdS nanoparticles by different colloidal chemical techniques *Colloid. Surface. A* **177** 3
2. Santra S, Yang H, Stanley J T, Holloway P H, Moudgil B M, Walterd G R and Mericle A 2005 Rapid and effective labelling of brain tissue using TAT-conjugated CdS: Mn/ZnS quantum dots *Chem. Commun.* **25** 3144
3. Chaudhary S, Ozkan M and Chan W C W 2004 Trilayer hybrid polymer-quantum dot light-emitting diodes *Appl. Phys. Lett.* **84** 2925
4. Song W S and Yang H 2012 Efficient white-light-emitting diodes fabricated from highly fluorescent copper indium sulphide core/shell quantum dots *Chem. Mater.* **24** 1961
5. Tan Z, Zhang F, Zhu T and Xu J 2007 Bright and colour-saturated emission from blue light-emitting diodes based on solution-processed colloidal nanocrystal quantum dots *Nano Lett.* **7** 3803
6. Shalom M, Ruhle S, Hod I, Yahav S and Zaban A 2009 Energy level alignment in CdS quantum dot sensitized solar cells using molecular dipoles *J. Am. Chem. Soc.* **131** 9876
7. Wang P, Wang L, Ma B, Li B and Qiu Y 2006 TiO_2 surface modification and characterization with nanosized PbS in dye-sensitized solar cells *J. Phys. Chem. B* **110** 14406
8. Lee H, Yoon S W, Kim E J and Park J 2007 In-situ growth of copper sulphide nanocrystals on multiwalled carbon nanotubes and their application as novel solar cell and amperometric glucose sensor materials *Nano Lett.* **7** 778
9. Mishra N, Mukherjee B, Xing G, Chakrabortty S, Guchhait A and Lim J Y 2016 *Cation* exchange synthesis of uniform PbSe/PbS core/shell tetra-pods and their use as near-infrared photodetectors *Nanoscale* **8** 14203
10. Koch D F A and McIntyre R J 1976 The application of reflectance spectroscopy to a study of the anodic oxidation of cuprous sulphide *J. Electroanal. Chem.* **71** 285
11. Grozdanov I and Najdoski M 1995 Optical and electrical properties of copper sulphide films of variable composition *J. Solid State Chem.* **114** 469
12. (a) Roy P, Mondal K and Srivastava S K 2008 Synthesis of twinned CuS nanorods by a simple wet chemical method *Cryst. Growth Des.* **8** 1530; (b) Roy P and Srivastava S K 2007 Low-temperature synthesis of CuS nanorods by simple wet chemical method *Mater. Lett.* **61** 1693; (c) Hsu S, On K and Tao A R 2011 Localized surface plasmon resonances of anisotropic semiconductor nanocrystals *J. Am. Chem. Soc.* **133** 19072; (d) Bryks W, Wette M, Velez N, Hsu S and Tao A R 2014 Supramolecular precursors for the synthesis of anisotropic Cu_2S nanocrystals *J. Am. Chem. Soc.* **136** 6175; (e) Hsu S, Bryks W and Tao A R 2012 Effects of Carrier Density and Shape on the Localized Surface Plasmon Resonances of $Cu_{2-x}S$ Nanodisks *Chem. Mater.* **24** 3765; (f) Hsu S, Ngo C and Tao A R 2014 Tuneable and directional plasmonic coupling within semiconductor nanodisk assemblies *Nano Lett.* **14** 2372
13. (a) Kumar B G and Muralidharan K 2011 Hexamethyldisilazane-assisted synthesis of indium sulphide nanoparticles *J. Mater. Chem.* **30** 11271; (b) Kumar B G and Muralidharan K 2013 Organic-Free Self-Assembled Copper Sulphide Microflowers *Eur. J. Inorg. Chem.* **32** 2102; (c) Gottapu S N and Muralidharan K 2016 Room temperature synthesis of organic surfactant-free PbS and PbSe nanoparticles exhibiting NIR absorption *New J. Chem.* **40** 832
14. Li B, Xie Y and Xue Y 2007 Controllable synthesis of CuS nanostructures from self-assembled precursors with biomolecule assistance *J. Phys. Chem. C* **111** 12181
15. Wang W, Germanenko I and El-Shal M S 2002 Room-temperature synthesis and characterization of nanocrystalline CdS, ZnS, and $Cd_xZn_{1-x}S$ *Chem. Mater.* **14** 3028
16. Chung J–S and Sohn H-J 2002 Electrochemical behaviours of CuS as a cathode material for lithium secondary batteries *J. Power Source* **108** 226
17. Mao G, Dong W, Kurth D G and Mohwald H 2004 Synthesis of copper sulphide nanorod arrays on molecular templates *Nano Lett.* **4** 249
18. (a) Gao L, Wang E, Lian S, Kang Z, Lan Y and Wu D 2004 Microemulsion-directed synthesis of different CuS nanocrystals *Solid State Commun.* **130** 309
19. (a) Kumar P, Gusain M and Nagarajan R 2012 Solvent-mediated room temperature synthesis of highly crystalline $Cu_9S_5(Cu_{1.8}S)$, CuSe, PbS, and PbSe from their elements *Inorg. Chem.* **51** 7945; (b) Kumar P, Gusain M and Nagarajan R 2011 Synthesis of $Cu_{1.8}S$ and CuS from copper-thiourea containing precursors; anionic (Cl^-, NO_3^-, SO_4^{2-}) influence on the product stoichiometry *Inorg. Chem.* **50** 3065
20. (a) Kovalenko M V, Scheele M and Talapin D V Colloidal nanocrystals with molecular metal chalcogenide surface ligands *Science* **324** 1417; (b) Talapin D V, Lee J S, Kovalenko M V and Shevchenko E V 2010 Prospects of colloidal nanocrystals for electronic and optoelectronic applications *Chem. Rev.* **110** 389; (c) Kilina S, Ivano S and Tretiak S 2009 Effect of surface ligands on optical and electronic spectra of semiconductor nanoclusters *J. Am. Chem. Soc.* **131** 7717
21. (a) Giannis A and Sandhoff K 1989 $LiBH_4$ $(NaBH_4)/Me_3SiCl$, an unusually strong and versatile reducing agent *Angew. Chem. lnt. Ed. Engl.* **28** 218; (b) Gemal A L and Luche J-L 1981 Lanthanoids in organic synthesis. 6. Reduction of alpha-enones by sodium borohydride in the presence of lanthanoid chlorides: synthetic and mechanistic Aspects *J. Am. Chem. Soc.* **103** 5454; (c) Vajo J J and Skeith S L 2005 Reversible storage of hydrogen in destabilized $LiBH_4$ *J. Phys. Chem. B* **109** 3719; (d) Zhang L, Shen X and Liang H 2010 A mild phosphine-free synthesis of alkylamine-capped CdSe nanocrystals *J. Nanosci. Nanotechnol.* **10** 4979; (e) Ramasamy K, Nejo A O, Ziqubu N, Rajasekhar P V S R, Nejo A A, Revaprasadu N and Paul O'Brien 2011 A new route to lead chalcogenide nanocrystals *Eur. J. Inorg. Chem.* 5196; (f) Moloto N, Moloto M J, Coville N J and Sinha Ray S 2009 Optical and structural characterization of nickel selenide nanoparticles synthesized by simple methods *J. Cryst. Growth* **311** 3924; (g) Oluwafemi O S and Revaprasadu N 2008 A new synthetic route to organically capped cadmium selenide nanoparticles *New J. Chem.* **32** 1432; (h) Kandasamy K, Singh H B and Kulahreshtha S K 2009 Synthesis and characterization of CdS and CdSe nanoparticles prepared from novel intramolecularly stabilized single-source precursors *J. Chem. Sci.* **121**

293; (i) Jain V K 2006 Synthesis and characterization of single-source molecular precursors for the preparation of metal chalcogenides *J. Chem. Sci.* **118** 547

22. (a) Sudeep P K, Page Z and Emrick T 2008 PEGylated silicon nanoparticles: synthesis and characterization *Chem. Commun.* 6126; (b) Cheng X, Gondosiswanto R, Ciampi S, Reeceb P J and Gooding J J 2012 One-pot synthesis of colloidal silicon quantum dots and surface functionalization via thiol–ene click chemistry *Chem. Commun.* **48** 11874; (c) Wang J, Sun S, Peng F, Cao L and Sun L 2011 Efficient one-pot synthesis of highly photoluminescent alkyl-functionalised silicon nanocrystals *Chem. Commun.* **47** 4941; (d) Rosso-Vasic M, Spruijt E, Popovic Z, Overgaag K, Lagen B V, Grandidier B, Vanmaekelbergh D, Nguez-Gutierrez D D, Cola L D and Zuilhof H 2009 Amine-terminated silicon nanoparticles: synthesis, optical properties and their use in bioimaging *J. Mater. Chem.* **19** 5926
23. Ghanta S R, Rao M H and Muralidharan K 2013 Single-pot synthesis of zinc nanoparticles, borane (BH_3) and closo-dodecaborate $(B_{12}H_{12})^{2-}$ using $LiBH_4$ under mild conditions *Dalton Trans.* **42** 8420
24. (a) Bhaskar Kanth J V and Periasamy M 1991 Selective reduction of carboxylic acids into alcohols using sodium borohydride and iodine *J. Org. Chem.* **56** 5964; (b) Bhanu Prasad A S, Bhaskar Kanth J V and Periasamy M 1992 Convenient methods for the reduction of amides, nitriles, carboxylic esters, acids and hydroboration of alkenes using $NaBH_4/I_2$ system *Tetrahedron* **48** 4623
25. (a) Giannis A and Sandhoff K 1989 $LiBH_4$ $(NaBH_4)/Me_3SiCl$, an unusually strong and versatile reducing agent *Angew. Chem. Int. Ed. Engl.* **28** 218; (b) Vajo J J and Skeith S L 2005 Reversible storage of hydrogen in destabilized $LiBH_4$ *J. Phys. Chem. B* **109** 3719
26. (a) Satyanarayana N and Periasamy M 1984 Hydroboration or hydrogenation of alkenes with $CoCl_2$-$NaBH_4$ *Tetrahedron Lett.* **25** 2501; (b) Periasamy M and Thirumalaikumar M 2000 Methods of enhancement of reactivity and selectivity of sodium borohydride for applications in organic synthesis *J. Organometallic Chem.* **609** 137
27. (a) Liu R, Jing L, Peng D, Li Y, Tian J and Dai Z 2015 Manganese (II) Chelate Functionalized Copper Sulfide Nanoparticles for Efficient Magnetic Resonance/Photoacoustic Dual-Modal Imaging Guided Photothermal Therapy *Theranostics* **5** 1144; (b) Poulose C, Veeranarayanan S, Mohamed M S, Nagaoka Y, Aburto R R, Mitcham T, Ajayan P M, Bouchard R R, Sakamoto Y, Yoshida Y, Maekawa T and SakthiKumar D 2015 Multi-stimuli responsive Cu_2S nanocrystals as trimodal imaging and synergistic chemo-photothermal therapy agents *Nanoscale* **7** 8378
28. Dutta A and Dolui S K 2008 Preparation of colloidal dispersion of CuS nanoparticles stabilized by SDS *Mater. Chem. Phys.* **112** 448
29. Wang Q, Li J X, Li G D, Cao X. J, Wang K J and Chen J S 2007 Formation of CuS nanotube arrays from CuCl Nanorods through a gas-solid reaction route *J. Cryst. Growth* **299** 386
30. Li B X, Xie Y and Xue Y 2007 Controllable synthesis of CuS nanostructures from self-assembled precursors with biomolecule assistance *J. Phys. Chem. C* **111** 12181
31. (a) Roy P and Srivastava S K 2007 Low-temperature synthesis of CuS nanorods by simple wet chemical method *Mater. Lett.* **61** 1693; (b) Hemakanthi G, Dhathsthreyan A Ramasami T and Möbius D 2001 Preparation of copper sulphide clusters in organic–inorganic composites of Langmuir–Blodgett films of amphiphilic Schiff bases *Proc. Indian Acad. Sci. (J. Chem. Sci.)* **113** 147
32. Zhu L Y, Xie Y, Zheng X W, Liu X and Zhou G E 2004 Fabrication of novel urchin-like architecture and snowflake-like pattern CuS *J. Cryst. Growth* **260** 494
33. Tan C H, Lu R, Xue P C, Bao C Y and Zhao Y Y 2008 Synthesis of CuS nanoribbons templated by hydrogel *Mater. Chem. Phys.* **112** 500
34. Zhang S, Wu C, Wu Z, Yu K, Wei J and Xie Y 2008 Construction of PbSe hierarchical superstructures via an alkaline etching method *Cryst. Growth Des.* **8** 2933
35. (a) Ostwald W Z 1900 About the supposed isomerism of red and yellow mercuric oxide and the surface tension of solids *Phys. Chem.* **34** 495; (b) Li B, Rong G, Xie Y, Huang L and Feng C 2006 Low-temperature synthesis of α-MnO_2 hollow urchins and their application in rechargeable Li^+ batteries *Inorg. Chem.* **45** 6404; (c) Li J H and Zeng C 2007 Hollowing Sn-doped TiO_2 nanospheres via Ostwald ripening *J. Am. Chem. Soc.* **129** 15839
36. (a) Weimarn V P P 1925 The Precipitation Laws *Chem. Rev.* **2** 217; (b) Nielsen A E 1960 The kinetics of calcium oxalate precipitation *Acta Chem. Scand.* **14** 1654; (c) Johnson R A and O'Rourke J D 1954 The Kinetics of Precipitate Formation: Barium Sulfate *J. Am. Chem. Soc.* **76** 2124; (d) Jr Day R A and Underwood A L 2013 *Quantitative Analysis* edn. 6 p.74; (e) Skoog D A, West D M, Holler F J and Crouch S R 2004 *Fundamentals of Analytical Chemistry* edn. 8 p.316
37. Gukathasan R R, Morris R H and Walker A 1983 Reactions of elemental sulphur with tetrakis (triphenylphosphine) platinum (0). Formation of a complex containing very nucleophilic bridging sulphido ligands *Can. J. Chem.* **61** 2490

Journal of Organometallic Chemistry 884 (2019) 59–65

Contents lists available at ScienceDirect

Journal of Organometallic Chemistry

journal homepage: www.elsevier.com/locate/jorganchem

Multicomponent click reaction catalyzed by organic surfactant-free copper sulfide (sf-CuS) nano/micro flowers

Venkateswara Rao Velpuri, Krishnamurthi Muralidharan*

School of Chemistry, University of Hyderabad, Prof. C. R. Road, Gachibowli, Hyderabad, Telangana, 500 046, India

ARTICLE INFO

Article history:
Received 27 November 2018
Received in revised form
17 January 2019
Accepted 23 January 2019
Available online 28 January 2019

Keywords:
Copper sulfide
Cycloaddition
Multicomponent synthesis
Triazoles
Micro flower architectures

ABSTRACT

The azide-alkyne cycloaddition (Huisgen reaction) is one of the most powerful and widely used copper-mediated reactions. In many such reactions, use of metal or metal oxide nanoparticles as the catalyst is more appealing because of the increased catalytic activity attributed to the large surface to volume ratio. However, the nano/micro particles are synthesized often in the presence of long chain organic molecules as capping or stabilizing agents. These organic molecules cover the active centers and restrict or reduce their catalytic activity. Therefore, we have synthesized the copper sulfide (sf-CuS) nano/micro particles without having organic surfactant molecules as the capping agent. These particles with a flower-like architecture (micro flowers, **mf**) were obtained readily under the supersaturated condition at room temperature. In these particles, the surface was freely available for adsorption and desorption reactions. When utilized as a catalyst in multicomponent cycloaddition reactions, the sf-CuS **mf** exhibited excellent catalytic activity compared with some other nanoparticles with surfactants. This sf-CuS **mf** catalyzed the one-pot synthesis of 1,2,3-triazole and β-hydroxy-1,2,3-triazole effectively from a variety of benzyl bromide derivatives epoxides respectively. Both these reactions proceeded in the presence of azide and phenylacetylene in the water at room temperature. The catalyst was reusable, and there was no catalyst leaching observed during reactions. Synthesis of β-hydroxy triazoles and 1,2,3-triazoles under exceptionally mild conditions with high yields proved the sf-CuS **mf** as the catalyst as a robust and recyclable catalyst.

1. Introduction

Synthesis of nano/micro particles is fascinating in organic chemistry since they are used as heterogeneous catalysts in organic reactions. The capping agents or surfactants that are used commonly in the synthesis of metal chalcogenides nanoparticles are; amines (hexadecyl amine, alkyl amine), oleic acid, polymers (PVP, PMMA), thiols (do-decane thiol, 1, 6-hexane dithiol) [1–3]. However, the collective properties of nanomaterials are not utilized fully [4–9] because of the presence of organic surfactant molecules around the nano/micro particles that are synthesized *via* conventional chemical synthetic methods. When the metal nano/micro particles are used as a catalyst, the chemical reaction occurs on the surface of the particles. The presence of capping molecules would hide the active centers and restrict or reduce the catalytic activity so that capping agents or surfactant molecules around the particles may contribute negatively to the target applications [10].

In recent years metal is decorated on nanomaterials and these materials are used as heterogeneous catalysts in organic reactions such as heck reaction (Pd/CuO) [11], Suzuki cross-coupling reaction (Pd–CuO@Hol S-1) [12], Sonagashira coupling reaction (Cu/CuO) [13], Heisenberg 1, 3-dipolar reaction (CuNPs/MagSilica) [14], copper(I)-catalyzed synthesis of azoles by Sharpless [15], copper(I)-catalyzed azide-alkyne [3 + 2] cycloaddition by Sharpless and Finn [16] and so on. The substituted triazoles are exciting materials in organic synthesis, coordination chemistry, and N-heterocyclic chemistry [17–21]. Substituted triazoles play an essential role in opening calcium channels in cells, particularly [22] at 1 and 4 positions of triazole. They also show biological activities as anti-cancer, anti-HIV therapy, anti-bacterial [23–27] and anti-allergy molecules [28–30]. Agricultural and industrial applications of such compounds include herbicides, fungicides, agrochemicals [31], optical brighteners [32], fluorescence chemosensory [33] corrosion retarding agents, dyes, and solar cells [34–37]. Further, the heterocyclic compounds that are rich in nitrogen atoms can be

* Corresponding author.
E-mail address: murali@uohyd.ac.in (K. Muralidharan).

https://doi.org/10.1016/j.jorganchem.2019.01.016
0022-328X/

used as high energy materials [38].

The formation of 1,2,3-triazole derivatives is known to proceed through heisenbug 1,3-dipolar cycloaddition of organic azides and alkynes using CuAAC as a catalyst [38–41]. In recent years, multicomponent click synthesis of 1,2,3-triazoles from both *in-situ* azidolysis of benzyl halide in the presence of alkynes and β-hydroxy-1,2,3-triazoles *via in-situ* azidolysis of epoxides in the presence of alkynes have been developed [42–44]. Some heterogeneous catalysts used in the dipolar cycloaddition are polyurea encapsulated copper(I) chloride [45], CuNP/C [46], $CuFe_2O_4$, [47] Cu/Cu_2O [48], [AQ_2Cu(II)-$APSiO_2$] [49], copper(I)@phosphorated SiO_2 [50] SiO_2–CuI [51], Clay–Cu(II)/$NH_2NH_2 \cdot H_2O$ [52], GO@PTA-Cu [53] and copper(I) in ionic liquids [54]. Albeit several catalytic systems have been used for dipolar cycloaddition, in pursuit of catalyst working under mild condition and developing simple method of production of nano catalyst, we have synthesized surfactant-free copper sulfide (sf-CuS) particles having micro flower (**mf**) like architecture formed by the self-assembly of nanoparticles.

Herein, we report the synthesis of surfactant-free copper sulfide micro flowers (**sf-CuS mf)** in an efficient and straightforward synthetic process, and its practical use in the synthesis of both benzyl halide linked 1,2,3- triazoles and β-hydroxy- 1,2,3-triazoles *via* dipolar cycloaddition of azide and alkyne in the presence of benzyl halide and epoxide. The synthesis described here was performed in water, and so it was safer, greener, and used inexpensive, recyclable surfactant free heterogeneous catalyst. The above synthetic procedure satisfied the most of green chemistry principles such as (a) one-pot multicomponent synthesis (atom economy) (b) reactions in a water medium (green solvent) (c) using of readily separable and recyclable heterogeneous catalyst (d) involving simple workup procedure.

2. Results and discussion

In recent times, the azide-alkyne cycloaddition (Huisgen reaction) has emerged as one of the most powerful and widely utilized copper-mediated reactions. However, many reactions catalyzed by metal or metal oxide nanoparticles are more appealing because of the increased catalytic activity attributed to the large surface to volume ratio. In general, the nano/micro particles used as the catalyst are produced in the presence of long chain organic molecules as capping or stabilizing agents. These capping agents on the nano/micro particles cover the active centers and restrict or reduce their catalytic activity. To outwit this problem, we have developed a method of synthesis of metal chalcogenides without capping agent so that the catalyst surface is freely available for adsorption and desorption reactions [10].

In the present work, we have prepared surfactant-free copper sulfide (**sf-CuS)** under the supersaturated condition in a simple chemical reaction wherein sulphur was dissolved while $LiBH_4$ and $Cu(CH_3COO)_2 \cdot H_2O$ were suspended in dry tetrahydrofuran (THF). The reaction was conducted for 1 h at room temperature and in an inert atmosphere to avoid any oxidation. The partial solubility of the metal source and fast reactivity in the presence of $LiBH_4$ provided a thermodynamically favorable condition [55] which induced the nucleation of particles. Since the reaction was at room temperature, the digestion process was avoided [56–60], which supplemented the formation of black powder of CuS having nano/micro flower like architecture. These micron-sized flower-like particles (**mf**) were formed by the self-assembly of nanoflakes [61]. These metal chalcogenide **mf** were formed under the supersaturated condition, and no surfactant molecules were used during synthesis. The particles were stable, and no agglomeration [10] was observed. The material was characterized by PXRD, SEM, and spectroscopic techniques (Fig. 1) [10]. Since no organic surfactant molecules were surrounding the particles, the catalyst surface was freely available for reactions and that significantly favored high activity in the reactions of click chemistry and epoxy ring opening.

The catalytic activity of sf-CuS **mf** having the unhindered surface in the multicomponent synthesis of 1, 2, 3-triazoles in the dipolar cycloaddition reactions was investigated. The experiments began with optimizing the reaction conditions for the multicomponent synthesis of 1, 2, 3-triazoles from benzyl halide, sodium azide and phenylacetylene (Scheme 1). Later the reaction was extended to the synthesis of β-hydroxy 1, 2, 3-triazoles from epoxy derivatives, sodium azide and phenylacetylene (Scheme 2). This reaction proceeded *via in-situ* ring opening of epoxides followed by the reaction with phenylacetylene. In both reactions, water was used as the solvent at room temperature. The results were very encouraging since the reactions completed in 5–12 h, and yielded of the desired products quantitatively.

In order to optimize the reaction conditions, the reactions were performed by varying the quantity of catalyst and using different solvents. Progress the reaction was monitored by means of TLC. At the end of the reaction, the catalyst was separated by filtration and worked up using ethyl acetate and water. There was no difference in yield and reaction time when catalyst loading was reduced to 15 mg, 10 mg, and 5 mg. However, when 2 mg of the catalyst was used, it required a longer time for the completion of the reaction (above 12 h). Consequently, it was decided to use 5 mg of the catalyst for further studies. Similarly, few more reactions were performed in various solvents to choose the medium of the reaction (Table 1). In DMF 45%, DMSO 20% yield was obtained. Among all solvents tried, water was the best solvent to produce the products in good yields. Other than these solvents no product spot was observed in TLC. Therefore, water was chosen as the reaction

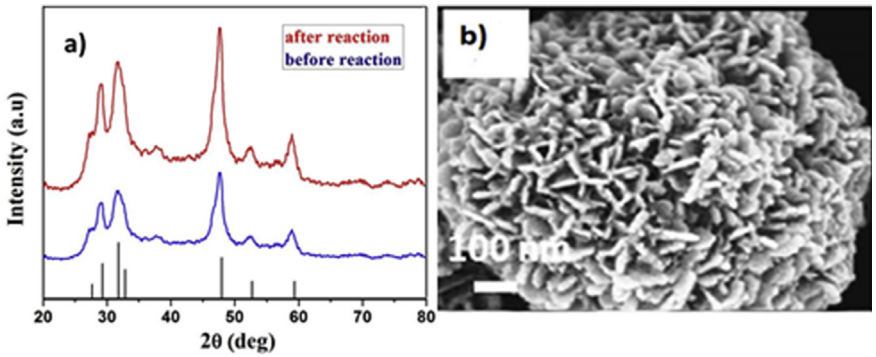

Fig. 1. (a) X-ray diffraction of sf-CuS mf, (b) SEM images of sf-CuS mf.

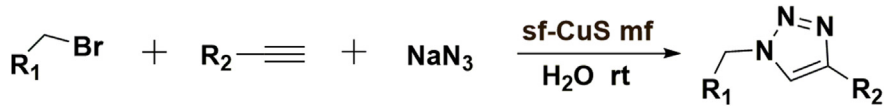

Scheme 1. Three component syntheis of 1,2,3-triazoles from organic halides catalysed by sf-CuS mf.

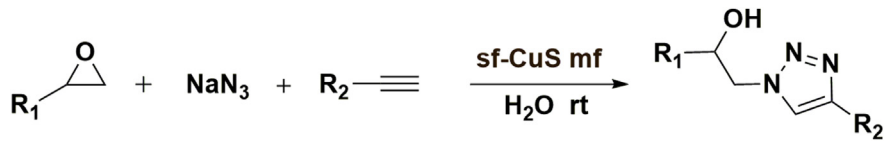

Scheme 2. Three component syntheis of β-hydroxy-1,2,3-triazoles from expoxides catalysed by sf-CuS mf in water.

Table 1
Solvent optimization of for the synthesis of Scheme 1 in the model reaction.

Entry	Solvent	time	Yield
1	CH_3OH	24 h	no
2	n-butanol	24 h	no
3	CH_3CN	24 h	no
4	$CHCl_2$	24 h	no
5	$CHCl_3$	24 h	no
6	DMSO	24 h	20%
7	DMF	24 h	45%
8	H_2O	6 h	92%

medium for all reactions.

Different benzyl bromides substituted with halides and methyl were reacted with sodium azide and terminal alkynes to form 1,2,3-triazoles using **sf-CuS mf** as catalyst under optimized condition (Table 2). Similarly, a series of different aryl epoxy, cyclic epoxy and alkyl-substituted epoxy derivatives, sodium azide, and terminal alkynes to form β-hydroxy 1,2,3- triazole using **sf-CuS mf** as catalyst and water as solvent at room temperature (Table 3). The crude products from all reactions were purified by column chromatography and then characterized by ^{1}H and ^{13}C NMR spectral data (Figs. S1–S18). Almost all these reactions (except Table 2, entries 3, 4 and 5) yielded the corresponding product in more 90% yield in water as the solvent.

Though many catalysts are known, the **sf-CuS mf** used here was obtained in a simple reaction condition, and the products were obtained in excellent yield. The performance of the various catalysts in the model reaction (styrene oxide, sodium azide, and phenylacetylene) was compared (Table 4) to understand the effect of **sf-CuS** micro flowers as the catalyst. Most of those catalysts were used at above 60 °C except for Cu/Cu_2O while our CuS was working at the room temperature (This work). Further, most of the literature on Scheme 1 type model reaction was only within benzyl azide and phenylacetylene (two reactants) whereas we are presenting the catalyst which can work in multicomponent reactions.

Leaching study was performed to confirm the heterogeneous catalysis for the reaction shown in Scheme 1. For this purpose, a reaction was stopped after the formation of around 20% product, and the catalyst was separated from the reaction mixture. The reaction was continued without the catalyst for 8 h, but no considerable product formation was observed. This observation explained that the reaction was working under heterogeneous catalysis.

The lifetime of the catalyst and its reusability play an essential role in the practical applications of such heterogeneous systems. In order to take advantage of heterogeneous nature of our catalyst, a set of experiments were performed in which both 1,2,3-triazole from *in-situ* azidolysis of benzyl halide in the presence of alkynes (Scheme 1) and epoxy ring opening followed by cycloaddition of azide (Scheme 2) and phenylacetylene using the recycled **sf-CuS mf**. After the completion of the first reaction, the product was extracted using ethyl acetate, and the catalyst was recovered by simple decantation and dried at 50 °C. A new reaction was performed with new reactants under the same conditions using the recovered **sf-CuS mf**. We have also performed a recycling experiment in Scheme 1 using 5 mmol of reagents. After completion of the reaction, the catalyst was recovered and reused for the next cycle thus confirming that **sf-CuS mf** could be reused for five times with little change in its activity (Fig. 2).

2.1. Experimental procedure

2.1.1. Synthesis of catalyst (sf-CuS)

Sulphur (40 mg, 1.3 mmol) was dissolved in 15 mL of dry tetrahydrofuran (THF) in a 50 mL two neck RB flask, to that $LiBH_4$ (59 mg, 2.5 mmol) and $Cu(CH_3COO)_2 \cdot H_2O$ (250 mg, 1.2 mmol) were added. The reaction mixture was stirred at room temperature under nitrogen atmosphere for 1 h. Initially, the color of the solution was dark brown, and after the completion of reaction it turned to dark green along with the evolution of gaseous side product(s). After 1 h, volatile side products and solvent were removed by applying high vacuum. The obtained crude product was washed with methanol (40 mL) followed by THF (40 mL) to remove side products (copper acetate, lithium salt) and unreacted S, and then centrifuged. The residue was dried under vacuum for 6 h to get catalyst as a black powder of **sf-CuS** micro flowers. The catalyst was characterized by PXRD and SEM techniques.

2.1.2. Synthesis of 1, 2, 3-triazole from benzyl bromide derivatives, sodium azide and alkyne

NaN_3 (65 mg, 1.0 mmol), the benzyl bromide (1 mmol), and the alkyne (1 mmol) were added to a suspension of sf-**CuS** (5 mg) in water. The reaction mixture was stirred at room temperature and monitored by TLC until all the starting materials were converted to products. The solid was obtained by filtration and washed by DCM (3 × 10 mL). The ex-traction of aqueous phase with DCM was also performed without loss of product, and collected organic phase were dried with anhydrous Na_2SO_4, and concentrated in vacuum. The product was purified through a silica gel column chromatography as corresponding β-hydroxy 1, 2, 3-triazoles. All the products were confirmed by usual spectral methods (^{1}H NMR, ^{13}C NMR) (*see* Supporting Information S1–S9).

For example: **1-benzyl-4-phenyl-1H-1, 2, 3-triazole:** white solid, mp:128–129 °C; ^{1}H NMR (500 MHz, $CDCl_3$) δ = 7.83–7.81 (m, 2H), 7.68 (s, 1H), 7.43–7.38 (m, 5H) 7.35–7.32 (m, 3H), 5.59 (s, 2H). ^{13}C NMR (400 MHz, $CDCl_3$) δ = 148.2, 134.6, 130.5, 129.1, 128.8, 128.1, 128.0, 125.7, 119.4 and 54.2., HRMS calculated for $C_{15}H_{13}N_3$ $[M+H]^+$: 236.1182, found: 236.1184. (See Supporting Information S1).

Table 2
Synthesis of 1, 2, 3 triazole derivatives by CuS.

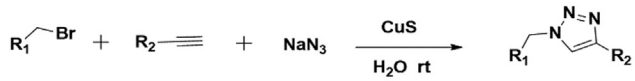

Entry	benzyl bromide (R1)	alkyne (R2)	time	product	yield%
1	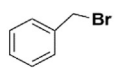	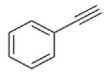	6h	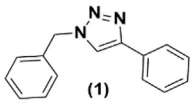 (1)	96%
2	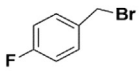	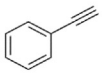	5h	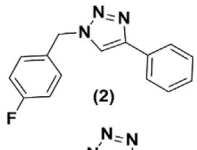 (2)	95%
3	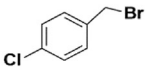	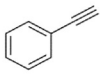	7h	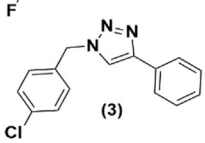 (3)	92%
4	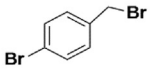	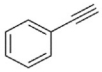	9h	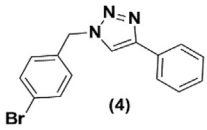 (4)	90%
5	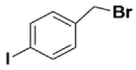	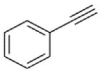	12h	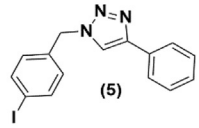 (5)	87%
6	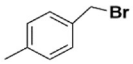	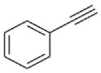	8h	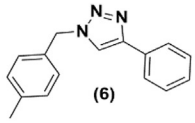 (6)	92%
7	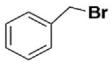	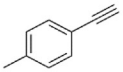	6h	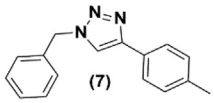 (7)	95%
8	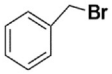	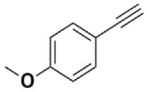	6h	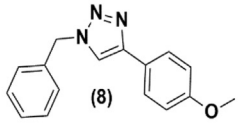 (8)	96%
9	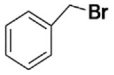	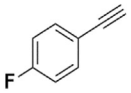	5h	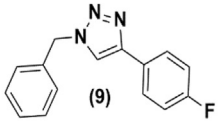 (9)	97%

2.1.3. Synthesis of β-hydroxy 1, 2, 3-triazole from benzyl bromide derivatives, sodium azide and alkyne

NaN_3 (65 mg, 1.0 mmol), the epoxide (1 mmol), and the alkyne (1 mmol) were added to a suspension of **sf-CuS** (5 mg). The reaction mixture was stirred at room temperature and monitored by TLC until all the starting materials were converted to products. The solid was obtained by filtration and washed by DCM (3 × 10 mL). The extraction of aqueous phase with DCM was also performed without loss of product, and collected organic phase were dried with anhydrous Na_2SO_4, and concentrated in vacuum. The product was isolated through a silica gel column chromatography as corresponding β-hydroxytriazoles. All the products were confirmed by usual spectral methods (^{1}H NMR, ^{13}C NMR) (See Supporting Information S10–S18).

For example: **3-Phenoxy-2-(4-phenyl-1H-1,2,3- triazol-1-yl) propan-1- ol:** pale yellow solid; mp:126–128 °C; ^{1}H NMR (500 MHz, $CDCl_3$) $\delta = 7.89$ (s, 1H), 7.78–7.75 (m, 2H), 7.43–7.39 (m, 2H), 7.34–7.35 (m, 1H), 7.32–7.30 (m, 1H) 7.03–6.99 (m, 1H),

Table 3
Synthesis of β-hydroxy 1, 2, 3-triazole derivatives by CuS.

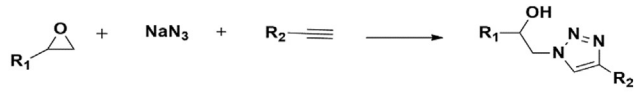

Entry	epoxide (R1)	alkyne (R2)	time	product	Yield%
1	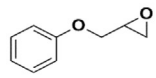	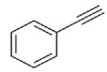	6h	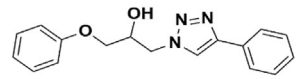 (10)	92%
2	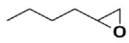	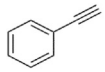	8h	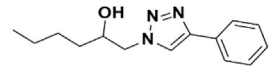 (11)	89%
3		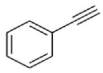	8h	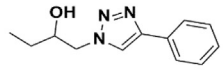 (12)	86%
4		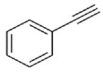	10h	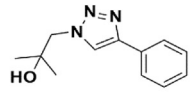 (13)	82%
5		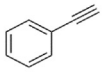	12h	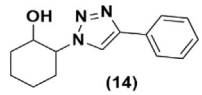 (14)	79%
6	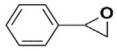	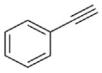	5h	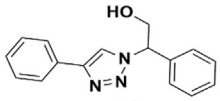 (15)	91%
7	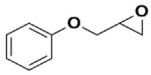	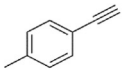	7h	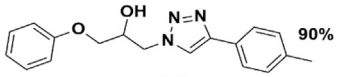 (16)	90%
8	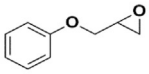	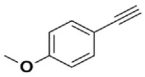	7h	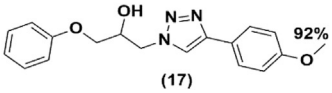 (17)	92%
9	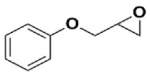	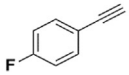	6h	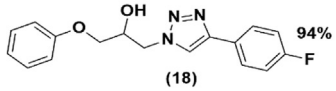 (18)	94%

6.95–6.92 (m, 2H), 4.75 (dd, $J = 3$ Hz, $J = 11$ Hz, 1H), 4.61–4.54 (m, 2H), 4.09–4.00 (m, 2H), 3.57 (s, 1H). ^{13}C NMR (400 MHz, $CDCl_3$) $\delta = 158.0$, 147.7, 130.2, 129.6, 129.5, 128.8, 128.2, 125.6, 121.6, 121.3, 114.5, 68.9, 68.7 and 53.03 HRMS calculated for $C_{17}H_{17}N_3O_2$ $[M+H]^+$: 296.1398, found: 296.1398. (See Supporting Information S10).

3. Conclusions

Surfactant-free copper sulfide (**sf-CuS)** catalyst has been utilized successfully for one-pot synthesis of triazoles by cycloaddition of both benzyl halide derivatives-alkyne and epoxide derivatives – alkyne in the presence of sodium azide. The desired products were obtained at ambient temperature while the reactions were performed in water. Most of the reactions proceeded faster with the exception of aliphatic epoxide in the case of epoxide derivatives. While in benzyl halide derivatives, less electronegative substituted benzyl halide derivative (Bromo and Iodo) were slower compared with other (flouro and chloro). The catalyst can be recycled and reused for five times without losing its activity.

Table 4
Comparison table of numerous catalysts with various Synthesis of 1, 4-disubstituted β-hydroxy-1, 2, 3-triazoles (for compound 15).

Catalyst	Substrate	Time	Temperature	Yield	Ref.
CPSi	Styrene Oxide	1 h	60 °C	94%	[50]
Cu/Cu_2O	Styrene Oxide	2 h	RT	75%	[48]
$AQ_2Cu(II)$-$APSiO_2$	Styrene Oxide	4 h	60 °C	82%	[49]
$CuFe_2O_4$	Styrene Oxide	6 h	60 °C	87%	[47]
Cu Nano particles	Styrene Oxide	8 h	100 °C	83%	[46]
Cu(I) in Ionic liquids	Styrene Oxide	10 h	80 °C	95%	[54]
Sf-CuS mf	Styrene Oxide	5 h	RT	91%	This work

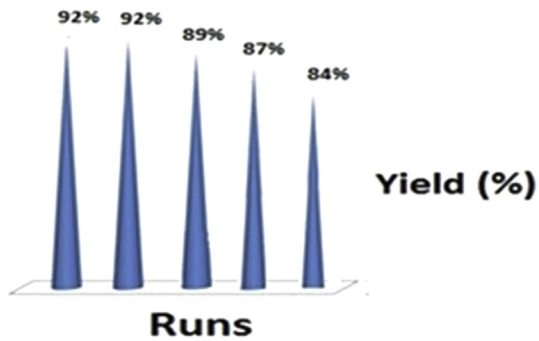

Fig. 2. Recycling results of the sf-CuS mf catalyst in the syntheis of triazoles.

Authors' contributions

Competing interests

No competing interest.

Consent for publication

Not applicable.

Ethics approval and consent to participate

Not applicable.

Acknowledgement

The authors thank the Centre for Nanotechnology at the University of Hyderabad for the TEM facility. V. R. Velpuri acknowledges UGC –BSR India for doctoral fellowship.

Appendix A. Supplementary data

Supplementary data to this article can be found online at https://doi.org/10.1016/j.jorganchem.2019.01.016.

Funding

The work is collectively supported by SERB (project No: SB/S1/IC- 47/2013), and UGC-CAS and DST-PURSE grants of the University of Hyderabad.

References

[1] Q. Lu, F. Gao, D. Zhao, Nano Lett. 2 (2002) 725.
[2] E.C. Greyson, J.E. Barton, T.W. Odom, Small 2 (2006) 368.
[3] A. Rabkin, N. Belman, J. Israelachvili, Y. Golan, Langmuir 28 (2012) 15119.
[4] P. Roy, K. Mondal, S. K Srivastava, Cryst. Growth Des. 8 (2008) 1530.
[5] P. Roy, S.K. Srivastava, Mater. Lett. 61 (2007) 1693.
[6] S. Hsu, K. On, A.R. Tao, J. Am. Chem. Soc. 133 (2011) 19072.
[7] W. Bryks, M. Wette, N. Velez, S. Hsu, A.R. Tao, J. Am. Chem. Soc. 136 (2014) 6175.
[8] S. Hsu, W. Bryks, A.R. Tao, Chem. Mater. 24 (2012) 3765.
[9] S. Hsu, C. Ngo, A.R. Tao, Nano Lett. 14 (2014) 2372.
[10] S. Gottepu, V.R. Velpuri, K. Muralidharan, J. Chem. Sci. 129 (2017) 1853.
[11] M. Nasrollahzadeh, S.M. Sajadi, A. Rostami-Vartooni, M. Bagherzadeh, J. Colloid Interface Sci. 448 (2015) 106.
[12] C. Dai, X. Li, A. Zhang, C. Liu, Song, X. Guo, RSC Adv. 5 (2015) 40297.
[13] J.H. Kou, A. Saha, C. Bennett-Stamper, R.S. Varma, Chem. Commun. 48 (2012) 5862.
[14] F. Nador, M.A. Volpe, F. Alonso, A. Feldhoff, A. Kirschning, G. Radivoy, Appl. Catal., A 455 (2013) 39.
[15] F. Himo, T. Lovell, R. Hilgraf, V.V. Rostovtsev, L. Noodleman, K.B. Sharpless, V.V. Fokin, J. Am. Chem. Soc. 127 (2005) 210–216.
[16] Qian Wang, Timothy R. Chan, Robert Hilgraf, Valery V. Fokin, K. Barry Sharpless, M.G. Finn, J. Am. Chem. Soc. 125 (2003) 3192–3193.
[17] A.S. Felten, N. Petry, B. Henry, N. Pellegrini-Moïse, K. Selmeczi, New J. Chem. 40 (2016) 1507.
[18] M. Bakthadoss, N. Sivakumar, A. Devaraj, P.V. Kumar, RSC Adv. 5 (2015) 93447.
[19] M. Rajeswari, S. Kumari, J.M. Khurana, RSC Adv. 6 (2016) 9297.
[20] S.Q. Bai, L. Jiang, A.L. Tan, S.C. Yeo, D.J. Young, T.S.A. Hor, Inorg. Chem. Front 2 (2015) 1011.
[21] S.Q. Bai, L. Jiang, D.J. Young, T.S.A. Hor, Aust. J. Chem. 69 (2016) 372.
[22] V. Calderone, I. Giorgi, O. Livi, E. Martinotti, E. Mantuano, A. Martelli, A. Nardi, Eur. J. Med. Chem. 40 (2005) 521.
[23] C. Menendez, A. Chollet, F. Rodriguez, C. Inard, M.R. Pasca, C. Lherbet, M. Baltas, Eur. J. Med. Chem. 52 (2012) 275.
[24] F.C. da Silva, M.C.B. de Souza, I.I. Frugulhetti, H.C. Castro, L.O. Silmara, T.M.L. de Souza, D.Q. Rodrigues, A.M. Souza, P.A. Abreu, F. Passamani, Eur. J. Med. Chem. 44 (2009) 373.
[25] T.W. Kim, Y. Yong, S.Y. Shin, H. Jung, K.H. Park, Y.H. Lee, Y. Lim, K.Y. Jung, Bioorg. Chem. 59 (2015) 1.
[26] J.N. Sangshetti, R.R. Nagawade, D.B. Shinde, Bioorg. Med. Chem. Lett 19 (2009) 3564.
[27] M.F. Mady, G.E. Awad, K.B. Jorgensen, Eur. J. Med. Chem. 84 (2014) 433.
[28] D.R. Buckle, D.J. Outred, C.J.M. Rockell, H. Smith, B.A. Spicer, J. Med. Chem. 29 (1986) 2267.
[29] D.R. Buckle, D.J. Outred, C.J.M. Rockell, H. Smith, B.A. Spicer, J. Med. Chem. 26 (1983) 251.
[30] C.J. Buckle, D.R. Rockell, J. Chem. Soc. 1 (1982) 627.
[31] M.Z. Griffiths, P.L.A. Popelier, J. Chem. Inf. Model. 53 (2013) 1714.
[32] N. Gouault, J.F. Cupif, A. Sauleau, M. David, Tetrahedron Lett. 41 (2000) 7293.
[33] E. Hao, T. Meng, M. Zhang, W. Pang, Y. Zhou, L. Jiao, J. Phys. Chem. 115 (2011) 8234;
(b) S.A. Ingale, F. Seela, J. Org. Chem. 77 (2012) 9352;
(c) C.Y. Wang, J.F. Zou, Z.J. Zheng, W.S. Huang, L. Li, L.-W. Xu, RSC Adv. 4 (2014) 54256.
[34] H. Wamhoff, A.R. Katritzky, C.W. Rees, Comprehens. Heterocyc. Chem. 5 (1984) 669.
[35] M. Gouault, N. Cupif, J.F. Sauleau, A. David, Tetrahedron Lett. 41 (2000) 7293.
[36] A.C. Lees, B. Evrard, T.E. Keyes, J.G. Vos, C.J. Kleverlaan, M. Alebbi, C.A. Bignozzi, Eur. J. Org. Chem. (1999) 2309.
[37] D. srinivas, V.D. Ghule, S.P. Tewari, K. Muralidharan, Chem. Eur J. 18 (2012) 15031.
[38] A. Domling, I. Ugi, Angew. Chem. Int. Ed. 39 (2000) 3169.
[39] R. Huisgen, Pure Appl. Chem. 61 (1989) 613.
[40] R. Huisgen, G. Szeimies, L. Moebius, Chem. Ber. 98 (1965) 4014.
[41] C.S. Radatz, L. do, A. Soares, E.F. Vieira, D. Alves, D. Russowsky, P.H. Schneider, New J. Chem. 38 (2014) 1410.
[42] G. Kumaraswamy, K. Ankamma, A. Pitchaiah, J. Org. Chem. 72 (2007) 9822.
[43] K.R. Reddy, C.U. Maheswari, M.L. Kantam, P.C. Division, Synth. Commun. 38 (2008) 2158.
[44] J.S. Yadav, B.V.S. Reddy, G.M. Reddy, D.N. Chary, Tetrahedron Lett. 48 (2007) 8773.
[45] Y. Chen, W.-Q. Zhang, B.-X. Yu, Y.-M. Zhao, Z.-W. Gao, Y.-J. Jian, L.-W. Xu, Green Chem. 18 (2016) 6357.
[46] F. Alonso, Y. Moglie, G. Radivoy, M. Yus, J. Org. Chem. 76 (2011) 8394.
[47] B.S.P. Anil Kumar, K.H.V. Reddy, G. Satish, R.U. Kumar, Y.V.D. Nageswar, Tetrahedron Lett. 53 (2012) 4595.
[48] H.E. Shahri, H. Eshghi, J. Lari, S.A. Rounagh, Appl. Organomet. Chem. (2017) e3947.
[49] H. Sharghi, A. Khoshnood, M.M. Doroodmand, R. Khalifeh, J. Iran. Chem. Soc. 9 (2012) 231.
[50] H. Naeimi, V. Nejadshafiee, New J. Chem. 38 (2014) 5429.
[51] T. Shamim, S. Paul, Catal. Lett. 136 (2010) 260–265.
[52] H.N. M Elnagdy, K. Gogoi, A.A. Ali, D. Sarma, Appl. Organomet. Chem. 32 (2018), e3931.
[53] H. Naeimi, Z. Ansarian, Inorg. Chim. Acta. 466 (2017) 417–442.
[54] N. Singh, C. R. Chimie. 2015, 18, 1257.
[55] B. Li, Y. Xie, Y. Xue, J. Phys. Chem. C 111 (2007) 12181.

[56] V.P.P. Weimarn, Chem. Rev. 2 (1925) 217.
[57] A.E. Nielsen, Acta Chem. Scand. 14 (1960) 1654.
[58] R.A. Johnson, J.D. O'ourke, J. Am. Chem. Soc. 76 (1954) 2124.
[59] R.A. Day Jr., A.L. Underwood, Quantitative Analysis, sixth ed., Pearson Education India, 2015 sixth ed.
[60] D.A. Skoog, D. M West, F. J Holler, S. R Crouch, Fundamental Analytical Chemistry, Cengage Learning, 2004.
[61] B.G. Kumar, K. Muralidharan, Eur. J. Inorg. Chem. 32 (2013) 2102.

Nano/micro particle as catalysts for organic reactions and carbon dioxide conversion into cyclic- and poly-carbonates

by Venkateswara Rao Velpuri

Nano/micro particle as catalysts for organic reactions and carbon dioxide conversion into cyclic- and poly-carbonates

ORIGINALITY REPORT

23%	9%	21%	6%
SIMILARITY INDEX	INTERNET SOURCES	PUBLICATIONS	STUDENT PAPERS

K. M

PRIMARY SOURCES

.K. MURALIDHARAN
Professor
School of Chemistry
University of Hyderabad
Hyderabad - 500 046.

1	Venkateswara Rao Velpuri, Krishnamurthi Muralidharan. "Multicomponent click reaction catalyzed by organic surfactant-free copper sulfide (sf-CuS) nano/micro flowers", Journal of Organometallic Chemistry, 2019 Publication	14%
2	www.patentsencyclopedia.com Internet Source	1%
3	rua.ua.es Internet Source	1%
4	Submitted to Jawaharlal Nehru Technological University Student Paper	<1%
5	patents.justia.com Internet Source	<1%
6	Submitted to University of Birmingham Student Paper	<1%
7	idoc.pub Internet Source	

Self plagiarism
K. M
25/1/21

.K. MURALIDHARAN
Professor
School of Chemistry
University of Hyderabad
Hyderabad - 500 046.

		<1%
8	repository.upenn.edu Internet Source	<1%
9	hdl.handle.net Internet Source	<1%
10	www.freepatentsonline.com Internet Source	<1%
11	Submitted to University College London Student Paper	<1%
12	www.thieme-connect.com Internet Source	<1%
13	scholarbank.nus.edu.sg Internet Source	<1%
14	www.thieme-connect.de Internet Source	<1%
15	A. Antony Muthu Prabhu, V.K. Subramanian, N. Rajendiran. "Excimer formation in inclusion complexes of β-cyclodextrin with salbutamol, sotalol and atenolol: Spectral and molecular modeling studies", Spectrochimica Acta Part A: Molecular and Biomolecular Spectroscopy, 2012 Publication	<1%
16	epub.uni-regensburg.de Internet Source	<1%

17	www.faqs.org Internet Source	<1%
18	pubs.acs.org Internet Source	<1%
19	scholarcommons.usf.edu Internet Source	<1%
20	Yuqin Jiang, Niu Guo, Xiyong Li, Yamin Sun, Weiwei Zhang. "Cu(II)-CMC: a mild, efficient and recyclable catalyst for the oxidative alkyne homocoupling reaction", Zeitschrift für Naturforschung B, 2017 Publication	<1%
21	Submitted to University of Hyderabad, Hyderabad Student Paper	<1%
22	www.rsc.org Internet Source	<1%
23	Andrew B. Lutjen, Mackenzie A. Quirk, Erin M. Kolonko. "Synthesis of Esters Via a Greener Steglich Esterification in Acetonitrile", Journal of Visualized Experiments, 2018 Publication	<1%
24	Apurba Kr. Barman, Sandeep Verma. "Solid state structures and solution phase self-assembly of clicked mannosylated	<1%

diketopiperazines", RSC Advances, 2013
Publication

25	Takizawa, A.. "Convergent synthesis of the common FGHI-ring part of ciguatoxins", Tetrahedron, 20060731 Publication	<1%
26	Min Lv, Peng Wang, Dan Yuan, Yingming Yao. "Conversion of Carbon Dioxide into Oxazolidinones Mediated by Quaternary Ammonium Salts and DBU", ChemCatChem, 2017 Publication	<1%
27	digital.lib.washington.edu Internet Source	<1%
28	Huanfeng Jiang, Li jiawei, Yanwei Ren, Chaorong Qi. "A Chiral Salen-based MOF Catalytic Material with highly thermal, aqueous and chemical stabilities", Dalton Trans., 2017 Publication	<1%
29	Sateesh Mulkapuri, Sathish Kumar Kurapati, Samar K. Das. " Carbonate encapsulation from dissolved atmospheric CO into a polyoxovanadate capsule ", Dalton Transactions, 2019 Publication	<1%
30	tsukuba.repo.nii.ac.jp Internet Source	<1%

31	www.google.com.ar Internet Source	<1%
32	Zidan Zhou, Xinwen Peng, Linxin Zhong, Xuehui Li, Runcang Sun. "Lignin Nanosphere-Supported Cuprous Oxide as an Efficient Catalyst for Huisgen [3+2] Cycloadditions under Relatively Mild Conditions", Polymers, 2018 Publication	<1%
33	Submitted to University of Witwatersrand Student Paper	<1%
34	jbcs.sbq.org.br Internet Source	<1%
35	Submitted to Savitribai Phule Pune University Student Paper	<1%
36	Hidetoshi Yamada, Mugio Nishizawa. "Syntheses of sweet tasting diterpene glycosides, baiyunoside and analogs", Tetrahedron, 1992 Publication	<1%
37	Sanyasinaidu Gottapu, Venkateswara Rao Velpuri, Krishnamurthi Muralidharan. "Surfactant free metal chalcogenides microparticles consisting of nano size crystallites: room temperature synthesis driven by the supersaturated condition", Journal of Chemical Sciences, 2017	<1%

Publication

38	Novak, P.. "Co- and homocyclotrimerization reactions of protected 1-alkynyl-2-deoxyribofuranose. Synthesis of C-nucleosides, C-di- and C-trisaccharide analogues", Tetrahedron, 20080526 Publication	<1%
39	www.survivin.net Internet Source	<1%
40	ir.soken.ac.jp Internet Source	<1%
41	Thomas P. Lockhart, Joseph C. Calabrese, Fredric. Davidson. "Structural studies of diorganotin(IV) carboxylates. X-ray and NMR structures of Me2Sn(OAc)2 and a 7-coordinate tin anion, Me2Sn(OAc)3NMe4.cntdot.2CHCl3", Organometallics, 1987 Publication	<1%
42	ueaeprints.uea.ac.uk Internet Source	<1%
43	Submitted to University of Newcastle upon Tyne Student Paper	<1%
44	Andre A. L. Goncalves, Ana C. Fonseca, Jorge F. J. Coelho, Armenio C. Serra. "Supported Catalysis in Carbon Dioxide Activation", Current Green Chemistry, 2015	<1%

Publication

45	Manoj B. Gawande, Anandarup Goswami, François-Xavier Felpin, Tewodros Asefa et al. "Cu and Cu-Based Nanoparticles: Synthesis and Applications in Catalysis", Chemical Reviews, 2016 Publication	<1%
46	Li, J.H.. "Amine- and phosphine-free palladium(II)-catalyzed homocoupling reaction of terminal alkynes", Tetrahedron, 20050214 Publication	<1%
47	pubs.rsc.org Internet Source	<1%
48	baadalsg.inflibnet.ac.in Internet Source	<1%
49	www.medal-project.eu Internet Source	<1%
50	Maya Shankar Singh, Sushobhan Chowdhury, Suvajit Koley. "Advances of azide-alkyne cycloaddition-click chemistry over the recent decade", Tetrahedron, 2016 Publication	<1%
51	www.patentgenius.com Internet Source	<1%
52	"Applications of Nanomaterials in Human Health", Springer Science and Business Media	<1%

LLC, 2020

Publication

Exclude quotes	On	Exclude matches	< 14 words
Exclude bibliography	On		